UNIVERSIDAD NACIONAL DE COLOMBIA

LEOPOLDO MÚNERA RUIZ
RECTOR

MARY LUZ ALZATE ZULUAGA
VICERRECTORA · SEDE MEDELLÍN

OSCAR DE JESÚS CÓRDOBA GAONA
DECANO · FACULTAD DE CIENCIAS AGRARIAS

COMITÉ CIENTÍFICO INTERNACIONAL

Rita M. Ávila de Hernández, Ph.D.
Universidad Centroccidental Lisandro Alvarado
Barquisimeto, Lara, Venezuela. ritaavila@ucla.edu.ve

Felipe Bravo Oviedo, D.Sc.
Universidad de Valladolid.
Valladolid, España. fbravo@pvs.uva.es

José Rafael Córdova, Ph.D.
Universidad Simón Bolivar y Universidad Central de
Venezuela. Baruta, Venezuela. jcordova45@yahoo.com

José Luis Crossa, Ph.D.
Centro Internacional de Mejoramiento de Maíz y Trigo
(CIMMYT). Texcoco, México. j.crossa@cgiar.org

Mateo Itzá Ortiz, D.Sc.
Universidad Autónoma de Ciudad Juárez
Chihuahua, México. mateo.itza@uacj.mx

Juan Pablo Damián, Ph.D.
Universidad de la República, Uruguay.
jpablodamian@gmail.com

Moncef Chouaibi, Ph.D.
Higher School of Food Industries of Tunisia (ESIAT),
Tunisia. moncef.chouaibi@yahoo.com.au

Walter Motta Ferreira, D.Sc.
Universidade Federal de Minas Gerais.
Belo Horizonte, Brasil. pereira3456@hotmail.com

Tomas Norton, Ph.D.
University of Leuven. Leuven, Flanders, Bélgica.
tnorton@harper-adams.ac.uk

Pepijn Prinsen, Ph.D.
University of Amsterdam. Holanda.
pepijnprinsen33@hotmail.com

Aixa Ofelia Rivero Guerra, Ph.D.
Centro Europeo de Estadística Aplicada.
Sevilla, España. rivero-guerra@hotmail.com

Antonio Roldán Garrigos, Ph.D.
Consejo Superior de Investigaciones Científicas.
Murcia, España. aroldan@cebas.csic.es

Elhadi M. Yahia, Ph.D.
Universidad Autónoma de Querétaro.
Querétaro, México. elhadiyahia@hotmail.com

Meisam Zargar, Ph.D.
RUDN University, Rusia.
zargar_m@pfur.ru

COMITÉ EDITORIAL

Período 2022-2024

Albeiro López Herrera, Ph.D. **Editor en Jefe**	Universidad Nacional de Colombia. Colombia alherrera@unal.edu.co
Flavio Alves Damasceno, Ph.D.	Universidade Federal de Lavras. Brasil flavioua@gmail.com
Luz Estela González de Bashan, Ph.D.	The Bashan Institute of Science, USA legonzal04@cibno.mx
Juan Diego León Peláez, Ph.D.	Universidad Nacional de Colombia. Colombia jdleon@unal.edu.co
Deyanira Lobo Luján, Ph.D.	Universidad Central de Venezuela. Venezuela lobo.deyanira@gmail.com
Sara Márquez Girón, Ph.D.	Universidad de Antioquia. Colombia saramariamarquezg@gmail.com
Jousset Alexandre, Ph.D.	Utrecht University. Países Bajos A.L.C.Jousset@uu.nl
Juan Gonzalo Morales Osorio, Ph.D.	Universidad Nacional de Colombia. Colombia jgmoraleso@unal.edu.co
Jaime Parra Suescún, Ph.D.	Universidad Nacional de Colombia. Colombia jeparrasu@unal.edu.co
Camilo Ramírez Cuartas, Ph.D.	Universidad de Antioquia. Colombia camilo.ramirez@udea.edu.co
Iang Schroniltgen Rondon B. M.Sc. Ph.D(c)	Universidad del Tolima. Colombia isrondon@ut.edu.co
Paola Andrea Sotelo Cardona, Ph.D.	World Vegetable Center (WorldVeg). Taiwan paola.sotelo@worldveg.org

EDICIÓN TÉCNICA

Mario Alejandro Vallejos Jiménez - Ingeniero Biológico. M.Eng. Química-
mavallejosj@unal.edu.co

Periodicidad: Cuatrimestral
Vol. 78 No. 2 - 2025

Admitida en las Bases Bibliográficas:
Scopus
Scielo (Scientific Electronic Library Online)
ISI-Scielo Citation Index
REDIB (Red Iberoamericana e innovación y conocimiento científico)
Cabi (www.cabi.org)
EBSCO Host
Google Scholar
DOAJ (Directory of Open Access Journals)
Ulrich's Periodicals Directory (Global Serials Directory)
Redalyc (Red de Revistas Científicas de América Latina, el Caribe, España y Portugal)
Latindex (Sistema Regional de Información en Línea para Revistas Científicas de América Latina, el Caribe, España y Portugal)
ProQuest
Teeal (The Essential Electronic Agricultural Library)
WZB (Berlin Social Science Center)
Cross ref
Cornell University
Field Crop Abstracts
Forestry Abstracts
Plant Breeding Abstracts
Índice Agrícola de América Latina y el Caribe
Índice Bibliográfico Nacional
Minciencias - Publindex
AGRIS-FAO

Portada: 112 años Facultad de Ciencias Agrarias - Tatiana Montero Ciro - Realizadora Audiovisual, Facultad de Ciencias Agrarias, Universidad Nacional de Colombia, Sede Medellín, Colombia - audiovisualfca_med@unal.edu.co

Contraportada: Klara Torres Restrepo

Dirección postal: Apartado Aéreo 568, Medellín, Colombia

Dirección electrónica: rfnagron_med@unal.edu.co

Página Web: http://www.revistas.unal.edu.co/index.php/refame

Teléfono: (*4) 430 90 06; Fax: (* 4) 230 04 20

Diagramación: Miryam Ospina Ocampo

Marcación: LandSoft S.A.

Diseño e Impresión: Centro de Publicaciones UN, Medellín.

Primera edición: Año 1939

ISSN: 0304-2847

ISSN formato web: 2248-7026

doi: 10.15446/rfnam

CC BY NC SA

Licencia Ministerio de Gobierno: 275/64

11057 **Growth models of *Hevea brasiliensis* genotypes in clonal fields of the Colombian Orinoquia**
Modelos de crecimiento de genotipos de *Hevea brasiliensis* en campos clonales de la Orinoquía colombiana

Sandra Liliana Castañeda-Garzón / Argenis Antonio Mora Garcés / Maribel Tarazona Yanes / David Ricardo Hernández Angarita

11069 **Gibberellic acid and warm incubation temperatures as germination stimulants in yellow kiwifruit seeds (*Actinidia chinensis* var. *chinensis*)**
Ácido giberélico y temperaturas cálidas de incubación como estimulantes de la germinación en semillas de kiwi amarillo (*Actinidia chinensis* var. *chinensis*)

Jhusua David Reina-García / Juan Guillermo Cruz-Castillo / Gustavo Almaguer-Vargas / Diana Guerra-Ramírez / Álvaro Castañeda-Vildozola

11077 **Protein concentrates from colombian cheese acid whey as a source of antioxidant hydrolysates obtained by proteolysis**
Concentrados proteicos a partir de lactosuero ácido de queso colombiano como una fuente de hidrolizados antioxidantes obtenidos por proteólisis

Sandra Zapata Bustamante /Héctor José Ciro Velásquez / José Uriel Sepúlveda Valencia / Diego Luis Durango Restrepo /Jesús Humberto Gil González

11089 **Characterization of rejected green banana flour: morphological, structural, and techno-functional properties**
Caracterización de la harina de banano verde de rechazo: propiedades morfológicas, estructurales y tecnofuncionales

Nelly Sánchez-Mesa / Katherine Manjarres-Pinzón / Eduardo Rodríguez-Sandoval / Jesus Gil-González / Guillermo Correa-Londoño

11103 **Silage production from agro-industrial by-products fermented with lactic acid bacteria isolated from the marine environment**
Producción de ensilados a partir de subproductos agroindustriales fermentados con bacterias ácido lácticas aisladas del ambiente marino

Emilio R. Marguet / Marisol Vallejo

11117 **Application of tomato peels (*Solanum lycopersicum* L.) in baking: effects on nutritional and sensory quality**
Aplicación de cáscaras de tomate (*Solanum lycopersicum* L.) en panificación: efectos en calidad nutricional y sensorial

Vilma Quitral / Adriana Escobar / Rocío Ávila / Marcos Flores / Ítalo Chiffelle / Carolina Araya-Bastías

11127 **Effect of turmeric flour on sensory rating and antioxidant capacity in spicy fruit sauce**
Efecto de Curcuma longa en la calificación sensorial y antioxidante de salsa picante de fruta

Maritza Barriga-Sánchez / Patricia Cristobal Alania

11141 **Effect of Trolox and resveratrol supplementation during the refrigeration of boar sperm**
Efecto de la suplementación con Trolox y resveratrol durante la refrigeración de semen porcino

Stephania Madrid Gaviria / Sergio Morado / Pablo Daniel Cetica / Mariana Córdoba

11151 **Interaction of biological soil crusts with edaphic parameters of carbon and nitrogen in desertified soils**
Interacción de las costras biológicas del suelo con los parámetros edáficos de carbono y nitrógeno en suelos desertificados

Juan Jair Rivera Padilla / Julian David Romero Conde / Lizeth Manuela Avellaneda-Torres

11161 **Physical and mechanical properties of cross-laminated timber made from *Pinus tecunumanii* wood**
Propiedades físicas y mecánica de madera contralaminada fabricada con *Pinus tecunumanii*

Jhon F. Herrera-Builes / Juan C. Sierra / Rodolfo Parra

11169 **Survival and oviposition of *Tetranychus urticae* Koch (Acari: Tetranychiidae) under exposure to unfractionated botanical extracts**
Supervivencia y oviposición de *Tetranychus urticae* Koch (Acari: Tetranychiidae) bajo exposición a extractos botánicos crudos

Daniel Rodríguez / Fernando Cantor / Ericsson Coy-Barrera

11181 ***Camellia cattienensis*: phytochemical and biological properties from the leaf extract**
Camellia cattienensis: propiedades fitoquímicas y biológicas del extracto de hojas

Hanh Thi Dieu Nguyen / Ngoc An Nguyen / Thi Nha Xuyen Nguyen / Trong Thao Nguyen / Le Pham Tan Quoc / Hong Thien Van / Thanh Tho Le / Van Hop Nguyen / Quoc Hung Nguyen / Tan Viet Pham

The ideas expressed in the articles published in this volume are exclusively those of the authors and do not necessarily reflect the opinion of the Facultad de Ciencias Agrarias

Las ideas de los trabajos publicados en esta entrega, son de exclusiva responsabilidad de los autores y no reflejan necesariamentela opinión de la Facultad de Ciencias Agrarias

EVALUADORES

El Comité Editorial dentro de sus políticas, envía los artículos a especialistas, con el fin de que sean revisados. Sus observaciones en adición a las que hacen los editores, contribuyen a la obtención de una publicación de reconocida calidad en el ámbito de las Ciencias Agrarias. Sus nombres son mencionados como una expresión de agradecimiento.

Alejandro Expósito. Departamento de Ingeniería Agroalimentaria y Biotecnología, Universitat Politècnica de Catalunya, BarcelonaTech, España. alejandro.exposito@upc.edu

Alexandra Úsuga Suárez. Facultad de Ciencias Agrarias, Universidad de Antioquia, Colombia. alexandra.usuga@udea.edu.co

Aramys Silva dos Reis. Federal University of Maranhão, Brazil. aramys.reis@ufma.br

Ariel Antonio Agudelo-Sánchez. Facultad de Ciencias Básicas, Universidad de la Amazonía, Colombia. ar.agudelo@udla.edu.co

Bruno Fonsêca Feitosa. University of Campinas, Faculty of Food Engineering, Brazil. brunofonsecafeitosa@live.com

Cassia Nespolo. Universidade Federal do Pampa, Brazil. cassianespolo@unipampa.edu.br

Christian Camilo Castañeda Cardona. Universidad de los Llanos, Colombia. christian.castaneda@unillanos.edu.co

Claudia E. Barraza-Zepeda. Northern Arizona University, United States of America. claudiabarraz@gmail.com

Eleana Spavento. Universidad Nacional de la Plata, Argentina. eleanaspavento@yahoo.com.ar

Francisca de los Angeles Mejía Betancourt. Universidad Nacional Agraria, Nicaragua. francisca.mejia@ci.una.edu.ni

Freddy Muñoz. Centro de Investigación en Innovación Forestal, Instituto Tecnológico de Costa Rica, Costa Rica. fmunoz@tec.ac.cr

García Mora C. Centro de Investigaciones Químicas, Universidad Autónoma del Estado de Hidalgo, México. coralgm19@gmail.com

Giovanni Restrepo Betancur. Facultad de Ciencias Agrarias, Universidad Nacional de Colombia, Sede Medellín, Colombia. grestre0@unal.edu.co

Huong Thi Lan Vu. Faculty of Biology- Biotechnoogy, University of Science, Vietnam National University of Ho Chi Minh City, Vietnam. vtlhuong@hcmus.edu.vn

Hüseyin Çelik. University of Ondokuz Mayis, Faculty of Agriculture, Department of Horticulture, Turkey. huscelik@omu.edu.tr

Jaime Alberto Moreno. Facultad del Medio Ambiente y Recursos Naturales, Universidad Distrital Francisco José de Caldas, Colombia. jmoreno@udistrital.edu.co

Jorge Figueroa Florez. Universidad de Sucre, Sincelejo, Colombia. jorge.figueroa@unisucre.edu.co

Jorge León Quispe. Facultad de Ciencias Biológicas, Universidad Nacional Mayor, Perú. jleonq@unmsm.edu.pe

Juan Carlos Gómez Daza. Universidad del Valle, Colombia. juan.gomez.d@correounivalle.edu.co

Julio César Chacón-Hernández. Instituto de Ecología Aplicada, Universidad Autónoma de Tamaulipas, México. jchacon@docentes.uat.edu.mx

Liana Claudia Salantă. Faculty of Food Science and Technology, University of Agricultural Sciences and Veterinary Medicine Cluj-Napoca, Romania. liana.salanta@usamvcluj.ro

Linette Salvo S._Universidad del Bío-Bío, Chile. lsalvo@ubiobio.cl

Marcy Rodrigues. Universidade do Vale do Taquarí, Brazil. marcy.rodrigues@univates.br

Maritza Barriga-Sánchez. Instituto Tecnológico de la Producción, Perú. mbarriga@itp.gob.pe

Nora Estela Ponce Fernández. Instituto Tecnológico Superior de Guasave, México. nponcef.itsg@gmail.com

Oscar de Jesú Córdoba Gaona. Facultad de Ciencias Agrarias, Universidad Nacional de Colombia, Sede Medellín, Colombia. ojcordobag@unal.edu.co

Quyen Bao Thuy Ho. Faculty of Biotechnoogy, Ho Chi Minh City Open University, Vietnam. quyen.hbt@ou.edu.vn

Saby Inés Zegarra Samamé. Universidad Peruana de Ciencias Aplicadas, Perú. pcnuszeg@upc.edu.pe

Sani Raquel Aguero Gauto. Facultad de Ciencias y Tecnología, Universidad Nacional de Itapúa, Paraguay. sanyraquel5@gmail.com

Shaimaa Fadhil Weshah. Food and Nutrition Department, College of Health and Medical Technologies, Northern Technical University-Al-Dour, Iraq. Shaimaa.fadhil@ntu.edu.iq

Sofía Loza-Cornejo. Laboratorio de Bioquímica, Centro Universitario de los Lagos. Universidad de Guadalajara, México. sofialo@culagos.udg.mx

Valentina Toledo. Universidad Pedagógica Experimental Libertador, Caracas, Venezuela. toledo.valentina@gmail.com

Victor Hugo Morales Peña. Universidad EARTH, Costa Rica. vmorales@earth.ac.cr

Yesim Bulak Korkmaz. Department of Plant Protection, Faculty of Agriculture, Ataturk University, Turkey. yesim.bulak@atauni.edu.tr

Yusuf Sudo Hadi. Department of Forest Products, Faculty of Forestry and Environment, IPB University, Indonesia. yshadi@indo.net.id

EDITORIAL

A History of Commitment to Agriculture and Knowledge: Over a Century of Cultivating Wisdom Among Furrows and Letters, Celebrating 111 Years of the Faculty of Agrarian Sciences and 85 Years of Its Journal

Una historia de compromiso con la agricultura y el saber: más de un siglo cultivando saberes entre surcos y letras, en los 111 años de la Facultad de Ciencias Agrarias y los 85 años de su Revista

La historia de la Facultad de Ciencias Agrarias es una narración de esfuerzo colectivo, visión educativa y contribución constante al desarrollo agrícola de Colombia. Sus raíces se remontan a la creación de la Escuela de Agricultura Tropical y Veterinaria, establecida mediante la Ordenanza N° 11 de la Asamblea Departamental de Antioquia el 23 de marzo de 1914. Esta institución nació de la convicción de que la agricultura constituía la base del progreso genuino de la nación, respondiendo al llamado de modernizar los métodos agrícolas y formar profesionales comprometidos con la transformación del campo.

La apertura oficial de la Escuela se llevó a cabo el 10 de octubre de 1916, iniciando labores con 104 estudiantes matriculados. Esta cifra pronto descendió a 84, reflejando las dificultades iniciales de consolidar una oferta educativa sólida y atractiva en un contexto social donde la migración hacia profesiones "de guante blanco" era una tendencia marcada. A pesar de ello, la Escuela mantuvo su propósito firme: formar profesionales capaces de extraer del suelo colombiano toda su riqueza mediante el empleo de los modernos procedimientos de la ciencia agrícola, como lo expresó el diario *El Colombiano* en su edición del 7 de octubre de 1916.

El espíritu de la Escuela no tardó en traducirse en iniciativas estudiantiles. En 1920, surgió el primer número de *El Agrónomo*, una revista dirigida por los propios alumnos, entre ellos Juvenal Posada, que reflejaba el entusiasmo académico y la necesidad de crear espacios de divulgación científica.

El año de 1926 marcó un punto de inflexión con la propuesta de reorganización liderada por el científico puertorriqueño Carlos Chardón, se impulsó un proyecto de desarrollo agrícola que incluía la compra de una nueva propiedad para la Escuela y la construcción de un edificio moderno, adecuado a las necesidades de la enseñanza agrícola contemporánea. La búsqueda de nuevos terrenos, que se extendió desde Itagüí hasta Girardota, y la activa participación de la Escuela en eventos como la Exposición Agropecuaria de Medellín, evidenciaron el esfuerzo por consolidar una infraestructura física y académica acorde con sus ideales de excelencia. Paralelamente, se cedieron terrenos de la Granja de Fontidueño para la creación de la Colonia Agrícola de la Casa de Menores, reafirmando el compromiso social de la institución.

El periodo de la denominada "Misión Chardón" en 1927 puso en evidencia una reflexión crucial sobre las tendencias sociales: el abandono del campo por parte de la juventud, en busca de profesiones urbanas consideradas más prestigiosas. La Escuela, no obstante, persistió en su misión de dignificar las labores agrícolas, destacando su valor fundamental para el progreso colectivo.

Los años treinta trajeron nuevos desafíos. En 1930, la Escuela debió cambiar de sede, abandonando la propiedad de Joaquín Santamaría y realizando los arreglos pertinentes para su devolución. Este mismo año, se incorporaron técnicos expertos internacionales quienes contribuyeron a fortalecer las capacidades técnicas de la Escuela. Sin embargo, las dificultades presupuestales obligaron en 1931 a sustituirlos por profesionales nacionales formados en la propia institución, como Francisco Luis Gallego y Ramón Mejía Franco.

La consolidación académica de la Escuela se vio reflejada en 1934 con su anexión a la Universidad de Antioquia mediante la Ordenanza N° 34 de la Asamblea Departamental. Esta incorporación significó un respaldo institucional y financiero que permitió a la Escuela y a la Estación Experimental Tulio Ospina articularse de manera más eficiente con otros programas de la Universidad, enriqueciendo su capacidad de investigación y formación.

En 1937, el proceso de expansión educativa alcanzó una dimensión nacional. La incorporación del Instituto Agrícola Nacional a la Universidad Nacional de Colombia, donde se convirtió en la primera Facultad de presencia nacional, sentó las bases de un sistema de educación agronómica de amplio alcance, que trascendía las fronteras departamentales.

El entusiasmo y la inquietud científica de los estudiantes no se detuvieron. En 1939, José Vicente Lafaurie Acosta y Jesús Atehortúa propusieron la creación de una revista científica que sirviera como órgano de divulgación académica de la Escuela. Esta iniciativa se concretó en 1940 con la fundación de la *Revista Facultad Nacional de Agronomía*, bajo la dirección de los mismos estudiantes.

La revista nació con el propósito de ser un vehículo de comunicación científica, reflejando el quehacer investigativo y académico de la Facultad. Desde sus primeros números, se caracterizó por su rigor técnico y su enfoque en problemáticas agrícolas relevantes para el país, contribuyendo significativamente a la consolidación de una cultura científica en el sector agrario.

Este recorrido histórico desde 1914 hasta 1940 no solo da cuenta de la evolución institucional de la actual Facultad de Ciencias Agrarias, sino que también ilustra un esfuerzo constante por responder a las necesidades del país, formar profesionales de excelencia, impulsar la investigación y promover el desarrollo rural. La creación de la *Revista Facultad Nacional de Agronomía* representa el cierre de una etapa de maduración institucional y el inicio de una nueva era en la divulgación del conocimiento agrícola en Colombia.

Hoy, al rememorar estos primeros pasos, se reafirma el compromiso de la Facultad y su revista con la construcción de una sociedad más justa, próspera y sustentable, enraizada en el conocimiento y la innovación agropecuaria.

Oscar de Jesús Córdoba Gaona
Decano Facultad de Ciencias Agrarias
Universidad Nacional de Colombia, Sede Medellín
ojcordobag@unal.edu.co

Research article

https://revistas.unal.edu.co/index.php/refame

Revista Facultad Nacional de Agronomía

Growth models of *Hevea brasiliensis* genotypes in clonal fields of the Colombian Orinoquia

Modelos de crecimiento de genotipos de *Hevea brasiliensis* en campos clonales de la Orinoquía colombiana

https://doi.org/10.15446/rfnam.v78n2.113865

Sandra Liliana Castañeda-Garzón[1]*, Argenis Antonio Mora Garcés[1], Maribel Tarazona Yanes[1] and David Ricardo Hernández Angarita[1]

ABSTRACT

In forest species, mathematical models have been useful for describing growth, development, biomass production, and carbon sequestration. However, the growth of *Hevea brasiliensis* in the Orinoquia region has not yet been characterized using models validated from field data. In this study, four growth models were evaluated and growth curve parameters and absolute growth rate (AGR) were calculated in the clonal fields of the La Libertad Research Center (Villavicencio, Meta) and the Taluma Experimental Farm (Puerto López, Meta) of Corporación colombiana de investigación agropecuaria (AGROSAVIA) to describe the growth pattern of seven clones of the CDC, FDR, MDF, and PMB series and the FX 3864 and RRIM 600 controls. At 8 years of age, the logistic function was identified as the best-fitting growth model. In the clonal fields of La Libertad and Taluma, clones FDR 5788 and PMB1 exhibited the largest trunk circumferences (69.89 and 57.47 cm) and higher AGR (10.92 and 9.63 cm per year), reaching their maximum growth rate (MGRs) at 3.9 and 3.7 years, respectively. The earliest maturing clones were RRIM 600 and CDC 312, with MGRs at 3.46 and 3.4 years, respectively. These findings provide critical insights into the growth dynamics of rubber tree clones and offer valuable guidance for the management and performance evaluation of rubber plantations in the Colombian Orinoquia.

Keywords:
Logit analysis
Plantations
Plant growth
Rubber

RESUMEN

En especies forestales, los modelos matemáticos han sido útiles para describir el crecimiento, desarrollo, producción de biomasa y captura de carbono. Sin embargo, el crecimiento de *Hevea brasiliensis* en la región de la Orinoquia aún no ha sido caracterizado mediante modelos validados con datos de campo. Con el objetivo de describir el patrón de crecimiento de siete clones de las series CDC, FDR, MDF, PMB y los testigos FX 3864 y RRIM 600, se evaluaron cuatro modelos de crecimiento, se calcularon los parámetros de la curva de crecimiento y la tasa absoluta de crecimiento (TAC) en los campos clonales del Centro de Investigación La Libertad (Villavicencio, Meta) y la Finca Experimental Taluma (Puerto López, Meta) de la Corporación colombiana de investigación agropecuaria - AGROSAVIA. A la edad de 8 años, el mejor modelo de crecimiento correspondió a la función logística. En los campos clonales de la Libertad y Taluma, los clones FDR 5788 y PBM1 presentaron las mayores circunferencias de tronco (69,89 y 57,47 cm, respectivamente) y las mayores AGR (10,92 y 9,63 cm por año), alcanzando la máxima tasa de crecimiento (MTC) a la edad de 3,9 y 3,7 años, respectivamente. Los clones más precoces fueron RRIM 600 y CDC 312, con MTC de 3,46 y 3,4 años, respectivamente. Estos hallazgos proporcionan información clave sobre la dinámica de crecimiento de clones de caucho y ofrecen una guía valiosa para la gestión y evaluación del rendimiento de plantaciones de caucho en la Orinoquía colombiana.

Palabras clave:
Análisis logit
Plantaciones
Crecimiento de plantas
Caucho

[1]Corporación colombiana de investigación agropecuaria - AGROSAVIA, Centro de investigación La Libertad, Colombia. slcastaneda@agrosavia.co, aamora@agrosavia.co, mtarazona@agrosavia.co, drhernandez@agrosavia.co
*Corresponding author

Received: October 26, 2024; Accepted: March 31, 2025
Rev. Fac. Nac. Agron. Medellín 78(2): 11057-11068. 2025
ISSN 0304-2847 / e-ISSN 2248-7026

CC BY NC SA

Rubber tree [*Hevea brasiliensis* (Willd. ex A.Juss.) Müll.Arg.] is a native species and the largest source of natural rubber worldwide, a raw material used to manufacture tires and other industrial products (Tangonyire 2019). In Colombia, it is one of the 10 species with commercial forest plantations and with the largest established area, exceeding 30,000 hectares in the Orinoquia region (Ministerio de Agricultura y Desarrollo Rural 2023). Of the total planted area, 51.5% corresponds to monoclonal plantations and 42.4% to polyclonal plantations. The remaining 6% corresponds to plantations of unidentified clones or sprouted trees (Correa-Pinilla et al. 2022).

Considering that the genetic base of commercially planted materials in the country consists of fewer than five clones—including RRIM 600 and FX 3864—it is necessary to select clones with higher performance, productivity, and tolerance to the main foliar diseases. To this end, clonal fields were established using *Hevea brasiliensis* genotypes from the breeding program initiated in 1992 by CIRAD-Michelin-Brazil as an alternative for cultivation in suboptimal regions and areas affected by South American leaf bling (SALB) (Rivano et al. 2013).

Mathematical models have been useful in timber forest species to describe development based on stem diameter or height and age, obtaining valuable site index curves in forest management plans. In *H. brasiliensis,* site index equations have been generated for clone IAN 710 plantations in Mexico (Rojo-Martínez et al. 2005), stem diameter growth (before and after tapping), and total and commercial heights have been modeled in plantations in Thailand (Nattharom et al. 2020).

Progress made in rubber trees includes model generation or validation to quantify biomass and carbon sequestration for the RRIM 600 clone in plantations in Tabasco, Mexico (López-Reyes et al. 2016), in Tolima, Colombia (Patiño et al. 2018), and also in agroforestry systems (AFS) with *Theobroma cacao* L. in Huánuco, Peru (Zavala Solórzano et al. 2019). Furthermore, large-scale biomass estimation has been performed in plantations in China (Li et al. 2023).

Among the studies developed in Colombia, the one carried out by Corporación colombiana de investigación agropecuaria (AGROSAVIA) and Centre de Coopération Internationale en Recherche Agronomique pour le Développement (CIRAD) stands out as it established clonal fields in the Department of Meta to evaluate the growth, the reaction to foliar diseases and rubber production of the *Hevea brasiliensis* genotypes of the CIRAD-Michelin Selection "CMS" Collection (Castañeda-Garzón et al. 2024). Moreover, in the Colombian Amazon region, growth has been described in clones CDC 56, CDC 312, GU 198, IAN 873, FX 4098, FX 2899 PI, MDF 180, FDR 4575, FDR 5597, and FDR 5788 in the municipalities of Florencia, Belén de los Andaquíes and San Vicente del Caguán (SINCHI 2019), as well as in plantations in Belén de los Andaquíes (Pardo-Rozo et al. 2021), and AFSs and plantations in Caquetá (Andrade et al. 2022).

On the other hand, the management of forest plantations requires monitoring tree growth, which is influenced by species, genotype, environment, and other factors. Description of the growth patterns of *H. brasiliensis* CMS clones using mathematic models validated from field data allows the identification of the most vigorous genotypes based on the minimum stem circumference to initiate tapping. So far, the growth models of *H. brasiliensis* genotypes in the Colombian Orinoquia region and specifically in the Department of Meta are unknown. For that reason, the study aimed to evaluate four growth models in nine *H. brasiliensis* clones to establish the maximum potential growth value reached by each clone, the time to achieve the maximum absolute growth rate, and the estimated value of the maximum absolute growth rate.

The results will allow the rubber producers in the Orinoquia region to understand the growth of *H. brasiliensis* clones of the CMS collection in their juvenile stage and the agroclimatic conditions of the La Libertad (Villavicencio, Meta) and Taluma (Puerto López, Meta) clonal fields. Tapping can start in some clones at an earlier age before reaching eight years, speeding up the start of latex harvesting and, consequently, generating economic benefits. However, the performance of these clones in the production stage is still being evaluated.

MATERIALS AND METHODS

Study site and plant material

The first study site is the La Libertad small-scale clonal field (SCCF) established in the La Libertad Research

Center of AGROSAVIA (Villavicencio), Vereda La Reforma (4°3'37.43" N, 73°27'52.47" W), at 335 meters above sea level (masl), in the Department of Meta, Colombia. It is located in a typical foothill landscape called Piedemonte Llanero. It was established in October 2013 with a planting distance of 6x3 m under an experimental randomized complete block (RCB) design with four repetitions, nine clones (CDC 312, CDC 56, FDR 4575, FDR 5597, FDR 5788, FX 3864, MDF 180, PMB 1, and RRIM 600) and 20 plants per experimental unit. The area has predominantly flat relief, and the soils have a sandy loam texture with low fertility; they are moderately deep and strongly acidic, have high aluminum content, good drainage, and low saturation (Castañeda-Garzón et al. 2024). The average climatic conditions from 2013 to 2022, registered by the meteorological station C.I. La Libertad, showed an annual precipitation of 2,676 mm, a temperature of 25.92 °C, and a relative humidity of 77.83% (Figure 1).

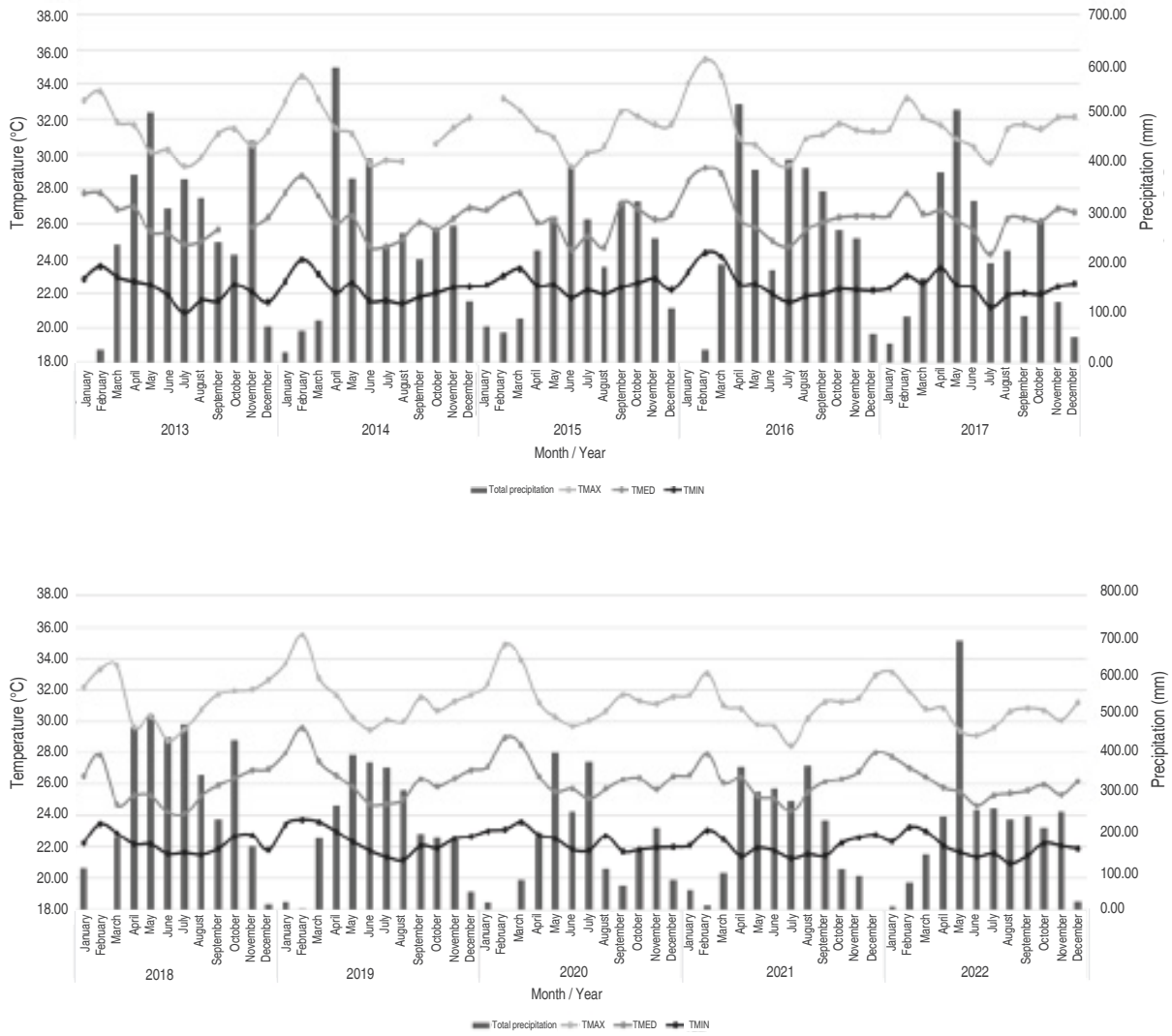

Figure 1. Monthly climate data at the La Libertad small-scale clonal field in Villavicencio, Meta, Colombia, from January 2013 to December 2022. TMAX (average maximum temperature), TMED (average temperature), TMIN (average minimum temperature).

The second study site is the Taluma large-scale clonal field (LSCF) established in the Taluma Experimental Farm of AGROSAVIA (Puerto López), Vereda Carubare (4°22'39.2" N, 72°13' 49.9" W), at 176 masl, in the

Department of Meta, Colombia. It was established in a typical high-plain landscape (Altillanura) in August 2013. The planting distance is 6x3 m under an experimental RCB design, with four repetitions, five clones (CDC 312, FDR 5788, FX 3864, PMB 1, and RRIM 600), and 84 plants per experimental unit. The area has predominantly flat relief, and the soils have a sandy loam-clay texture with low fertility; they are moderately deep and strongly acidic and have high aluminum content, good drainage, and low saturation (Castañeda-Garzón et al. 2024). The average climatic conditions from 2013 to 2022 showed an annual precipitation of 2,806 mm, a temperature of 26.51 °C, and a relative humidity of 80.27% (NASA 2021) (Figure 2).

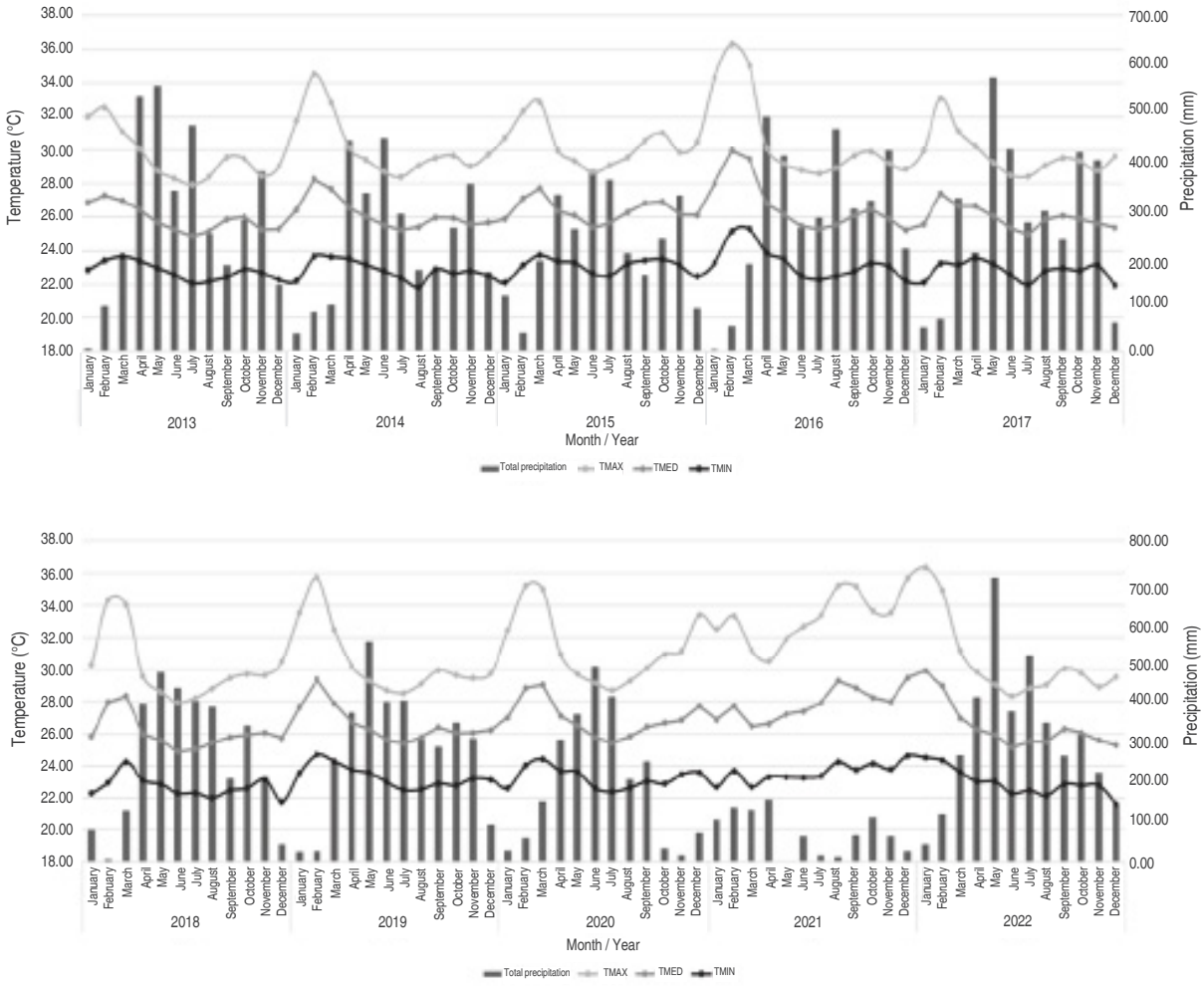

Figure 2. Monthly climate data in the Taluma large-scale clonal field in Puerto López, Meta, Colombia, from January 2013 to December 2022. TMAX (average maximum temperature), TMED (average temperature), TMIN (average minimum temperature).

In these clonal fields, the commercial controls were FX 3864 and RRIM 600, and the genotypes of the CMS Collection were CDC 312, CDC 56, FDR 4575, FDR 5597, FDR 5788, MDF 180, and PMB 1. CIRAD recommended these clones based on the results obtained in clonal fields in Brazil and Ecuador, where they were evaluated for growth, resistance to the South American leaf disease, and latex yield (Rivano et al. 2013). The management practices carried out corresponded to replanting and chemical and mechanical weed control in lanes and decks. At the CCPE La Libertad and the CCGE Taluma, a fertilization plan was used in the third

year with the following proportions: Urea (54%), KCL (27%), and DAP (19%), in a dosage of 370 g per plant. At the CCPE La Libertad, in the fourth and seventh years, the proportions were: Urea (22%), KCL (44%), Amidas® (225), MAP® (8%), and Borozinco® (3%), in a dosage of 800 g per plant. At CCGE Taluma in the fifth year, the proportions were: Urea (40%), KCL (20%), DAP (11%), Sulcamag® (11%), and Borozinco® (2%), in a dosage of 380 g per plant. There was no pruning and phytosanitary control. In both locations from 2013 to 2022, the dry season occurred between December and February-March (Figures 1 and 2).

Variable evaluated

The growth of *H. brasiliensis* clones was evaluated by measuring the stem circumference (CIRC) in 100% of the live trees in each clonal field, 1 masl (Rivano et al. 2013), using a tape measure with a frequency of 6 months for 8 years and before starting to tap. The survival was monitored during the evaluation period, and growth models were evaluated based on the records obtained.

Model evaluation and statistical analysis

Growth curves are mathematical functions that describe a sigmoidal growth pattern and are an important group of non-linear functions that allow describing plant growth in several of their attributes (e.g., total height, biomass, stem or bole thickness, and leaf area, among others), as well as be used as modifiers in simulation models based on physiological processes (Archontoulis and Miguez 2015). In this study, four non-linear growth models (Equations 1, 2, 3, and 4) were adjusted to establish the maximum potential growth value reached by each clone ($CIRC_{max}$, cm), the time to achieve the maximum absolute growth rate (MAGR, years), and the estimated value of the maximum absolute growth rate (MAGRe, cm per year). The structure of the functions is described below.

Logistics model:

$$CIRC = \frac{CIRC_{max}}{1 + e^{-k(age - T.pi)}} \quad (1)$$

Gompertz:

$$CIRC = CIRC * e^{-e^{-k(age - T.pi)}} \quad (2)$$

Chapman-Richards:

$$CIRC = CIRC_{max} * (1 - e^{-k * age})c \quad (3)$$

Beta:

$$CIRC = CIRC_{max}\left[1 + \frac{T_e - age}{T_e - T.pi}\right] * \left[\frac{age}{T_e}\right]^{\frac{T_e}{T_e - T_{.pi}}} \quad (4)$$

Where $CIRC_{max}$ is the maximum stem circumference (CIRC, cm) value reached; k controls the inclination of the curve; $T_{.pi}$ is the time at which the tree reaches its maximum growth rate (MGR, years); and T_e is the year when the tree reached the maximum CIRC value.

Each model was fitted using the maximum likelihood method (Pinheiro and Bates 2000), and they were compared according to the following goodness-of-fit measures: a) coefficient of determination adjusted according to the number of parameters of each model, b) the Akaike information criterion (AIC) and the standard error of the residuals; when the latter two show lower values, the model is classified as having the best fit. Based on the best growth model, this model was adjusted to each tree and per clone to compare the performance of the clones according to the parameters related to $CIRC_{max}$, $T_{.pi}$, and T_e. Only trees with complete CIRC records during the evaluation years were used to ensure the convergence of the models fitted for each tree within each clone. The model parameters were compared between clones through an analysis of variance, and in those cases where significant differences were found at 5%, a minimum significant difference test was applied. All statistical analyses were carried out with the R software [free software] (R Core Team 2023) and the "nlraa" library.

RESULTS AND DISCUSSION

In La Libertad SCCF and Taluma LSCF, the growth model based on the CIRC with the best fit corresponded to the logistic function, in which the AIC value is lower (Tables 1 and 2). Rojo-Martínez et al. (2005) indicate that depending on tree age, allometric variables, such as standard diameter, height, or volume, follow a pattern that can be represented by a logistic curve, which, in turn, is described by an equation. In forest management, growth models are developed to estimate future production and

growth under conditions where data do not exist (Rojo-Martínez et al. 2005). In this case, the generated models are useful for describing the growth of rubber clones of the CMS collection in conditions of the Piedemonte Llanero and Altillanura landscapes in Orinoquia, localities in which field data are not yet available.

Table 1. Fitted models and goodness-of-fit measures to describe the growth curve of *H. brasiliensis* clones evaluated in the La Libertad small-scale clone field (Villavicencio, Meta, Colombia).

Fitted model	Adjusted R^2	AIC	σ_e
Logistic	0.727	35036.24	9.641
Gompertz	0.726	35037.73	9.643
Chapman-Richards	0.727	35045.86	9.651
Beta	0.727	35038.08	9.643

R^2: Adjusted coefficient of determination; AIC: Akaike Information Criterion; σ_e: Standard error of residuals.

Table 2. Fitted models and goodness-of-fit measures to describe the growth curve of *H. brasiliensis* clones established in the Taluma large-scale clone field (Puerto López, Meta, Colombia).

Fitted model	Adjusted R^2	AIC	σ_e
Logistic	0.846	63045.91	6.227
Gompertz	0.843	63142.78	6.259
Chapman-Richards	0.847	63059.35	6.232
Beta	0.847	63053.32	6.23

R^2: Adjusted coefficient of determination; AIC: Akaike Information Criterion; σ_e: Standard error of residuals.

Based on the above, the growth curve of the *H. brasiliensis* clones evaluated was adjusted with the logistic function. In the La Libertad SCCF during the evaluation period (8 years), clone FDR 5788 presented the highest growth in CIRC (69.89 cm), followed by clones FX 3864 (64.05 cm), RRIM 600 (63.77 cm), CDC 312 (63.14 cm), PMB 1 (61.34 cm), CDC 56 (59.11 cm), FDR 4575 (54.52 cm), MDF 180 (52.65 cm), and FDR 5597 (42.91 cm) (Figure 3). This contrasts with what was observed in Belén de los Andaquíes (Caquetá) by Sterling et al. (2019) with the following values: FDR 5788 (44.04 cm), FDR 5597 (42.75 cm), CDC 56 (38.21 cm), FDR 4575 (36.97 cm), MDF 180 (36.30 cm), and CDC 312 (36.16 cm).

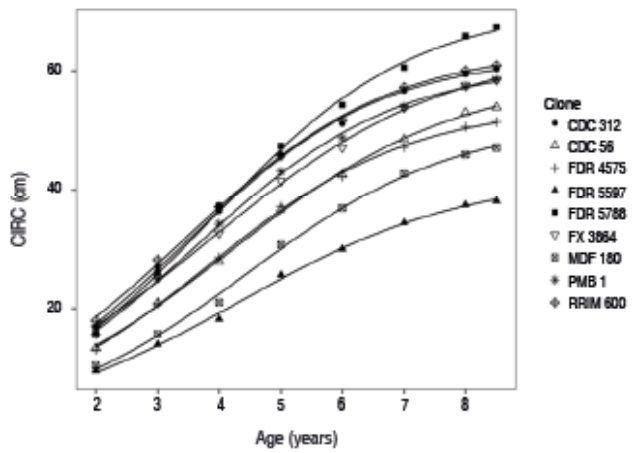

Figure 3. Fitting of the growth curve with the logistic function of the clones of *H. brasiliensis* evaluated in the La Libertad small-scale clone field (Villavicencio, Meta, Colombia). CIRC (cm): circumference.

By comparing the parameters of the growth curve and the AGR of clones in the La Libertad SCCF, the FDR 5788 clone presented higher CIRC (69.89 cm) and AGR (10.92 cm per year), reaching the MGR at the age of 3.9 years (Table 3). The earliest clone was RRIM 600 (MGR 3.46 years) and ranked third in $CIRC_{max}$ (63.77 cm) and AGR (9.65 cm per year). Clones MDF 180 and FDR 5597 showed the lowest performance in $CIRC_{max}$, MGR, and AGR and the lowest survival (76.25 and 57.5%, respectively). Statistical differences were evident between the clones, and survival ranged between 57.5 and 85% (FDR 5788).

Table 3. Comparison of the growth curve and the absolute growth rate parameters for the La Libertad small-scale clone field (Villavicencio, Meta, Colombia). Age: 8 years.

Clone	$CIRC_{max}$ (cm)	MGR (years)	AGR (cm per year)
FDR 5788	69.89±12.11^{a}	3.9±0.16^{bcd}	10.92±1.86^{a}
FX 3864	64.05±5.93^{ab}	3.89±0.23^{bcd}	8.51±1.08^{bcd}
RRIM 600	63.77±7.22^{ab}	3.46±0.15^{a}	9.65±1.07^{abc}
CDC 312	63.14±7.74^{ab}	3.6±0.6^{ab}	9.89±1.7^{ab}
PMB 1	61.34± 6.96^{bc}	3.64±0.23^{ab}	9.5±1.03^{bc}
CDC 56	59.11±11.02^{bcd}	4.11±0.63^{cd}	8.29±1.59^{cd}
FDR 4575	54.52±5.11^{cd}	3.83±0.16^{abc}	8.29±1.25^{cd}
MDF 180	52.65±11.12^{d}	4.58±0.69^{e}	7.66±1.88^{d}
FDR 5597	42.91±4.8^{e}	4.31±0.44^{de}	5.86±0.84^{e}

$CIRC_{max}$: Maximum circumference value reached; MGR: Time at which the maximum growth rate is achieved; AGR: Absolute growth rate based on the logistic model. Values with the same letter in each column are statistically similar at 5% significance.

On the other hand, in the Taluma LSCF during the 8 years of evaluation, clones PMB 1 (57.47 cm) and FDR 5788 (56.12 cm) registered higher growth, surpassing in $CIRC_{max}$, the values recorded for clones FX 3864 (51.91 cm), CDC 312 (49.18 cm), and RRIM 600 (45.60 cm) (Figure 4). These values exceed those observed at the age of 8 years in an LSCF in Caquetá for FDR 5788 (44.04 cm) and CDC 312 (36.16 cm) (Sterling et al. 2019), as well as for FDR 5788 in a large-scale clonal field in San Vicente del Caguán, Belén of the Andaquíes and Florencia (Caquetá) at the age of 10 years (51, 48, and 50 cm, respectively) (SINCHI 2020a).

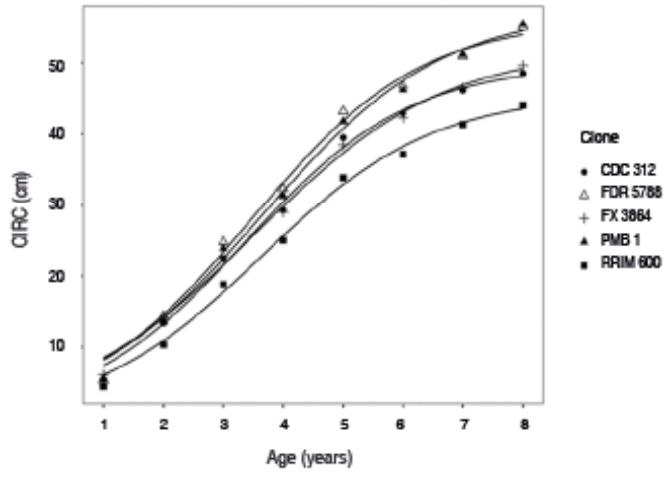

Figure 4. Fitting of the growth curve with the logistic function of the *H. brasiliensis* clones evaluated in the Taluma large-scale clone field (Puerto López, Meta, Colombia). CIRC (cm): circumference.

In the Taluma LSCF, the PMB 1 clone had a higher $CIRC_{max}$ (57.47 cm) and AGR (9.63 cm per year), reaching the maximum growth rate at the age of 3.7 years (Table 4). The earliest clone was CDC 312 (MGR 3.40 years), which ranked fourth with respect to $CIRC_{max}$ (49.78 cm) and presented a higher AGR (9.11 cm per year) compared to the commercial controls. Statistical differences between clones were evident. Survival in this locality ranged between 91.07% (RRIM 600) and 92.86% (PMB 1).

Table 4. Comparison of the growth curve and the absolute growth rate parameters for the Taluma large-scale clonal field (Puerto López, Meta, Colombia). Age: 8 years.

Clone	$CIRC_{max}$ (cm)	MGR (years)	AGR (cm per year)
PMB 1	57.47±4.80[a]	3.7±0.24[a]	9.63±1.15[a]
FDR 5788	56.12±5.28[a]	3.5±0.23[a]	9.95±1.05[a]
FX 3864	51.92±5.17[b]	3.5±0.28[b]	8.34±0.93[c]
CDC 312	49.78±5.29[c]	3.4±0.27[b]	9.11±1.18[b]
RRIM 600	45.60±3.63[d]	3.6±0.24[c]	8.01±0.74[d]

$CIRC_{max}$: Maximum CIRC value reached; MGR: Age at which the maximum growth rate is reached; AGR: Absolute growth rate based on the logistic model. Values with the same letter in each column are statistically similar at 5% significance.

Under the conditions of the Piedemonte Llanero and Altillanura regions of Colombia, the clones FDR 5597 (La Libertad SCCF), CDC 312 and RRIM 600 (Taluma LSCF) did not reach the maximum CIRC of 50 cm at the age of 8 years (Tables 3 and 4), reference value to open the tapping panel, evidencing a possible effect of the edaphoclimatic conditions of the localities. Similar behavior was observed in the LSCF San Vicente del Caguán (Caquetá), in which the clones FX 3899 P1, FDR 4575, FDR 5578, GU 198 and FDR 5597 presented an acceptable average CIRC value (>52 cm) at the end of the pre-tapping stage and an acceptable CIRC (<58 cm) in the first year of tapping (year 10) (Sterling et al. 2020). This corroborates what was stated by other authors, regarding that rubber trees need a considerable period (years) to start latex harvesting and reach 50 cm of CIRC at 120 cm above the graft union to open the tapping panel (Nadeeshani et al. 2021).

However, when reviewing the age at which the maximum growth rate (MGR) was reached in the La Libertad SCCF, the CMS clones with the highest precocity were RRIM 600, CDC 312, PMB 1, and FDR 4575 (Table 3). For the Piedemonte Llanero area, these values are a useful reference for rubber plantations with genotypes different from commercial clones. In the Taluma LSCF, the CDC 312 genotype was the earliest, although only by a minimal difference compared to the other clones (Table 4). In this locality, the size of the plot allows observing the behavior of the genotypes on a semi-commercial scale; therefore, these values are valuable for the Altillanura region since in Puerto López, the largest extensions of commercial rubber plantations in the Department of Meta are found. Regarding precocity in growth, it is important to remember that in rubber, a rapid increase in height and vigor means a reduction of the immaturity period, allowing the opening of the panel at younger ages of the plantation (Sterling et al. 2012).

In the two clonal fields, AGR values higher than 9 cm per year were obtained in FDR 5788, CDC 312, RRIM 600, and PMB 1 in the La Libertad SCCF, in contrast to the Taluma LSCF in which clones FDR 5788, PMB 1 and CDC 312 stood out (Tables 3 and 4). In LSCF in Ecuador, clones MDF 180, CDC 56, CDC 312, and FDR 5788, at the age of 4 years, presented a CIRC $\geq$40 cm and an average increase of 10 cm per year (Rivano et al. 2013), surpassing what was observed at that age in the La Libertad and Taluma clonal fields (Figures 3 and 4). In FDR 5597, lower growth was evident in the La Libertad SCCF (Table 3 and Figure 3), with behavior similar to that reported for Brazil and Ecuador. Therefore, as Rivano et al. (2013) stated, "This clone is not recommended for commercial plantations because its production begins two years after any commercial clone." The *H. brasiliensis* clones from the CMS collection with the greatest vigor, based on the minimum trunk circumference for opening a tapping panel

at an age under seven years, were FDR 5788, CDC 312, and PMB 1 in the La Libertad LSCF, and PMB 1 and FDR 5788 in the Taluma LCCF (Castañeda-Garzón et al. 2024).

When comparing the parameters of the growth curve and the AGR of the clones of *H. brasiliensis*, higher $CIRC_{max}$, and AGR were observed for the genotypes in the La Libertad SCCF, while MGR varied in the localities. The differential growth in the genotypes can be attributed to the edaphoclimatic conditions and agronomic management during the juvenile stage of the rubber trees (Castañeda-Garzón et al. 2024). According to some authors, climatic conditions play a vital role in the physiology and growth of rubber trees (Nadeeshani et al. 2021). According to Rojo-Martínez et al. (2005), growth results from a "very complex biological process that interweaves heredity, environmental factors, and cultivation practices."

In traditional rubber-growing areas of Colombia, such as the Amazon, progress has been made in the evaluation of promising materials, thus expanding the genetic base of *H. brasiliensis* (Sterling et al. 2020), with vigorous clones with productive potential, adaptive capacity, and tolerance to pests and diseases (SINCHI 2020b). Likewise, the idea of converting the traditional monoculture model into an AFS that includes promising native fruit or timber species has also been adopted (Sterling et al. 2015). Hence, the growth of *H. brasiliensis* has been evaluated in monoclonal plantations (age: 4 to 5 years) associated with the promising fruit tree copoazú (*Theobroma grandiflorum* (Willd. ex Spreng.) Schum.) materials, in which average CIRC values of 43.46 cm (FX 3864) and 4.50 cm (FX 4098) were recorded (SINCHI 2015), surpassing what was registered for FX 3864 in the La Libertad and Taluma clonal fields at the age of 5 years (41.5 and 38.51 cm, respectively).

In San Vicente del Caguán (Caquetá) after the second year of establishment, the highest CIRC averages in rubber were obtained when cultivated in an AFS associated with *T. grandiflorum*, Hartón plantain (Musa AAB) and the FX 4098 clone (Sterling et al. 2015). In this regard, Snoeck et al. (2013) affirm that the association of crops with *H. brasiliensis* can favor its growth compared to monoculture, optimizing land use and generating higher income for producers. Moreover, it improves the physical characteristics of soils in terms of depth and penetrability (Rosas et al. 2015), acts as a barrier against strong winds protecting rubber trees, increases production, and optimizes the cultivation system and productivity (Qi et al. 2021). Therefore, in sustainable agroecosystem management and climate change mitigation contexts, using some *H. brasiliensis* clones of the CMS collection in AFSs would be an attractive short-term possibility to contemplate in Orinoquia.

Usually, the growth of *H. brasiliensis* had been described in terms of the CIRC reached at a specific age (Rivano et al. 2013; Sterling et al. 2020; Sterling et al. 2015), and thus, identifying in this way the most vigorous and promising clones in each region. In this study, the description was not only obtained for clonal fields from two landscapes in the Orinoquia region (Piedmonte and Altillanura), but it was also complemented with growth curve parameters (CIRCmax, MGR, and AGR), which allow identifying the age at which maximum growth is reached and the absolute growth rate. These variables provide additional information for selecting promising clones in each landscape or associating them with other production systems. Likewise, it allows producers to glimpse the agronomic management period before latex harvesting.

Future studies should include the climate variability and the long period required to evaluate the growth of *H. brasiliensis* trees to obtain further field data and generate mathematical models that more accurately describe their development during the juvenile and early stages of tapping. Likewise, the fluctuating availability of financial resources for optimal agronomic management is a challenge; despite this, clones have demonstrated their growth potential in the study locations. Possible sources of error include staff turnover in conducting the assessments; however, compliance with the measurement methodology was verified.

CONCLUSION

The logistic model was the one that best expressed the growth in the juvenile and pre-tapping stage of the *Hevea brasiliensis* clones in the La Libertad and Taluma clonal fields located in the municipalities of Villavicencio and Puerto López (Meta). The statistical robustness of the model allows for the prediction, with acceptable precision, of the growth of CMS clones in edaphoclimatic conditions similar to those that occurred in the localities evaluated during the first 8 years of genotype development. Significant

differences were found in $CIRC_{max}$, MGR, and AGR, adjusted according to the logistic model, which reveals the effect of the genotype on growth and the influence of the environments in which the clones were evaluated.

In the La Libertad SCCF, a higher CIR_{max} and AGR were recorded in the *H. brasiliensis* clones evaluated, while MGR presented less variation in the Taluma LSCF (3.4 to 3.7 years). With respect to the CIRC in the La Libertad SCCF, clone FDR 5788 (69.89 cm) stood out, and in the Taluma LSCF, clone PMB 1 (57.47 cm) was highlighted. Likewise, for AGR, this was evidenced in clone FDR 5788 with values of 10.92 and 9.95 cm per year (La Libertad SCCF and Taluma LSCF, respectively). These differences highlight the importance of considering local conditions when comparing and evaluating the growth of clones of *H. brasiliensis* from the CMS collection to carry out management according to its development.

ACKNOWLEDGMENTS

This publication is derived from the results and information obtained within the project "Evaluation of the behavior of rubber clones in the early productive stage, in four rubber regions of Colombia," executed by Corporación colombiana de investigación agropecuaria (AGROSAVIA) and Centre de Coopération Internationale en Recherche Agronomique pour Le Développement (CIRAD) within the scope of the Corporate Dynamic Agenda, financed with public resources through the Ministry of Agriculture and Rural Development of Colombia. Many thanks to the CIRAD-Michelin consortium for providing the CMS clones for evaluation in Colombia. To Franck Rivano from CIRAD for his technical support and to Ferney López, Hernán Camacho, and Oscar Triana for their support in data collection in the field.

DATA AVAILABILITY

The data used in this research is available upon reasonable request through the following email: reservasinfo@agrosavia.co

CONFLICT OF INTERESTS

The authors declare that it is an original work and that there is no conflict of interest of any kind in the preparation and publication of the manuscript.

REFERENCES

Andrade H, Orjuela J and Hernández C (2022) Modelos de biomasa aérea y subterránea de *Hevea brasiliensis* y *Theobroma grandiflorum* en la Amazonía colombiana. Colombia forestal 25(2): 57-69. https://doi.org/10.14483/2256201X.18464

Archontoulis S and Miguez F (2015) Nonlinear Regression Models and Applications in Agricultural Research. Agronomy Journal 107(2): 786-798. https://doi.org/10.2134/agronj2012.0506

Castañeda-Garzón S, Rivano F and Mora Garcés A (2024) Crecimiento de clones de *Hevea brasiliensis* (Willd. Ex A.Juss.) Müll. Arg. en etapa juvenil establecidos en campos clonales, Meta, Colombia. Temas Agrarios 29(1): 53-65. https://doi.org/10.21897/5099hh92

Correa-Pinilla D, Gutiérrez-Vanegas A, Gil-Restrepo J, Martínez-Atencia J and Córdoba-Gaona O (2022) Agroecological and South American leaf blight escape zones for rubber cultivation in Colombia. Agronomy Journal 114(5): 2830-2844. https://doi.org/10.1002/agj2.21068

Li X, Wang X, Gao Y, Wu J, Cheng R et al (2023) Comparison of different important predictors and models for estimating large-scale Biomass of rubber plantations in Hainan Island, China. Remote Sensing 15(13): Art. 13. https://doi.org/10.3390/rs15133447

López-Reyes L, Domínguez-Domínguez M, Martínez-Zurimendi P, Zavala-Cruz J et al (2016) Carbono almacenado en la biomasa aérea de plantaciones de hule (*Hevea brasiliensis* Müell. Arg.) de diferentes edades. Madera y Bosques 22(3): 49-60. https://doi.org/10.21829/myb.2016.2231456

Ministerio de Agricultura y Desarrollo Rural (2023) 7° Boletín estadístico forestal Marzo 2023. https://fedemaderas.org.co/boletin-forestal-2023/

Nadeeshani A, Palihakkara I and Kudaligama K (2021) Assessing growth and physiological parameters of young *Hevea brasiliensis* to identify adaptable clones for WL1a agroecological region in Sri Lanka. Journal of Food and Agriculture 14(2): Art. 2. https://doi.org/10.4038/jfa.v14i2.5261

NASA - The National Aeronautics and Space Administration (2021) NASA POWER Prediction of worldwide energy resources. https://power.larc.nasa.gov/

Nattharom N, Roongtawanreongsri S and Bumrungsri S (2020) Growth prediction for rubber tree and intercropped forest trees to facilitate environmental services valuation in South Thailand. Biodiversitas Journal of Biological Diversity 21(5): Art. 5. https://doi.org/10.13057/biodiv/d210528

Pardo-Rozo Y, Andrade-Castañeda H, Muñoz-Ramos J and Velásquez-Restrepo J (2021) Carbon capture in three land use systems in the Colombian Amazonia. Revista de Ciencias Agrícolas 38(2): 111-123. https://doi.org/10.22267/rcia.213802.160

Patiño S, Suárez L, Andrade H and Segura M (2018) Captura de carbono en biomasa en plantaciones forestales y sistemas agroforestales en Armero-Guayabal, Tolima, Colombia. Revista de Investigación Agraria y Ambiental 9(2): Art. 2. https://hemeroteca.unad.edu.co/index.php/riaa/article/view/2312

Pinheiro J and Bates D (2000) Mixed-Effects Models in S and S-PLUS (First edition). Springer. https://link.springer.com/book/10.1007/b98882

Qi D, Wu Z, Yang C, Xie G, Li Z, Yang X and Li D (2021) Can

intercropping with native trees enhance structural stability in young rubber (*Hevea brasiliensis*) agroforestry system. European Journal of Agronomy 130: 126353. https://doi.org/10.1016/j.eja.2021.126353

R Core Team (2023) R: A Language and Environment for Statistical Computing. R: The R Project for Statistical Computing. https://www.r-project.org/

Rivano F, Mattos C, Cardoso S, Martinez M, Cevallos V et al (2013) Breeding *Hevea brasiliensis* for yield, growth and SALB resistance for high disease environments. Industrial Crops and Products 44: 659-670. https://doi.org/10.1016/j.indcrop.2012.09.005

Rojo-Martínez G, Jasso-Mata J, Zazueta-Angulo X et al (2005) Modelos de índice de sitio para *Hevea brasiliensis* Müll. Arg. del clon IAN710 en el norte de Chiapas. Ra Ximhai 1(1): 153-166. https://doi.org/10.35197/rx.01.01.2005.10.GR

Rosas G, Ramos J and Suárez J (2015) Incidencia de sistemas agroforestales con *Hevea brasiliensis* (Willd. Ex A.Juss.) Müll.Arg. sobre propiedades físicas de suelos de lomerío en el departamento de Caquetá, Colombia. Acta Agronómica 65: 122. http://www.scielo.org.co/pdf/acag/v65n2/v65n2a02.pdf

SINCHI - Instituto Amazónico de Investigaciones Científicas (2015) Evaluación inicial del asocio caucho – copoazú en el Caquetá: Una alternativa de enriquecimiento agroforestal con potencial para la Amazonia colombiana (A. Sterling Cuéllar, C. H. Rodríguez León, & L. M. Melgarejo-Muñoz, Eds.). Instituto Amazónico de Investigaciones Científicas - SINCHI. Bogotá. 231p. https://sinchi.org.co/files/publicaciones/novedades%20editoriales/pdf/Agrosilvícola%20Final_baja.pdf

SINCHI - Instituto Amazónico de Investigaciones Científicas (2019) Valoración y análisis de la biodiversidad y servicios ecosistémicos asociados a campos clonales de caucho en Caquetá, Amazonia Colombiana (A. Sterling Cuéllar & C. H. Rodríguez León, Eds.). Instituto Amazónico de Investigaciones Científicas - SINCHI. Bogotá. 154p. https://sinchi.org.co/index.php/valoracion-y-analisis-de-la-biodiversidad-y-servicios-ecosistemicos-asociados-a-campos-clonales-de-caucho-en-caqueta-amazonia-colombiana

SINCHI - Instituto Amazónico de Investigaciones Científicas (2020a) Valoración de nuevos clones de *Hevea brasiliensis* con proyección para la Amazonia colombiana: Fases de pre y post-sangría temprana en el Caquetá (A. Sterling Cuéllar & C. H. Rodríguez León, Eds.). Instituto Amazónico de Investigaciones Científicas SINCHI. Bogotá. 322p. https://sinchi.org.co/files/publicaciones/novedades%20editoriales/pdf/Valoracion%20Nuevos%20Clones.pdf

SINCHI - Instituto Amazónico de Investigaciones Científicas (2020b) Valoración inicial del potencial productivo de *Hevea brasiliensis* en la Amazonia colombiana mediante la evaluación de nuevos clones promisorios para la región (A. Sterling Cuéllar & Rodríguez León, Eds.). Bogotá. 108p. https://sinchi.org.co/valoracion-inicial-del-potencial-productivo-de-hevea-brasiliensis-en-la-amazonia-colombiana-mediante-la-evaluacion-de-nuevos-clones-promisorios-para-la-region

Snoeck D, Lacote R, Kéli J, Doumbia A et al (2013) Association of hevea with other tree crops can be more profitable than hevea monocrop during first 12 years. Industrial Crops and Products 43: 578-586. https://doi.org/10.1016/j.indcrop.2012.07.053

Sterling A, Martinez E, Pimentel G, Suarez Y, Fonseca-Restrepo J and Diaz Y (2019) Dynamics of adaptive responses in growth and resistance of rubber tree clones under South American leaf blight non-escape conditions in the Colombian Amazon. Industrial Crops and Products 141: 111811. https://doi.org/10.1016/j.indcrop.2019.111811

Sterling A, Martínez-Viuche E, Suárez-Córdoba Y, Agudelo-Sánchez A, Fonseca-Restrepo J et al (2020) Assessing growth, early yielding and resistance in rubber tree clones under low South American Leaf Blight pressure in the Amazon region, Colombia. Industrial Crops and Products 158: 112958. https://doi.org/10.1016/j.indcrop.2020.112958

Sterling A, Rodríguez C, Dussán I, Castillo J, Ruiz P and Jara L (2012) Desempeño de diez clones de caucho natural en campo clonal a gran escala en condiciones de la Amazonía Colombiana. Revista Colombia Amazónica 5: 161-175. https://www.sinchi.org.co/files/publicaciones/revista/pdf/5/9%20desempen%CC%83o%20de%20diez%20clones%20de%20caucho%20natural%20en%20campo%20clonal%20a%20gran%20escala%20en%20condiciones%20de%20la%20amazonia%20colombiana.pdf

Sterling A, Suárez J, Rodrídguez D, Rodríguez C, Salas-Tobón Y and Virgüez-Díaz Y (2015) Crecimiento inicial de clones promisorios de *Hevea brasiliensis* (Willd. Ex A. Juss.) Müll. Arg. en sistema agroforestal en Caquetá, Colombia. Colombia Forestal 18(2): Art. 2. https://doi.org/10.14483/udistrital.jour.colomb.for.2015.2.a01

Tangonyire D (2019) Assessing the growth performance of two different *Hevea brasiliensis* clones (IRCA 41 and GT 1) in the Guinea savanna soil in the northern region of Ghana. Malaysian Journal of Sustainable Agriculture 3(2): 46-55. https://doi.org/10.26480/mjsa.02.2019.46.55

Zavala Solórzano J, Mansilla L, Zavala S and Merino É (2019) Mitigación del cambio climático a través del secuestro y almacenamiento del carbono y evaluación de los servicios ambientales del SAF caucho o jebe (*Hevea brasiliensis*) y cacao (*Theobroma cacao* L.) en Tingo María. Anales Científicos 80(2): 462-475. https://revistas.lamolina.edu.pe/index.php/acu/article/view/1478

Research article

https://revistas.unal.edu.co/index.php/refame

Revista Facultad Nacional de Agronomía

Gibberellic acid and warm incubation temperatures as germination stimulants in yellow kiwifruit seeds (*Actinidia chinensis* var. chinensis)

Ácido giberélico y temperaturas cálidas de incubación como estimulantes de la germinación en semillas de kiwi amarillo (*Actinidia chinensis* var. chinensis)

https://doi.org/10.15446/rfnam.v78n2.115017

Jhusua David Reina-García[1,3]*, Juan Guillermo Cruz-Castillo[2], Gustavo Almaguer-Vargas[3], Diana Guerra-Ramírez[4] and Álvaro Castañeda-Vildozola[5]

ABSTRACT

The kiwifruit (*Actinidia chinensis* var. chinensis) is a deciduous fruit tree belonging to the *Actinidiaceae* family. Its industry in Mexico is still incipient, making it necessary to introduce new cultivars with diverse pulp colors and flavors. To achieve this, a population of seed-derived plants was used; however, these exhibited dormancy and low germination rates. This study aimed to evaluate pre-germination treatments to improve seed germination capacity. A completely randomized design with a factorial arrangement was applied, evaluating five concentrations of gibberellic acid (GA_3) [0, 1,000, 2,000, 4,000, and 6,000 ppm] in combination with three constant temperature levels (25, 30, and 35 °C) for 68 days. Prior to treatment application, seeds were stratified at 4 °C for 31 days and then immersed for 24 hours in their respective GA_3 solutions and water. Each experimental unit consisted of 50 seeds, with three replications. The variables evaluated included germination percentage (GP), mean germination rate (MGR), mean germination time (MGT), and days to dormancy release (DL), using ANOVA and Tukey's test ($P \leq 0.05$). Significant differences were found for all variables except MGT. The best results were obtained at 25 °C with any GA_3 concentration, where dormancy period was shortened (2.63 days), and both GP (6.35%) and MGR (0.5 seeds/day) increased. Constant temperatures above 30 °C negatively affected these variables.

Keywords:
Deciduous
Latency
Stimulation
Temperature

RESUMEN

El kiwi (*Actinidia chinensis* var. chinensis) es un frutal caducifolio de la familia *Actinidiaceae* cuya industria en México aún es incipiente, por lo que se requiere la introducción de nuevos cultivares con pulpas de distintos colores y sabores. Para ello, se utilizó una población de plantas obtenidas por semilla, las cuales presentaron latencia y bajo porcentaje de germinación. El objetivo de este estudio fue evaluar tratamientos pre-germinativos para mejorar su capacidad germinativa. Se aplicó un diseño completamente al azar con un arreglo factorial, evaluando cinco concentraciones de ácido giberélico (GA_3) [0, 1.000, 2.000, 4.000 y 6.000 ppm], combinadas con tres niveles de temperatura constante (25, 30 y 35 °C) por 68 días. Previo a la aplicación de los tratamientos, las semillas fueron estratificadas a 4 °C durante 31 días y posteriormente sumergidas por 24 horas en las respectivas soluciones de GA_3 y agua. Cada unidad experimental estuvo compuesta por 50 semillas, con tres repeticiones. Se evaluaron las variables: porcentaje de germinación (PG), velocidad media de germinación (VMG), tiempo medio de germinación (TMG) y días a latencia (DL), utilizando ANOVA y prueba de Tukey ($P \leq 0,05$). Se encontraron diferencias significativas en todas las variables, excepto en TMG. Las mejores respuestas se obtuvieron a 25 °C con cualquier concentración de GA_3, donde se redujo el tiempo de latencia (2,63 días) y se incrementaron el PG (6,35 %) y la VMG (0,5 semillas/día). Temperaturas superiores a 30 °C afectaron negativamente estas variables.

Palabras clave:
Caducifolio
Latencia
Estimulación
Temperatura

[1]Programa de Ingeniería Agronómica, Facultad de Ciencias Agropecuarias y Recursos Naturales, Universidad de los Llanos. Meta-Colombia. jhosuadavid11@hotmail.com
[2]Centro Académico Regional Oriente, Universidad Autónoma Chapingo, Huatusco, Veracruz, México. jcruzc@chapingo.mx
[3]Departamento de Fitotecnia, Universidad Autónoma Chapingo, Chapingo, Estado de México, México. galmaguerv@chapingo.mx
[4]Departamento de Preparatoria Agrícola, Universidad Autónoma Chapingo, Chapingo, Estado de México, México. dguerrar@chapingo.mx
[5]Facultad de Ciencias Agrícolas, Universidad Autónoma del Estado de México, Campus "El Cerrillo", Piedras Blancas, Toluca, Estado de México, México. acastanedav@uaemex.mx
*Corresponding author

Received: January 30, 2025; Accepted: March 28, 2025
Rev. Fac. Nac. Agron. Medellín 78(2): 11069-11076. 2025
ISSN 0304-2847 / e-ISSN 2248-7026

CC BY NC SA

The kiwifruit (*Actinidia chinensis* var. chinensis), belonging to the *Actinidiaceae* family, is a deciduous climbing plant of the genus *Actinidia* (Windauer et al. 2016). In Mexico, the kiwifruit industry is still emerging, making it necessary to introduce new cultivars with different pulp colors and flavors to expand the domestic market supply (Maghdouri et al. 2021). Conventional or commercial kiwifruit propagation is typically carried out by cutting and/or grafting, using rootstocks obtained from seed-propagated plants. However, the presence of dormant embryos poses a challenge, as it increases seed population losses and complicates seedling uniformity (Maghdouri et al. 2021).

It is understood that seed dormancy is the inability of viable and intact seeds to complete germination, even under favorable environmental conditions (Gao and Ayele 2014). This physiological mechanism functions as an adaptive strategy in many plant species, allowing them to regulate the timing of germination to maximize seedling establishment success (Sekhukhune et al. 2018b). However, in agricultural contexts, dormancy represents a significant limitation for the uniform propagation of crops, which has prompted the evaluation of various techniques aimed at overcoming it (Escobar et al. 2015).

Among the most used methods is cold stratification, which involves exposing seeds to low temperatures (typically between 4 and 6 °C) for a set period. This treatment simulates winter conditions that many seeds require to activate their metabolic processes and break dormancy (Castillo et al. 2013; Sekhukhune et al. 2018b; Zhang et al. 2018).

Likewise, the use of plant growth regulators, such as gibberellic acids (GAs), has proven highly effective in overcoming dormancy. These phytohormones, belonging to the diterpenoid group, are involved in key processes of plant growth and development, including germination activation (Yamaguchi 2008).

Although more than a hundred gibberellins have been identified, only a few possess biological activity, with GA_1, GA_3, GA_4, and GA_7 being the most relevant. The exogenous application of GA_3 has been widely used, as it stimulates the expression of genes and enzymes associated with reserve mobilization, facilitating radicle emergence and seedling development (Yamaguchi 2008). In kiwifruit seeds, dormancy-breaking treatments have primarily involved the use of GA_3 at various concentrations, applied through 24-hour seed immersion prior to incubation (Sekhukhune et al. 2018a).

Bishwas et al. (2018) evaluated the germination response of three kiwifruit varieties (*Abbot*, *Allison*, and *Bruno*) pretreated with GA_3 concentrations of 2,000, 4,000, and 6,000 ppm. The results showed a significantly higher germination percentage in the *Bruno* variety (68.67%), followed by *Allison* (47.33%) at 6,000 ppm. *Bruno* also recorded the fastest average germination rate (0.059 seeds per day) with an average germination time of 17 days.

In another study, seeds of *A. arguta* and *A. chinensis* were stratified at 4 °C for 28 and 42 days, followed by treatments with GA_3 at concentrations of 500, 1,000, 1,500, 2,000, and 2,500 ppm (Sekhukhune et al. 2018b). Seeds stratified for 28 days showed germination percentages of only 8% in *A. arguta* and 20% in *A. chinensis.* However, the combination of cold stratification (28 days) followed by GA_3 treatments at 1,435 and 1,610 ppm resulted in optimal germination of 88% in *A. arguta*, with an average germination time of 23 days. In *A. chinensis*, optimal germination (80%) was achieved with GA_3 concentrations of 1,565 and 2,050 ppm, reducing the average germination time to 25 days (Kumar et al. 2020).

Based on this background, this study aimed to determine the most effective pre-germination treatment for stimulating germination in kiwifruit seeds (*Actinidia chinensis* var. chinensis) collected from Huatusco, Veracruz. Five different concentrations of gibberellic acid (GA_3) [0, 1,000, 2,000, 4,000, and 6,000 ppm], were evaluated in combination with three constant temperature levels (25, 30, and 35 °C) for 68 days. Prior to treatment application, all seeds were subjected to stratification at 4 °C for 31 days, followed by a 24-hour immersion in their respective GA_3 solutions and in water.

MATERIALS AND METHODS

Study area

The study was conducted in the seed laboratory of the Department of Phytotechnology at the Universidad Autónoma Chapingo, Mexico, located at 19°51' N latitude and 98°88' W longitude, at an altitude of 2,377 meters

above sea level (masl). The experimental activities were carried out during the winter period of 2022-2023 under controlled conditions that ensured the stability of environmental variables throughout the development of the research.

Seed Acquisition

Kiwifruit seeds (*Actinidia chinensis* var. chinensis) were used, obtained from ripe, yellow-fleshed fruits collected in the community of Elotepec, municipality of Huatusco, state of Veracruz, Mexico. This location is situated at an altitude of 1,851 masl, with geographical coordinates of 19°11'21" N latitude and 97°01'59" W longitude. The fruits were collected during the autumn of 2022, selecting those with an average weight of 70 to 90 g, free of physical damage and signs of disease, to ensure the quality of the seeds used in the study.

The seed extraction process consisted of cutting the fruits in half and manually extracting the seeds along with the attached pulp. Subsequently, this mixture was placed in plastic containers for fermentation at room temperature for three days, which facilitated the separation of the seeds from the pulp through the decomposition of surrounding tissues. After fermentation, the seeds were carefully washed with distilled water to remove any pulp residues and other impurities. Finally, they were dried in the shade on paper towels and stored in paper envelopes at room temperature until their use in the germination trials, following the methodology proposed by González-Puelles et al. (2018). To determine seed viability, the tetrazolium test was conducted using a representative sample of 20 seeds per replicate (three replicates). This analysis was carried out following the protocol described by Lastuvka et al. (2021) and Windauer et al. (2016).

Experimental design

The experiment was conducted using a completely randomized design with a factorial arrangement (5x3), where the effects of five levels of gibberellic acid concentration, combined with three incubation temperatures were evaluated. Prior to treatment application, all seeds were stratified at 4 °C for 31 days, followed by a 24-hour immersion in their respective GA_3 solutions and water. The methods and factors evaluated in the germination process are detailed in Table 1.

Table 1. Description of pre-germination treatments for kiwifruit (*Actinidia chinensis* var chinensis) seeds.

Treatments	GA_3 [ppm]	Immersion time (h)	Incubation temperature (°C)
1	0 (water)	24	25±2
2			30±2
3			35±2
4	1,000	24	25±2
5			30±2
6			35±2
7	2,000	24	25±2
8			30±2
9			35±2
10	4,000	24	25±2
11			30±2
12			35±2
13	6,000	24	25±2
14			30±2
15			35±2

GA_3: Gibberellic acid.

Each experimental unit consisted of 50 seeds, uniformly distributed in Petri dishes (100 mm in diameter) with moistened filter paper. Each treatment was replicated three times simultaneously. Incubation conditions were kept constant using germination chambers with controlled temperature and 85% humidity, ensuring treatment homogeneity. The moisture of the filter paper was checked daily to prevent desiccation, and germination observations were recorded every two days over a period of 68 days after sowing.

Stratification method

Prior to the process with gibberellic acid and disinfection, all seeds were subjected to a stratification period in a cold chamber at 4 °C for 31 days. This treatment aimed to simulate winter conditions necessary to break seed dormancy, promoting the synchronization of metabolic processes associated with germination, as recommended by various studies on *Actinidia* species (Zhang et al. 2018).

Disinfection process

After stratification, the seeds were disinfected to prevent potential microbial contamination during the germination process. Initially, the seeds were immersed in 70% ethanol for 1 minute to eliminate surface contaminants. Subsequently, they were placed in a 1% sodium hypochlorite solution for 5 minutes, ensuring deep disinfection without compromising seed viability. Finally, four consecutive washes with sterile distilled water were performed to remove any residual disinfectant agents, following the methodology described by Zhang et al. (2018).

Experiment management

After stratification and disinfection, the seeds were treated with different concentrations of gibberellic acid (GA_3) [0, 1,000, 2,000, 4,000, and 6,000 ppm], according to the experimental treatments established by Çelik et al. (2006) and Kumar et al. (2020). Subsequently, the seeds were rinsed thoroughly with distilled water to remove any residual growth regulator.

The Petri dishes were placed in SEEDBURO® germination chambers under dark conditions for the first five days, at constant temperatures of 25±2, 30±2 and 35±2 °C, depending on the corresponding treatment. Throughout the experiment, the filter paper was kept consistently moist with daily applications of distilled water, ranging from 3 to 13 mL depending on hydration needs as seeds germinated and metabolic activity increased.

Evaluated variables

Seed germination was visually evaluated every two days over a period of 68 days after sowing, until germination stabilized, as no new germination events were recorded after day 57. The following variables were determined based on the collected data**:**

-Germination Percentage (GP) = Number of germinated seeds / total number of seeds, expressed as (%) (Maghdouri et al. 2021). According to Equation 1:

$$PG = \frac{ni}{N} \times 100\% \quad (1)$$

Where ni is the number of germinated seeds and N is the total number of seeds.

-Mean Germination Rate (MGR) = Expressed as germinated seeds per day (seeds per day) (Sharma et al. 2021).

-Mean Germination Time (MGT) = The time elapsed in days from when the seeds are sown until 50% of the germinated seeds are reached (Sharma et al. 2021). According to Equation 2:

$$MGT = \frac{\sum ni * di}{N} \quad (2)$$

Where ni is the number of seeds germinated on day ddd, di is the number of days since the start of the germination trial, and N is the total number of seeds germinated by the end of the trial.

-Days to Latency (DL): The number of days elapsed between sowing and the start of germination of the first seed (Bishwas et al. 2018).

Statistical analysis

After completing the germination evaluations, the following response variables were calculated: germination percentage (GP), mean germination rate (MGR), mean germination time (MGT), and days to latency (DL). Since these variables did not follow a normal distribution according to the Shapiro-Wilk test ($P \leq 0.05$), a square root transformation was applied to normalize the data

and meet the assumptions required for the analysis of variance (ANOVA).

ANOVA was used to determine the existence of significant differences among the evaluated treatments, considering the factors of stratification, gibberellic acid concentration, incubation temperatures, and their interaction. Tukey's multiple comparison test at a 95% confidence level was applied to identify which treatments showed significant differences. All statistical analyses were performed using the Infostat software version 2020 (Di Rienzo et al. 2020).

RESULTS AND DISCUSSION

According to the results obtained from the mean comparisons, significant differences ($P \leq 0.05$) were found in all evaluated variables, except for the mean germination time (MGT). This suggests that *Actinidia chinensis* var. chinensis seeds responded differently to the various constant temperature levels used during the incubation process (25, 30 and 35 °C).

It is noteworthy that at a temperature of 35 °C, germination was completely inhibited (0%), indicating that elevated temperatures induce thermal stress that prevents the activation of the metabolic processes necessary for germination (Fernández and Johnston 2006) (Table 2). These results are consistent with previous studies (Çelik et al. 2006), where temperatures above 30 °C showed negative effects on germination in other *Actinidia* species.

Table 2. Comparison of means for germination variables in kiwifruit (*Actinidia chinensis* var chinensis) seeds subjected to different temperatures.

Temperature (°C)	GP	MGR	DL	MGT
25	5.96[a]	0.54[a]	2.63[a]	6.51[a]
30	4.52[b]	0.30[b]	3.46[b]	6.27[a]
HSD	0.65	0.11	0.46	0.37

Different letters between treatments denote significant differences (Tukey test, $P \leq 0.05$); HSD: honestly significant difference; GP: germination percentage; MGR: mean germination rate; MGT: mean germination time; DL: days to latency.

The results obtained demonstrated that seeds incubated at 25 °C for 68 days achieved the highest values of germination percentage (GP) and mean germination rate (MGR), with 5.96% and 0.54 seeds germinated per day, respectively. Additionally, these seeds completed the germination process in the shortest time (DL=2.63 days), which represents a shorter duration than that reported by Çelik et al. (2006). These findings suggest that 25 °C provides optimal conditions for activating the physiological and biochemical processes involved in kiwifruit seed germination, promoting greater efficiency in reserve mobilization and enzymatic activity required for radicle emergence (Fernández and Johnston 2006; Rosabal et al. 2014).

When analyzing temperature as an independent factor, it was determined that once seed tissues are rehydrated at a constant temperature of 25 °C, they regulate the biochemical reactions necessary for germination more efficiently (Pérez 2003). This suggests that thermal stability within this range favors the synchronization of metabolic events prior to germination, preventing potential adverse effects associated with temperature fluctuations (Fernández and Johnston 2006). Similar behavior was observed by Çelik et al. (2006), indicating that as temperature increases, GP decreases. In particular, temperatures above 30 and 35 °C negatively affected these variables, possibly due to the denaturation of essential proteins for germination or an increase in the respiration rate that prematurely depletes the seed's energy reserves (Fernández and Johnston 2006).

On the other hand, various studies have demonstrated that exogenous application of gibberellic acid in pre-germination treatments has positive effects on kiwifruit seed germination (Çelik et al. 2006; Ahmad 2010; Zhang et al. 2018; Bishwas et al. 2018). This plant growth regulator plays a key role in activating hydrolytic enzymes, facilitating reserve degradation, and promoting cell elongation necessary for seedling emergence. However, although gibberellic acid is widely recognized as a stimulator of the germination process in this and other species, the results of this study did not show significant differences

in the evaluated variables across different concentrations of this phytohormone (Table 3). This suggests that the concentrations used in the experiment have the same capacity to effectively break kiwifruit seed dormancy and significantly increase the germination rate compared to the control, where values were null. It is possible that the doses evaluated have already reached a maximum response threshold, so additional increases in gibberellic acid concentration would not generate significant improvements in germination.

Table 3. Comparison of means for germination variables in kiwifruit (*Actinidia chinensis* var chinensis) seeds subjected to different concentrations of gibberellic acid (GA_3).

Treatments GA_3 [ppm]	GP	MGR	DL (days)	MGT
1,000	5.24[a]	0.42[a]	3.18[a]	6.1[a]
2,000	6.63[a]	0.50[a]	2.92[a]	6.25[a]
4,000	4.63[a]	0.30[a]	3.19[a]	6.59[a]
6,000	5.45[a]	0.45[a]	2.88[a]	6.62[a]
HSD	1.25	0.2	0.88	0.7

Different letters between treatments denote significant differences (Tukey test, $P \leq 0.05$); HSD: honestly significant difference; GP: germination percentage; MGR: mean germination rate; MGT: mean germination time; DL: days to latency.

Gibberellic acid produces a wide variety of responses in seed development and germination control, making it a key factor in inducing dormancy break after seed imbibition (Amador-Alférez et al. 2013). Its effect on seeds lies in reducing the environmental requirements necessary for germination, such as chilling hours, light conditions, and temperature, counteracting the effects of other plant hormones such as abscisic acid (ABA), and stimulating both germination and embryo growth (Gazzarrini and Tsai 2015).

Çelik et al. (2006) concluded that the influence of a single factor in germination studies is not sufficient. However, when it interacts or combines with other factors, the germination percentage (GP) increases. Therefore, in the double interaction of the factors evaluated in this study, significant differences were observed in all variables except for the mean germination time (MGT) (Table 4).

The treatments subjected to constant temperatures of 35 °C without the application of gibberellic acid were

Table 4. Comparison of means for germination variables in kiwifruit (*Actinidia chinensis* var chinensis) seeds subjected to the double interaction of the evaluated factors.

Treatments	Description	GP	MGR	DL (days)	MGT
4	1,000 ppm+25 °C	6.13[ab]	0.62[ab]	2.87[a]	6.21[a]
5	1,000 ppm+30 °C	4.34[b]	0.29[ab]	3.5[a]	5.98[a]
7	2,000 ppm+25 °C	6.14[ab]	0.58[ab]	2.71[a]	6.17[a]
8	2,000 ppm+30 °C	5.12[ab]	0.41[ab]	3.14[a]	6.33[a]
10	4,000 ppm+25 °C	5.21[ab]	0.38[ab]	2.63[a]	6.89[a]
11	4,000 ppm+30 °C	4.06[b]	0.22[b]	3.74[a]	6.29[a]
13	6,000 ppm+25 °C	6.35[a]	0.56[a]	2.3[a]	6.74[a]
14	6,000 ppm+30 °C	4.54[ab]	0.27[ab]	3.46[a]	6.49[a]
	HSD	2.15	0.38	1.51	1.2
	CV	14.5	16.44	17.58	6.7

Different letters between treatments denote significant differences (Tukey test, $P \leq 0.05$); HSD: honestly significant difference; CV: coefficient of variation.

not included in the tables due to the lack of satisfactory germination results (0%). Although previous studies, such as that of Çelik et al. (2006), reported germination rates of 45.3, 50, 51.7, and 48.2% under 35 °C conditions combined with 0, 2,000, 4,000, and 6,000 ppm of gibberellic acid, respectively, complete inhibition of germination was observed in the present study. This suggests that seeds of this *Actinidia chinensis* var. chinensis species do not require high temperatures to activate their metabolism and that thermal stress at 35 °C may have negatively affected seed viability.

In contrast, the interaction between a constant temperature of 25 °C and the different concentrations of gibberellic acid effectively broke dormancy and stimulated germination. In the absence of the growth regulator (control, data not shown), no germination was recorded (0%), while treatment 13 achieved a germination rate of 40.6%. These findings are consistent with those reported by Çelik et al. (2006), who determined that the optimal temperature for germination in other kiwifruit species, such as *A. arguta* and *A. kolomikta*, ranges between 20 and 25 °C.

Furthermore, Çelik et al. (2006) evaluated the interaction of three factors—temperature, growth medium, and gibberellic acid concentration—on the germination process of *Actinidia chinensis* cv. Hayward seeds. Their study analyzed four temperature levels (20, 25, 30, and 35 °C), three types of substrates (peat, perlite + heating humus, and soil mixture), and four gibberellic acid (GA_3) concentrations [1,000, 2,000, 4,000, and 6,000 ppm]. Results indicated that seeds treated with 6,000 ppm of GA_3 and sown in peat achieved the highest germination rate (79%), a value considerably higher than that obtained in the present study (40.6%).

Discrepancies between the two studies could be attributed to differences in seed genetics, experimental conditions, or the interaction between uncontrolled environmental factors. These results highlight the importance of evaluating multiple factors simultaneously to optimize kiwifruit seed germination, emphasizing the crucial role of temperature and gibberellic acid in the germination process.

CONCLUSION

The interaction between the application of gibberellic acid (GA_3) and a constant incubation temperature of 25 °C significantly promoted the germination process of kiwifruit seeds (*Actinidia chinensis* var. chinensis) collected in Huatusco, Veracruz. This pre-germination treatment proved to be the most effective, as it reduced the dormancy period and increased both the germination percentage and the mean germination rate, without notable differences among the GA_3 concentrations evaluated. In contrast, temperatures above 30 °C had a negative effect on all germination variables, completely inhibiting germination. These findings reaffirm the effectiveness of combining GA_3 with controlled thermal conditions as a viable strategy to overcome seed dormancy in kiwifruit under tropical environments. Further research is recommended on incubation conditions below 25 °C and intermediate GA_3 concentrations (2,000 and 4,000 ppm) to refine propagation protocols and support the establishment of cultivars adapted to Mexico's agroclimatic conditions.

ACKNOWLEDGMENTS

We express our gratitude to the National Council of Humanities, Science, and Technology (CONAHCyT Spanish acronym), technician Mateo Barrientos Reyes, and Universidad Autónoma Chapingo for their valuable contribution and support during the development of this experiment.

CONFLICT OF INTERESTS

The author declares no conflict of interest.

REFERENCES

Amador-Alférez KA, Díaz-González J, Loza-Cornejo S and Bivián-Castro EY (2013) Efecto de diferentes reguladores de crecimiento vegetal sobre la germinación de semillas y desarrollo de plántulas de dos especies de *Ferocactus* (Cactaceae). Polibotánica, 35: 109-131. https://www.scielo.org.mx/pdf/polib/n35/n35a7.pdf

Ahmad MF (2010) Enhancement of seed germination in kiwifruit by stratification and gibberellic acid application. Indian Journal of Horticulture 67(1): 34-36. https://www.indianjournals.com/ijor.aspx?target=ijor:ijh&volume=67&issue=1&article=007&type=pdf

Bishwas KC, Kumar A, Santosh S, Raj-Kumar KC and Dipendra R (2018) Effect of GA_3 on germination parameters of different varieties of kiwi. Current Investigations in Agriculture and Current Research 4(3): 516-522. https://doi.org/10.32474/CIACR.2018.04.000186

Castillo JCC, Medina EL, Zavaleta SC, Mendoza MW and Gonza CA (2013) Efecto de la estratificación en la germinación de semillas del ciruelo europeo, *Prunus domestica*. Revista REBIOLEST 1(1): 49-53. https://revistas.unitru.edu.pe/index.php/ECCBB/article/view/181

Çelik H, Zenginbal H and Özcan M (2006) Enhancing germination of kiwifruit seeds with temperature, medium and gibberellic acid. Horticultural Science 33(1): 39-45. https://doi.org/10.17221/3738-HORTSCI

Di Rienzo JA, Casanoves F, Balzarini MG, Gonzalez L, Tablada M and Robledo CW (2020) InfoStat versión 2020. Centro de Transferencia InfoStat, FCA, Universidad Nacional de Córdoba, Argentina. http://www.infostat.com.ar

Escobar DF and Cardoso VJ (2015) Seed germination and dormancy of *Miconia chartacea* (Melastomataceae) in response to light, temperature and plant hormones. Revista de Biología Tropical 63(4): 1169-1184. https://doi.org/10.15517/rbt.v63i4.17955

Fernández G and Johnston M (2006) Capítulo XX: Crecimiento y Temperatura. Pp 1-28. In: Squeo FA and Cardemil L (ed). Fisiología Vegetal. Ediciones Universidad de La Serena, Chile. v210806. http://www.biouls.cl/librofv/web/pdf_word/Capitulo%2020.pdf

Gao F and Ayele BT (2014) Functional genomics of seed dormancy in wheat: advances and prospects. Frontiers in Plant Science 5: 458. https://doi.org/10.3389/fpls.2014.00458

Gazzarrini S and Tsai AY (2015) Hormone cross-talk during seed germination. Essays in biochemistry 58: 151–164. https://doi.org/10.1042/bse0580151

González-Puelles JE, Landín M, Gallego PP and Barreal ME (2018) Deciphering kiwifruit seed germination using neural network tools. Acta Horticulturae 1218: 359–366. http://doi.org/10.17660/actahortic.2018.1218.50

Kumar A, Ali A, Khalil A and Sharma A (2020) Chapter 6: Kiwifruit (*Actinidia deliciosa* Chev.). pp. 184-221. In: Ghosh SN, Kumar A and Tarai RK (Ed) Plant growth regulators in temperate and underutilized fruit crops. First edition. Editorial Jaya Publishing House, Nueva Delhi India.

Lastuvka M, Benech-Arnold R and Windauer L (2021) A stratification thermal time-based model as a tool for designing efficient methodologies to overcome seed dormancy constraints to kiwifruit seedling production. Scientia Horticulturae 277: 109796. https://doi.org/10.1016/j.scienta.2020.109796

Maghdouri M, Ghasemnezhad M, Rabiei B, Golmohammadi M and Atak A (2021) Optimizing seed germination and seedling growth in different kiwifruit genotypes. Horticulturae 7(9): 314. https://doi.org/10.3390/horticulturae7090314

Pérez F (2003) Capitulo 7: Germinación y dormición de semillas. 177-199. In: Consejería de Medio Ambiente (eds). Material vegetal de reproducción: manejo, conservación y tratamiento Junta de Andalucía, Andalucía, España. 229 p.

Rosabal AL, Martínez GL, Reyes GY, Dell'Amico RJ and Núñez VM (2014) Aspectos fisiológicos, bioquímicos y expresión de genes en condiciones de déficit hídrico. Influencia en el proceso de germinación. Cultivos Tropicales 35(3): 24-35. http://scielo.sld.cu/pdf/ctr/v35n3/ctr03314.pdf

Sharma A, Devkota D, Thapa M and Bista B (2021) Improving germination and stand establishment of kiwifruit (*Actinidia deliciosa* cv. Hayward) seed through media selection and hormonal use in Dolakha, Nepal. Tropical Agrobiodiversity 2(1): 16-21. http://doi.org/10.26480/trab.01.2021.16.21

Sekhukhune MK, Nikolova RV and Maila MY (2018a) Effect of cold stratification and gibberellic acid on *in vitro* germination of *Actinidia arguta* and *Actinidia chinensis.* Acta Horticulturae 1204: 65–76. http://doi.org/10.17660/actahortic.2018.1204.9

Sekhukhune MK, Maila MY, Nikolova RV and Mphosi MS (2018b) Preliminary studies on *in vivo* germination of *Actinidia arguta* and *Actinidia chinensis.* Acta Horticulturae 1204: 123–132. http://doi.org/10.17660/actahortic.2018.1204.16

Windauer LB, Insausti P, Biganzoli F, Benech-Arnold R and Izaguirre MM (2016) Dormancy and germination responses of kiwifruit (*Actinidia deliciosa*) seeds to environmental cues. Seed Science Research 26(4): 342-350. https://doi.org/10.1017/S0960258516000192

Yamaguchi S (2008) Gibberellin metabolism and its regulation. Annual Review of Plant Biology 59 (1): 225-251. https://doi.org/10.1146/annurev.arplant.59.032607.092804

Zhang Y, Zhang H, Kong L and Tang H (2018) Effects of different treatment methods on seed germination of kiwifruit. In: IOP Conference Series: Materials Science and Engineering 394(2): 022-034. http://doi.org/10.1088/1757-899X/394/2/022034

Research article

https://revistas.unal.edu.co/index.php/refame

Revista Facultad Nacional de Agronomía

Protein concentrates from Colombian cheese acid whey as a source of antioxidant hydrolysates obtained by proteolysis

Concentrados proteicos a partir de lactosuero ácido de queso colombiano como una fuente de hidrolizados antioxidantes obtenidos por proteólisis

https://doi.org/10.15446/rfnam.v78n2.110709

Sandra Zapata Bustamante[1,2*], Héctor José Ciro Velásquez[3], José Uriel Sepúlveda Valencia[3], Diego Luis Durango Restrepo[4] and Jesús Humberto Gil González[3**]

ABSTRACT

Protein concentration and hydrolysis have been widely used in sweet whey to produce a variety of food products, while the use of acid whey has been limited due to its high salinity and acidity, hence this study aimed to obtain different protein concentrates from Colombian double-cream cheese acid whey by ultrafiltration (UF), salt treatment (ST), and thermal precipitation (TP); and to evaluate their potential application in the production of antioxidant hydrolysates by enzymatic hydrolysis with alcalase (ALC), chymotrypsin (CHY), and flavourzyme (FLA). Regarding the protein concentration, the UF, TP, and ST concentrates presented a protein content of 49, 75, and 53% and protein yield of 46, 28, and 43%, respectively. After enzymatic hydrolysis, the soluble protein content decreased in the UF and ST concentrates, while the free amino acid concentration increased in all concentrates. The UF and ST concentrates showed a higher degree of hydrolysis with ALC (33.76 and 33.57%, respectively) and FLA (40.35 and 31.60%, respectively). Concerning antioxidant activity, the UF and ST concentrates treated with ALC (5,675 and 5,199 µmol Trolox L^{-1}, respectively) and CHY (4,663 and 4,419 µmol Trolox L^{-1}, respectively) were the most effective in scavenging the ABTS radical. All the FLA hydrolysates presented higher reducing power (152-183 µmol Trolox L^{-1}) and the UF concentrate, and its hydrolysates showed greater iron-chelating activity. In conclusion, UF and ST are valuable methods for acid whey protein recovery and concentration, which could be converted into potential antioxidant peptides by proteolytic processes.

Keywords:
Acid whey
Antioxidant activity
Bioactive peptides
Enzymatic hydrolysis
Protein concentrate

RESUMEN

La concentración e hidrólisis de proteínas se han aplicado ampliamente en el lactosuero dulce para producir una variedad de productos alimenticios, mientras que el uso de lactosuero ácido ha sido limitado debido a su alta salinidad y acidez, por lo tanto este estudio tuvo como objetivo obtener diferentes concentrados de proteína a partir de lactosuero ácido de queso colombiano mediante ultrafiltración (UF), tratamiento con sal (ST) y precipitación térmica (TP); así como evaluar su potencial aplicación en la producción de hidrolizados antioxidantes por hidrólisis enzimática con alcalasa (ALC), quimotripsina (CHY) y flavourzima (FLA). Respecto a la concentración de proteína, los concentrados de UF, TP y ST presentaron un contenido de proteína de 49, 75 y 53% y un rendimiento de proteína de 46, 28 y 43%, respectivamente. Después de la hidrólisis enzimática, el contenido de proteína soluble disminuyó en los concentrados de UF y ST, mientras que la concentración de aminoácidos libres aumentó en todos los concentrados. Los concentrados de UF y ST mostraron un mayor grado de hidrólisis con ALC (33,76 y 33,57%, respectivamente) y FLA (40,35 y 31,60%, respectivamente). En cuanto a la actividad antioxidante, los concentrados de UF y ST tratados con ALC (5.675 y 5.199 µmol Trolox L^{-1}, respectivamente) y CHY (4.663 y 4.419 µmol Trolox L^{-1}, respectivamente) fueron los más efectivos en atrapar el radical ABTS. Todos los hidrolizados de FLA presentaron mayor poder reductor (152-183 µmol Trolox L^{-1}) y el concentrado de UF y sus hidrolizados mostraron mayor actividad quelante de hierro. En conclusión, UF y ST son métodos valiosos para la recuperación y concentración de proteínas de lactosuero ácido, las cuales podrían convertirse en potenciales péptidos antioxidantes mediante procesos proteolíticos.

Palabras clave:
Lactosuero ácido
Actividad antioxidante
Péptidos bioactivos
Hidrólisis enzimática
Concentrado proteico

[1]Grupo de Investigación Síntesis y biosíntesis de metabolitos naturales, Universidad Nacional de Colombia, Sede Medellín, Colombia.
[2]Instituto Tecnológico Regional Suroeste, Universidad Tecnológica del Uruguay, Paysandú, Uruguay. sandra.zapata@utec.edu.uy
[3]Facultad de Ciencias Agrarias, Universidad Nacional de Colombia, Sede Medellín, Colombia. hjciro@unal.edu.co, jusepul@unal.edu.co, jhgilg@unal.edu.co,
[4]Facultad de Ciencias, Universidad Nacional de Colombia, Sede Medellín, Colombia. dldurango@unal.edu.co
*Corresponding author
**Corresponding author

Received: June 6, 2024; Accepted: October 23, 2024
Rev. Fac. Nac. Agron. Medellín 78(2): 11077-11088. 2025

ISSN 0304-2847 / e-ISSN 2248-7026

CC BY NC SA

Whey proteins are a mix of globular proteins obtained from whey including β-lactoglobulin (~50%), α-lactoalbumin (~20%), bovine serum albumin (~10%), immunoglobulins (~10%), and other minor protein fractions of low abundance. These proteins constitute about 20% of the total milk protein content, which have excellent nutritional, biological, and functional properties. Whey proteins are rich in essential and branched-chain amino acids (Khaire and Gogate 2019), they are also precursors of bioactive peptides (Olvera-Rosales et al. 2023), have emulsifying, gelling, and foaming properties, and possess a high digestibility (Embiriekah et al. 2018). All these characteristics make whey a valuable dairy raw material in the food industry for developing value-added products.

Whey proteins are highly diluted in whey, which contains 6-7% of total solids; for that reason, the implementation of techniques for their isolation and concentration is necessary. Methods, such as precipitation and membrane separation, have been used for the recovery of whey proteins, and both methods depend on the physicochemical properties of whey (Jiménez et al. 2012; Yadav et al. 2014). Precipitation of whey proteins is achieved by heating or adding specific chemicals (salts) that cause the insolubility of whey proteins for their easy removal. The membrane separation allows the fractionation of whey components depending on their molecular size. Specifically, ultrafiltration is the most used industrial method for the recovery of whey proteins (Khaire and Gogate 2019). These processes may influence the yield as well as the nutritional and biological properties of proteins (Jiménez et al. 2012).

Whey proteins can be enzymatically hydrolyzed to produce hydrolysates containing peptides with various functions (Olvera-Rosales et al. 2023). These hydrolysates have been reported to act as antioxidants by different mechanisms: inactivation of reactive oxygen species, free radical scavenging, inhibition of lipid peroxidation, chelation of metal ions, or a combination of these mechanisms (Olvera-Rosales et al. 2023). The composition of hydrolysates and their bioactivity can be affected by the enzyme specificity, the nature, concentration, and extent of denaturation of protein substrate, and physicochemical conditions applied during the enzymatic process. These factors can impact the accessibility of enzymes to protein substrate, which may result in the production of hydrolysates with a diversity of peptides of different sizes and structures that can exhibit a wide range of biological activities (Zou et al. 2016; Olvera-Rosales et al. 2023).

Different whey protein products, such as whey protein concentrates (WPC), isolates (WPI), and hydrolysates (WPH), are mainly manufactured from sweet whey, which is obtained by enzymatic coagulation of milk. In contrast, the use of acid whey, which is obtained by fermentation or the addition of organic or mineral acids, is limited due to its high acidity and salinity (Nishanthi et al. 2017). Both sweet and acid whey have different compositions, which could affect the final composition of hydrolysates obtained from them and thus their biological properties. In Colombia, acid whey can be produced during the manufacture of double-cream cheese, a stretched-curd and non-matured cheese traditionally made from a mixture of fresh and acidified cow milk. It is one of the most widely marketed cheeses in the country (representing approximately 30% of total cheese consumption) (Londoño-Zapata et al. 2017), with a monthly production of around 3,000 tons in 2023 that has increased in recent years (Ministerio de Agricultura y Desarrollo Rural 2024). A limited number of studies appear in the literature on the comparison of methods for the acid whey protein concentration and the enzymatic hydrolysis of these products to obtain hydrolysates with different compositions that may exhibit antioxidant capacity. This demonstrates the need to conduct further research in this area, which could contribute to the generation of alternatives that add value to acid whey. For this reason, this study aimed to obtain different whey protein concentrates from Colombian double-cream cheese acid whey by ultrafiltration and precipitation methods, and to evaluate their potential application in the production of antioxidant hydrolysates by enzymatic hydrolysis.

MATERIALS AND METHODS

Materials

Double-cream cheese whey was obtained from the Laboratory of Dairy Products of the Universidad Nacional de Colombia (Medellín, Colombia). Enzymes used for hydrolysis: Alcalase 2.4 L and Flavourzyme 1,000 L were supplied by Novozymes, while α-Chymotrypsin was purchased from Sigma-Aldrich. All other chemicals and reagents of analytical grade were purchased from Merck.

Preparations and characterization of whey protein concentrate

Ultrafiltration, salt treatment, and thermal precipitation were used for the whey protein concentration. A whey sample (500 mL) containing 0.7% of the protein was used in all tests. For ultrafiltration (UF), whey was processed in a tangential ultrafiltration module Vivaflow 50R equipped with a 10 kDa regenerated cellulose membrane. The sample was concentrated 20-fold and lyophilized. Salt treatment (ST) was carried out according to the method described by Lozano et al. (2008), with some modifications. The precipitation was performed with 50% ammonium sulfate (291 g ammonium sulfate per Liter of whey) at 4 °C. The precipitate was recollected by centrifugation (5,000×*g*, 20 min, 4 °C), dissolved in distilled water and desalinated using 10 kDa cut-off membrane (Vivaflow 50R). Then, the desalinated sample was freeze-dried. Thermal precipitation (TP) was performed according to Tari et al. (2021), with some modifications. Whey was heated in a water bath (Memmert WNB14) to 85 °C for 5 min, cooled on ice and recollected by centrifugation at 5,000×*g* for 20 min at 4 °C. The precipitate was recovered and freeze-dried.

Whey protein concentrates were characterized by analysis of the following parameters: protein, α-lactalbumin (α-La), β-lactoglobulin (β-Lg), lactose, fat, and moisture. The total protein content was determined by the Kjeldahl method of the AOAC (AOAC 2002). α-La and β-Lg were analyzed by HPLC-DAD on a Shimadzu Prominense liquid chromatography equipped with Diode Array Detector (SPD-M20A), with the following conditions: column, RP JUPITER C18 (5 µm, 250×4.6 mm, 300 Å, Phenomenex); elution system: eluent A, 0.1% (v/v) of trifluoroacetic acid in water; eluent B, 90% (v/v) of acetonitrile and 0.09% (v/v) of trifluoroacetic acid in water; gradient, 0-20 min linear from 75% A to 45% A, 20-25 min 45% A, 25-35 min linear to 100% A, 35-36 min linear from 100% A to 75% A; column temperature, 35 °C; sample temperature, room temperature.; injection volume, 10 µL; acquisition time, 36 min; flow rate, 1 mL min^{-1}; UV detector: λ=228 nm. LabSolutions Software (Shimadzu, LC solution Version 1.22 SP1) was used for data analysis (Waters Co.). Lactose concentration was determined by the dinitrosalicylic acid (DNS) method (Ghasemi et al. 2017). Fat was extracted with hexane (3×10 mL), sonicated (15 min), and centrifuged (5,000×*g*, 10 min). The supernatants were collected, and fat content was then determined gravimetrically after hexane was evaporated in a vacuum rotary evaporator (40 °C). Moisture content was carried by a gravimetric method (105 °C - Memmert UFE 400) (AOAC 2002).

Protein yield was also determined using Equation (1):

$$\text{Protein yield (\%)} = \left(\frac{\text{g of protein in WPC}}{\text{g of protein in acid whey}} \text{x } 100 \right) \quad (1)$$

Where WPC is whey protein concentrate.

Enzymatic hydrolysis

Each whey protein concentrate was suspended in deionized water at a concentration of 1% (w/v) on a protein equivalent basis, and pH was adjusted by 1 M NaOH to obtain the optimal value for the enzyme using a pH-meter. The hydrolysis was performed using various enzymes under the following parameters: enzyme/substrate ratio, 1/50 (w/w); pH=8.0 for Alcalase and Chymotrypsin and pH=7.0 for Flavourzyme; temperature, 45 °C. The digestion was allowed for 24 h with continuous stirring. Samples were removed at 0, 4, and 24 h, heated at 85 °C for 10 min, and placed in an ice bath to inactivate the enzymes. The insoluble solids were recollected by centrifugation at 5,000×*g* for 10 min and the obtained supernatants were adjusted to pH=7.0 and stored at -20 °C.

Degree of hydrolysis (DH)

The degree of hydrolysis (DH) was determined using the *o*-phthaldialdehyde (OPA) method (Spellman et al. 2003). The OPA reagent (100 mL) was prepared by combining the following solutions: 10 mL of 50 mM OPA (in methanol) and 10 mL of 50 mM N-acetyl-L-cysteine (NAC), 5 mL of 20% (w/v) sodium dodecyl sulfate (SDS) and 75 mL of borate buffer (0.1 M, pH=9.5). The reagent was protected from light and stirred at least 1 h before use. For the assay, 10 µL of sample (or standard) was mixed with 1.2 mL of OPA reagent and the absorbance was recorded at 340 nm after 2 min using an UV-Vis spectrophotometer. A calibration curve was prepared using leucine (0–2 mg mL^{-1}). The degree of hydrolysis (DH) was calculated according to the methodology described by Anzani et al. (2018) as indicated in Equation 2:

$$DH(\%) = (N_{free}/N_{total}) \text{ x } 100 \quad (2)$$

Where N_{free} are the moles of free nitrogen atoms from α-amino groups of amino acids after hydrolysis measured

by the OPA assay, and N_{total} are the total moles of nitrogen atoms in solution before hydrolysis calculated by the ratio of total grams of proteins and the average residual amino acid molecular mass (MW 110 Da).

Protein and free amino acids concentration

The soluble protein content in the supernatant of the hydrolysates was determined by the Bradford method (Nwachukwu and Aluko 2019), using bovine serum albumin as a standard. The free amino acid content was estimated by the ninhydrin method (Quintanilla et al. 2019), using leucine as the standard.

Antioxidant activity

The *in vitro* antioxidant activity was evaluated by measuring the ABTS radical scavenging activity, reducing power, and Iron (II) chelating capacity. ABTS radical cation was generated according to the method described by Corrêa et al. (2014). 10 µL of hydrolysate (or standard) was mixed with 1 mL of diluted ABTS solution. After 6 min, the absorbance was registered at 734 nm and the results were reported as Trolox equivalents (µmol Trolox L^{-1}) using a Trolox calibration curve.

The reducing power of the hydrolysates was assessed according to the method of Jayanthi and Lalitha (2011), with slight modifications. A 250 µL sample (or standard) was mixed with 250 µL of phosphate buffer (0.2 M, pH=6.6) and 250 µL of a potassium ferricyanide solution (1%, w/v). After 20 min of incubation at 50 °C, 250 µL of a trichloroacetic acid solution (10%, w/v) was added and the resulting mixture was centrifuged at 3,000×*g* for 10 min. Then, 500 µL of supernatant was mixed with 500 µL of distilled water and 100 µL of a ferric chloride solution (0.1%, w/v). The absorbance was read at 700 nm and the results were expressed as Trolox equivalents (µmol Trolox L^{-1}).

The iron (II) chelating capacity was determined according to the method described by Corrêa et al. (2014), with some modifications. A 100 µL sample (or standard) was mixed with 840 µL of distilled water, 20 µL of 2 mM ferrous sulfate and 40 µL of 5 mM ferrozine (3-(2-pyridyl)-5,6-bis(4-phenyl-sulfonic acid)-1,2,4-triazine). After 10 min, the absorbance was registered at 562 nm. Distilled water and EDTA (40 µg mL^{-1}) were used as negative and positive controls, respectively. The results were expressed using Equation 3:

$$\text{Activity chelating}(\%) = \left[1 - \left(\frac{\text{Absorbance of sample}}{\text{Absorbance of control}}\right)\right] \times 100 \quad (3)$$

Figure 1 shows the methodology described above in the preparation of the whey protein concentrates and hydrolysates and their characterization.

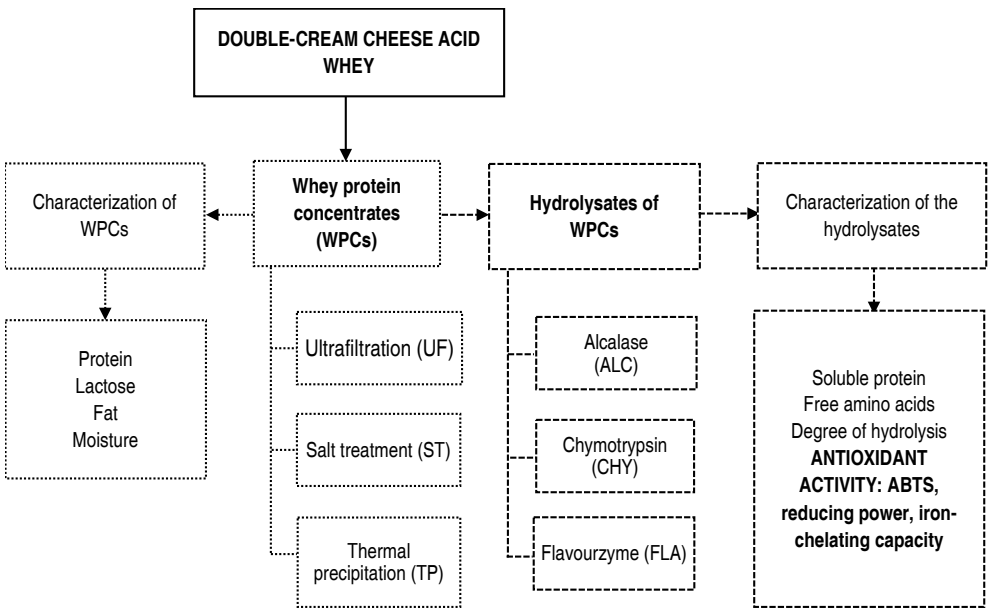

Figure 1. Outline of the preparation of the whey protein concentrates and hydrolysates and their characterization.

Statistical analysis

The methods of protein concentration were compared using one-way analysis of variance (ANOVA) followed by the least significant difference (LSD) test using Statgraphics Centurion XVI (Statpoint Technologies, Inc.). For enzymatic hydrolysis, three-way repeated measures ANOVA were carried out to analyze the effects of the method of protein concentration, enzyme used, and hydrolysis time on the soluble protein content, free amino acid concentration, degree of hydrolysis, and antioxidant activity, using SAS University Edition Software (SAS Institute, Inc.). All determinations were done in triplicate and values were expressed as mean ± standard deviation, and differences between means were considered statistically significant at $P<0.05$.

RESULTS AND DISCUSSION

Composition of whey protein concentrates

A whey protein concentrate (WPC) is a processed form of whey proteins containing at least 25% protein, which is obtained by removing sufficient amounts of non-protein components (lactose, fat, and minerals) from whey by different protein separation and concentration techniques (Kilara and Vaghela 2018). In this study, three WPCs were obtained by ultrafiltration (UF), salt treatment (ST), and thermal precipitation (TP) from double-cream cheese whey and their chemical composition is shown in Table 1. These products contained approximately 49-75% protein, 5-35% lactose, 2-5% fat, and 7-8% moisture.

Table 1. Chemical composition of whey protein concentrates obtained by ultrafiltration (UF), salt treatment (ST), and thermal precipitation (TP).

Composition (%)	Whey protein concentration method		
	UF	ST	TP
Protein	48.87±3.78^a	74.85±0.21^b	52.67±5.98^a
α-*Lactalbumin*	7.90±1.11^a	18.88±1.94^b	-
β-*Lactoglobulin*	27.29±3.49^a	19.98±1.39^b	-
Protein yield	46.29±2.80^a	27.72±4.05^b	43.00±2.43^a
Lactose	34.70±1.06^a	5.30±0.19^b	16.49±0.37^c
Fat	5.36±0.55^a	3.34±0.26^b	2.16±0.07^c
Moisture	8.09±0.47^a	7.89±0.69^a	7.28±0.05^a

Results represent the mean of three experimental repetitions ± standard deviation (n=6). Different letters in each row represent significant ($P<0.05$) differences between mean values.

The composition of the UF concentrate and the protein content of the TP concentrate were similar to those of WPC50. In the case of the ST concentrate, the protein content was consistent with WPC75, and the lactose and fat contents were close to those reported by Jiménez et al. (2012), as shown in Table 2.

Table 2. Chemical composition of whey protein products.

Whey protein concentrates	Protein (%)	Lactose (%)	Fat (%)	References
WPC50	50-52	33-37	5-6	U.S. Dairy Export Council 2006 Kilara and Vaghela (2018)
WPC75	75-78	-	-	U.S. Dairy Export Council 2006
Other WPC obtained by ST	-	5.67	3.3	Jiménez et al. (2012)

All these methods had a significant effect (P<0.05) on protein recovery with a yield of 28-46% in the different products (Table 1). No statistically significant differences (P>0.05) were found in total protein content and yield in the products obtained by TP and UF, respectively. ST produced a higher protein content with a lower yield level compared to TP and UF. This concentrate was subjected to a desalination step that could increase purity with a decrease in yield due to possible loss of protein material. The different protein separation and concentration techniques allowed to obtain WPCs from Colombian double-cream cheese whey with a protein content and yield comparable to that of previous studies. Jiménez et al. (2012) obtained different WPCs by precipitation, ultrafiltration, and freeze drying with a protein content of 20–35% and protein yield of 40-53%. They reported that higher protein content was obtained by ultrafiltration and ammonium sulfate precipitation. Yadav et al. (2014) reported a maximum soluble protein recovery of 53% from the supernatant of *K. marxianus* fermented cheese whey using thermal precipitation (100 °C, pH=4.5 and 10 min of incubation).

Statistically significant differences in α-La and β-Lg content in the products from UF and ST were observed (Table 1). With respect to the total whey protein content, α-La and β-Lg comprised about 16 and 56% in UF concentrate, and 25 and 27% in ST concentrate, respectively. Poor solubility of the TP concentrate was shown, causing difficulties for the determination of α-La and β-Lg. O'Loughlin et al. (2012) reported that heating of WPI results in the loss of native protein (α-La, β-Lg, and bovine serum albumin), aggregate formation, and insolubilization. They detected a reduction of solubility from 90±1 to 31±2% when samples were heated at 80 °C for 10 min compared to the unheated sample. Jiménez et al. (2012) found α-La, β-Lg, bovine serum albumin, and other minority proteins (lactoferrin and immunoglobulin) in WPCs obtained by UF and ammonium sulfate precipitation, while they were not detected when thermal precipitation was used. In addition, there were no modifications to protein structure during the ultrafiltration process, which is important for biopeptide production.

Enzymatic hydrolysis of whey protein concentrates

WPCs were subjected to enzymatic hydrolysis using different enzymes (ALC, CHY, and FLA), and the progress of the hydrolysis was evaluated by determining the soluble protein content, free amino acid concentration, and degree of hydrolysis (Figure 2). Higher protein solubility was observed in the UF and ST concentrates at time 0, as shown in Figure 2A, which is important for the hydrolytic process. Concerning the TP concentrate, thermal denaturation is one of the effects of heating on the protein structure and functionality. This denaturation can be reversible or irreversible, leading to partial unfolding or aggregate formation involving covalent bonds, and electrostatic, and hydrophobic interactions (Wijayanti et al. 2014). Solubility in the TP concentrate could be affected by thermal treatment (85 °C, 5 min) as reported by O'Loughlin et al. (2012). As hydrolysis progressed, a decrease in the protein content in the UF and ST concentrates was detected. Their protein structure was principally affected by ALC and CHY. No statistically significant changes in the soluble protein content of the TP concentrate were presented with any enzyme during hydrolysis. During heat treatment, whey proteins undergo conformational changes exposing reactive groups that can lead to sulfhydryl (–SH)/disulfide (S–S) interchange reactions or other intra- and intermolecular interactions, forming aggregates, and affecting the solubility of the proteins (Wijayanti et al. 2014). In contrast, the free amino acid content increased in all concentrates over time during hydrolysis (Figure 2B). The results obtained are consistent with other studies. Embiriekah et al. (2018) also detected a decrease in the soluble protein content while an increase in the free amino acid concentration in whey protein hydrolysates prepared with pepsin and trypsin. In addition, increments in the free amino acid content in sheep protein whey hydrolysates were reported by Corrêa et al. (2014). Notably, the UF and ST hydrolysates had higher free amino acids when hydrolyzed with FLA followed by those obtained using ALC after 24 h of hydrolysis. In general, all CHY hydrolysates presented lower free amino acid content. ALC is an endopeptidase from *Bacillus licheniformis* with broad specificity (Corrochano et al. 2019), and FLA is an enzymatic complex from *Aspergillus orysae* with both exo- and endopeptidase activity (Merz et al. 2015). Thus, both enzymes could cause greater release of amino acids compared to CHY, which cleaves at the carboxylic side of aromatic and bulky amino acids (Gauthier and Pouliot 2003).

The extent of whey protein hydrolysis was evaluated by measuring the degree of hydrolysis (DH), which can be quantified by the determination of free amino acids released

during the hydrolytic process using compounds such as *o*-phthaldialdehyde (OPA) (Spellman et al. 2003). DH increased in all concentrates during enzymatic hydrolysis (Figure 2C), reaching about 18-40, 13-34, and 7-34% in the UF, ST, and TP concentrates at 24 h, respectively. After 24 h of hydrolysis, the UF concentrate treated with FLA presented higher DH followed by all ALC hydrolysates and the ST concentrate hydrolyzed with FLA. Lower DH in the TP concentrate treated with FLA and the CHY hydrolysates were observed. A high DH with ALC and FLA and a low DH with CHY is consistent with the fact that the ALC and FLA hydrolysates presented greater free amino acid content, and the CHY hydrolysates had the lowest concentration. A high release of free amino acids could relate to a high DH as reported in previous work (Embiriekah et al. 2018). The type of protein substrate (WPC), enzyme specificity, and time of hydrolysis could influence the DH values. After 4 h of hydrolysis with ALC, no statistically significant differences in DH were found in all concentrates. The same was observed at 24 h. When the concentrates were treated with CHY, there were no statistical differences in the UF and ST concentrates after 4 and 24 h of hydrolysis. During the digestion with FLA, the UF concentrate showed higher DH compared to the ST and TP concentrates after 4 and 24 h of hydrolysis. It is important to note that the DH of the ALC and FLA hydrolysates increased as the time of hydrolysis increased. In addition, the UF and ST concentrates were more sensitive to the enzymatic action of ALC and FLA. Souza et al. (2019) reported high DH in a WPC obtained by UF when hydrolyzed with ALC. Additionally, as mentioned above, ALC and FLA are enzymes with broad specificity that can cleave protein substrates non-specifically, consistent with the high degree of hydrolysis (DH) and free amino acid content observed in the UF and ST concentrates treated with these enzymes. In contrast, CHY cleaves specific regions in the sequence, producing hydrolysates with lower values for these characteristics.

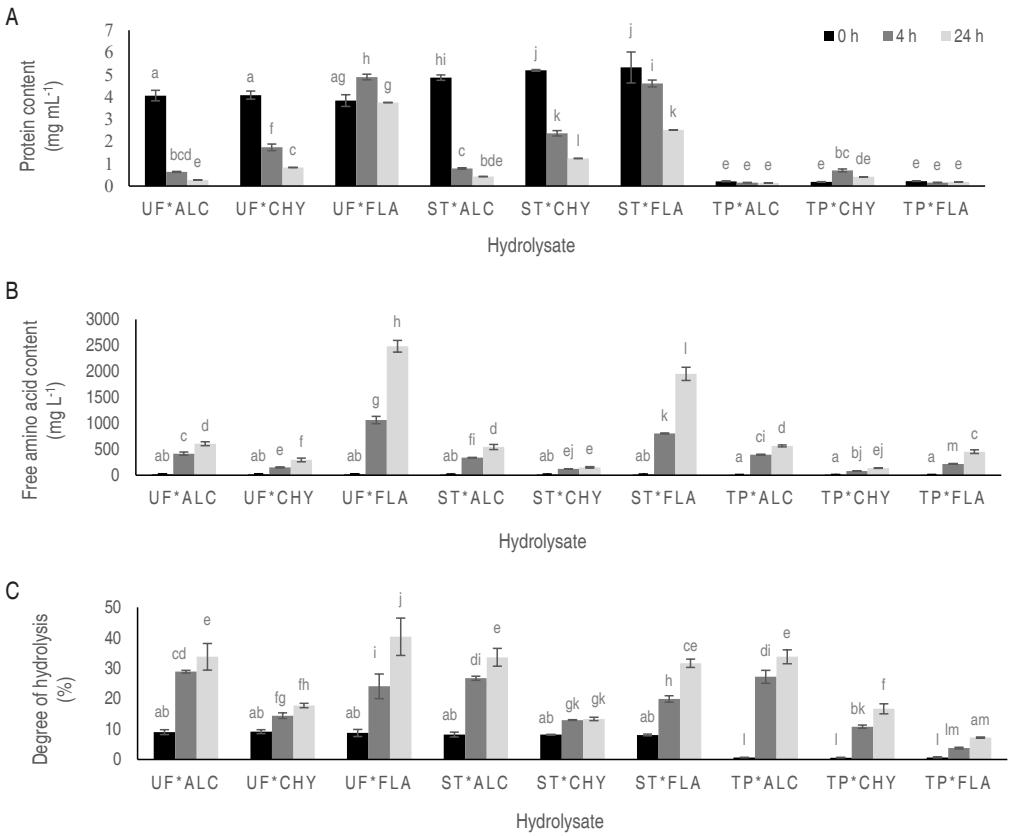

Figure 2. Soluble protein (A), free amino acids (B), and degree of hydrolysis (C) of whey protein concentrates obtained by ultrafiltration (UF), salt treatment (ST), and thermal precipitation (TP) hydrolyzed with alcalase (ALC), chymotrypsin (CHY), and flavourzyme (FLA) at 0 (black), 4 (gray), and 24 h (light gray) of hydrolysis. Results represent the meaning of three experimental repetitions ± standard deviation. Samples with different letters are significantly different (P<0.05).

Antioxidant activity of whey protein hydrolysates

Antioxidant activity of the UF, ST, and TP concentrates hydrolyzed with ALC, CHY, and FLA was examined *in vitro* by measuring the ABTS cation radical scavenging ability, reducing power, and iron-chelating capacity (Figure 3).

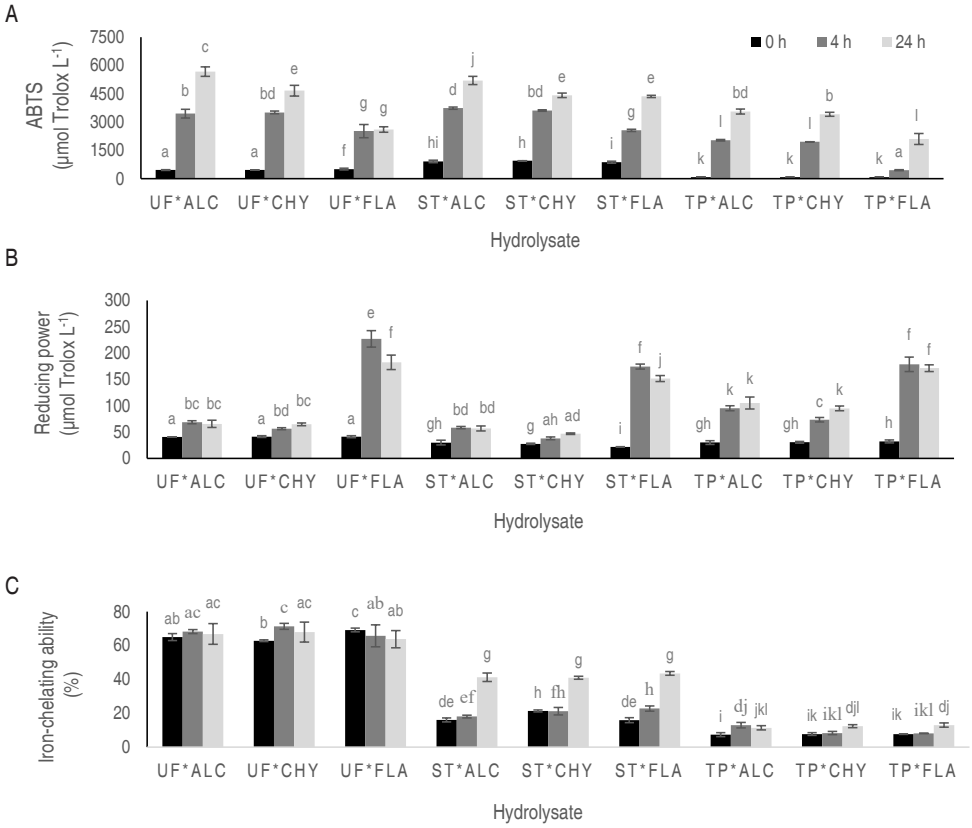

Figure 3. Antioxidant activity measured by ABTS assay (A), reducing power (B), and iron-chelating capacity (C) of whey protein concentrates obtained by ultrafiltration (UF), salt treatment (ST), and thermal precipitation (TP) hydrolyzed with alcalase (ALC), chymotrypsin (CHY), and flavourzyme (FLA) at 0 (black), 4 (gray), and 24 h (light gray) of hydrolysis. Results represent the meaning of three experimental repetitions±standard deviation. Samples with different letters are significantly different (P<0.05).

Both WPCs and their hydrolysates showed *in vitro* antioxidant activity. The enzymatic hydrolysis improved ABTS radical scavenging capacity and reduced the power of all concentrates, and iron-chelating activity of the ST and TP concentrates. As shown in Figure 3A, antioxidant activity determined by ABTS assay ranged from 2,523 to 3,448, 2,567 to 3,742, and 454 to 2,039 µmol Trolox L^{-1} in the UF, ST, and TP concentrates after 4 h of hydrolysis; and from 2,609 to 5,675, 4,360 to 5,199, and 2,101 to 3,560 µmol Trolox L^{-1} in the same concentrates at 24 h of hydrolysis, respectively. ABTS radical scavenging capacity increased with hydrolysis time. Concerning unhydrolyzed WPCs (0 h), this property increased 5-8-, 3-4-, and 5-24-fold after 4 h of hydrolysis, and 5-12-, 5-6-, and 24-42-fold after 24 h of digestion in the UF, ST, and TP concentrates, respectively. Although higher increases were detected in the TP concentrate, the UF and ST hydrolysates presented greater ABTS radical scavenging ability when compared at the same hydrolysis time. After 4 h of hydrolysis, this property was stronger when both concentrates were treated with ALC and CHY, and no statistically significant differences were detected between them. In addition, better radical scavenging capacity was exhibited in the UF and ST concentrates digested with ALC at 24 h of hydrolysis. These results suggest that the UF and ST methods could produce substrates that processed with ALC and CHY, generate hydrolysates with ABTS radical scavenging ability. The free

radical scavenging capacity of the hydrolysates may be attributed to peptides containing aromatic or hydrophobic residues that act through hydrogen donation (Shazly et al. 2017). Previous studies have revealed the antioxidant properties of whey protein hydrolysates measured by the ABTS assay. A WPC obtained by UF was hydrolyzed with alcalase, flavourzyme, and a mix of these enzymes, showing antioxidant activity by ABTS and ORAC, and its activity was higher when treated with ALC (Souza et al. 2019). Corrochano et al. (2019) prepared whey protein hydrolysates with alcalase, neutrase and bromelain from a bovine WPI, and evaluated their antioxidant properties. These hydrolysates exhibited ABTS radical scavenging ability, and their activity was higher in comparison with the unhydrolyzed counterpart.

Reducing power was also determined in all hydrolysates in order to measure the ability of each of them to donate electrons to iron (Figure 3B). Reducing power varied from 56 to 227, 38 to 174, and 73 to 179 µmol Trolox L^{-1} after 4 h of hydrolysis, and from 65 to 183, 47 to 152, and 95 to 171 µmol Trolox L^{-1} at 24 h of hydrolysis in the UF, ST, and TP concentrates, respectively. This property increased at 4 h of hydrolysis and a slight decrease was detected after 24 h in all concentrates treated with FLA. No statistically significant differences in the concentration hydrolyzed with ALC at 4 and 24 h of hydrolysis. Reducing power increased 1-6-, 1-8-, and 2-6-fold at 4 h, and 2-4-, 2-7-, and 3-5-fold at 24 h in the UF, ST, and TP concentrates, respectively, when hydrolyzed with ALC, CHY, and FLA, compared to time 0 h. All concentrates hydrolyzed with FLA showed higher reducing power, followed by the TP hydrolysates obtained with ALC and CHY. Previous studies have shown that the enzymatic hydrolysis of whey protein improved the reducing power. This property evaluated in a sheep whey hydrolysate obtained with a *Bacillus* sp. enzymatic preparation was 115% higher than the unhydrolyzed concentrate (Corrêa et al. 2014). Corrochano et al. (2019) found that the enzymatic hydrolysis significantly increased the reducing power of a WPI when hydrolyzed with alcalase, neutrase, and bromelain; and higher antioxidant activity by ABTS, ORAC, and reducing power was exhibited in the alcalase hydrolysate compared to the neutrase and bromelain hydrolysates. It is important to note that the presence of peptides, with specific sequences and determined sizes, in the hydrolysates could be responsible for the radical scavenging ability and reducing power by donating hydrogens or electrons, respectively. For example, aromatic amino acids can contribute to antioxidant potential by proton or electron transfer mechanisms (Zou et al. 2016; Shazly et al. 2017; Corrochano et al. 2019; Olvera-Rosales et al. 2023). Regarding the reducing power, the FLA hydrolysates showed a higher content of free amino acids and DH, and possibly contained short-chain peptides that could favor the reducing capacity. It has been reported that the low-molecular-weight peptides present in the whey hydrolysates can positively influence antioxidant properties (Zou et al. 2016). Additionally, higher antioxidant activity was observed in casein hydrolysates containing small peptides (Shazly et al. 2017).

Iron is a transition metal that can act as a promoter of the Fenton reaction for the generation of hydroxyl radicals. Its chelation could limit the iron available in free form to participate in this reaction (Zou et al. 2016). As observed in Figure 3C, the iron-chelating capacity of the UF, ST, and TP concentrates ranged from 66 to 71, 18 to 23, and 8 to 13% after 4 h of hydrolysis, and 64 to 68, 41 to 44, and 11 to 13% at 24 h of enzymatic digestion, respectively. The UF concentrate and its hydrolysates showed higher iron-chelating capacity, which was comparable to EDTA (62% at 40 µg mL^{-1}). No changes in the chelating ability of the UF concentrate treated with ALC were observed after 4 and 24 h compared to time 0 h. An increase in the chelating capacity of this concentrate when hydrolyzed with CHY, while a slight decrease when digested with FLA were detected in comparison with the unhydrolyzed UF concentrate. The ST and TP concentrates showed higher chelating properties at 24 h of hydrolysis with approximately 1.9-2.7- and 1.5-1.7-fold increments, respectively. Whey proteins can bind iron ions as observed in the different concentrates at time zero. Greater chelating capacity was detected in the UF concentrates, which might be due to that the UF process affects less the native protein structure compared to the precipitation methods, as indicated by Jiménez et al. (2012), where heating or the addition of chemical components (salts) may cause perturbations in the structure that could interfere with chelate formation. The iron-chelating activity of whey proteins and their hydrolysates have been reported previously. The ability of the main whey proteins, such as α-La and β-Lg, to bind iron has been indicated (Sugiarto et al. 2009). Moreover, sheep whey hydrolysates with ferrous-chelating ability were obtained by enzymatic hydrolysis using a protease

preparation from *Bacillus* sp. Their chelating capacity increased after 2 h of hydrolysis from 13.8% (unhydrolyzed concentrate) to 50.1% (Corrêa et al. 2014). Cruz-Huerta et al. (2016) obtained iron-binding peptides by hydrolysis of a WPI with alcalase, pancreatin, and flavourzyme. The iron-chelating capacity of hydrolysates could be related to the presence of peptides with similar structural characteristics; for example, carboxyl and amino groups in the amino acid side chain can influence (Athira et al. 2021). Cruz-Huerta et al. (2016) identified several iron-binding peptides rich in negatively charged amino acids, such as Asp and Glu. The ferrous-chelating capacity of WPI hydrolysate fractions obtained by enzymatic hydrolysis and ultrafiltration were also examined by O'Loughlin et al. (2015), where the 1-kDa permeate fraction showed chelating ability and had an abundant positively charged amino acid content, as Arg, His, and Lys. It is important to note that chelation could facilitate and enhance the bioavailability of iron and other minerals in humans in order to supply mineral deficiencies (Olvera-Rosales et al. 2023).

Enzymatic hydrolysis of different WPCs released peptides, which were able to scavenge free radicals, act as electron donors, and chelate metal ions such as iron. All these properties can contribute to the antioxidant activity of the hydrolysates produced (Zou et al. 2016; Olvera-Rosales et al. 2023). Differences in the antioxidant activity of hydrolysates were found depending on the method of protein concentration (UF, ST, and TP), type of enzyme (ALC, CHY, and FLA), and hydrolysis time (4 and 24 h) used in the hydrolytic process. WPCs obtained by UF and ST were more susceptible to enzymes in order to produce antioxidant hydrolysates. These processes could affect the protein structure, and thus the accessibility of enzymes to the protein substrate. Jiménez et al. (2012) indicated that protein structure in WPC is maintained after UF, which would be appropriate for the production of bioactive peptides, and structural conformation could be modified by the addition of chemicals (salts) to concentrate proteins. When ST is used, UF or dialysis are necessary for the removal of salts. Enzyme specificity can influence the composition of whey protein hydrolysates. ALC and FLA are non-specific peptidases (Merz et al. 2015; Corrochano et al. 2019), while CHY has substrate specificity (Gauthier and Pouliot 2003). As these enzymes cleave in different sites, the hydrolysates could be composed of peptides with different sizes and sequences, which can affect antioxidant activity (Zou et al. 2016). Possibly, ALC and CHY released principally peptides with radical scavenging ability and chelating capacity, while FLA produced mostly peptides containing electron donor residues. Regarding the physicochemical conditions used during hydrolysis, hydrolysis time can influence protein proteolysis. It is important to establish an accurate time to produce hydrolysates with biological activity (Corrêa et al. 2014). In this study, antioxidant activity measured by ABTS assay and chelating capacity increased as hydrolysis progressed in the mostly hydrolysates while reducing power was superior in the FLA hydrolysates obtained at 4 h of digestion.

CONCLUSION

The techniques used for whey protein recovery can significantly affect the final composition and yield of whey protein concentrates (WPCs). In turn, enzymatic hydrolysis can be influenced by the method of protein concentration, enzyme specificity, and time of hydrolysis, all of which impact the composition of the hydrolysates and their antioxidant activity. In this study, ultrafiltration (UF) and salt treatment (ST) were effective for the separation and concentration of proteins from Colombian double-cream cheese acid whey, leading to the production of WPCs, and subsequently antioxidant hydrolysates. The enzymatic hydrolysis of the WPCs enhanced their *in vitro* antioxidant properties. Specifically, the concentrates obtained by UF and ST showed better antioxidant capacity according to the ABTS assay and iron-chelating capacity when treated with ALC and CHY. Additionally, the concentrates enzymatically processed with FLA exhibited greater reducing power against iron. To gain a deeper understanding of these findings, future studies on the purification and characterization of hydrolysates are needed to establish possible relationships between structure and antioxidant activity. Furthermore, the use of UF, as a concentration method, and commercial enzymes, such as ALC and FLA, could be promising in obtaining antioxidant hydrolysates from acid whey, and further research on scaling these methods for industrial applications is deemed appropriate.

ACKNOWLEDGMENTS

This study was supported by Universidad Nacional de Colombia, Medellín Headquarters, Colombia (Project No. 201010017878), and Minciencias, Bogotá, Colombia (National Doctoral Program No. 647).

CONFLICT OF INTERESTS

The authors have no conflict of interest.

REFERENCES

Anzani C, Prandi B, Tedeschi T et al (2018) Degradation of collagen increases nitrogen solubilisation during enzymatic hydrolysis of fleshing meat. Waste Biomass Valorization 9:1113–1119. https://doi.org/10.1007/s12649-017-9866-4

AOAC (2002) Official Methods of Analysis, 16th edition. Washington DC

Athira S, Mann B, Sharma R et al (2021) Preparation and characterization of iron-chelating peptides from whey protein: An alternative approach for chemical iron fortification. Food Research International 141:110133. https://doi.org/10.1016/j.foodres.2021.110133

Corrêa APF, Daroit DJ, Fontoura R et al (2014) Hydrolysates of sheep cheese whey as a source of bioactive peptides with antioxidant and angiotensin-converting enzyme inhibitory activities. Peptides 61:48–55. https://doi.org/10.1016/j.peptides.2014.09.001

Corrochano AR, Sariçay Y, Arranz E et al (2019) Comparison of antioxidant activities of bovine whey proteins before and after simulated gastrointestinal digestion. Journal of Dairy Science 102(1):54–67. https://doi.org/10.3168/jds.2018-14581

Cruz-Huerta E, Maqueda DM, Recio I et al (2016) Short communication: Identification of iron-binding peptides from whey protein hydrolysates using iron (III)-immobilized metal ion affinity chromatographyand reversed phase-HPLC-tandem mass spectrometry. Journal of Dairy Science 99(1):77–82. https://doi.org/10.3168/jds.2015-9839

Embiriekah S, Bulatović M, Borić M et al (2018) Antioxidant activity, functional properties and bioaccessibility of whey protein hydrolysates. International Journal of Dairy Technology 71(1):243–252. https://doi.org/10.1111/1471-0307.12428

Gauthier SF and Pouliot Y (2003) Functional and biological properties of peptides obtained by enzymatic hydrolysis of whey proteins. Journal of Dairy Science 86:E78–E87. https://doi.org/10.3168/jds.S0022-0302(03)74041-7

Ghasemi M, Ahmad A, Jafary T, Azad AK, Kakooei S, Daud WRW and Sedighi M (2017) Assessment of immobilized cell reactor and microbial fuel cell for simultaneous cheese whey treatment and lactic acid/electricity production. International Journal of Hydrogen Energy 42(14):9107-9115. https://doi.org/10.1016/j.ijhydene.2016.04.136

Jayanthi P and Lalitha P (2011) Reducing power of the solvent extracts of *Eichhornia crassipes* (Mart.) Solms. International Journal of Pharmacy and Pharmaceutical Sciences 3 Suppl. 3: 126-128.

Jiménez XT, Cuenca AA, Jurado AT et al (2012) Traditional methods for whey protein isolation and concentration: effects on nutritional properties and biological activity. Journal of the Mexican Chemical Society 56(4):369–377 https://doi.org/10.29356/jmcs.v56i4.246

Khaire RA and Gogate PR (2019) Chapter 7 - Whey proteins. pp 193–223. In: Galanakis CM (ed) Proteins: Sustainable Source, Processing and Applications. Academic Press, London. 345 p.

Kilara A and Vaghela MN (2018) Chapter 4 - Whey proteins. pp 93–126. In: Yada RY (ed) Proteins in Food Processing, Second edition. Woodhead Publishing, Duxford. 654 p.

Londoño-Zapata AF, Durango-Zuleta MM, Sepúlveda-Valencia JU and Herrera CXM (2017) Characterization of lactic acid bacterial communities associated with a traditional Colombian cheese: Double cream cheese. LWT-Food Science and Technology 82(1): 39-48. https://doi.org/10.1016/j.lwt.2017.03.058

Lozano JM, Giraldo GI and Romero CM (2008) An improved method for isolation of β-lactoglobulin. International Dairy Journal 18(1): 55–63. https://doi.org/10.1016/j.idairyj.2007.05.003

Merz M, Eisele T, Berends P et al (2015) Flavourzyme, an enzyme preparation with industrial relevance: automated nine-step purification and partial characterization of eight enzymes. Journal of Agricultural and Food Chemistry 63(23): 5682–5693. https://doi.org/10.1021/acs.jafc.5b01665

Ministerio de Agricultura y Desarrollo Rural (2024) Comportamiento de los Precios de principales productos derivados lácteos en planta de proceso. In: Unidad de Seguimiento de Precios de Leche - USPL. https://uspleche.minagricultura.gov.co/Lacteos.html

Nishanthi M, Chandrapala J and Vasiljevic T (2017) Properties of whey protein concentrate powders obtained by spray drying of sweet, salty and acid whey under varying storage conditions. Journal of Food Engineering 214: 137–146. https://doi.org/10.1016/j.jfoodeng.2017.06.032

Nwachukwu ID and Aluko RE (2019) A systematic evaluation of various methods for quantifying food protein hydrolysate peptides. Food Chemistry 270: 25-31. https://doi.org/10.1016/j.foodchem.2018.07.054

O'Loughlin IB, Kelly PM, Murray BA et al (2015) Molecular characterization of whey protein hydrolysate fractions with ferrous chelating and enhanced iron solubility capabilities. Journal of Agricultural and Food Chemistry 63(10): 2708–2714. https://doi.org/10.1021/jf505817a

O'Loughlin IB, Murray BA, Kelly PM et al (2012) Enzymatic hydrolysis of heat-induced aggregates of whey protein isolate. Journal of Agricultural and Food Chemistry 60(19): 4895–4904. https://doi.org/10.1021/jf205213n

Olvera-Rosales LB, Cruz-Guerrero AE, García-Garibay JM et al (2023) Bioactive peptides of whey: obtaining, activity, mechanism of action, and further applications. Critical Reviews in Food Science and Nutrition 63(30): 10351-10381. https://doi.org/10.1080/10408398.2022.2079113

Quintanilla P, Beltrán MC, Molina A, Escriche I and Molina MP (2019) Characteristics of ripened Tronchón cheese from raw goat milk containing legally admissible amounts of antibiotics. Journal of Dairy Science 102(4): 2941-2953. https://doi.org/10.3168/jds.2018-15532

Shazly AB, He Z, El-Aziz MA, Zeng M, Zhang S, Qin F and Chen J (2017) Fractionation and identification of novel antioxidant peptides from buffalo and bovine casein hydrolysates. Food Chemistry 232(1): 753–762. https://doi.org/10.1016/j.foodchem.2017.04.071

Souza RSC de, Tonon RV, Stephan MP et al (2019) Avaliação do potencial antioxidante de proteínas do soro de leite concentradas por ultrafiltração e hidrolisadas por diferentes proteases comerciais. Brazilian Journal of Food Technology 22: 1–11. https://doi.org/10.1590/1981-6723.02118

Spellman D, McEvoy E, O'Cuinn G and FitzGerald RJ (2003) Proteinase and exopeptidase hydrolysis of whey protein: Comparison of the TNBS, OPA and pH stat methods for quantification of degree of hydrolysis. International Dairy Journal 13(6): 447–453. https://doi.org/10.1016/S0958-6946(03)00053-0

Sugiarto M, Ye A and Singh H (2009) Characterisation of binding of iron to sodium caseinate and whey protein isolate. Food Chemistry 114(3): 1007–1013. https://doi.org/10.1016/j.foodchem.2008.10.062

Tari NR, Gaygadzhiev Z, Guri A and Wright A (2021) Effect of pH and heat treatment conditions on physicochemical and acid gelation properties of liquid milk protein concentrate. Journal of Dairy Science 104(6): 6609-6619. https://doi.org/10.3168/jds.2020-19355

U.S. Dairy Export Council (2006) Reference manual for US whey and lactose products. Arlington, VA, USA. 226 p.

Wijayanti HB, Bansal N and Deeth HC (2014) Stability of whey proteins during thermal processing: A review. Comprehensive Reviews in Food Science and Food Safety 13(6): 1235–1251. https://doi.org/10.1111/1541-4337.12105

Yadav JSS, Yan S, More TT et al (2014) Recovery of residual soluble protein by two-step precipitation process with concomitant COD reduction from the yeast-cultivated cheese whey. Bioprocess and Biosystems Engineering 37: 1825–1837. https://doi.org/10.1007/s00449-014-1155-z

Zou T Bin, He TP, Li H Bin et al (2016) The structure-activity relationship of the antioxidant peptides from natural proteins. Molecules 21(1): 72. https://doi.org/10.3390/molecules21010072

Research article

https://revistas.unal.edu.co/index.php/refame

Revista Facultad Nacional de Agronomía

Characterization of rejected green banana flour: morphological, structural, and techno-functional properties

Caracterización de la harina de banano verde de rechazo: propiedades morfológicas, estructurales y tecnofuncionales

https://doi.org/10.15446/rfnam.v78n2.114205

Nelly Sánchez-Mesa[1], Katherine Manjarres-Pinzón[1], Eduardo Rodríguez-Sandoval[2]*, Jesus Gil-González[2] and Guillermo Correa-Londoño[3]

ABSTRACT

Green banana flour (GBF) stands out as a promising raw material for agribusiness due to its techno-functional and nutritional properties. In this study, the characterization of flour obtained from rejected green bananas (*Musa acuminata* AAA, cv. Cavendish) produced in the department of Magdalena, Colombia, located north of the country on the Caribbean coast, was made. Physicochemical, proximate, morphological, structural, and techno-functional parameters were evaluated, as well as their thermal properties and pasting parameters. GBF had a high ash content (2.89%) and a low-fat content (0.6%), which contributes to a high mineral content and flour stability, respectively. The BET mathematical model showed the best fit to describe water absorption in GBF. X-ray diffraction analysis showed a combination of type A and B starch crystallinity. Raman spectroscopy analyses identified characteristic bands, functional groups and molecular interactions related to starch, amylose, and amylopectin (476, 941, and 2,914 cm^{-1}) in the flour. GBF had a pasting temperature around 79.58 °C, good resistance to shear stress at high temperature, and a high tendency to retrogradation. The GBF gelatinization had an enthalpy value of 12.97 J g^{-1}, while the retrogradation enthalpy was 8.19 J g^{-1}. The thermal and pasting values support the starch tendency in GBF to retrograde; this is an attractive property to use GBF as a functional ingredient. This study established the potential of GBF as a promising solution to reduce post-harvest losses of rejected green bananas.

Keywords:
Cavendish
Isotherms
Microstructure
Starch
Thermal properties

RESUMEN

La harina de plátano verde (HBV) se destaca como una materia prima prometedora para la agroindustria por sus propiedades tecnofuncionales y nutricionales. En este estudio, se realizó la caracterización de una harina obtenida de plátano verde de rechazo (*Musa acuminata* AAA, cv. Cavendish) producido en el departamento de Magdalena, Colombia, ubicado al norte del país, en la costa Caribe. Se evaluaron parámetros fisicoquímicos, proximales, morfológicos, estructurales y tecnofuncionales, así como sus propiedades térmicas y parámetros de empastamiento. La HBV tuvo un alto contenido de cenizas (2,89%) y bajo contenido de grasas (0,6%), que contribuyen a un alto contenido mineral y estabilidad, respectivamente. El modelo matemático BET mostró el mejor ajuste para describir la absorción de agua en la HBV. El análisis de difracción de rayos X mostró una combinación de cristalinidad de almidón tipo A y B. Los análisis de espectroscopía Raman identificaron bandas características, grupos funcionales e interacciones moleculares relacionadas con el almidón, la amilosa y la amilopectina (476, 941 y 2.914 cm^{-1}) en la harina. La HBV tuvo una temperatura de gelatinización cercana al 79,58 °C, buena resistencia al esfuerzo cortante a alta temperatura y tendencia a la retrogradación. La gelatinización de la HBV tuvo un valor de entalpía de 12,97 J g^{-1}, mientras que la entalpía de retrogradación fue de 8,19 J g^{-1}. Los valores térmicos y de empastamiento apoyan la tendencia a la retrogradación del almidón en la HBV; esta es una propiedad atractiva para utilizar la HBV como ingrediente funcional. Este estudio estableció el potencial de la HBV como una solución prometedora para reducir las pérdidas postcosecha de plátanos verdes de rechazo.

Palabras clave:
Cavendish
Isotermas
Microestructura
Almidón
Propiedades térmicas

[1]Corporación Natural SIG. Biodiversity, Territory and People Research Group (BIOTEGE). Santa Marta DTCH, Colombia. coordinacion.tecnica@naturalsig.org, directoracientifica@naturalsig.org
[2]Departamento de Ingeniería Agrícola y Alimentos, Facultad de Ciencias Agrarias, Universidad Nacional de Colombia, Sede Medellín, Colombia. edrodriguezs@unal.edu.co, jhgilg@unal.edu.co
[3]Departamento de Ciencias Agronómicas, Facultad de Ciencias Agrarias, Universidad Nacional de Colombia, Sede Medellín, Colombia. gcorrea@unal.edu.co
*Corresponding author

Received: January 24, 2025; Accepted: March 14, 2025
Rev. Fac. Nac. Agron. Medellín 78(2): 11089-11102. 2025
ISSN 0304-2847 / e-ISSN 2248-7026

CC BY NC SA

Bananas are one of the most consumed fruits in tropical and subtropical regions (Singh et al. 2016). This fruit is also known for its high nutritional value (Singh et al. 2016). The largest producers of bananas in the world are India, China, and Indonesia, with a representation of 48%; followed by South American countries that participate with 16%: Ecuador and Brazil contribute 5% each, while Colombia ranks ninth with 3% of the world production (Minagricultura 2021).

In 2022, Colombia exported 108 million boxes (20 kg) of bananas from the Caribbean region. The Urabá Antioqueño exported 64 million boxes; while the rest of the Caribbean region, made up of the departments of Magdalena, Guajira, and Cesar sold 44 million boxes abroad (AUGURA 2022). However, there is a percentage of green bananas that do not meet the premium quality requirements of international markets, such as variety, number, size of fingers per bunch, color, appearance, calibration, packaging, and phytosanitary conditions for export (Stanley 2017). This generates economic losses for producers and environmental problems due to the natural degradation of the fruits, which produce toxic gases and leachates that affect water resources and soil quality. Consequently, it is necessary to find alternatives for processing rejected green bananas that favor their conservation and consumption. Due to their high perishability, bananas need to be dried during processing for longer shelf life and storability, as is the case with banana flour (Amarasinghe et al. 2021). The drying process is key and seeks to reduce the weight of the product, facilitating its transport and storage while preserving some of its original properties, such as protein and mineral content. Green banana flour (GBF) preserves the nutritional value of the fruit and also benefits the producer of fresh bananas economically, socially, and environmentally. Its potential as a functional ingredient in food systems could also be explored. Nevertheless, production in banana-growing regions is still artisanal due to the lack of specialized equipment and procedures for its transformation.

Some studies indicate that GBF has a starch content between 58.01 and 81.66% (dry basis) (Wang et al. 2012; Velandia 2019; Kumar et al. 2019; Ahmed et al. 2020; Chang et al. 2022), protein between 2.96 and 5.88%, ash between 1.89 and 3.68%, fat between 0.13 and 4.12% (Kumar et al. 2019; Ahmed et al. 2020; Amarasinghe et al. 2021; Chang et al. 2022; Alam et al. 2023). Moreover, some technofunctional properties of GBF have been reported, e.g., oil absorption index (OAI) from 1.1 to 1.83 (g g^{-1}), swelling capacity (SC) from 2.7 to 4.92 (g g^{-1}), water absorption index (WAI) from 0.93 to 2. 9 (g g^{-1}), and water solubility index (WSI) from 0.28 to 0.36 (g g^{-1}) (Ahmed et al. 2020; Amarasinghe et al. 2021; Alam et al. 2023), Carr's index from 9.38 to 12.06, and Hausner ratio from 1.11 to 1.14 (Alam et al. 2023). These characteristics suggest that GBF is an ingredient suitable for preparing functional products that could help reduce cholesterol and relieve constipation (Anyasi et al. 2015). In addition, GBF could be used to supplement bakery products, pasta, cookies, and baby foods (Aurore et al. 2009). The functionality of starch —the main component of GBF— can vary even within the same cultivar depending on environmental factors; there are structural and functional differences in green banana flour according to its origin and cultivar (Kumar et al. 2019). This research aims to characterize the flour obtained from rejected green banana (*Musa acuminata* AAA, cv. Cavendish) produced in the department of Magdalena, Colombia, by determining physicochemical, morphological, thermal, pasting, structural, and techno-functional properties. This could lay the foundations to establish its potential as a functional ingredient in the food industry.

MATERIALS AND METHODS

Plant material

The plant material was rejected green banana (*Musa acuminata* AAA, cv. Cavendish) from the municipalities of Aracataca, Ciénaga, and Zona Bananera (Department of Magdalena, Colombia). Bananas' ripeness stage was between 1 and 2 (green) (Ortega 2016; Jaramillo-Garcés et al. 2023).

Characterization of the raw material

The soluble solids content (°Brix), pH, titratable acidity, and moisture content were determined according to AOAC (2005) to characterize green banana pulp. Its water activity (a_w) was measured using a dew point hygrometer (AquaLab 3TE Series, Decagon Devices, Inc., Pullman WA, Pullman WA, USA) (Manjarres-Pinzon et al. 2024).

Obtaining GBF

Slices of the pulp with a thickness of 5 mm were obtained and immersed in an anti-browning solution. Subsequently,

they were dried in a convection oven (UF750, Memmert, Germany) at 55 °C for 15 h, then ground and stored at room temperature (25 °C) in metalized bags until further analysis (Jaramillo-Garcés et al. 2023).

Physicochemical and proximate characterization of GBF

The following physicochemical parameters of the GBF were determined: pH, titratable acidity, moisture content, and water activity (a_w) (AOAC 2005). Color parameters were determined according to the CIELAB color scale: L*=0 (black) to L*=100 (white), –a* (green) to +a* (red), and –b* (blue) to +b* (yellow). Color parameters L*, a*, b*, chroma (C*), and hue angle (h*) were measured; in addition, the yellowness (YI) and whiteness (WI) indices were calculated using Equations (1) and (2) proposed by Borneo et al. (2016), respectively.

$$YI = \frac{142.86b}{L} \quad (1)$$

$$WI = 100 - ((100 - L)^2 + a^2 + b^2)^{1/2} \quad (2)$$

GBF sorption isotherms were determined using the static gravimetric method, as described by Gutiérrez et al. (2018). The moisture content of the samples was measured after reaching equilibrium at specific water activities maintained using saturated salt solutions, including potassium acetate (CH_3COOK), magnesium chloride ($MgCl_2$), potassium carbonate (K_2CO_3), magnesium nitrate ($Mg(NO_3)_2$), potassium iodide (KI), sodium chloride (NaCl), and potassium chloride (KCl). These experiments were performed at temperatures of 15, 25, and 35 °C. Thymol (0.5 g) was added to containers with an a_w>0.5 to prevent microbial growth. Initial sample weights were recorded, and final weights were measured after 40 days when equilibrium was reached. Sorption isotherms were fitted using several models, including GAB (Guggenheim-Anderson-de Boer), BET (Brunauer-Emmett-Teller), SMITH and OSWIN. Non-linear regression was used to calculate model parameters, minimizing the root mean square error between the experimental data and the model predictions. The moisture content of the sample was determined after having reached equilibrium with the air of known relative moisture (a_w between 0.234 and 0.859) at 15, 25, and 35 °C. Proximate analyses of GBF were conducted according to AOAC (2005) to determine levels of crude protein, ash, fat, native starch, and total fiber. The amylose content was determined by adding 10 mg of sample (dry basis) to 10 mL of DMSO (95% w/w). The suspension was heated in a water bath at 80 °C for 15 min under constant stirring. The mixture was cooled to room temperature and allowed to stand for 15 min. A solution of I_2/KI (100 µL) and distilled water (1,800 µL) was then added to 100 µL of the sample and allowed to react for 20 min in the dark. Finally, the absorbance was measured at a wavelength of 620 nm in a spectrophotometer (Thermo Scientific, Genesys 10S). The calibration curve was established using potato amylose and maize amylopectin standards at concentrations between 0-100% w/v (Figueroa-Flórez et al. 2024).

Morphological characterization of GBF

The birefringence of GBF samples was determined by observation under polarized light of GBF suspensions in deionized water; a binocular microscope (Leica, DM1000 led, Japan) with 40X magnification and equipped with a digital camera (Leica, ICC50W, Japan) was employed. The granular morphology of the GBF samples was evaluated with a Scanning Electron Microscope (SEM) (Zeiss, EVO MA10). Samples were placed in a sample holder with electroconductive carbon tape and covered with a platinum/gold alloy. The observation conditions of the samples were established at 15 kV, 30 mA, and magnifications of 400X and 800X.

Structural characterization of GBF

Particle size distribution was estimated by light scattering using a particle analyzer (Mastersizer 3000E, Malvern Instruments Ltd., UK); a refractive index value of 1.52, an absorption index of 0.05, and a mode of operation using air as a dispersing agent were employed. Particle size was expressed as a function of mean diameters D (10), D (50), D (90), D [3;2], and D [4;3]. The diffraction patterns of the samples were obtained on an X-ray diffractometer (X'Pert Pro- MPD, Panalytical, Italy). Intensities were detected in a range of Bragg 2θ angles of 5-70°, with a current of 30 mA and 40 kV of operation. The degree of crystallinity was estimated from the ratio of the crystalline areas and the total area (crystalline + amorphous) obtained by data processing using Matlab R2019a (MathWorks, R2019a, USA) (Padhi and Dwivedi 2022). The data were then smoothed using the Savitzky–Golay algorithm and the deconvolution process was developed using the Gaussian

function in the 5–30° region (Figueroa-Flórez et al. 2024). The intensity values of the XRD patterns were normalized by dividing them by the maximum intensity of the most prominent peak. Crystalline peaks were identified using a peak-finding algorithm in Matlab, which detected local maxima above a predefined threshold. The areas under the crystalline peaks were then integrated. The Raman spectra of the samples were collected using a Raman spectrometer (Horiba Scientific, LabRAM HR Evolution) with a 600 nm laser source, 5 mW power, 1 s acquisition time, and a 50X objective lens.

Thermal properties and pasting parameters of GBF

The thermal properties of the flour samples were determined using a differential scanning calorimeter (DSC 250, TA Instruments, USA). Flour/water suspensions (3.4 mg flour/10 µL water) were prepared in aluminum capsules, sealed, and kept refrigerated for 24 h. The thermal properties of each treatment were evaluated using a heating ramp from 30 to 120 °C at 10 °C min^{-1}; followed by a cooling ramp down to 30 °C at 25 °C min^{-1}. Subsequently, the capsule containing the gelatinized starch was stored at refrigeration temperature (4 °C); after 15 days, the thermal properties were determined under the same operating parameters of the DSC. An empty aluminum capsule was used as a reference. The following parameters were obtained from the thermograms and the TA Universal Analysis software (TA Instruments, USA): onset temperature (To), peak temperature (Tp), end temperature (Tf), gelatinization enthalpy (J g^{-1}) (ΔH), and retrogradation enthalpy (J g^{-1}) (ΔHr).

Pasting parameters were measured on a micro visco-amylograph (Brabender GmbH & Co. KG, Duisburg, Germany) coupled to a thermostat bath (F-12ED, Julabo, Baden-Wuerttemberg, Germany). The GBF/water suspension (5 g GBF/110 mL water) was heated from 30 to 95 °C at a rate of 7.5 °C min^{-1}, temperature was maintained at 95 °C for 5 min; subsequently, the sample was cooled to 50 °C at a rate of 7.5 °C min^{-1}; finally; the temperature was maintained for 5 min. Viscosities were recorded in Brabender Units (BU) and parameters such as pasting temperature, peak viscosity, breakdown, setback, and final viscosity were determined.

Techno-functional properties of GBF

The oil absorption index (OAI), swelling capacity (SC), water absorption index (WAI), and water solubility index (WSI) were determined according to the methodologies employed by Rodríguez-Sandoval et al. (2014). The bulk density was calculated by weighing 2 g of flour and measuring its volume in a 10 mL test tube. Subsequently, in the same tube, manual vibration was applied to the flour, and the volume was measured again to calculate the compacted density. The Carr index and Hausner ratio were calculated with bulk density and tapped density using the equations proposed by Moravkar et al. (2020). Finally, to determine the minimum gelation concentration (MGC) in test tubes, aqueous suspensions of GBF (5 mL) were prepared at concentrations of 2, 4, 6, 8, 10, 12, 14, 16, 18, 20 and 22%. Subsequently, the suspensions were vortexed for 30 seconds at 3,000 rpm and brought to a water bath (with stirring) for 45 min at 85 °C. The suspensions were then cooled with ice-water and stored at 4 °C for 24 h. The minimum gelation concentration was determined as the concentration at which the sample did not slip from the inverted test tube.

Statistical Analysis

All experiments were done in triplicate. The mean and standard deviation of all properties were calculated using Statgraphics (Centurion XVIII). In the isotherms, model parameters were estimated using the DATAFIT 9 non-linear regression software (Oakdale Engineering).

RESULTS AND DISCUSSION

Characterization of the raw material

Results of the physicochemical analysis of rejected green banana pulp are shown in Table 1. Its physicochemical parameters vary depending on cultivar, ripening stages, and environmental conditions (Melgarejo 2012). However, some of the values obtained for the Cavendish cultivar coincide with the parameters reported by different authors for other green-ripening banana cultivars (Ahmed et al. 2020; Anyasi et al. 2015). In particular, the pH and acidity values obtained from the pulp agree with the results reported by De Souza et al. (2021) for the same cultivar; however, substantial differences were obtained with respect to the soluble solids content (1.39 compared to values close to 11%). This could be associated with the ripening stage of the fruit. In this study, it was approximately 11 (Brix/acidity), which indicates that the fruits used to obtain GBF were at the first stage (Khoozani et al. 2019). Acidity is closely

related to the taste of the fruit (Ahmed et al. 2020) and is mainly represented by malic, citric, and oxalic acids; the latter contributes significantly to the astringency of the green fruit. High moisture and a_w values indicate microbiological instability; however, this can be mitigated by the low acidity and pH values found in the pulp. With a moisture of 74.06%, the net dry matter weight (flour) is expected to be around 26%.

Table 1. Physicochemical characterization of fresh green banana pulp.

Analysis	Mean ± standard deviation
Moisture (%)	74.06±0.98
a_w	0.983±0.01
pH	5.61±0.13
Acidity (%)*	0.13±0.07
°Brix	1.39±0.30

*Expressed as a percentage of malic acid.

Physicochemical and proximate characterization of GBF

GBF was obtained with a yield of 10% and with a moisture content of 7.2% (Table 2). This value meets the quality standard limits (<10%) for banana flours in Colombia (ICONTEC 2020) and is lower than that recommended for fruit powders (13%). A low-moisture product is considered stable against microbial spoilage (Pragati et al. 2014). Moisture content and a_w were similar to those reported in GBF dehydrated by convection at 50 °C (5.09% and 0.25) (Khoozani et al. 2019). These parameters, which assess the availability of water for use by microorganisms, are indicators of the physical, chemical, and microbial stability of the product and, therefore, the shelf life of food (Khoozani et al. 2019).

Table 2. Physicochemical results for green banana flour.

Analysis	Mean ± standard deviation
Moisture (%)[2]	7.2±0.8
Acidity[1]	0.16±0.04
pH	5.36±0.15
a_w	0.227±0.031
Native starch (%)[2]	81.95±4.45
Amylose (%)	23.94±1.27
Crude protein content (%)[2]	4.45±0.35
Ash (%)[2]	2.89±0.54
Fat content (%)[2]	0.6±0.14
Total Dietary Fiber (%)[2]	7.85±1.06
Color	
L*	44.88±6.03
a*	1.24±0.29
b*	8.46±0.94
C*	8.56±0.94
WI	44.20±0.94
YI	27.06±1.96
h*	81.58±1.98

Table 2

Analysis	Mean ± standard deviation
Particle Size	
D (10) (µm)	29.4±7.2
D (50) (µm)	230.1±89.2
D (90) (µm)	1,377.1±213.0
D [3;2] (µm)	75.6±16.8
D [4;3] (µm)	487.3±91.3

[1]Expressed as a percentage of malic acid. [2]Results expressed on a dry basis. WI: whiteness index. YI: yellowness index. h*: Hue angle.

The values of pH and acidity in GBF are low because they are related to the ripeness state of the raw material (green). The presence of various oxo acids has been reported in the pulp of green bananas; oxalic, malic, and citric acids contribute to the acidity of green banana flour (Drapal et al. 2024).

The ash content was high compared to the reported values (1.89-3.25%) in GBF obtained from different banana varieties (Kumar et al. 2019). The quality of the flour depends on the ash content, which provides the Cavendish variety with minerals, especially sodium and magnesium (Pragati et al. 2014). The fat content was less than 0.50 g 100 g^{-1}, thus favoring the stability of the flour because oxidative rancidity reactions are not favored. GBF samples have a starch content of more than 80%, which is higher than that reported for other cultivars (Ahmed et al. 2020; Chang et al. 2022), and an amylose percentage similar to that reported in the literature (Campuzano et al. 2018; Chang et al. 2022).

Color is a sensory attribute that impacts the degree of consumer acceptance. Variability in the luminosity (L*) of GBF samples could be associated with darkening reactions caused by the action of polyphenol oxidase (Zamudio et al. 2010), or by non-enzymatic browning associated with the reaction of starch with proteins during drying. Furthermore, the values of a* —which represents the coordinate of the red-green colors—, and b* —which represents the coordinates of the yellow-blue colors— were 1.24±0.29 and 8.46±0.94, respectively. These values agree with a reddish (a*) and yellowish (b*) hue of the flour. This result, as well as the C* values, could be related to the presence of carotenes and other pigments in the pulp and enzymatic reactions (Campuzano et al. 2018). Likewise, the C* value of food increases along with the concentration of pigment and decreases markedly as the samples darken.

The hue (h*) of GBF tends towards yellow, with values close to 90°. In addition, chromaticity resulted in 8.56±0.94, with a more saturated coloration. The whiteness index (WI) (44.20±0.94) and the yellowness index (YI) (27.06±1.96) are the result of the effect of temperature on the color and quality of GBF. High WI and low YI values are preferable because incorporating flours into a food matrix (e.g., baking) should not affect the color of the final product (Padhi and Dwivedi 2022). Kumar et al. (2019) reported higher WI (>80) and YI (15 to 40) values in GBF obtained from different banana cultivars.

The particle size distribution of GBF is shown in Table 2. The average values of D (10), D (50), and D (90) represent GBF particles smaller than the average particle size in flour samples (i.e., 10, 50, and 90%) (Wu et al. 2022). Results show a fraction of starch granules corresponding to type A (5-60 µm) (Vogel et al. 2018). Although the values of D (50) and D [4;3] suggest a high proportion of small particles related to intense milling conditions, 90% of the mass of the particles has a size equal to or less than 1,377.1 µm, and the remaining 10% of the particles are larger than that, thus indicating a heterogeneous distribution. These values are important considering that in powdered products used in food preparation, a higher degree of solubility and dispersibility is observed when they have smaller and finer particles. When the specific surface area is important, the mean Sauter diameter D [3;2] is measured, as it is more sensitive to the presence of fine particles in the size distribution. Whereas the volume means diameter D [4;3] reflects the size of the particles that make up the bulk of the sample volume and

is more sensitive to the presence of large particles in the size distribution.

Isotherms and sorption models

Four mathematical models (GAB, BET, SMITH, and OSWIN) were adjusted to describe the water sorption behavior of GBF at 15, 25, and 35 °C, and some indices were calculated to determine the quality of the adjustment. Figure 1 shows the BET working isotherms obtained for GBF at different temperatures. They show the relationship between water activity and equilibrium moisture content. The isotherms obtained are sigmoidal type II; these are common in foods such as fruits and vegetables, and in foods that have a high starch content (Ayala-Aponte 2016). According to Cardoso and Pena (2014), these types of isotherms are models with an adequate level of adjustment for GBF and can also indicate a porous structure of the flour. Similarly, the equilibrium moisture increased with the increase in the a_w value; several authors found a similar behavior (Bezerra et al. 2013; Susilo et al. 2019).

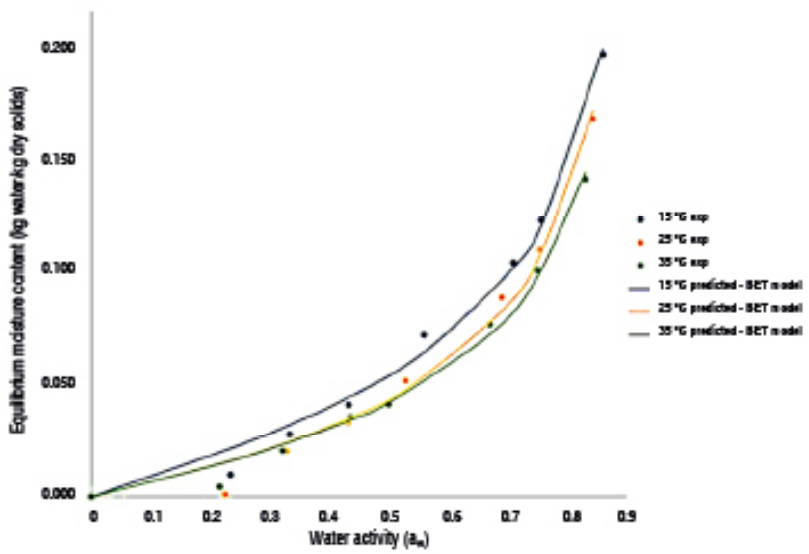

Figure 1. Moisture adsorption isotherms of green banana flour at 15, 25, and 35 °C.

Starch sorption may be influenced by hydrogen bonds between water molecules and available hydroxyl groups on amylose and amylopectin chains, especially in amorphous areas and on crystal surfaces (Aguirre-Cruz et al. 2010). The crystalline regions of the starch show a lower permeability to solvents. As a result, the presence of water acts as a plasticizer of the amorphous areas and affects the starch structure.

The exponential behavior of isotherms for a_w levels greater than 0.6 indicated that GBF peaked at 0.20, 0.17, and 0.14 kg water/kg dry solids at 15, 25, and 35 °C, respectively. Some authors indicate that relative humidity (RH) values below 0.60 guarantee the stability of some products under storage conditions (Gutiérrez et al. 2018; Cardoso and Pena 2014).

The adjusted parameters of the used sorption models are presented in Table 3. The BET, OSWIN, and SMITH models had the lowest CME and E_{RMS}. values, respectively. This suggests that they have the best fit to the experimental data and good accuracy of the models in predicting data compared to the GAB model, which showed higher CME and E_{RMS}. values. It was also observed that the BET and OSWIN models presented low *P* values, thus indicating a statistically significant adjustment to the experimental data. Similarly, different trends are observed when examining the predictor variables of the models as a function of temperature. In GAB and BET, they presented the highest Wm value (moisture content of the monolayer) at 35 °C, indicating that water sorption is more pronounced at this temperature. Likewise, C showed an increase in BET at 35 °C, suggesting a higher rate of water adsorption. In

the case of the OSWIN model, the value of "a" decreases as the temperature increases, which may be due to a lower water adsorption capacity at higher temperatures. Finally, in the SMITH model, the parameters "a" and "b" appear to be independent of temperature, as they remained constant under the three evaluated conditions.

Table 3. Estimated parameters and adjustment indices of various sorption models for banana flour.

Model	Constant	15 °C	25 °C	35 °C
GAB $M = W_m \frac{Ca_w}{(1-Ka_w)(1-Ka_w+CKa_w)}$	Wm	0.87890	0.68664	1.01997
	C	0.17383	0.19410	0.11791
	k	0.39458	0.42454	0.39240
	R^2	0.92888	0.94260	0.94810
	P	0.00563	0.00491	0.00307
	CME	0.00141	0.00098	0.00061
	E_{RMS}.	0.00035	0.00031	0.00019
BET $M = W_m \frac{Ca_w}{(1-a_w)(1-a_w+Ca_w)}$	Wm	0.29957	0.14209	0.16401
	C	0.28664	0.28664	0.37861
	R^2	0.99177	0.98797	0.99116
	P	0.00026	0.00030	0.00016
	CME	$2.586x10^{-05}$	$5.081x10^{-05}$	$2.586x10^{-05}$
	E_{RMS}.	$1.608x10^{-05}$	$1.906x10^{-05}$	$9.696x10^{-06}$
SMITH $M = a - b\ln(1-a_w)$	a	$1.000x10^{-02}$	$1.000x10^{-02}$	$1.000x10^{-02}$
	b	0.09288	0.08223	0.07425
	R^2	0.99113	0.9937	0.9961
	CME	$5.6999x10^{-04}$	$5.5351x10^{-4}$	$3.6595x10^{-4}$
	E_{RMS}.	$1.4250x10^{-04}$	0.000172972	$1.1436x10^{-4}$
OSWIN $M = a\left[\frac{a_w}{1-a_w}\right]^b$	a	0.05352	0.04363	0.04187
	b	0.73784	0.82608	0.79217
	R^2	0.99004	0.9876	0.9901
	CME	$7.13035x10^{-05}$	$6.01137x10^{-05}$	$3.23386x10^{-05}$
	E_{RMS}.	$1.78259x10^{-05}$	$1.87855x10^{-05}$	$1.01058x10^{-05}$

M: equilibrium moisture content; a_w: water activity; a, b, C and k: model parameters estimated by least squares; Wm: moisture content of the monolayer.

The BET model for equilibrium moisture content showed better fits with respect to the experimental data, it presents the lowest CME and E_{RMS}. values for the temperatures tested.

The data obtained showed that GBF tends to absorb more water with increasing temperature at a certain aqueous activity. This can be attributed to the increased mobility of water molecules and the adsorption energy of water as temperature increases (Ayala-Aponte 2016). In addition, the mathematical models GAB, BET, and OSWIN showed changes in their parameters as a function of temperature, indicating a significant dependence of GBF sorption behavior on temperature.

Birefringence and Scanning Electron Microscopy (SEM)

Micrographs obtained by polarized light microscopy (Figure 2) show elongated and oval-shaped granules, similar to those found by Chávez-Salazar et al. (2017). In addition, the formation of the Maltese cross indicates that there is a high degree of molecular orientation within the granule, and that these did not undergo internal decomposition or gelatinization during the drying and

grinding process (Chávez-Salazar et al. 2017). The Maltese cross also indicates that the starch is native, and that the crystal arrangement is anisotropic.

Generally, birefringence studies are linked to the study of starch gelatinization, a process by which starch granules absorb water when heated to a temperature close to 65 °C (depending on the starch) and a dispersion above 30% moisture content. Once the granules reach their maximum volume, they partially break down and leach amylose and amylopectin, leading to the loss of the original organization of the granule and birefringence.

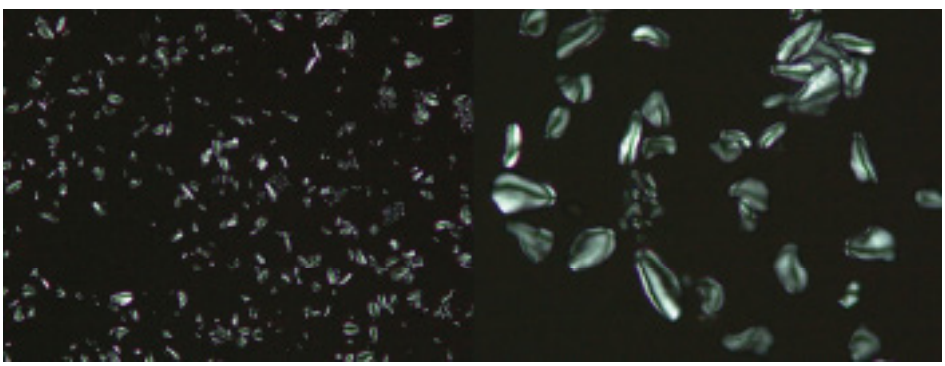

Figure 2. Polarized light microscopy of the starch granules present in GBF observed with 10X and 40X lenses.

Figure 3 shows GBF morphology at 400X and 800X magnification. Granules of unequal sizes, between 19 and 76 µm, and irregular shapes were observed; the elongated shape was predominant. The shape of these granules was similar to that found by Chang et al. (2022) in 6 varieties of green bananas from Tanzania, also finding a variation in sizes between 25.27 and 65.83 µm. The image also showed a layer that covers the granules and is mainly composed of pectin and cellulose (Salvador et al. 2000); moreover, the granules exhibited their complete shape because starch did not disintegrate during drying.

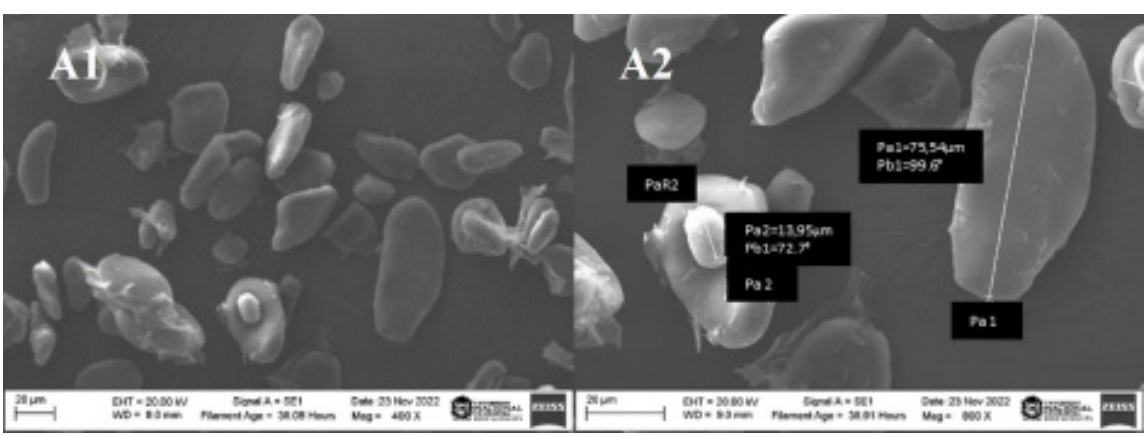

Figure 3. Scanning electron micrographs of GBF (A1:400X, A2:800X).

X-ray diffraction and RAMAN Spectrum

Green banana pulp contains up to 70-80% starch by dry weight; starches are generally classified into three types: A, B, and C according to the type of X-ray diffraction pattern shown by their crystalline lamellae. The type of diffraction pattern depends mainly on the arrangement of amylopectin double helices chains and the agronomic and environmental conditions of the crop (Vega-Rojas et al. 2021). Kumar et al. (2019) reported that banana flour made of the Grand Naine, Monthan, and Saba varieties have a crystallinity of 12.22, 15.31, and 9.38%, respectively. Crystallinity will vary according

to the banana cultivar used for the analysis and to the influence of the chemical composition of the flour, i.e., ash, lipid, protein, and fiber content (Padhi et al. 2022).

The X-ray diffraction pattern and Raman spectrum for the GBF sample are shown in Figure 4. The diffractogram (Figure 4A) presented the characteristics of a mixture of type A and B starch crystallinity with strong peaks at approximately 15, 18, and 23°, similar to that reported by Kumar et al. (2019) in five GBFs obtained from different banana varieties. The percentage of crystallinity calculated for GBF was 31.30%, a value similar (29.29%) to that reported by Campuzano et al. (2018) in GBF from the cultivar *Musa acuminata* (AAA), var. Cavendish.

In the Raman spectrum (Figure 4B), spectral bands between 400 and 800 cm^{-1} are attributed to the bending vibrations of C–C–C and C–C–O and torsional vibrations C–O (Mir and Bosco 2014). Some characteristic starch bands have been reported at 400, 430, 469, 518, 708, and 758 cm^{-1} (Czekus et al. 2019). The band at 476 cm^{-1} is considered typical of the starch skeleton. The vibrations originating from the α-1,4 glycosidic bonds can be observed as strong Raman bands in the region of 920–960 cm^{-1}; in fact, the band observed at 941cm^{-1} has been assigned to the skeletal mode vibrations of the α-1,4 glycosidic bond (C–O–C) in starch (Mir and Bosco 2014). Finally, the strong band at 2914 cm^{-1} has been related to the symmetrical and asymmetrical stretching of the C-H

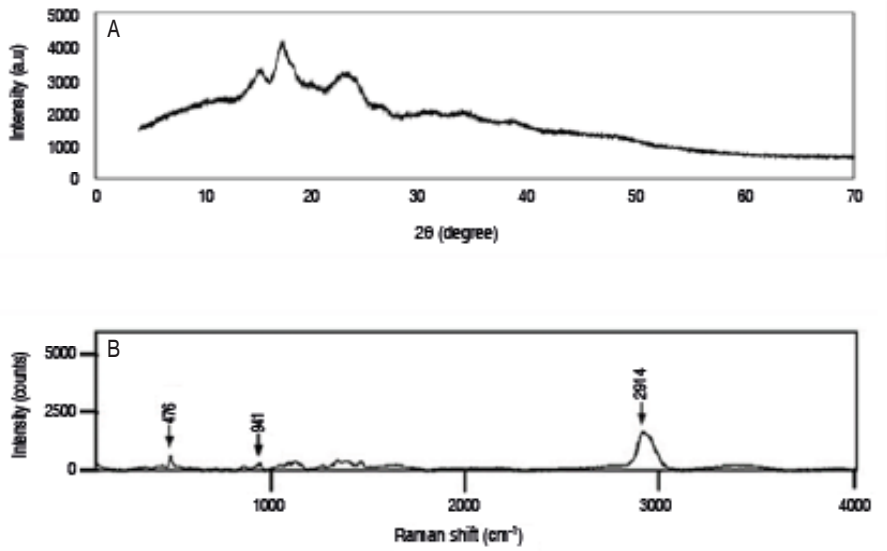

Figure 4. GBF X-ray diffraction (A) and Raman spectroscopy (B).

bond. According to Kizil et al. (2002), intensity changes in this range can be largely attributed to variations in the amount of amylose and amylopectin present in starches.

Thermal and pasting properties of GBF

Results obtained from differential calorimetry analysis of GBF are presented in Table 4. The gelatinization initiation and termination temperature ranged between 74.93±0.15 and 82.17±0.32 °C, respectively, with a peak or gelatinization temperature of 78.35±0.21 °C and a gelatinization enthalpy of 12.97±1.55 J g^{-1}. It has been reported that peaks with a narrow temperature range indicate lower heterogeneity of amylopectin crystals because they become disorganized during heating in a lower temperature range. Similar values were reported by Tribess et al. (2009) for different GBFs obtained from *Musa acuminata* (AAA), cv. Cavendish, under different drying conditions. The Tp and ΔHg values were lower and ranged from 67.95±0.31 to 68.63±0.28 °C and from 9.04±1.71 J g^{-1} to 11.63±1.74 J g^{-1}, respectively. These differences occur because the thermal transitions of starch depend on factors typical of the grain, such as its shape, the type of association of amylose molecules with amylopectin and lipids (complexes), and the alignment of hydrogen bonds in the crystalline region, among others.

During retrogradation, water-dispersed amylose and amylopectin molecules rearrange during storage to form ordered structures. The retrogradation tendency of gelatinized starches is commonly measured by thermal analysis (DSC). The amount of energy required to dissociate the annealed amylopectin molecules after 15 days of storage in GBF was 8.19±1.37 J g^{-1}, lower than that observed during GBF gelatinization. However, it indicates the high content of retrograde starch that can be obtained from GBF. Additionally, lower transition temperatures (Tor, Tpr, and Tfr) were compared to those obtained in gelatinization, indicating that the reassociation of amylopectin during storage is not similar to the ordering present in the native state.

Pasting parameters play an important role in the choice of flour, since they make it possible to analyze the behavior of a suspension formed by flour and water in a heating/cooling cycle. These properties depend on the type of processing used to obtain the flour, the amylose, protein and lipid content and the stiffness of the starch granules, which also influence their swelling capacity (Devi and Haripriya 2014). Moreover, these properties make it possible to determine the function of flour in the food industry to be used as a thickener, binder, or for any other use.

The results obtained for GBF are summarized in Table 4. The found pasting temperature was similar to that reported (72.51 °C) by Chang et al. (2022). The pasting temperature is affected by the presence of other flour components that compete for water, such as proteins. The flour was consistent after cooling and reached a higher final viscosity value compared to the peak viscosity. It also exhibited good shear strength at high temperature (95 °C), with a decrease in peak viscosity of approximately 6 BU. Finally, the setback value may indicate a tendency of flour to gel formation or rapid retrogradation associated with amylose (López-Ochoa et al. 2022). This could be associated with a high content

Table 4. Thermal and pasting properties of GBF.

Pasting Properties	Mean ± standard deviation
Peak Viscosity (BU)	113.38±5.35
Breakdown (BU)	5.75±1.73
Setback (BU)	18.88±4.27
Final viscosity (BU)	137.38±14.15
Pasting temperature (°C)	79.58±0.61
Thermal properties (gelatinization, day 0)	
To (°C)	74.93±0.15
Tp (°C)	78.35±0.21
Tf (°C)	82.17±0.32
ΔHg (J g^{-1})	12.97±1.55
Thermal properties (retrogradation, day 20)	
Tor (°C)	46.11±1.18
Tpr (°C)	65.85±0.41
Tfr (°C)	78.89±0.70
ΔHr (J g^{-1})	8.19±1.37

*BU: Brabender units.

of resistant starch in green banana flour, as reported by several authors (Kumar et al. 2019; Khoozani et al. 2019).

Techno-functional properties of GBF

The influence of the flow and compression properties of banana flour on its quality was evaluated (Table 5). The Hausner ratio (HR) and the Carr index (CI) were determined, which are obtained from the apparent and compacted densities of the material. HR is a measure of the degree of cohesion between particles of the powder, while CI is a measure of the variation of the density of the material when subjected to an external force. The results showed low fluidity and a

tendency to agglomeration, which could negatively affect its handling and processing. Banana flour was also found to have moderate compressibility. Similar results were reported by Grisi et al. (2021) in flour obtained from juca (*Libidibia ferrea*) and higher compared to GBF results from different drying methods (Alam et al. 2023). This feature can make it difficult to accurately dose flour in production processes and could compromise the performance and quality of the final product. Findings suggest that drying conditions, adding anti-agglomerating agents, among other possible solutions, are required in banana flour to obtain more uniform particles and optimize its use in the food industry. Similarly, Table 5 shows the results of the hydration, solubility, and gelling properties of GBF. In flours, the water absorption index (WAI) is an indicator of the yield of fresh dough, while the oil absorption index (OAI) is related to the hydrophobic character of the starch present in it. The content and nature of starch, the amount of protein and insoluble fiber in flour can influence those values.

Table 5. Techno-functional properties of rejected green banana flour.

Parameters	Value
Hausner ratio	1.340±0.069
Carr Index	25.202±3.781
WAI (g g^{-1})	3.060±0.158
WSI (g g^{-1})	6.326±0.730
SC (g g^{-1})	3.269±0.173
OAI (g g^{-1})	0.760±0.071
MGC (%)	6±0

Khoozani et al. (2019) reported similar WAI values (3.01) for GBF obtained at 50 °C but found higher OAI values (2.77) compared to those obtained in this study.

While the WSI is related to the number of soluble solids in the flour, SC represents the interaction between the starch chains within the amorphous and crystalline domains of the starch granule and is influenced by the characteristics of amylose and amylopectin. Bezerra et al. (2013) found lower WSI values (1.22-1.9 g g^{-1}) in GBF obtained at 80 and 90 °C. In contrast, the GBF SC values were lower than those reported by Ortega (2016) and Bezerra et al. (2013), although closer to those reported by Padhi and Dwivedi (2022), who found a SC of 2.54±0.45. A low SC value indicates the presence of higher binding forces inside the starch granules and a higher importance of the amylose-lipid complexes, but the latter would not be the case due to the low lipid content of the samples. Finally, the value obtained for MGC indicated gelling properties of GBF at a relatively low concentration (6%), which could be advantageous in the formulation of food products that require a gelatinous texture, such as soups, sauces, and desserts, among others.

CONCLUSION

Green banana flour (GBF) possesses techno-functional, physicochemical, physical, structural, and morphological properties that make it a suitable food ingredient for use across a wide spectrum of the food industry. Its fat content was low, which was beneficial to the stability of the flour. The whiteness index and the yellowness index of GBF were intermediate, indicating that this flour can be incorporated into a food matrix without significantly affecting its color. Although the values of D(50) and D[4;3] indicate a high proportion of small particles, 90% of the particle mass is equal to or smaller than 1,377.1 µm; the remaining 10% are larger, thus indicating a heterogeneous distribution. The starch granules of GBF are elongated and oval-shaped. Furthermore, the Hausner ratio and Carr index results showed low fluidity and a tendency to agglomerate, which could adversely affect its handling and processing. Moderate compressibility was also found. GBF also exhibited consistency after cooling, high temperature shear strength, and thermal and pasting values, supporting starch retrogradation behavior, which is attractive for use as a functional ingredient in a variety of foods.

During the drying and milling process, starch granules maintained their integrity without undergoing decomposition or gelatinization. This was corroborated by SEM and Raman, which showed characteristic bands of starch structure. In addition, the BET, OSWIN and SMITH models have the best fits to the experimental data and the accuracy of the models in predicting the data is good when compared to the GAB model. Better fits to the experimental data were obtained with the BET model for equilibrium moisture content. Moreover, it was determined that GBF presented a crystallinity of 31.30%, corresponding to a combination of type A and B starches in its composition. This research contributes to the growing body of knowledge on the valorization of rejected green bananas by transforming them into a valuable food ingredient. The detailed characterization of GBF's

properties provides a scientific basis for its application in the food industry. Further research is needed to evaluate other important nutritional properties, such as digestibility, resistant starch content, and antioxidant activity, as well as the performance of GBF in specific food matrices, including bakery products, pasta, and gluten-free formulations.

ACKNOWLEDGMENTS

Tecniban project BPIN code 2020000100698 and Hermes code 51045, Corporación Natural SIG, and Universidad Nacional de Colombia – Medellín Headquarters. K. Manjarres-Pinzon thanks Minciencias Call 935 for contract CT 195-2023.

CONFLICT OF INTERESTS

The authors declare that they have no known competing financial interests or personal relationships that could have appeared to influence the work reported in this paper.

REFERENCES

Aguirre-Cruz A, Alvarez-Castillo A, Castrejón-Rosales T, Carmona-García R et al (2010) Moisture adsorption behavior of banana flours (*Musa paradisiaca*) unmodified and modified by acid-treatment. Starch-Stärke 62: 658-666. https://doi.org/10.1002/star.201000028

Ahmed ZFR, Taha EMA, Abdelkareem NAA and Mohamed WM (2020) Postharvest properties of unripe bananas and the potential of producing economic nutritious products. International Journal of Fruit Science 20: S995-S1014. https://doi.org/10.1080/15538362.2020.1774469

Alam M, Biswas M, Hasan MM, Hossain MF, Zahid MA, Al-Reza MS and Islam T (2023) Quality attributes of the developed banana flour: Effects of drying methods. Heliyon 9(2023): e18312 https://doi.org/10.1016/j.heliyon.2023.e18312

Amarasinghe NK, Wickramasinghe I, Wijesekara I, Thilakarathna G and Deyalage ST (2021) Functional, physicochemical, and antioxidant properties of flour and cookies from two different banana varieties (*Musa acuminata* cv. Pisang awak and *Musa acuminata* cv. Red dacca). International Journal of Food Science, 2021(1): 6681687. https://doi.org/10.1155/2021/6681687

Anyasi TA, Jideani AIO and Mchau GA (2015) Morphological, physicochemical, and antioxidant profile of noncommercial banana cultivars. Food Science and Nutrition 3: 221–232. https://doi.org/10.1002/fsn3.208

AOAC - Association of Official Analytical Chemists (2005) Official methods of analysis of the AOAC International. 18th edition. Gaithersburg, MD.

AUGURA – Asociación de bananeros de Colombia (2022) Coyuntura bananera, análisis del mercado del banano. https://augura.com.co/wp-content/uploads/2022/04/COYUNTURA-BANANERA-2021.pdf

Aurore G, Parfait B and Fahrasmane L (2009) Bananas, raw materials for making processed food products. Trends in Food Science and Technology 20: 78–91. https://doi.org/10.1016/J.TIFS.2008.10.003

Ayala-Aponte AA (2016) Thermodynamic properties of moisture sorption in cassava flour. Dyna 83: 138-144. https://doi.org/10.15446/dyna.v83n197.51543

Bezerra CV, Amante ER, de Oliveira DC, Rodrigues AM and da Silva LHM (2013) Green banana (*Musa cavendishii*) flour obtained in spouted bed–Effect of drying on physico-chemical, functional and morphological characteristics of the starch. Industrial Crops and Products 41: 241-249. https://doi.org/10.1016/j.indcrop.2012.04.035

Borneo R, Alba N and Aguirre A (2016) New films based on triticale flour: Properties and effects of storage time. Journal of Cereal Science 68: 82-87. https://doi.org/10.1016/j.jcs.2016.01.001

Campuzano A, Rosell CM and Cornejo F (2018) Physicochemical and nutritional characteristics of banana flour during ripening. Food Chemistry. 256: 11–17. https://doi.org/10.1016/j.foodchem.2018.02.113

Cardoso JM and Pena RDS (2014) Hygroscopic behavior of banana (*Musa* ssp. AAA) flour in different ripening stages. Food and Bioproducts Processing 92: 73–79. https://doi.org/10.1016/j.fbp.2013.08.004

Chang L, Yang M, Zhao N, Xie F et al (2022) Structural, physicochemical, antioxidant and *in vitro* digestibility properties of banana flours from different banana varieties (*Musa* spp.). Food Bioscience. 47: 101624. https://doi.org/10.1016/j.fbio.2022.101624

Chávez-Salazar A, Bello-Pérez LA, Agama-Acevedo E, Castellanos-Galeano FJ et al (2017) Isolation and partial characterization of starch from banana cultivars grown in Colombia. International Journal of Biological Macromolecules 98: 240–246. https://doi.org/10.1016/j.ijbiomac.2017.01.024

Czekus B, Pećinar I, Petrović I, Paunović N et al (2019) Raman and Fourier transform infrared spectroscopy application to the Puno and Titicaca cvs. of quinoa seed microstructure and perisperm characterization. Journal of Cereal Science 87: 25–30. https://doi.org/10.1016/j.jcs.2019.02.011

De Souza AV, de Mello JM, da Silva Favaro VF, dos Santos TGF et al (2021) Metabolism of bioactive compounds and antioxidant activity in bananas during ripening. Journal of Food Processing and Preservation 45: e15959. https://doi.org/10.1111/jfpp.15959

Devi K and Haripriya S (2014) Pasting behaviors of starch and protein in soy flour-enriched composite flours on quality of biscuits. Journal of Food Processing and Preservation 38: 116–124. https://doi.org/10.1111/j.1745-4549.2012.00752.x

Drapal M, Amah D, Uwimana B, Brown A, Swennen R and Fraser P D (2024) Evidence for metabolite composition underlying consumer preference in sub-Saharan African *Musa* spp. Food Chemistry 435: 137481. https://doi.org/10.1016/j.foodchem.2023.137481

Figueroa-Flórez J, Cadena-Chamorro E, Salcedo-Mendoza J, Rodríguez-Sandoval E, Ciro-Velásquez H and Serna-Fadul T (2024) Enzymatic biocatalysis processes on the semicrystalline and morphological order of native cassava starches (*Manihot esculenta*). Revista Facultad Nacional de Agronomía Medellín. 77(3): 10839-10852. https://doi.org/10.15446/rfnam.v77n3.111270

Grisi CVB, de Magalhães AMT, de Carvalho AS, Vieira AF et al (2021) Nutritional, anti-nutritional and technological functionality of flour from *Libidibia ferrea*. Revista Principia-Divulgação Científica e Tecnológica do IFPB 53: 206-217. https://pdfs.semanticscholar.org/0717/d97db9da9531e38c573499be39d731c73428.pdf

Gutiérrez BL, Márquez-Cardozo CJ and Ciro-Velásquez HJ (2018) Thermodynamic study of adsorption properties of rocoto pepper (*Capsicum pubescens*) obtained by freeze-drying. Advance Journal of Food Science and Technology 15: 91–98. https://doi.org/10.19026/AJFST.14.5877

ICONTEC - Instituto Colombiano de Norma Técnica (2020) Harina plátano, banano verde. NTC 2799-2020. Colombia

Jaramillo-Garcés Y, Sacchet-Pérez M, Manjarres-Pinzon G, Manjarres-Pinzon K et al (2023) Effect of low-temperature storage time on rejected green banana for flour production. Revista Facultad Nacional

de Agronomía Medellín 76: 10517-10526. https://doi.org/10.15446/rfnam.v76n3.105789

Khoozani AA, Bekhit AEDA and Birch J (2019) Effects of different drying conditions on the starch content, thermal properties and some of the physicochemical parameters of whole green banana flour. International Journal of Biological Macromolecules 130: 938–946. https://doi.org/10.1016/j.ijbiomac.2019.03.010

Kizil R, Irudayaraj J and Seetharaman K (2002) Characterization of irradiated starches by using FT-Raman and FTIR spectroscopy. Journal of Agricultural and Food Chemistry 50: 3912–3918. https://doi.org/10.1021/JF011652P

Kumar PS, Saravanan A, Sheeba N and Uma S (2019) Structural, functional characterization and physicochemical properties of green banana flour from dessert and plantain bananas (*Musa* spp.). Lwt - Food Science and Technology 116: 108524. https://doi.org/10.1016/j.lwt.2019.108524

López-Ochoa JD, Cadena-Chamorro E, Ciro-Velasquez H and Rodríguez-Sandoval E (2022) Enzymatically modified cassava starch as a stabilizer for fermented dairy beverages. Starch-Stärke 74: 2100242. https://doi.org/10.1002/star.202100242

Manjarres-Pinzon G, Castro-Sanchez A, Lopez-Ochoa JD, Gil-Gonzalez J and Rodriguez-Sandoval E (2024) Efectos del reemplazo parcial de harina de trigo con harina de banano verde sobre las propiedades reológicas de la masa y las propiedades de calidad de pan. Investigación e Innovación en Ingenierías, 12(1): 45-54. https://doi.org/10.17081/invinno.12.1.6573

Melgarejo LM (2012) Ecofisiología del cultivo de la gulupa (*Passiflora edulis* Sims). First edition. Universidad Nacional de Colombia, Bogotá. 144p

Minagricultura - Ministerio de Agricultura y Desarrollo Rural (2021) Sistema de información de gestión y desempeño de organizaciones de cadenas. https://sioc.minagricultura.gov.co/Banano/Pages/default.aspx

Mir SA and Bosco SJD (2014) Cultivar difference in physicochemical properties of starches and flours from temperate rice of Indian Himalayas. Food Chemistry 157: 448–456. https://doi.org/10.1016/j.foodchem.2014.02.057

Moravkar KK, Korde SD, Bhairav BA, Shinde SB et al (2020) Traditional and advanced flow characterization techniques: a platform review for development of solid dosage form. Indian Journal of Pharmaceutical. Science 82: 945-957. https://doi.org/10.36468/pharmaceutical-sciences.726

Ortega Alvardo JE (2016) Estudio de las propiedades fisicoquímicas y funcionales de la harina de banano (*Musa acuminata* AAA) de rechazo en el desarrollo de películas biodegradables (trabajo de grado). Universidad de Ambato, Ambato, Ecuador. 88 p.

Padhi S and Dwivedi M (2022) Physico-chemical, structural, functional and powder flow properties of unripe green banana flour after the application of refractance window drying. Future Foods 5: 100101. https://doi.org/10.1016/j.fufo.2021.100101

Padhi S, Murakonda S and Dwivedi M (2022) Investigation of drying characteristics and nutritional retention of unripe green banana flour by refractance window drying technology using statistical approach. Journal of Food Measurement and Characterization 16: 2375–2385. https://doi.org/10.1007/s11694-022-01349-7

Pragati S, Genitha I and Ravish K (2014) Comparative study of ripe and unripe banana flour during storage. Journal of Food Processing and Technology 5: 1-6. https://doi.org/10.4172/2157-7110.1000384

Rodríguez-Sandoval E, Franco CML and Manjarres-Pinzon K (2014) Effect of fructooligosaccharides on the physicochemical properties of sour cassava starch and baking quality of gluten-free cheese bread. Starch/Staerke 66: 678–684. https://doi.org/10.1002/star.201300233

Salvador LD, Suganuma T, Kitahara K, Tanoue H and Ichiki M (2000) Monosaccharide composition of sweetpotato fiber and cell wall polysaccharides from sweetpotato, cassava, and potato analyzed by the high-performance anion exchange chromatography with pulsed amperometric detection method. Journal of Agricultural and Food Chemistry 48: 3448–3454. https://doi.org/10.1021/JF991089Z

Singh B, Singh JP, Kaur A and Singh N (2016) Bioactive compounds in banana and their associated health benefits - A review. Food Chemistry 206: 1–11. https://doi.org/10.1016/J.FOODCHEM.2016.03.033

Stanley R (2017) Commercial feasibility of banana waste utilization in the processed food industry. https://www.horticulture.com.au/globalassets/laserfiche/assets/project-reports/ba09025/ba09025-final-report-341.pdf

Susilo B, Maharani DM, Hawa LC and Fitri DNK (2019) Study of sorption isotherm and isosteric heat of Kepok Banana (*Musa paradisiaca* F.) slice. IOP Conference Series: Earth and Environmental Science 230 :012017. https://doi.org/10.1088/1755-1315/230/1/012017

Tribess TB, Hernández-Uribe JP, Méndez-Montealvo MGC, Menezes EW et al (2009) Thermal properties and resistant starch content of green banana flour (*Musa cavendishii*) produced at different drying conditions. LWT - Food Science and Technology 42: 1022–1025. https://doi.org/10.1016/j.lwt.2008.12.017

Vega-Rojas LJ, Londoño-Restrepo SM and Rodriguez-García ME (2021) Study of morphological, structural, thermal, and pasting properties of flour and isolated starch from unripe plantain (*Musa paradisiaca*). International Journal of Biological Macromolecules 183: 1723–1731. https://doi.org/10.1016/j.ijbiomac.2021.05.144

Velandia WL (2019) Producción y comercialización de banano en la finca el mango del municipio de Támara Casanare (trabajo de grado). Universidad Santo Tomás. Bogotá, Colombia. 71 p.

Vogel C, Scherf KA and Koehler P (2018) Effects of thermal and mechanical treatments on the physicochemical properties of wheat flour. European Food Research and Technology 244: 1367–1379. https://doi.org/10.1007/s00217-018-3050-3

Wang Y, Zhang M and Mujumdar AS (2012) Influence of green banana flour substitution for cassava starch on the nutrition, color, texture and sensory quality in two types of snacks. LWT- Food Science and Technology 47: 175–182. https://doi.org/10.1016/J.LWT.2011.12.011

Wu Z, Ameer K, Hu C, Bao A et al (2022) Particle size of yam flour and its effects on physicochemical properties and bioactive compounds. Food Science and Technology. (Brazil) 42: e43921. https://doi.org/10.1590/fst.43921

Zamudio FPB, Vargas A, Gutiérrez F and Bello LA (2010) Caracterización fisicoquímica de almidones doblemente modificados del plátano. Agrociencia 44: 283–295. https://www.uaeh.edu.mx/investigacion/icap/LI_IntGenAmb/Juana_Fons/22.pdf

Research article

https://revistas.unal.edu.co/index.php/refame

Revista Facultad Nacional de Agronomía

Silage production from agro-industrial by-products fermented with lactic acid bacteria isolated from the marine environment

Producción de ensilados a partir de subproductos agroindustriales fermentados con bacterias ácido lácticas aisladas del ambiente marino

https://doi.org/10.15446/rfnam.v78n2.115273

Franco M. Sosa[1,2,3], Emilio R. Marguet[1] and Marisol Vallejo[1]*

ABSTRACT

The increase in demand for food induces food industry activity, generating waste that could be used as silage for animal feed through biological fermentation. This study evaluated the evolution of physicochemical parameters of biological silage (BS) using by-products from food industries through a seven-day fermentation process. The silages of fish muscle and whey (F+W), and fish muscle and residual brewer's yeast (F+RBY) were inoculated with lactic acid bacteria (LAB), previously selected. The drop in pH, water-soluble protein fraction, trichloroacetic acid-soluble protein fraction and antimicrobial activity were registered in both matrices. The total protein content, antioxidant activity, trypsin inhibition, phytase activity, free phosphorus determination and Ca^{2+}, Fe^{2+}, Mg^{2+} concentrations were registered in F+RBY. A pH drop was registered in both matrices (F+RBY=5.4; F+W=5.47). In both cases, the soluble peptide concentration in water and trichloroacetic acid increased during the fermentation process, and the antimicrobial activity was registered from day one of the fermentation process. Complimentary assays were carried out only with F+RBY. An increase in the antioxidant capacity of BS was detected with DPPH and CUPRAC methods. The total protein content displays no significant differences during assays. The phosphate concentration remained stable, with values of 2.06 and 1.72 mg g^{-1} of silage for the control and BS, respectively. Low phytase activity was registered through the fermentation process, and the concentration of divalent cations remained stable during the fermentation process. Trypsin inhibitory activity was not registered. The use of matrices from discards of the feed industry, fermented with LAB, used for animal feed suggests a potential application for the revaluation of by-products.

Keywords:
Food industry wastes
Lactic fermentation
Residual brewer's yeast
Whey

RESUMEN

El aumento en la demanda de alimentos induce la actividad industrial alimentaria, generando residuos que podrían ser utilizados como ensilados para la alimentación animal mediante fermentación biológica. Este estudio evaluó la evolución de parámetros fisicoquímicos de ensilados biológicos (EB) utilizando subproductos de las industrias alimentarias, mediante un proceso de fermentación de siete días. Ensilados de músculo de pescado y lactosuero (P+LS) y, músculo de pescado y residuo de levadura cervecera (P+RLC) fueron inoculados con bacterias ácido lácticas (BAL), previamente seleccionadas. Se registró el descenso del pH, la fracción proteica soluble en agua, en ácido tricloroacético y la actividad antimicrobiana. Se registró en P+RLC el contenido total de proteínas, la actividad antioxidante, inhibición de tripsina, actividad fitasa, determinación de fósforo libre y las concentraciones de Ca^{2+}, Fe^{2+}, Mg^{2+}. Se registró una caída del pH en ambas matrices (P+RLC=5,4; P+LS=5,47). En ambos casos, la concentración de péptidos solubles en agua y ácido tricloroacético aumentó durante el proceso de fermentación, y la actividad antimicrobiana se registró desde el primer día del proceso de fermentación. En P+RLC, se detectó un aumento en la capacidad antioxidante del EB con los métodos DPPH y CUPRAC. El contenido total de proteínas no exhibió diferencias significativas. La concentración de fosfato se mantuvo estable, con valores de 2,06 y 1,72 mg g^{-1} de ensilaje para el control y EB, respectivamente. El proceso de fermentación registró una baja actividad fitásica y la concentración de cationes divalentes se mantuvo estable. No se registró actividad inhibidora de tripsina. El uso de matrices procedentes de descartes de la industria alimentaria, fermentadas con BAL, utilizadas para la alimentación animal sugiere una potencial aplicación para la revalorización de subproductos.

Palabras clave:
Residuos de la industria alimentaria
Fermentaciones lácticas
Residuo de levadura cervecera
Suero

[1]Laboratorio de Biotecnología Bacteriana, Facultad de Ciencias Naturales y Ciencias de la Salud. Universidad Nacional de la Patagonia San Juan Bosco. Trelew, Chubut, Argentina. Franco.m.sosa94@gmail.com, emarguet@yahoo.com.ar, soltrelew@gmail.com
[2]Consejo Nacional de Investigaciones Científicas y Técnicas (CONICET). Buenos Aires, Argentina.
[3]Secretaría de Ciencia y Tecnología. Chubut, Argentina.
*Corresponding author

Received: February 16, 2025; Accepted: April 6, 2025
Rev. Fac. Nac. Agron. Medellín 78(2): 11103-11116. 2025
ISSN 0304-2847 / e-ISSN 2248-7026

CC BY NC SA

Currently, there is a growing demand for food due to global population growth. Consequently, the food industry has increased production, generating waste during the elaboration process or after sales. The world´s production of aquatic animals by capture fisheries is estimated at 90 million tons. Argentina, which has a vast coastal region, is among the leading producers of capture fisheries, with 0.82 million tons of live weight (FAO 2022a). Some of the waste produced during processing is used in ornamental fish feed, while another large amount is reduced into fish oil and fishmeal. However, this processing would not be economically sustainable in small-scale processing, such as the distribution of whole fish for sale (Toppe et al. 2018).

World dairy production in 2022 hovered around 930 million tons, an increase derived mainly from volumetric expansions in Asia, Central America, and the Caribbean. In South America, milk production was 65.6 million tons (FAO 2022b). In Argentina, according to the Observatory of the Argentine Dairy Chain (OCLA), the volume produced was 11,557.4 million liters, equivalent to 11,904.12 million tons.

In addition to its direct consumption, the fate of milk is derivative production, among which cheese stands out. The significant by-product produced is whey, whereas its discard tends to damage the environment due to the high amount of organic matter (Sakr et al. 2021).

Beer is the most consumed alcoholic beverage worldwide, with approximately 177.50 billion liters in 2020 (Santacruz et al. 2023). The high production worldwide results in significant amounts of waste, estimating that for every 100 liters of beer brewed, between 14-20 kg of grain, 0.2-0.4 liters of hot trub, and 1.5-3 kg of yeast are produced. Considering only the three largest producers (China, USA, and Brazil), world beer production reaches almost 84 billion liters annually, making approximately 143 million kg of grains, 2.5 million kg of residual brewing yeast, and 19 million kg of residual yeast (Mathias et al. 2016).

The wastes mentioned above have much organic matter that can be used for animal and fish nutrition. One method for using by-products is through the production of silage by the use of acid preservation (acid silage) or anaerobic microbial fermentation (microbial silage), thus reducing the waste produced and the production costs in aquaculture or livestock farming. The latter is of greater interest because they are relatively cheaper and easier to make, taking advantage of the metabolic characteristics of the bacteria used during the fermentation process, thus obtaining a nutritious, stable product with antimicrobial capacity (Peña et al. 2020). Furthermore, biological silage is advantageous because it enhances the availability of nutrients and minerals generated by the fermentation of processed wastes (Marti-Quijal et al. 2020).

Lactic acid bacteria (LAB) have gained relevance in recent years due to their use in elaborating functional foods. Their proteolytic activity, antimicrobial agents' synthesis, and antioxidant capacity result in a product with better nutritional properties than raw food or chemical processing. LAB is a group of microorganisms located in the *Clostridia* branch of gram-positive bacteria, which includes non-spore-forming cocci, coccobacilli, anaerobes, or aerotolerant, with a DNA base composition of less than 50% in G+C. LAB have a proteolytic system composed of proteinases, peptidases, and specific transport proteins, allowing them to degrade and consume high molecular weight proteins in the medium. On the other hand, they can ferment sugars into lactic acid, thus obtaining the necessary energy for their development in anaerobic conditions (Kieliszek et al. 2021).

The acid environment produced in biological silages by LAB, together with the ability to synthesize compounds with antimicrobial activity, prevents or inhibits the development of possible pathogenic and food spoilage organisms and contributes to preserving the nutritional value and energy content through the metabolic capacity of the bacteria (Baños et al. 2019).

Moreover, phosphorus (P) is a crucial mineral to be considered in animal feed because it improves growth, development, and firmness in the muscle of animals raised in the fields of livestock and aquaculture (Wen et al. 2015). In modern livestock production, cereal grains and oilseeds have their P source as phytates, finding about 70% of the phosphorus in barley like this compound. The degrading inefficiency of phytate is a problem in P that may be related to some organisms that do not possess phytase, a digestive enzyme necessary to hydrolyze the phytate molecule. Some microorganisms, such as LAB and yeasts, harbor this enzyme and metabolize phytic acid, leaving P

bioavailable in phosphate groups. The achievement of the latter points depends mainly on selecting adequate strains that could be used as inoculums during the fermentation process (Toppe et al. 2018).

The concept of circular economy is currently taking resonance through a change in the traditional "take-make-waste" model. Using industrial by-products in new productive chains and reducing untreated waste is a new trend toward cleaner food production through a "cascading" use (Cerdá and Khalilova 2016).

This study evaluated the evolution of physicochemical parameters of biological silage using by-products from the brewing, dairy, and fishing industries through a seven-day process. The silage was inoculated with LAB previously selected based on their technological properties.

MATERIALS AND METHODS

Selection of lactic acid bacteria

Strains from marine organisms belonging to the Bacterial Biotechnology laboratory (Facultad de Ciencias Naturales y Ciencias de la Salud, Universidad Nacional de la Patagonia San Juan Bosco, Trelew), were selected based on their biotechnological potential. The *Lactococcus lactis* subsp. *lactis* Tw34 strain was selected based on its antimicrobial and phytase activity (Marguet et al. 2013). *Enterococcus mundtii* Tw278 strain was selected based on its antimicrobial and antioxidant capacity (Sosa et al. 2022; Sosa et al. 2023), and *Lactobacillus* sp. Tw93 strain was selected based on its proteolytic activity. All strains were replicated in Man Rogosa Sharpe (MRS) agar (Biokar, France) for 24 h at the optimum temperature.

Silage preparation and fermentation process

The silage was prepared based on combinations of waste from the fishing, dairy, and brewing industries. Common hake (*Merluccius hubbsi*) muscle discards were collected from a local fish market in Rawson Harbor, province of Chubut (longitude -65.0532532, latitude -43.3325653). Lactic whey was obtained from an artisanal producer of Trelew, province of Chubut (longitude -65.30505, latitude -43.3325653) after cheese-making. Residual brewing yeast was provided by Cerveceria Rijavec, located in Rawson, province of Chubut (longitude -65.1078894 latitude -43.3022935. The substrates for biological silage were carried out by mixing 70% fish homogenate with 28% lactic whey or residual brewing yeast; after homogenization, 1% potassium sorbate (Productos Químicos, Argentina) and 1% edible yeast (Titan, France) were added to both mixtures (Figure 1). The selected strains were incubated overnight in MRS broth at the optimum temperature. Furthermore, the cultures were centrifuged at 4,000 g for 15 min, and the supernatants were discarded. After that, pellets were washed twice and resuspended in sterile distilled water.

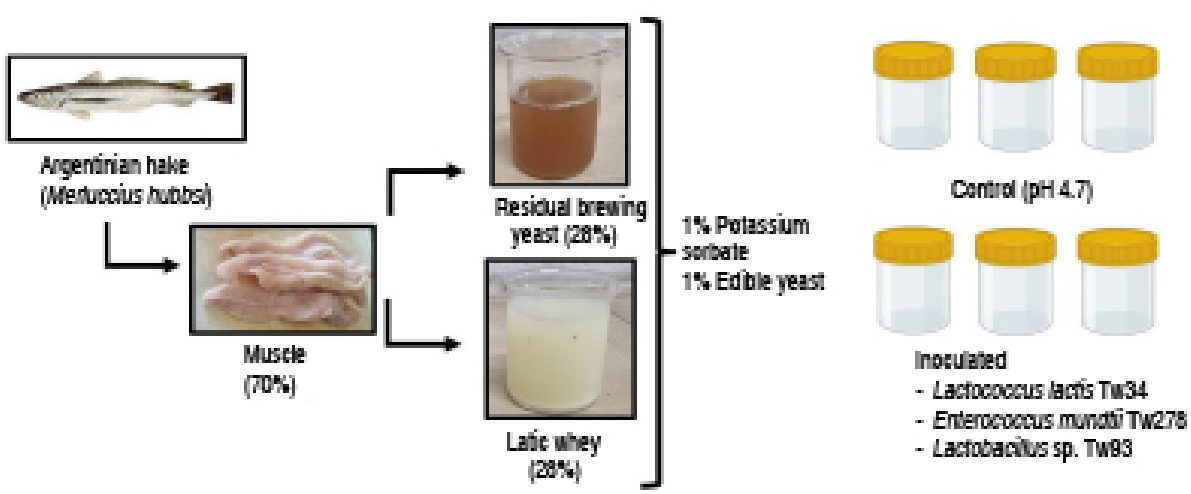

Figure 1. Silage preparation and fermentation process treatments.

The biological silage (BS) was subjected to a fermentation process for 7 days at 18 °C. Inoculation was carried out with 1% of the resuspended pellet of each selected strain. Silage previously treated with lactic acid (Fluka – Switzerland) was prepared as a control until the pH reached 4.7. Samples of 1 g of silage were collected in a Falcon tube and 0.5 g in an Eppendorf tube every 24 h until the end of the experiment. The tests were carried out in triplicate, and the samples obtained were stored at -30 °C until processing.

pH determination

During the fermentation process, the pH of the silage was measured daily with an Orion Model 410A pH- meter with an Orion 8135BN solids electrode.

Determination of protein fraction

The protein fractions were determined following the methodology described by Marguet et al. (2017). Briefly, 10 mL of distilled water was added to 1 g of the sample and homogenized with a vortex mixer. After storing at 4 °C for 24 h, the mixtures were centrifuged at 2,000 g for 15 min. The O-phthalaldehyde technique was used to evaluate the concentration of water-soluble peptides in the supernatant (Church et al. 1983).

The soluble protein fraction in trichloroacetic acid was determined by mixing 500 µL of the processed sample of the water-soluble fraction with 500 µL of trichloroacetic acid (TCA) and subjected to vigorous agitation for 1 min, and was incubated for 10 min. The sample was centrifuged at 12,000 g for 2 min, and the concentration of soluble peptides in the supernatant was determined with the O-phthalaldehyde assay. Absorbance values of water-soluble and TCA-soluble peptides were measured at 590 nm in a UV/vis Jenway 6405 spectrophotometer. The results were expressed in mg equivalents of leucine per 100 grams of silage.

Evaluation of antimicrobial activity during fermentation process

A 500-mg sample was resuspended with 500 µL of sterile distilled water and vigorously mixed with a vortex. After centrifugation at 12,000 g for 2 min, 50 µL of supernatants was placed in wells of 6 mm in diameter cut in Brain Heart Infusion (Biokar, France) plates seeded with a stationary phase cell suspension of *Listeria innocua* ATCC 33090, *L. innocua* Tw67 and *L. monocytogenes* Scott A, used as indicator microorganisms. After incubation for 24 h at 37 °C, a clear zone around the wells was considered inhibitory activity.

Total protein determination

The crude protein content was determined at the beginning and the end of the assay of control and BS using Kjeldahl digestion (N factor=6.25) (Method 976.05) (AOAC 1990). It was also determined the moisture content of control and biological silage by drying the samples in an oven at 95 °C until a constant weight was achieved (Method 934.01) (AOAC 1990).

Determination of antioxidant capacity during the fermentation process

Antioxidant activity by reduction of 2,2 diphenyl-1-picryhydrazyl (DPPH): The DPPH assay was carried out following the recommendations of Zhang et al. (2013). In brief, 1 mL of DPPH reagent was inoculated with 100 µL of the sample (1 g of silage sample homogenized in 10 mL of distilled water) and incubated in the dark for 30 min. Afterward, the absorbance was measured at 517 nm. The antioxidant capacity results were expressed as mmol ascorbic acid equivalents per gram of silage.

Cupric Ion Reducing Antioxidant Capacity (CUPRAC): The CUPRAC assay was performed following the recommendations of Apak et al. (2004). The reaction reagent was prepared with 1 mL neocuproine (1 mg mL^{-1} in ethanol), 1.5 mL of sodium acetate buffer (0.05 M, pH=6.0), and 0.5 mL of $CuCl_2$ (0.01 M). The samples were prepared as explained in "Determination of protein fraction" section. After centrifugation, 100 µL were inoculated in 900 µL of CUPRAC reagent and incubated at 37 °C for 1 h. The absorbance was read at 450 nm, and the results obtained were expressed as mmol ascorbic acid equivalents per gram of silage.

Determination of free phosphorus

The concentration of free phosphorus in the BS was determined as proposed by Marguet et al. (2017). A phosphate reagent containing 0.6 M H_2SO_4, 2% ascorbic acid, and 0.5% ammonium molybdate was prepared. Initially, 100 µL of the sample was seeded in 900 µL of reagent and incubated for 30 min at room temperature. Subsequently, the absorbance reading was performed

at 820 nm. The results were compared with a calibration curve of a KH_2PO_4 solution.

Determination of phytase activity

The determination of phytase activity was carried out following the method proposed by Marguet et al. (2013). In brief, 100 µL of the sample was seeded in 900 µL of a reaction mixture of 1 mg mL^{-1} sodium phytate dissolved in 0.1 M acetate buffer pH=5.5 and incubated at 35 °C for 30 min. Subsequently, the reaction was stopped by adding 1 mL of trichloroacetic acid (10% v/v). Afterward, 100 µL were inoculated in 900 µL of the previously used phosphate reagent and incubated at room temperature for 1 h. Finally, the absorbance at 820 nm was measured. The phytase enzymatic unit (EU) was defined as the enzyme required to liberate 1 µmol of phosphate per minute from sodium phytate under stated pH and temperature conditions.

Trypsin inhibitory activity determination

The substrate was composed of azocasein (10 mg mL^{-1} in TRIS buffer, 0.1 M and pH=8.5) treated with trypsin (0.5 mg mL^{-1}). Then, the mixture was divided into aliquots of 1 mL and 100 µL of the silage sample was inoculated. After incubation at 37 °C, the reaction was stopped by adding 100 µL of 24% TCA and centrifuged at 13,000 g for 2 min. The obtained supernatant was treated with 600 µL of 0.5 M NaOH. The absorbance reading was performed at 450 nm. The trypsin inhibitory activity was calculated following Liu and Markakis (1989) Equation (1), as follows:

$$\text{Trypsin Inhibitory Unit (TIU)} = \frac{(A^r_{450} - A^s_{450}) \times 100}{\text{mL of sample}} \quad (1)$$

Where A^r is the absorbance of the reagents and A^s is the absorbance of the silage sample.

Determination of divalent cations

For sample preparation, a 500-mg sample was resuspended with 500 µL of sterile distilled water and vigorously mixed with a vortex. The determination of Calcium (Ca^{2+}), Iron (Fe^{2+}), and Magnesium (Mg^{2+}) were carried out using the following techniques.

Determination of Ca^{2+}

Calcium determination was carried out as Ray and Chauhan (1967) proposed. Briefly, 50 µL of control and BS were mixed with 1.0 mL of O-Cresolphthalein and 8-hydroxyquinoline and 1.0 mL of aminomethyl propanol and incubated at 25 °C for 5 min. Finally, the absorbance was measured at 570 nm. A standard curve of $CaCl_2$ was used to determine calcium concentration.

Determination of Fe^{2+}

Iron determination was determined as proposed by Jeitner (2014). Briefly, 300 µL of control and BS samples were mixed with 20 µL of ascorbic acid 1 M, and 80 µL of 50 mg ferrozine per milliliter potassium acetate buffer (500 mM). The reaction was carried out at 37 °C for 135 min. Finally, the absorbance was measured at 562 nm, and the result was compared with an absorbance standard curve using known concentrations of $FeCl_3$.

Determination of Mg^{2+}

In brief, 10 µL of control and BS were mixed with 1.0 mL of a reaction mixture of xylidyl blue 0.1 mM and EGTA 0.04 mM on Tris buffer (0.22 M, pH=11.3), and incubated for 5 min at 25 °C. The absorbance was measured at 510 nm and the results were compared with a curve using known concentrations of MgO (Kafesa et al. 2021).

Statistical analysis

All assays were performed independently and in triplicate. The data were subjected to an analysis of variance (ANOVA), and the significant differences between the means were determined using Tukey's test (P<0.05). The statistical software Statgraphics Centurion XV (15.1.02, Statsoft, The Plains, Virginia – USA) was used.

RESULTS AND DISCUSSION

Drop in pH during the fermentation process

Figure 2 shows the evaluation of pH as a function of time for all residue combinations. In all cases, the combinations of residues from the dairy and brewing industry with by-products from the fishing industry allowed the development of LAB, observing a reduction in pH during the experiment. A final pH value of 5.4 was obtained with fish muscle and residual brewing yeast and 5.47 in the combination of fish muscle and whey.

Lactic acid generated by the LAB inoculated at the beginning of fermentation produces pH drop values. Similar results of pH were obtained by Fernández et al. (2015), who made silages with hake waste

supplemented with yogurt as a fermentative agent in different proportions, reaching a stabilization between 5.1 and 5.3. On the other hand, Castillo et al. (2019) obtained a drop in pH between 4.2 and 4.7 after 30 days of fermentation, and Peña et al. (2020) obtained at the end of the experiment a pH of 4.5. In both cases, these biological silages were composed of fisheries residues, supplemented with 25% molasses.

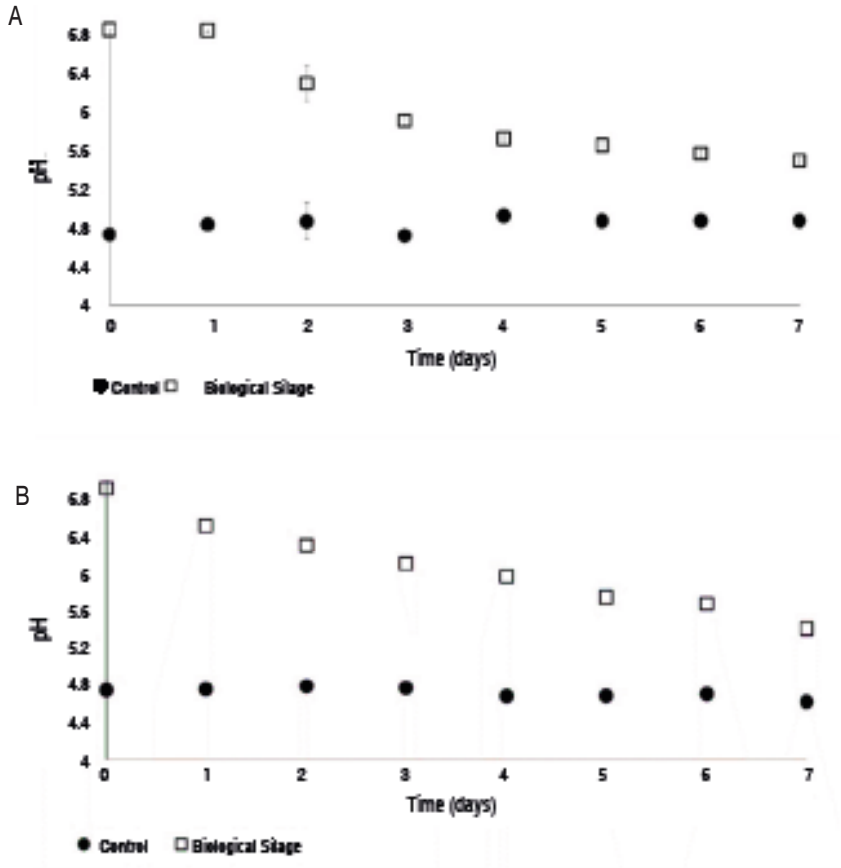

Figure 2. pH drop during fermentation process. The values obtained correspond to the mean and standard deviation in triplicate. A. Fish muscle + whey and B. Fish muscle + residual brewing yeast.

Differences in the pH values obtained may be due to differences in the concentration of fermentable sugars. For the production of the fermentation matrix, 28% of the residual brewing yeast added corresponds to 0.52% of reducing sugars, according to the composition of sugar previously determined, and the 28% of the whey used is equivalent to 1.4% of lactose according to the concentration of fermentable sugars present in this waste, according to Ramirez (2012). Differences are observed in terms of the origin and concentration of sugars used in other fermentation matrices, such as the example of Raeesi et al. (2021), who supplemented the silage of fish residues with 15% (w/w) beet molasses. These differences result in a higher concentration of fermentable sugars for the development of bacterial inoculum and the production of lactic acid, producing a more significant decrease in pH values.

Another reason may be related to the fermentation temperature. In this study, the fermentation was carried out at 18 °C, taking into account the possibility of productive scale-up, where high temperatures translate into an increase in production costs, and a decrease in the probability of contamination. In another research, the temperatures of the fermentation processes were developed within a range between 24-30 °C (Peña et al.

2020; Raeesi et al. 2021), close to the optimal temperature for growth and development of the LAB.

During the growth and development of LAB, different metabolites are produced, including lactic acid, which plays a fundamental role in the fermentation matrices, influencing nutritional and sensory properties (such as texture and aroma). In addition, they exert a preservative effect on the products, improving their safety and shelf life by inhibiting the growth of undesirable microorganisms without favoring the development of antimicrobial resistance (Cortés et al. 2024).

Determination of protein fractions

Water-soluble protein fraction (WSP)

In Figure 3, an increase during the fermentation process of the peptides soluble in water can be observed compared to the control. Differences observed in the results depend on adding whey or residual brewing yeast, the latter exhibiting a higher concentration value, possibly due to the contribution of high molecular weight proteins from the residual brewing yeast (Mathias et al. 2014), which could be a substrate of proteolytic enzymes. The increase in the concentration of soluble peptides in water is mainly related to proteases from fish tissue, which exhibit their activity at acidic pH, as is the case with cathepsins. These proteolytic enzymes are located in the lysosomes of fish muscle and, through tissue disruption, can be released and produce protein lysis (Yoshida et al. 2015). During the silage process, these proteases are activated, improving the digestibility of proteins in fish muscle, such as actin, tropomyosin, α-actinin, and myosin, among others (Cortés et al. 2024). The peptides determined in the soluble fraction correspond to medium-large peptides. Additionally, this proteolytic activity was complemented with LAB proteases. These results were similar to those obtained by Marguet et al. (2017), who exhibited an increase in the concentration of soluble peptides during the fermentation process, with a maximum between 1,189-1,244 mg eq. of leucine per 100 g of silage.

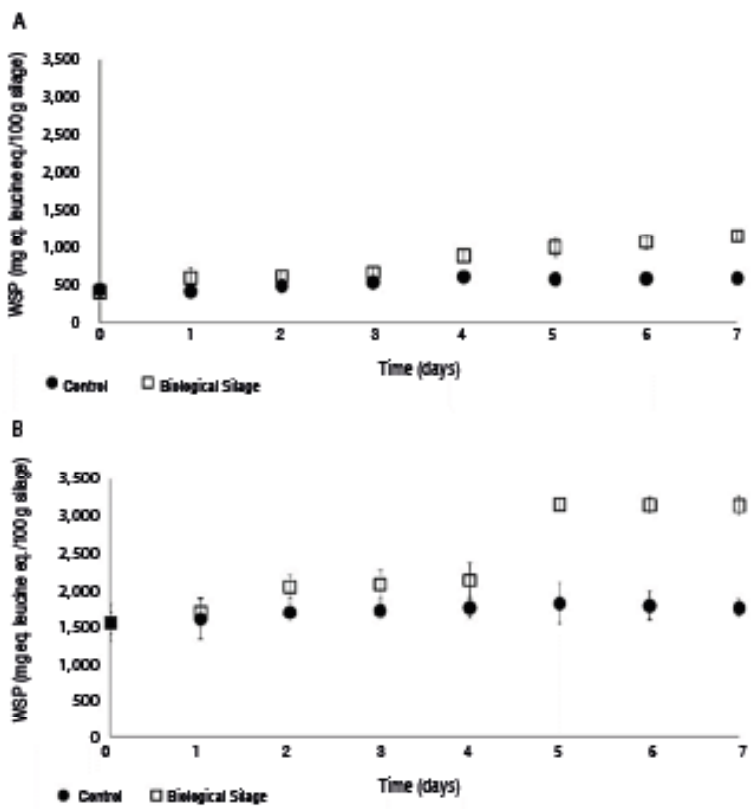

Figure 3. Concentration of water-soluble peptides during the fermentation process. The values obtained correspond to the mean and standard deviation in triplicate. A. Fish muscle + whey and B. Fish muscle + residual brewing yeast.

Trichloroacetic acid soluble protein fraction (TSP)

Figure 4 shows the results obtained for the different combinations tested. An increase in the concentration of soluble peptides in TCA was observed during the fermentation process compared to that obtained in the control. Differences were observed in the concentration values obtained from the addition of whey and residual brewing yeast, with the brewing residue showing the highest concentrations. Peptides soluble in TCA are characterized by their small size, which may reflect the activity of the proteolytic system of the LAB inoculated at the start of the fermentation process. Similar concentrations of soluble peptides were observed when compared to the results of the water-soluble fraction. This suggests a synergistic effect between fish muscle proteases and microbial proteases, which reduced the size of the peptides in the silage, resulting in small peptides as the final product. The values obtained in this study are higher than those obtained by Marguet et al. (2017), who made silage with residues of hake and barley grains as a carbon source, supplemented with *Lactococcus lactis* subsp. *lactis* Tw34, obtaining values of soluble peptides in TCA between 771 and 840 mg of leucine per 100 grams of silage. LAB strains possess a proteolytic system composed of proteinases, peptidases, and specific transport proteins, classified as exopeptidases or endopeptidases that process proteins and peptides into free amino acids, di, tri, and oligopeptides (Kieliszek et al. 2021). The increase in small peptide concentration improves digestibility and palatability, which is related to a higher efficiency of animal food intake and a lower amount of environmental waste (Marguet et al. 2017).

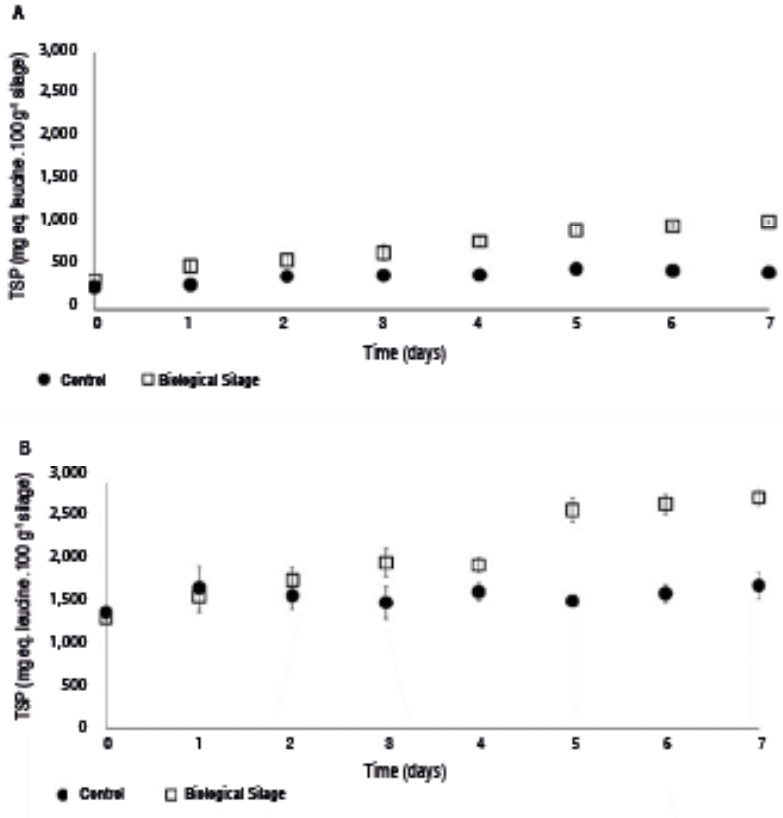

Figure 4. Concentration of soluble peptides in trichloroacetic acid during the fermentation process. The values obtained correspond to the mean and standard deviation in triplicate. A. Fish muscle + whey; B. Fish muscle + residual brewing yeast.

Evaluation of antimicrobial activity during the fermentation process

In Figure 5, the inhibition halos of the growth of *Listeria* strains can be observed due to the antimicrobial activity of the silages. In the control, no antagonist activity can be observed throughout the process. Meanwhile, in the

inoculated silages, supplemented with residual brewing yeast or whey, the antimicrobial activity against the strains *L. innocua* ATCC 33090, *L. innocua* Tw67, and *L. monocytogenes* Scott A was registered after 24 h of incubation, and was maintained throughout the test. These results contrast with those obtained by Ozyurt et al. (2017), who did not observe inhibitory activity in spray-dried fish silage against gram-positive and negative bacteria tested.

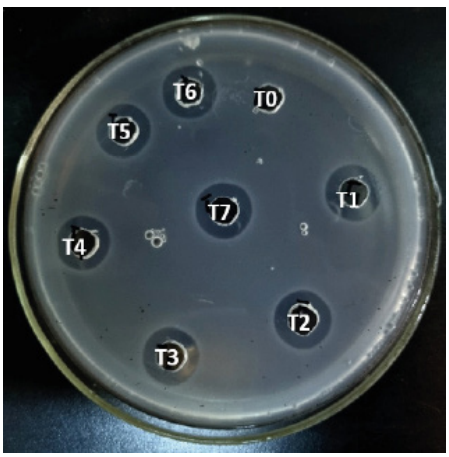

Figure 5. Antimicrobial activity against *Listeria* strains of silage inoculated during the fermentation process.

One of the LAB's selection criteria for silage production was antimicrobial activity, observing its effective development in the matrix of fish and waste. The antimicrobial capacity could be associated with diverse membrane compounds or the production of bacteriocins, ribosomally synthesized peptides active against phylogenetically related microorganisms (Baños et al. 2019). In particular, the production levels of bacteriocins produced by LAB depend on the strain, medium compounds, and physical parameters. In previous research, Sosa et al. (2022) demonstrated that the strain *E. mundtii* Tw278 reached the highest inhibitory activity when a mixture of cheese whey and hot tub was used for cell growth. The production of metabolites with antimicrobial activity is a characteristic of interest for selecting potentially usable microorganisms in fermentative processes, since they prevent the appearance of pathogenic or food spoilage bacteria, avoiding chemical preservatives.

According to the results obtained, the silage model composed of fish muscle and residual brewing yeast from the brewing industry was considered for the following tests.

Determination of total protein

The total protein content for the control was 15.81% at the start of fermentation and 15.23% at the end of fermentation, with a moisture content of 81.5 and 81.26%, respectively. In the case of BS, 16.03% total protein was recorded at the beginning of fermentation and 15.08% on the seventh day of the trial, with a moisture content of 81.57 and 80.38%, respectively. These results were comparable with those of Leonarduzzi et al. (2014), who obtained an average total protein content of 15.84% and a moisture content of 79.25% when performing the proximal analysis on muscle samples of *M. hubbsi*.

Determination of antioxidant capacity

The results of antioxidant capacity obtained by DPPH and CUPRAC methods are shown in Table 1. The antioxidant capacity of the DPPH method is observed through the interaction of free radicals with proton-donating antioxidant compounds, causing a decrease in absorbance compared with the control. The CUPRAC method is based on measuring the reducing power of antioxidant compounds to convert Cu^{2+} ions to Cu^{+}, being a variation of the FRAP assay, where the reduction of the Fe^{+3} ion to Fe^{2+} is evaluated (Shahidi and Zhong 2015). During the fermentation process, the antioxidant capacity of the fermented silage with LAB remains constant. Significant differences between control and inoculated treatments were determined (P<0.05).

Table 1. Determination of antioxidant capacity by DPPH and CUPRAC methods.

	Antioxidant Capacity (mM ascorbic acid equivalent per gram of silage)			
	DPPH		CUPRAC	
	Control	BS	Control	BS
T0	12.96±3.42^{a}	26.05±2.19^{b}	14.14±6.22^{a}	39.60±3.05^{b}
T1	14.72±2.12^{a}	23.72±0.49^{b}	15.67±1.48^{a}	37.17±1.87^{b}
T2	17.07±2.52^{a}	23.33±1.03^{b}	15.54±3.63^{a}	35.39±0.89^{b}
T3	12.88±0.75^{a}	25.04±1.63^{b}	14.54±3.73^{a}	35.49±1.91^{b}
T4	13.12±1.57^{a}	26.39±1.81^{b}	14.89±0.53^{a}	36.18±4.75^{b}
T5	12.56±0.85^{a}	25.52±1.08^{b}	11.69±2.18^{a}	32.85±2.52^{b}
T6	13.15±3.12^{a}	26.15±0.97^{b}	14.01±2.56^{a}	34.02±3.44^{b}
T7	13.13±2.54^{a}	26.72±0.85^{b}	15.83±2.53^{a}	36.71±3.75^{b}

The results are equivalent to the three independent experiments' average and standard deviation. Means with different letters indicate significant differences (P<0.05). BS = Biological silage.

The results of DPPH are comparable with those obtained by Chen et al. (2021), where it is observed that, during the LAB fermentation process, there is an increase in the antioxidant capacity. Similar results were obtained by Yang et al. (2019), who observed an increase in the antioxidant capacity in fermented soybeans with *Bacillus amyloliquefaciens* SWJS22 60 h after fermentation.

Similar behavior was observed in Chen et al. (2018), where a fluctuation in the antioxidant capacity was observed in *Lactobacillus acidophilus* and *L. plantarum* strains during the 48 h fermentations in papaya juices. On the other hand, Jin et al. (2018), who tested six probiotic strains in mango liquid sludge, obtained values between 14-18 mM Trolox equivalents L^{-1} after 48 h of fermentation. These results highlight the development of antioxidant capacity in different by-products. However, it is difficult to compare the results of this study due to the differences between the units used for each experiment's results.

In both cases, the antioxidant capacity, expressed in ascorbic acid equivalents per g of silage, displays differences between the control and inoculated silage, the latter being higher. The results obtained from the antioxidant capacity of the control may be due to the bioactive compounds of the hydrolysate (Martínez 2011), and the existing difference with the samples of the inoculated silage may be due to both the contribution of compounds with antioxidant capacity present on the LAB strains (Sosa et al. 2023), as well as also the increase in the degree of hydrolysis by microorganisms to the silage matrix.

Bhagwat and Annapure (2019) suggest different methods to assess antioxidant capacity due to microorganisms´ different radical scavenging systems. The presence of compounds with antioxidant capacity in food attracts the industry since artificial antioxidants usually used to prevent oxidative deterioration are avoided (Martínez 2011), and it must be considered that the biosynthesis of EPSs by LAB and the increase of amino acids during the fermentation process contribute to the antioxidant activity of the silage (Sharma et al. 2024).

Phytase activity and determination of free phosphorus

At the beginning of the experience, both control and inoculated mixtures exhibited a low enzymatic activity (0.06 and 0.09 EU g^{-1} of silage). Phytase activity in the control remained stable during the 7 days of the process. The inoculated silage showed a slight increase in activity on day 3 (0.11 EU g^{-1} of silage) due to the contribution of phytase of LAB; however, at the end of the process, values between control and inoculated silage were comparable (0.06 and 0.08 EU g^{-1} of silage, respectively). Phytase activity involves the hydrolysis of phytic acid and the release of phosphorus and essential minerals (Zn^{2+}, Fe^{2+}, Ca^{2+}, Mg^{2+}) (Belda 2022).

Despite cereals exhibiting phytase activity, the results are insufficient to improve the phosphorus and mineral bioavailability. Adding exogenous phytase or including high phytase active LAB or yeast to food processing can be overcome this drawback. Previous studies demonstrated that the selection and inclusion of LAB with high phytase activity degrades phytate efficiently and increases the free phosphorus concentration when whole grains are used in animal feed silage (Marguet et al. 2013). In the same direction, several attempts have been made to select phytase-active yeasts for grain-based food and beer elaboration (Nuobariene et al. 2011).

In this study, the addition of residual brewing yeast to fish muscle results in a high concentration of free phosphorus in the control and inoculated mixture (approximately 1.89 and 1.72 mg of phosphate g^{-1} of silage, respectively). Both concentrations remained stable until the end of the experience, displaying values of 2.06 mg phosphate per gram of sample and 1.77 mg of phosphate per gram of silage for the control and inoculated mixture, respectively.

The high amount of free phosphate on the control and inoculated matrices is related to the use of a residue resulting from the previous fermentation of barley grains with *Saccharomyces cerevisiae* for beer production (Nuobariene et al. 2011). The yeast displays a high phytase activity that hydrolyzes the phytic acid and derivatives present in the whole grain and releases free phosphates. The low increase of the inducible phytase of LAB during the fermentation suggests that the yeast's enzymatic activity during the beer production process hydrolyzed most of the phytic acid.

Phosphorus is essential in animal feed; however, when wholegrain products or derivatives are included, those metabolites that can inhibit or diminish intestinal absorption should be considered. Phytic acid is the principal storage molecule for phosphorus and acts as a strong chelator of cations (Zn^{2+}, Fe^{2+}, Ca^{2+}, Mg^{2+}); these forms of phytate result unavailable for absorption in the intestinal tract. In order to avoid these adverse effects, degradation of phytates by enzymatic activity is needed (Nuobariene et al. 2011).

Determination of divalent cations

The results of the divalent cations are presented in Table 2.

Table 2. Concentrations of divalent cations during the fermentation process.

	Minerals (mg 100 g^{-1})			
	Control		BS	
	T0	T7	T0	T7
Ca	19.37±2.14	18.47±1.95	19.43±2.49	19.33±2.34
Mg	19.93±2.25	18.77±1.35	19.83±2.25	18.33±1.93
Fe	0.40±0.15	0.36±0.12	0.35±0.11	0.34±0.09

The results are equivalent to the three independent experiments' average and standard deviation.

There were no significant differences (P>0.05) between control and BS during fermentation in the Ca^{2+}, Mg^{2+}, and Fe^{2+} concentrations. According to the absence of enzymatic induction of phytase activity, and the concentration of phosphorus obtained in this study demonstrated that most of the phytic acid was degraded during the brewing process. Moreover, the stability of divalent cations detected during the experience confirmed that they were not in chelated form with phytic acid. According to Samtiya et al. (2020), eliminating this compound increases the availability of minerals, allowing silages to be considered potential raw materials for developing diets for animal feed.

Trypsin inhibitory activity determination

This study assayed trypsin inhibitory activity because it is one of the most used techniques to determine an anti-nutritional parameter. The results showed that at the beginning of the experiment, the control and the BS displayed low inhibitory activity and remained without significant changes throughout the 7 days of incubation.

Besides phytic acid, several antinutritional compounds, such as glucosinolates, tannins, and protein inhibitors, are known to reduce the absorption of nutrients, including vitamins, minerals, and proteins, and inhibit proteolytic

enzyme activity. Trypsin inhibitors in diets can reduce protein digestion and, subsequently, the bioavailability of amino acids, leading to a decrease in the growth rate (Samtiya et al. 2020). Several processing techniques and methods, such as germination, fermentation, autoclaving, soaking, etc., are used to reduce the anti-nutrient content of foods (Liu 2021). In this case, germination and heating eliminated most of the phytic acid. The other potential trypsin inhibitors, such as glucosinolates, polyphenols, and tannins, are eliminated during fermentation due to the enzymatic activity of LAB (Parada et al. 2023). Glucosinolates are effectively transformed into nitriles by myrosinase activity (Hsieh et al. 2024), and tannins are degraded to simpler compounds, such as gallic acid, by tannase activity (Parada et al. 2023). Phenolic compounds are transformed by LAB by esterase, reductase, and decarboxylase activity (Gaur and Gänzle 2023). These enzymatic activities during fermentation reduce the concentration of antinutritional compounds and improve the availability of their components, which interfere with the nutritional value of the products, by reducing protein digestibility and mineral absorption (Samtiya et al. 2020)

CONCLUSION

The matrices from discards of the fishing industry, supplemented with by-products from the dairy and brewing industries, provide a favorable environment for developing LAB. The use of waste from the food industry for animal feed suggests a potential advantage from the point of view of a circular economy. Silage production is an economical, safe, and versatile technology that is easy to implement, has minimal energy requirements, and is potentially applicable at artisanal and industrial levels, with the advantage of generating economic income from discards. Revaluing by-products through fermentation using lactic acid bacteria (LAB) with desirable biotechnological traits—such as pH reduction and the production of metabolites with antioxidants and antimicrobial properties—offers a cost-effective alternative to the use of preservatives and chemical antibiotics. Additionally, these food matrices are considered rich in essential minerals necessary for animal development. When combined with the proteolytic system of LAB, they promote protein degradation in silage into small peptides, which may enhance digestibility and nutrient absorption during passage through the animal's digestive tract. The high concentration of phosphorus and the absence of enzymatic induction of phytase activity during the fermentation demonstrated that most of the phytic acid was degraded during the brewing process. The stability and high concentration of divalent cations detected during the experience confirmed that they were not in chelated form with phytic acid. This study could be registered as the first time that waste from the dairy and brewing industry is used as an alternative carbon source to produce fermentation matrices and obtain fermented silage potentially applicable to animal feed. In future studies, a complete proximate analysis of the components present in the silage should be carried out, as well as the formulation and effect of the diet *in vivo*.

CONFLICT OF INTERESTS

The authors declare they have no conflict of interest.

REFERENCES

Apak R, Güçlü K, Özyürek M and Karademir SE (2004) Novel total antioxidant capacity index for dietary polyphenols and vitamins C and E, using their cupric ion reducing capability in the presence of neocuproine: CUPRAC method. Journal of Agricultural and Food Chemistry 52(26): 7970–7981. https://doi.org/10.1021/jf048741x

Baños A, Ariza JJ, Nuñez C, Gil-Martínez L, García-López JD et al (2019) Effects of *Enterococcus faecalis* UGRA10 and the enterocin AS-48 against the fish pathogen *Lactococcus garvieae*. Studies *in vitro* and *in vivo*. Food Microbiology 77: 69–77. https://doi.org/10.1016/j.fm.2018.08.002

Belda Palazón C (2022) La fermentación aplicada a la mejora de las propiedades funcionales de residuos y subproductos de alimentos de origen vegetal (Tesis de maestría). Universitat Politècnica de València. Valencia. España. 32p. https://riunet.upv.es/entities/publication/5f51e5b7-c342-4a70-a6e2-1f2a17c9da69

Bhagwat A and Annapure U (2019) *In vitro* assessment of metabolic profile of *Enterococcus* strains of human origin. Journal of Genetic Engineering and Biotechnology 17(11): 1–11. https://doi.org/10.1186/s43141-019-0009-0

Castillo García WE, Sánchez Suárez HA and Ochoa Mogollón GM (2019) Evaluación del ensilado de residuos de pescado y de cabeza de langostino fermentado con *Lactobacillus fermentus* aislado de cerdo. Revista de Investigaciones Veterinarias del Perú 30(4): 1456-1469. http://www.scielo.org.pe/scielo.php?script=sci_arttext&pid=S1609-91172019000400007

Cerdá E and Khalilova A (2016) Economía circular. Economía Industrial 401: 11–20. https://dialnet.unirioja.es/servlet/articulo?codigo=5771932

Chen L, Hui Y, Gao T, Shu G and Chen H (2021) Function and characterization of novel antioxidant peptides by fermentation with a wild *Lactobacillus plantarum* 60. LWT - Food Science and Technology 135. https://doi.org/10.1016/j.lwt.2020.110162

Chen R, Chen W, Chen H, Zhang G and Chen W (2018) Comparative evaluation of the antioxidant capacities, organic acids, and volatiles of papaya juices fermented by *Lactobacillus acidophilus* and *Lactobacillus plantarum*. Journal of Food Quality. https://doi.org/10.1155/2018/9490435

Church, FC Swaisgood HE, Porter DH and Catignani GL (1983) Spectrophotometric assay using o-phthaldialdehyde for determination of

proteolysis in milk and isolated milk proteins. Journal of Dairy Science 66(6): 1219–1227. https://doi.org/10.3168/jds.S0022-0302(83)81926-2

Cortés-Sánchez ADJ, Jaramillo-Flores ME, Díaz-Ramírez M, Espinosa-Chaurand LD and Torres-Ochoa E (2024) Biopreservation and the safety of fish and fish products, the case of lactic acid bacteria: a basic perspective. Fishes 9: 303. https://doi.org/10.3390/fishes9080303

FAO – Food and Agriculture Organization of the Nations (2022a) El estado mundial de la pesca y la acuicultura 2022. Hacia la transformación azul. In FAO. https://doi.org/10.4060/cc0461es

FAO – Food and Agriculture Organization of the Nations (2022b) Dairy Market Review - Emerging trends and outlook. Rome. https://www.fao.org/3/cc3418en/cc3418en.pdf

Fernández Herrero AL, Fernández Compás A and Manca E (2015) Ensayo preliminar de obtención de ensilado biológico de anchoita (*Engraulis anchoita*), utilizando hez de malta de cebada (*Hordeum vulgare L*) como fuente de hidratos de carbono. Revista Electrónica de Veterinaria 16(3): 1–13. https://www.redalyc.org/pdf/636/63638740004.pdf

Gaur G and Gänzle MG (2023) Conversion of (poly)phenolic compounds in food fermentations by lactic acid bacteria: Novel insights into metabolic pathways and functional metabolites. Current Research in Food Science 6. https://doi.org/10.1016/j.crfs.2023.100448

Hsieh CC, Liu YH, Lin SP, Santoso SP, Jantama K et al (2024) Development of High-Glucosinolate-retaining lactic-acid-bacteria-co-fermented cabbage products. Fermentation 10(12). https://doi.org/10.3390/fermentation10120635

Jeitner TM (2014) Optimized ferrozine-based assay for dissolved iron. Analytical Biochemistry 454: 36-37. http://doi.org/10.1016/j.ab.2014.02.026

Jin X, Chen W, Chen H, Chen W and Zhong Q (2018) Comparative evaluation of the antioxidant capacities and organic acid and volatile contents of mango slurries fermented with six different probiotic microorganisms. Journal of Food Science 83(12): 3059–3068. https://doi.org/10.1111/1750-3841.14373

Kafesa A, Lutfi NNH and Wahyu C (2021) Chemometric analysis of serum magnesium calculations using Mg-Xylidyl Blue-I method based on molar absorptivity. Indonesian Journal of Medical Laboratory Science and Technology 3(1): 9–18.

Kieliszek M, Pobiega K, Piwowarek K and Kot AM (2021) Characteristics of the proteolytic enzymes produced by lactic acid bacteria. Molecules 26. https://doi.org/10.3390/molecules26071858

Leonarduzzi E, Rodrigues KA and Macchi GJ (2014) Proximate composition and energy density in relation to Argentine hake females (*Merluccius hubbsi*) morphometrics and condition indices. Fisheries Research 160: 33-40. http://doi.org/10.1016/j.fishres.2014.04.017

Liu K (2021) Trypsin inhibitor assay: expressing, calculating, and standardizing inhibitor activity in absolute amounts of Trypsin inhibited or trypsin inhibitors. JAOCS - Journal of the American Oil Chemists' Society 98(4): 355–373. https://doi.org/10.1002/aocs.12475

Liu K and Markakis P (1989) An improved colorimetric method for determining antitryptic activity in soybean products. Cereal Chemistry 66(5): 415–422. http://www.aaccnet.org/publications/cc/backissues/1989/Documents/66_415.pdf

Marguet ER, Ledesma P and Vallejo M (2013) Disponibilidad de fósforo soluble en ensilado experimental fermentado con una cepa de *Lactococcus lactis* subsp. *lactis* con alta actividad de fitasa. Revista de la Sociedad Venezolana de Microbiología 33: 116–121. https://ve.scielo.org/scielo.php?script=sci_arttext&pid=S1315-25562013000200006

Marguet E, Vallejo M, Schulman G, Ledesma P and Parada R (2017) Biosilo de residuos de merluza y harina de cebada fermentados con bacterias ácido lácticas seleccionadas. Biotecnología en el Sector Agropecuario y Agroindustrial 15(2): 112–120.

Marti-Quijal FJ, Remize F, Meca G, Ferrer E, Ruiz MJ and Barba FJ (2020) Fermentation in fish and by-products processing: an overview of current research and future prospects. Current Opinion in Food Science 31: 9–16. https://doi.org/10.1016/j.cofs.2019.08.001

Martínez Álvarez O (2011) Estado actual el aprovechamiento de subproductos de la industria pesquera mediante la obtención de productos de alto valor añadido. Alimentaria: Revista de Tecnología e Higiene de Los Alimentos 429: 71–80.

Mathias TRDS, Fernandes de Aguiar P, Batista de Almeida E Silva J et al (2016) Brewery waste reuse for protease production by lactic acid fermentation. food technology and biotechnology 55(2): 218-224. https://www.doi.org/10.17113/ftb.55.02.17.4378

Mathias TRDS, Moretzsohn de Mello PP and Camporese Servulo CS (2014) Solid wastes in brewing process: A review. Journal of Brewing and Distilling 5(1): 1–9. https://doi.org/10.5897/jbd2014.0043

Nuobariene L, Hansen AS, Jespersen L and Arneborg N (2011) Phytase-active yeasts from grain-based food and beer. Journal of Applied Microbiology 110(6): 1370–1380. https://doi.org/10.1111/j.1365-2672.2011.04988.x

Ozyurt G, Boga M, Uçar Y, Boga EK and Polat A (2017) Chemical, bioactive properties and *in vitro* digestibility of spray-dried fish silages: comparison of two discard fish (*Equulites klunzingeri* and *Carassius gibelio*) silages. Aquaculture Nutrition 24: 998–1005. https://doi.org/10.1111/anu.12636

Parada RB, Marguet E, Campos C and Vallejo M (2023) Improved antioxidant capacity of three *Brassica* vegetables by two-step controlled fermentation using isolated autochthone strains of the genus *Leuconostoc* spp. And *Lactiplantibacillus* spp. Food Chemistry: Molecular Sciences 6: 1-9. https://doi.org/10.1016/j.fochms.2023.100163

Peña García P, Querevalú Ortiz J, Ochoa Mogollón G and Sánchez Suárez H (2020) Ensilado biológico de residuos de langostino fermentado con bacterias ácido-lácticas: Uso como biofertilizante en cultivo de pasto y como alimento para cerdos de traspatio. Scientia Agropecuaria 11(4): 459–471.

Raeesi, R Shabanpour B and Pourashouri P (2021) Quality evaluation of produced silage and extracted oil from rainbow trout (*Oncorhynchus mykiss*) wastes using acidic and fermentation methods. Waste and Biomass Valorization 12(9): 4931–4942. https://doi.org/10.1007/s12649-020-01331-8

Ramirez Navas SJ (2012) Aprovechamiento industrial de lactosuero mediante procesos Fermentativos. Revista Especializada en Ingeniería de Procesos en Alimentos y Biomateriales 6: 69–83. https://doi.org/10.22490/25394088.1100

Ray Sarkar BC and Chauhan PS (1967) A new method for determining micro quantities of calcium in biological materials. Analytical Biochemistry 20: 155-166. https://doi.org/10.1016/0003-2697(67)90273-4

Samtiya M, Aluko RE and Dhewa T (2020) Plant food anti-nutritional factors and their reduction strategies: an overview. Food Production, Processing and Nutrition 2(6): 1-14. https://doi.org/10.1186/s43014-020-0020-5

Sakr EAE, Massoud MI and Ragaee S (2021) Food wastes

as natural sources of lactic acid bacterial exopolysaccharides for the functional food industry: A review. International Journal of Biological Macromolecules 189: 232–241. https://doi.org/10.1016/j.ijbiomac.2021.08.135

Santacruz-Salas AP, Antunes MLP, Gomez-Herrera S, Velez Lozano JA and Donnini Mancini S (2023) Sostenibilidad en la industria cervecera: una revisión crítica de los residuos generados y su gestión. Biotecnología en el Sector Agropecuario y Agroindustrial 21(1). https://doi.org/10.18684/rbsaa.v21.n2.2023.2167

Shahidi F and Zhong Y (2015) Measurement of antioxidant activity. Journal of Functional Foods 18: 757–781. https://doi.org/10.1016/j.jff.2015.01.047

Sharma P, Sharma A and Lee HJ (2024) Antioxidant potential of exopolysaccharides from lactic acid bacteria: A comprehensive review. International Journal of Biological Macromolecules 281. https://doi.org/10.1016/j.ijbiomac.2024.135536

Sosa FM, Parada RB, Marguet ER and Vallejo M (2022) Utilization of agro-industrial byproducts for bacteriocin production using *Enterococcus* spp. strains isolated from patagonian marine invertebrates. Current Microbiology 79(16): 1–12. https://doi.org/10.1007/s00284-021-02712-5

Sosa FM, Parada RB, Sánchez-Cabrera MA, Marguet ER and Vallejo M (2023) Capacidad antioxidante de bacterias lácticas aisladas de peces e invertebrados marinos de la provincia de Chubut, Patagonia-Argentina. Revista de Ciencias Marinas y Costeras 15(1): 99–112. https://www.redalyc.org/articulo.oa?id=633775558006

Toppe J, Olsen R, Peñarubia O and James DG (2018) Producción y utilización del ensilado de pescado. Organizaciones de las Naciones Unidas para la Alimetación y la Agricultura 1-28. http://www.fao.org/3/i9606es/I9606ES.pdf

Wen J, Jiang W, Feng L, Kuang S, Jiang J, Tang L, Zhou X and Liu Y (2015) The influence of graded levels of available phosphorus on growth performance, muscle antioxidant and flesh quality of young grass carp (*Ctenopharyngodon idella*). Animal Nutrition 1(2): 77–84. https://doi.org/10.1016/j.aninu.2015.05.004

Yang J, Wu XB, Chen HL, Sun-waterhouse D, Zhong H and Cui C (2019) A value-added approach to improve the nutritional quality of soybean meal byproduct: Enhancing its antioxidant activity through fermentation by *Bacillus amyloliquefaciens* SWJS22. Food Chemistry 272: 396–403. https://doi.org/10.1016/j.foodchem.2018.08.037

Yoshida A, Ohta M, Kuwahara K, Cao MJ, Hara K and Osatomi K (2015) Purification and characterization of cathepsin B from the muscle of horse mackerel *Trachurus japonicus*. Marine Drugs 13: 6550-6565. https://doi.org/10.3390/md13116550

Zhang L, Liu C, Li D, Zhao Y, Zhang X, Zeng X, Yang Z and Li S (2013) Antioxidant activity of an exopolysaccharide isolated from *Lactobacillus plantarum* C88. International Journal of Biological Macromolecules 54(1): 270–275. https://doi.org/10.1016/j.ijbiomac.2012.12.037

Research article

https://revistas.unal.edu.co/index.php/refame

Revista Facultad Nacional de Agronomía

Incorporation of tomato peel (*Solanum lycopersicum* L.) into scones: effects on nutritional composition, fatty acids, and sensory traits

Incorporación de cáscara de tomate (*Solanum lycopersicum* L.) en scones: efectos sobre la composición nutricional, ácidos grasos y características sensoriales

https://doi.org/10.15446/rfnam.v78n2.112944

Vilma Quitral[1], Adriana Escobar[1], Rocío Ávila[1], Marcos Flores[2], Ítalo Chiffelle[3] and Carolina Araya-Bastías[4]

ABSTRACT

Food losses and waste correspond to environmental, economic, ethical, and nutritional problems affecting the world. Since most waste is generated at the household level, developing initiatives to recover and revalue it is essential. The present study evaluated the incorporation of tomato (*Solanum lycopersicum* L.) peels (CT) as an ingredient in scones when replacing milk and part of margarine. Scones were formulated with the addition of CT at 20, 25, and 30% of the weight of the dough, and a control sample (M1) was kept. The prepared samples' nutritional composition, carotenoid content, instrumental color, specific volume, and sensory acceptability were evaluated. The fatty acid profile was analyzed in M1 and another sample with CT. A 9-point hedonic scale per parameter was used for sensory evaluation. Incorporating CT in scones made it possible to produce healthier products, with lower fat content, higher dietary fiber content, carotenoids, and lower caloric intake. The specific volume decreased in the scones with CT. The color acquired red tones and, the luminosity decreased. Sensory acceptability was high, with higher ratings for the sample with 30% CT. In the fatty acid profile, saturated fatty acids increased, monounsaturated and polyunsaturated decreased, compared to M1. It was concluded that the incorporation of CT in the preparation of scones is feasible, healthier products were obtained, and well qualified in sensory acceptability.

Keywords:
Bakery
Sensory
Specific volume
Waste

RESUMEN

Las pérdidas y desperdicios de alimentos son un problema ambiental, económico, ético y nutricional que afectan al mundo. Dado que la mayor parte de los residuos se genera a nivel doméstico, es esencial desarrollar iniciativas para su recuperación y valorización. El presente estudio evaluó la incorporación de cáscara de tomate (*Solanum lycopersicum* L.) (CT) como ingrediente en bollitos en reemplazo de leche y parte de la margarina. Los bollitos se formularon con adición de CT en un 20, 25 y 30% del peso de la masa y se conservó una muestra control (M1). De las muestras preparadas se evaluó la composición nutricional, el contenido de carotenoides, el color por método instrumental, el volumen específico y la aceptabilidad sensorial. El perfil de ácidos grasos se analizó en M1 y otra muestra con CT. Para la evaluación sensorial se aplicó una escala hedónica de 9 puntos por parámetro. La incorporación de CT en scones permitió elaborar productos más saludables, con menor contenido de grasa, mayor contenido de fibra dietética, carotenoides y menor aporte calórico. El volumen específico disminuyó en los bollitos con CT. El color adquirió tonos rojos y la luminosidad disminuyó. La aceptabilidad sensorial fue positiva, con calificaciones más altas para la muestra con 30% de CT. En el perfil de ácidos grasos, aumentaron los ácidos grasos saturados, disminuyeron los monoinsaturados y poliinsaturados, en comparación con M1. Se concluyó que la incorporación de CT en la preparación de bollitos es factible, se obtuvieron productos más saludables y bien calificados en aceptabilidad sensorial.

Palabras clave:
Productos horneados
Sensorial
Volumen específico
Desperdicios

[1]Escuela de Nutrición y Dietética, Facultad de Salud, Universidad Santo Tomás, Santiago de Chile, Chile. vilmaquitral@santotomas.cl, a.escobar10@alumnos.santotomas.cl, r.avila2@alumnos.santotomas.cl
[2]Departamento de Horticultura, Facultad de Ciencias Agrarias, Universidad de Talca, Talca, Chile. marcos.flores@utalca.cl
[3]Departamento de Agroindustria y Enología. Facultad de Ciencias Agronómicas, Universidad de Chile, Santiago, Chile. ichiffel@uchile.cl
[4]School of Cardiovascular and Metabolic Health, College of Medical, Veterinary and Life Sciences, University of Glasgow, United Kingdom. c.araya-bastias.1@research.gla.ac.uk
*Corresponding author

Received: October 4, 2024; Accepted: April 24, 2025
Rev. Fac. Nac. Agron. Medellín 78(2): 11117-11125. 2025
ISSN 0304-2847 / e-ISSN 2248-7026

CC BY NC SA

According to FAO (2019) data, 14% of food, with an estimated value of US$ 400 billion, is lost between harvest and distribution worldwide, and 17% is wasted in distribution and among final consumers (PNUMA 2021). This is an economic, environmental, ethical, and nutritional problem. Consumers can reduce "waste" by taking advantage of what is commonly known as "inedible parts" of some foods, such as vegetable peels. When revaluing these, their nutrients and bioactive compounds are used, since, in several vegetables, the peels contain more nutrients, dietary fiber, polyphenols, and other bioactive compounds than the pulp (Rocha da Costa et al. 2023). Further, its use allows to reduce waste.

Data from a household survey in Santiago, Chile, indicate that the average food waste was 0.96 kg per week per capita, and the main group of wasted food corresponds to fruits and vegetables (Cáceres-Rodríguez et al. 2021). The waste products must be revalued as they contain nutrients, pigments, and bioactive compounds that enhance processed foods, such as bakery products.

Several studies have explored the use of fruits and vegetable peels as partial substitutes for flour in baked products, increasing the content of dietary fiber and bioactive compounds while reducing caloric intake. Some studies have shown an increase in satiety because of the higher dietary fiber content. When vegetable peels are added, the dough changes, and the leavening effect is diminished. The concentrations at which they are added must be carefully monitored as in some cases, the products acquire strong or uncharacteristic residual aroma and flavor (Martins et al. 2017; Santos et al. 2022; Quitral et al. 2022, 2023).

Baked products are a highly consumed food by a large part of the population (Moretton et al. 2023). They are consumed at breakfast as snacks, and to accompany other meals. They are made with flour, butter, margarine or oil, eggs, sugar, milk, and other ingredients. Their caloric intake in general is high, attributed to the fat they contain and carbohydrates. Scones, or English rolls, are characterized by their flavor and soft texture; they are very pleasant and have high acceptability among consumers, despite their high caloric intake.

In this type of product, vegetable peels can be used to replace part of other ingredients and provide nutrients and bioactive compounds. The incorporation of vegetable peels alters the color of baked products (measured instrumentally) in various cases, the specific volume decreases, and the sensory characteristics are favored or harmed depending on the concentration of peels incorporated (Martins et al. 2017).

Tomato peels are interesting to research due to their attractive color produced by carotenoids and their high availability since tomato is a widely consumed vegetable. It is consumed fresh, in culinary preparations, and processed products. It is rich in carotenoids, especially lycopene, which is a powerful antioxidant, and contains tocopherols, polyphenols, organic acids, vitamins, and other components beneficial to health. At an industrial and domestic level, tomato by-products are eliminated, which must be valued and rescued to take advantage of their nutrients and bioactive compounds (Navarro-González et al. 2011).

This study aimed to assess the impact of replacing milk and part of margarine with fresh tomato peel on the nutritional composition, fatty acid profile, carotenoid content, physical properties, and sensory acceptability of scones.

MATERIALS AND METHODS

Formulations

This study employs a quantitative experimental design to formulate scones with tomato peels (CT) at varying concentrations, substituting milk and a portion of the margarine. The independent variable is the concentration of CT in scones. The dependent variables are nutritional composition, total carotenoid content, color, specific volume, sensory acceptability, and fatty acid profile. CT was obtained from household discards through the manual peeling of tomatoes, the inclusion of the red layer attached to the skin. The peels were washed exhaustively with water, dried with absorbent paper, and ground in a manual grinder.

Scones were made for a traditional recipe based on flour, eggs, margarine, milk, sugar, baking powder, and salt. Three formulations were developed in which milk was

eliminated; the margarine concentration was reduced by 25, 35, and 50%; and CT was added at 20, 25, and 30% of the total mass. A control sample, without tomato peel, was also prepared. The dough was divided into units of 50 g and baked in an oven at 175 °C for 20 minutes. The formulations are presented in Table 1.

Table 1. Scone formulations with tomato peel (CT).

Ingredients/formulations	M1	M2	M3	M4
Flour (g)	52	52	52	52
Eggs (g)	6	6	6	6
Sugar (g)	3	3	3	3
Baking powder (g)	2	2	2	2
Salt (g)	1	1	1	1
Milk (mL)	25	0	0	0
Margarine (g)	11	8.25	7.15	5.5
Tomato peel (CT) (g)	0	20	25	30
Water (mL)	0	7.75	3.85	0.5

Chemical analysis

The nutritional composition was determined using official methods (AOAC 2012). Humidity was measured by the thermogravimetric oven drying method at 105 °C. Fat content was determined by solvent extraction using the Soxhlet method. Proteins were analyzed according to the Kjeldahl method. Ash content was measured by the thermogravimetric method, with incineration in a muffle furnace at 550 °C. Total dietary fiber (TDF) was determined using a gravimetric enzymatic method, with soluble (SDF) and insoluble fiber (IDF) components assessed separately. Carbohydrates were calculated by difference. Caloric intake was estimated by multiplying the values for proteins, fats, and carbohydrates by the Atwater factors. Total carotenoids were evaluated using a spectrophotometric method, and the fatty acid profile was determined by chromatography (AOAC 2012).

Determination of color

Instrumental color was evaluated for CIELab values with a Hunter colorimeter and specific volume according to the seed displacement method (AACC 2010).

Sensory analysis

Acceptability test with a 9-point hedonic scale for parameters (Abalos et al. 2023; Sugumar and Guha 2022). The test was applied to 93 consumers, 50 women, and 43 men, aged 20 to 60. Single-blind study. Each scone sample was evaluated individually. A sample and the answer sheet were given to the evaluator. Each description was assigned a numerical value from 1 to 9 (1 for "I dislike it too much" and 9 for "I love it"), and the average was calculated for each parameter per sample.

Statistical analysis

The data were analyzed by analysis of variance (ANOVA) and Tukey's test to establish significant differences between the samples at $P<0.05$. All experiments and analyses were conducted in triplicate to ensure the reliability of the results.

RESULTS AND DISCUSSION

The incorporation of CT in the scone dough was effective, readily integrating with the other ingredients to produce a dough with suitable properties. Consistent with this observation, Gu et al. (2020) reported that CT exhibits high water retention capacity (7.9 g g^{-1}), water solubility (18%), oil retention capacity (4.5 g g^{-1}), and swelling capacity (12.4 mL g^{-1}), due to its dietary fiber content, which likely facilitated its convenient addition and homogeneous mixing with the other components.

As shown in Table 2, the protein and ash content do not exhibit statistically significant differences between the analyzed samples. In contrast, the fat content was significantly higher ($P<0.05$) in the control sample and demonstrated a reduction with increasing CT incorporation. The carbohydrate content was significantly higher ($P<0.05$)

in sample M1. Statistically significant differences (P<0.05) were observed in the total dietary fiber (TDF) content, with M1 displaying the lowest value and M4 the highest. A similar trend was observed for soluble dietary fiber (SDF) and insoluble dietary fiber (IDF). The caloric intake is significantly higher in M1 and significantly lower in M4 (P<0.05).

Table 2. Nutritional composition and carotenoids in scones in 100-gram dry weight (dw).

	M1	M2	M3	M4
Proteins (g)	10.9±0.367^{a}	10.8±0.286^{a}	11.3±0.474^{a}	11.3±0.242^{a}
Fat (g)	10.5±0.345^{b}	7.1±0.421^{a}	6.5±0.420^{a}	6.3±0.227^{a}
Ashes (g)	4.1±0.514^{a}	4.2±0.188^{a}	3.7±0.043^{a}	3.7±0.201^{a}
Carbohydrates (g)	68.0±0.989^{b}	64.5±1.152^{a}	64.9±0.834^{a}	63.4±0.489^{a}
Total dietary fiber (TDF) (g)	6.4±0.303^{a}	12.9±0.536^{b}	13.6±0.376^{b}	15.3±0.324^{c}
Soluble dietary fiber (SDF) (g)	1.8±0.220^{a}	2.7±0.294^{b}	2.9±0.169^{b}	4.3±0.179^{c}
Insoluble dietary fiber (IDF) (g)	4.6±0.270^{a}	10.1±0.406^{b}	10.8±0.207^{bc}	11.0±0.302^{c}
Energy (kcal)	411±4.400^{c}	365±2.645^{b}	363±2.449^{b}	355±1.391^{a}
Carotenoid totals (mg)	ND	2.7±0.147^{a}	2.9±0.312^{a}	3.2±0.310^{a}

M1: control sample; M2: sample with 20% of CT, 25% margarine reduction; M3: sample with 25% of CT, 35% margarine reduction; M4: sample with 30% of CT, 50% margarine reduction; ND: not detected. The detection limit is $\leq$0.60 mg 100 g^{-1}. Different letters indicate significant differences between the samples (P<0.05).

Eliminating milk from formulations and substituting part of the margarine with tomato peels resulted in a significant decrease in fat content of 32, 38, and 40% in M1, M2, and M3, respectively, compared to M1. The incorporation of CT also led to a reduction in caloric intake in M2, M3, and M4 by 11, 12, and 14%, respectively. Furthermore, a significant increase in dietary fiber, primarily in IDF, was observed. A negative correlation was found between the CT content in scones and both fat and energy (R^2=0.994, 0.960, and 0.780, respectively). From a nutritional perspective, scone formulations incorporating CT appear healthier due to their lower fat, carbohydrate, and caloric content, coupled with a higher DF contribution. These findings align with other studies demonstrating that the addition of vegetable peels can reduce caloric intake while enhancing dietary fiber content (Martins et al. 2017; Quitral et al. 2022).

The carotenoid content in CT was measured at 15.5 mg 100 g^{-1}, and its concentration in the scone samples increased with higher CT concentrations in the formulations. No statistically significant differences in carotenoid content were observed among the scone samples containing CT. Notably, the total carotenoid concentration in CT is higher than that reported by Beltrán et al. (2012) for common raw tomato (2.66 mg 100 g^{-1}) and by Pataro et al. (2018) for tomato skin (10 mg 100 g^{-1}). It is important to note that the carotenoid content in tomatoes is generally higher in the peel than in the pulp (Meléndez-Martínez et al. 2023).

Carotenoids are susceptible to degradation by heat; the baking temperature of 175 °C is relatively high, likely to affect the carotenoid concentration in the scone samples. Burešová et al. (2021) reported a 26% loss of carotenoids in bread baked al 220 °C. Elevated temperatures can induce degradation, isomerization, and oxidation of carotenoids (Shen et al. 2015). Conversely, thermal processing of food can lead to interaction with other lipophilic constituents, potentially modifying the quantity of carotenoids released from the food matrix (Kotíková et al. 2016).

The incorporation of tomato peels into flour-based products increases the carotenoid concentration, offering potential health benefits due to their antioxidant properties and provitamin A activity. Furthermore, they impart reddish hues to foods, which can be a desirable attribute (Salanţă and Fărcaş 2024). The addition of peels or other fruit and vegetable by-products to baked goods introduces bioactive compounds, such as polyphenols and carotenoids, thereby enhancing the antioxidant capacity of the products (Santos et al. 2022).

Table 3 presents the luminosity (L*), which shows no significant differences between the samples. However, the a* (redness) and b* (yellowness) values increased noticeably with CT incorporation. Chroma (C*) and hue angle (H*) were also higher in samples containing CT. The color difference (ΔE*) compared to the control sample did not show significant differences between among the CT-containing samples.

The instrumental color analysis results are consistent with a study on bread incorporating tomato pomace, which also reported an increase in a* and b* values (Martins et al. 2017). The intense red color of tomatoes and their peels contributes to this coloration in the final products. The observed increase in a* and b* aligns with the findings of Bhat and Ahsan (2015) in cookies containing tomato pomace powder (OTP). However, their study reported a decrease in L* with OTP addition, which the authors attributed to the reduced flour concentrations as OTP concentration increased.

By incorporating CT in scones, the specific volume decreases proportionally, as seen in Table 3 and

Table 3. Instrumental color and specific volume of scone samples.

	M1	M2	M3	M4
L*	66±4.00^{a}	68±4.36^{a}	68±6.08^{a}	69±6.56^{a}
a*	0.3±0.20^{a}	8.2±0.46^{b}	7.8±0.53^{b}	9.1±1.99^{b}
b*	23.4±1.60^{a}	35.6±2.29^{b}	36.0±3.04^{b}	35.1±1.05^{b}
ΔE*	-	14.8±0.21^{a}	16.5±5.17^{a}	16.7±3.44^{a}
C*	23.4±1.60^{a}	36.5±2.13^{b}	36.8±3.10^{b}	36.3±0.79^{b}
H*	0.01±0.01^{a}	0.23±0.03^{b}	0.21±0.01^{b}	0.25±0.06^{b}
Specific volume ($cm^3 g^{-1}$)	2.28±0.07^{a}	2.23±0.11^{a}	2.20±0.10^{a}	2.17±0.21^{a}

M1: control sample; M2: sample with 20% of CT, 25% margarine reduction; M3: sample with 25% of CT, 35% margarine reduction; M4: sample with 30% of CT, 50% margarine reduction. Different letters indicate significant differences between the samples (P<0.05).

Figure 1. Tomato peel contains dietary fiber, which weakens the structure of gluten, causing less CO_2 retention in the scones (Bora et al. 2019).

Figure 1 presents the differences in color and shape of the samples. The color differences in the crumb are more noticeable than in the crust. The specific volume of

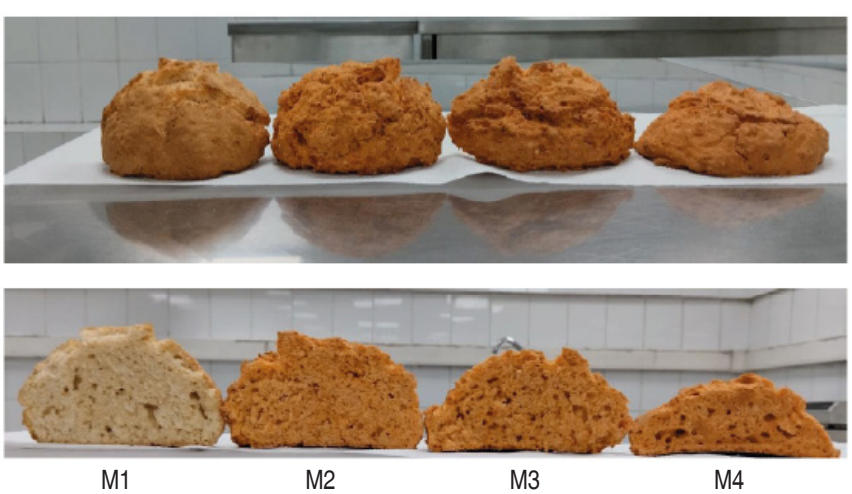

Figure 1. Scones samples. M1: control sample; M2: sample with 20% of CT, 25% margarine reduction; M3: sample with 25% of CT, 35% margarine reduction; M4: sample with 30% of CT, 50% margarine reduction.

the samples is lower than the values reported by other researchers for bread, which typically exceed 3 cc g^{-1} (Mudgil et al. 2016; Ding et al. 2019). However, the results of this study are comparable to those observed in gluten-free bread and muffins by Gostin (2019) and Bora et al. (2019). According to Burton and Lightowler (2006), this reduction in specific volume could be advantageous as it is associated with a lower glycemic index and increased satiety.

A strong negative correlation (-0.946) was observed between the specific volume of the scones and increasing CT concentration. This phenomenon can be attributed to the incorporation of dietary fiber from CT. Specific volume is a critical characteristic of baked products, influencing the perception of a light and spongy texture. It is primarily determined by gas production and retention during baking, a process largely dependent on gluten development. The samples containing CT exhibited significantly higher DF content, and increasing its concentration in the dough has been shown to reduce the rate of hydration and gluten development (Xu et al. 2021), consequently affecting the specific volume. Furthermore, the reduction in fat content, which plays a crucial role in air bubble incorporation and contributes to increased volume and a porous structure, also likely influenced this result. Fat also aids in moisture retention, leading to a moist and tender crumb, and interacts with starch to form lipid-amylose complexes, thereby inhibiting retrogradation (Garvey et al. 2020).

Overall, the samples demonstrated high sensory acceptability, as illustrated in Figure 2. Appearance was rated significantly higher (P<0.05) in M1 and M4. No significant differences were found in the color of the samples. Regarding aroma, significant differences (P<0.05) were observed, with M4 receiving the highest acceptability score and M2 the lowest. Flavor acceptability was significantly higher (P<0.05) in M1, M2, and M4. Texture was also rated significantly higher (P<0.05) in M1 and M4.

Despite the variations in individual attributes, all samples exhibited high overall sensory acceptability. No significant correlation was found between the amount of CT incorporated into the samples and the ratings of the sensory attributes evaluated using a 9-point hedonic scale. Based on the overall evaluation, sample M4 was the preferred formulation.

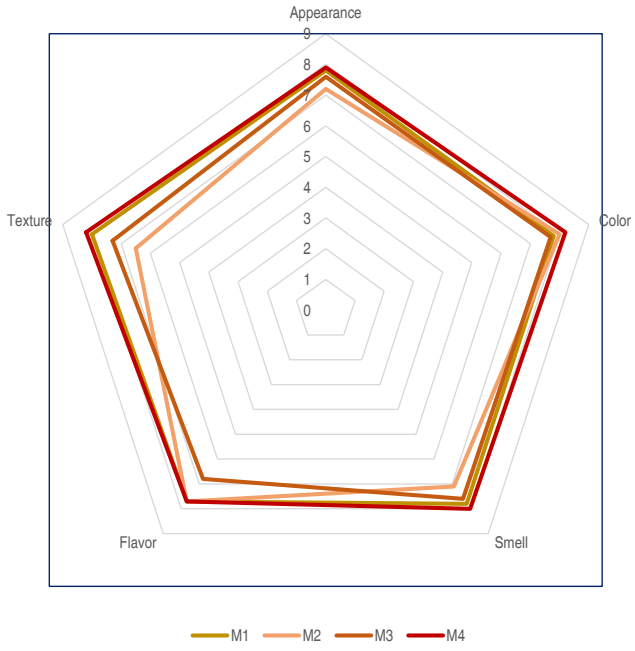

Figure 2. Sensory test radial graph – 9-point hedonic scale. M1: control sample, M2: sample with 20% of CT, 25% margarine reduction, M3: sample with 25% of CT, 35% margarine reduction, and M4: sample with 30% of CT, 50% margarine reduction.

In contrast to the results obtained in this study, Bhat et al. (2015) reported that the incorporation of tomato pomace powder negatively impacted the sensory parameters of appearance, color, texture, and flavor in cookies, recommending a maximum addition of 5%. In this study, the addition of fresh tomato peel, without dehydration, as a substitute for milk and part of margarine, yielded more favorable sensory outcomes.

Based on the results presented in Table 4, sample M4 exhibits a higher proportion of saturated fatty acids compared to M1. The amount of monounsaturated fatty acids is similar between the samples, while polyunsaturated fatty acids are present at a slightly higher concentration in M1. Notably, sample M4 contains linolenic acid, whereas trans fatty acid content is below 0.1% in both samples.

Table 4. Fatty acid profile of scone samples.

Fatty acid	M1	M4
Saturated (%) methyl esters	-	-
C6:0 caproic	0.21	-
C8:0 caprilic	0.63	0.37
C10:0 capric	0.77	0.33
C12:0 lauric	7.34	5.52
C14:0 miristic	3.72	2.35
C15:0 pentadecanoic	0.13	0.04
C16:0 palmitic	14.19	24.91
C17:0 heptadecanoic	0.14	0.13
C18:0 stearic	8.89	9.07
C22:0 docosanoic	0.43	0.33
C24:0 tetracosanoic	0.12	-
The sum of saturated fatty acids	36.58	43.18
Monounsaturated % methyl esters	-	-
C14:1 ω 5 miristoleic	0.11	-
C16:1 ω 7 palmitoleic	0.51	0.39
C18:1 ω 9 oleic	25.39	28.10
C18:1 ω 7 oleic	1.24	0.84
C20:1 ω 15 eicosaenoic	3.98	-
C20:1 ω 9 eicosaenoic	0.39	0.25
The sum of monounsaturated fatty acids	31.62	29.59
Polyunsaturated (%) Methyl esters	-	-
C18:2 ω 6 linoleic acid	31.63	25.27
C18:3 ω 3 linolenic acid	-	1.87
C20:4 ω 6 eicosatetraenoic acid	0.17	0.10
The sum of polyunsaturated fatty acids	31.80	27.23
Isomers trans (%) methyl esters	<0.1	<0.1

M1: Control sample, M4: sample with 30% of CT, 50% margarine reduction.

The fatty acid profile reveals that in M4, saturated fatty acids increased by 18% compared to the control sample, while monounsaturated and polyunsaturated fatty acids decreased by 6.4 and 14.4%, respectively. Different results might have been anticipated, given that M4 is formulated without milk, a significant source of saturated fatty acids, and relatively low in polyunsaturated fatty acids. However, margarine, an ingredient in M4, does

contribute saturated fatty acids. Consequently, while the concentration of SFAs in M4 is lower compared to milk-containing formulations, their presence is still attributable to the inclusion of margarine. Linolenic acid was detected in sample M4 but not in M1. Sample M4 had a lower margarine content and did not contain milk; the primary lipid source in this formulation was eggs. Among individual fatty acids, palmitic acid and oleic acid concentrations were 75 and 11% higher in M4 compared to M1, respectively. These fatty acids are constituents of eggs, an ingredient present at a higher ratio to margarine in M4 (1.1:1) than in M1 (0.5:1). The concentration of palmitic acid, oleic acid, and linolenic acid were significantly elevated in M4. According to Elbadrawy and Sello (2016), tomato peel contains 15.2% palmitic acid, 19.1% oleic acid, and 4.3% linolenic acid. The latter two are particularly beneficial for health: oleic acid is associated with a reduced incidence of cardiovascular disease, and linolenic acid is an essential fatty acid and a precursor to EPA and DHA. Tomato peel also contains linoleic acid, another essential fatty acid.

A key strength of this study is its demonstration that vegetable peels can be utilized at the consumer level with minimal processing (simply washing) and still yield positive nutritional and sensory outcomes. Common baked goods like scones often have a high fat content, which can be effectively reduced through the incorporation of vegetable peels, leading to healthier products.

CONCLUSION

Incorporating fresh tomato peels as an ingredient in scones, substituting part of the margarine and all the milk, yielded favorable outcomes. From a nutritional standpoint, this approach effectively reduced total fat content and caloric intake while increasing dietary fiber. Furthermore, carotenoids were successfully incorporated into the scones. The addition of CT influenced the color, resulting in predominantly red tones and a decrease in luminosity. However, the specific volume was negatively affected, indicating a need to explore alternative strategies to mitigate this issue. Scone samples containing CT demonstrated high sensory acceptability, with sample M4 (containing 30% CT and 50% margarine reduction) identified as the most promising formulation. This sample exhibited significantly high levels of TDF, SDF, and IDF, along with a lower caloric content and a distinct fatty acid profile compared to the control sample M1, notably including linolenic acid. This study contributes to the growing body of knowledge regarding the utilization of vegetable peels, specifically fresh tomato peels, in this case, as functional ingredients in flour-based foods. Future research should focus on investigating methods to enhance the specific volume of scones incorporating CT, determining their shelf life, and evaluating their potential for industrial-scale applications.

ACKNOWLEDGMENTS

This study was financially supported by the Internal Project of Universidad Santo Tomás, titled "*Incorporation of vegetable peel as an ingredient in baked products*" ERP-11320023. We thank the UST-Santiago School of Nutrition for its willingness and support to carry out the study.

CONFLICT OF INTERESTS

The authors have no conflict of interest.

REFERENCES

AACC – American Association of Cereal Chemists (2010) Approved Methods of Analysis**.** Method 10-05.01 Guidelines for Measurement of Volume by Rapeseed Displacement.

AOAC – Association of Official Analytical Chemists (2012) Official Methods of Analysis of Association of Official Analytical Chemists International. 19th edition. Dr. William Horwitz, and Dr. George Latimer, Jr Editors.

Abalos RA, Aviles MV, Naef E and Gómez MB (2023) Development and characterization of a ready-to-eat vegetable millefeuille enriched with polyphenols. Revista Española de Nutrición Humana y Dietética 27(2): 163 – 172. https://doi.org/10.14306/renhyd.27.2.1839

Beltrán B, Estévez R, Cuadrado C, Jiménez S and Alonso BO (2012) Base de datos de carotenoides para valoración de la ingesta dietética de carotenos, xantofilas y de vitamina A; utilización en un estudio comparativo del estado nutricional en vitamina A de adultos jóvenes. Nutrición Hospitalaria 27(4): 1334-1343.

Bhat MA and Ahsan H (2015) Physico-Chemical characteristics of cookies prepared with tomato pomace powder. Journal of Food Processing & Technology 7: 543. https://doi.org/10.4172/2157-7110.1000543

Bora P, Ragaee S and Abdel-Aal ES (2019) Effect of incorporation of goji berry by-product on biochemical, physical and sensory properties of selected bakery products. LWT-Food Science and Technology 112: 108225. https://doi.org/10.1016/j.lwt.2019.05.123

Burešová B, Paznocht L, Kotíková Z, Giampaglia B et al (2021) Changes in carotenoids and tocols of colored-grain wheat during unleavened bread preparation. Journal of Food Composition and Analysis 103: 104108. https://doi.org/10.1016/j.jfca.2021.104108

Burton P and Lightowler HJ (2006) Influence of bread volume

on glycaemic response and satiety. British Journal of Nutrition 96: 877-882. https://doi.org/10.1017/BJN20061900

Cáceres-Rodríguez P, Morales-Zúñiga M, Jara-Nercasseau M, Huentel-Sanhueza C et al (2021) Encuesta sobre comportamiento familiar frente al desperdicio de alimentos y determinación del costo nutricional de éste, en una muestra de hogares en Chile: Resultados de un estudio piloto. Revista Española de Nutrición Humana y Dietética 25(3): 279-293. https://doi.org/10.14306/renhyd.25.3.1242

Ding S, Peng B, Li Y and Yang J (2019) Evaluation of specific volume, texture, thermal features, water mobility, and inhibitory effect of staling in wheat bread affected by maltitol. Food Chemistry 283: 123-130. https://doi.org/10.1016/j.foodchem.2019.01.045

Elbadrawy E and Sello A (2016) Evaluation of nutritional value and antioxidant activity of tomato peel extracts. Arabian Journal of Chemistry. 9(2): S1010-S1018. https://doi.org/10.1016/j.arabjc.2011.11.011

FAO (2019) Pérdida y Desperdicios de Alimentos. https://www.un.org/es/observances/end-food-waste-day/background

Garvey EC, O'Sullivan MG, Kerry JP and Kilcawley KN (2020) Factors influencing the sensory perception of reformulated baked confectionary products. Critical Reviews in Food Science and Nutrition 60(7): 1160-1188. https://doi.org/10.1080/10408398.2018.1562419

Gostin AI (2019) Effects of substituting refined wheat flour with wholemeal and quinoa flour on the technological and sensory characteristics of salt-reduced breads. LWT-Food Science and Technology 114: 108412. https://doi.org/10.1016/j.lwt.2019.108412

Gu M, Fang H, Gao Y, Su T et al (2020) Characterization of enzymatic modified soluble dietary fiber from tomato peels with high release of lycopene. Food Hydrocolloids 99: 105321. https://doi.org/10.1016/j.foodhyd.2019.105321

Kotíková Z, Šulc M, Lachman J, Pivec V et al (2016) Carotenoid profile and retention in yellow-, purple- and red-fleshed potatoes after thermal processing. Food Chemistry 197 (Part A): 992-1001. https://doi.org/10.1016/j.foodchem.2015.11.072

Martins ZE, Pinho O and Ferreira IMPLVO (2017) Food industry by-products used as functional ingredients of bakery products. Trends in Food Science and Technology 67: 106-128. http://doi.org/10.1016/j.tifs.2017.07.003

Meléndez-Martínez AJ, Esquivel P and Rodríguez-Amaya DB (2023) Comprehensive review on carotenoid composition: Transformations during processing and storage of foods. Food Research International 169: 112773. https://doi.org/10.1016/j.foodres.2023.112773

Moretton M, Cattaneo C, Mosca AC, Proserpio C et al (2023) Identification of desirable mechanical and sensory properties of bread for the elderly. Food Quality and Preference 104:104716. https://doi.org/10.1016/j.foodqual.2022.104716

Mudgil D, Barak S and Khatkar BS (2016) Optimization of bread firmness, specific loaf volume and sensory acceptability of bread with soluble fiber and different water levels. Journal of Cereal Science 70: 186-191. http://doi.org/10.1016/j.jcs.2016.06.009

Navarro-González I, García-Valverde V, García-Alonso J and Periago MJ (2011) Chemical profile, functional and antioxidant properties of tomato peel fiber. Food Research International 44 (5):1528-1535. http://doi.org/10.1016/j.foodres.2011.04.005

Pataro G, Carullo D, Bakar Siddique MdA et al (2018) Improved extractability of carotenoids from tomato peels as side benefits of PEF treatment of tomato fruit for more energy-efficient steam-assisted peeling. Journal of Food Engineering 233: 65-73. https://doi.org/10.1016/j.jfoodeng.2018.03.029

PNUMA - Programa de las Naciones Unidas para el Medio Ambiente (2021) Informe anual. https://www.unep.org/es/resources/informe-anual-de-2021

Quitral V, Sepúlveda M, Figueroa D, Saa V and Flores M (2022) Cáscaras de frutas y vegetales como ingrediente en pan: aporte nutricional, saciedad y preferencia sensorial: Análisis de pan con cáscaras como ingrediente. Revista Española de Nutrición Humana Y Dietética 26(1): e1467. https://doi.org/10.14306/renhyd.26.S1.1467

Quitral V, Flores M, Plaza K, Quezada F and Arce H (2023) Carrot peel flour as an ingredient in the preparation of cookies. Revista Chilena de Nutrición 50(2): 226-232. https://doi.org/10.4067/s0717-75182023000200226

Rocha da Costa CA, Machado GGL, Rodrigues LJ, Araújo de Barros H et al (2023) Phenolic compounds profile and antioxidant activity of purple passion fruit's pulp, peel and seed at different maturation stages. Science Horticulturae 321: 112244. https://doi.org/10.1016/j.scienta.2023.112244

Salanţă LC and Fărcaş AC (2024) Exploring the efficacy and feasibility of tomato by-products in advancing food industry applications. Food Bioscience 62: 105567. https://doi.org/10.1016/j.fbio.2024.105567

Santos D, Lopes da Silva JA and Pintado M (2022) Fruit and vegetable by-products flours as ingredients: A review on production process, health benefits and technological functionalities. LWT-Food Science and Technology 154:112707. http://doi.org/10.1016/j.lwt.2021.112707

Shen R, Yang S, Zhao G, Shen Q and Diao X (2015) Identification of carotenoids in foxtail millet (*Setaria italica*) and the effects of cooking methods on carotenoid content. Journal of Cereal Science 61: 86–93. https://doi.org/10.1016/j.jcs.2014.10.009

Sugumar JK and Guha P (2022) Comparative study on the hedonic and fuzzy logic based sensory analysis of formulated soup mix. Future Foods. 5: 100115. https://doi.org/10.1016/j.fufo.2022.100115

Xu J, Li Y, Zhao Y, Wang D and Wang W (2021) Influence of antioxidant dietary fiber on dough properties and bread qualities: A review. Journal of Functional Foods 80: 104434. https://doi.org/10.1016/j.jff.2021.104434

Research article

https://revistas.unal.edu.co/index.php/refame

Revista Facultad Nacional de Agronomía

Effect of turmeric flour on the sensory properties, antioxidants and antidiabetic activity of a spicy fruit sauce

Efecto de harina de *Curcuma longa* en las propiedades sensoriales, actividad antioxidante y antidiabética de salsa picante de fruta

https://doi.org/10.15446/rfnam.v78n2.113684

Maritza Barriga-Sánchez[1]* and Patricia Cristobal Alania[1,2]

Keywords:
α-glucosidase
Charapita chili
Mangifera indica
Solanum sessiliflorum

ABSTRACT

Peru is one of the largest exporters of turmeric. In this sense, it is important to use turmeric in new products for national consumption to achieve its revalorization with other national resources, such as mango, cocona, and charapita chili of Amazonian origin. Due to the growing interest in functional foods, the aim of this study was to evaluate the effect of the addition of turmeric (*Curcuma longa* L.*)* flour (TF) to a spicy fruit sauce (SFS), in the sensory rating, total phenolic compounds (TPC), and antioxidant activity. A factorial experiment design of two factors was carried out: TF content (6, 7, 8, and 9%) and type of fruit (mango and cocona). The proximal composition was determined, and spectrophotometric methods were used to measure the TPC, total curcuminoids, and antioxidant activity: DPPH, FRAP, and ABTS; the colorimetry method was used to measure the color of the samples; and atomic absorption spectroscopy was used to measure the mineral content. The antidiabetic activity was determined for the optimized sample. The optimal SFS was mango-based with 8% TF, with 5.01±0.23 mg curcuminoids g^{-1}, 4.29±0.13 mg GAE $g^{-1,}$ and a higher flavor rating (4.39). The antioxidant capacity DPPH, FRAP, and ABTS was: 15.01±2.38, 14.59±0.04, and 42.01±2.11 µmol TE g^{-1}, respectively; and the α-glucosidase inhibition test resulted in IC_{50} of 69.81±9.42 µg mL^{-1}. In conclusion, TF provides TPC, curcuminoids, antioxidants, and antidiabetic activity. This suggests possible future applications of TF in the development of functional food with antioxidant and antidiabetic effects.

Palabras clave:
α-glucosidasa
Ají Charapita
Mangifera indica
Solanum sessiliflorum

RESUMEN

El Perú es uno de los mayores exportadores de cúrcuma fresca. En ese sentido, es importante emplear la cúrcuma en nuevos productos de consumo nacional para lograr su revalorización junto a otros recursos nacionales, como el mango, cocona y ají charapita de origen amazónico. Dado el creciente interés en alimentos funcionales, este estudio tuvo como objetivo evaluar el efecto de la adición de harina de *Curcuma longa* L (HC) en una salsa picante (SP), analizando la calificación sensorial, compuestos fenólicos (CFT) y actividad antioxidante. Se realizó un diseño experimental factorial de dos factores: HC (6, 7, 8 y 9%) y tipo de fruta (mango y cocona). Se determinó la composición proximal, se usaron métodos espectrofotométricos para los CFT, curcuminoides totales y la actividad antioxidante: DPPH, FRAP y ABTS, se usó un colorímetro para medir el color de las muestras, y el espectrofotómetro de absorción atómica para medir el contenido de minerales. A la muestra optimizada se le determinó la actividad antidiabética. La SP óptima fue la de mango con 8% de HC, con 5,01±0,23 mg curcuminoides g^{-1} y 4,29±0,13 mg GAE g^{-1}. La capacidad antioxidante DPPH, FRAP y ABTS fue :15,01±2,38, 14,59±0,04 y 42,01±2,11 µmol TE g^{-1}, respectivamente y la prueba de inhibición de la α-glucosidasa resultó en IC_{50} de 69,81±9,42 µg mL^{-1}. En conclusión, la HC aporta CFT, curcuminoides, actividad antioxidante y antidiabética. Esto sugiere posibles aplicaciones de la harina de cúrcuma en el desarrollo de productos alimenticios funcionales dirigidos a efectos antioxidantes y antidiabéticos.

[1]Laboratorio de Compuestos bioactivos de la Dirección de Investigación, Desarrollo, Innovación y Transferencia Tecnológica (DIDITT). Instituto Tecnológico de la Producción (ITP), Perú. mbarriga@itp.gob.pe
[2]Escuela Profesional de Ingeniería Alimentaria, Facultad de Oceanografía Pesquería, Ciencias Alimentarias y Acuicultura (FOPCAA), Universidad Nacional Federico Villarreal (UNFV), Perú. patricia27ca@gmail.com
*Corresponding author

Received: October 17, 2024; Accepted: April 28, 2025
Rev. Fac. Nac. Agron. Medellín 78(2):11127-11140. 2025
ISSN 0304-2847 / e-ISSN 2248-7026

CC BY NC SA

Turmeric (*Curcuma longa* L.) is a plant commonly used in many countries, especially in Asia; its rhizome is used as a spice to flavor or color foods and dishes. In 2022, Peru exported 2,734,764 tons of turmeric (*Curcuma longa*), 80.9% fresh, 15.9% in powder, and 3.2% in juice and coloring presentations, among others (CIEN 2023).

It is used in traditional Indian medicine to treat anorexia, cough, diabetic wounds, urinary tract infections and liver disorders, and it also has a similar action to insulin (Mohanty et al. 2004). Likewise, Seclén (2015) mentions that diabetes is a public health problem in Peru, especially for middle-aged people, since approximately a quarter of the adult population of Peru has a higher risk of diabetes.

Slowing glucose absorption by inhibiting the activities of carbohydrate digestive enzymes is considered an effective treatment for diabetes mellitus type 2 (Perez 2016). Tshiyoyo et al. (2022) evaluated the ability of curcumin, and rosmarinic acid to inhibit α-amylase, α-glucosidase and hepatic lipid accumulation. Although several synthetic drugs have been used to treat diabetes, efforts are needed to develop new effective inhibitors against α-amylase and α-glucosidase. Metformin is the most prescribed and recommended drug for type 2 diabetes mellitus because of its better tolerability, pleiotropic benefits, and cost-effectiveness. However, it has secondary effects such as abdominal distension, flatulence, bloating and the possibility of diarrhea (Chaudhary et al. 2024).

The incorporation of fresh *Curcuma longa* or its extract into food matrices provides phenolic compounds and a notable antioxidant capacity. In this regard, Awaeloh et al. (2025) developed gluten-free extruded snacks based on green banana and rice flour enriched with turmeric microcapsules, observing an increase in antioxidant activity while maintaining high sensory acceptability. Similarly, Modi and Sahota (2024) optimized a fermented beverage with fresh turmeric using a response surface methodology. Hutachok et al. (2023) evaluated macaroni fortified with turmeric and green tea extract, which not only has high antioxidant activity but also demonstrated hypolipidemic effects in diabetic rat models by using serum triglyceride levels. These findings support the use of turmeric as a functional ingredient and justify its incorporation into innovative products such as the fruit-based spicy sauce evaluated in this study.

The health benefits of turmeric, including its α-glucosidase inhibitory effects, are well recognized. Although studies have explored its use in food matrices through extracts, microencapsulated forms, and fresh turmeric, there remains a lack of research on the potential antidiabetic and antioxidant effects of new product formulations using turmeric flour in combination with other ingredients, particularly those that have undergone thermal processing. In this study, the inhibition of α-glucosidase of the optimized SFS formulation was demonstrated. At the same time, it contributes to the food sector with a proposal for the productive diversification of turmeric to provide added value to this resource. This study addresses a novel topic, as no prior research was found on the incorporation of turmeric into spicy fruit sauces.

The aim of this study was to assess the impact of turmeric flour (TF) incorporation on the sensory properties, curcuminoid and total phenolic contents, antioxidant capacity, and α-glucosidase inhibitory activity of a spicy fruit sauce.

MATERIALS AND METHODS

Turmeric

Plants of *C. longa L.*, from the Zingiberaceae family, were identified by the Amazonian Herbarium (AMAZ) and registered with code AMAZ 42787. Rhizomes were sown in the Caserío Angel Cárdenas from San Juan, Maynas, Loreto (2'58.954" S, 73°25'46.047" W) at 132 meters above sea level (masl). The humid tropical climate of the area had a temperature range from 20 to 32° C and a rainfall of 2,500 mm per year. In January 2022, 8 months after sowing, the plants with rhizomes at the phenological flowering stage were harvested by digging up. Then, 250 kg of rhizome were washed and sorted. Yellow and orange rhizomes with 5 – 8 cm length and 1.5 – 2 cm diameter were selected and disinfected with 2% sodium hypochlorite for 30 min. They were cut with a steel knife to a thickness of 3 mm to improve the drying process, then dried in a drying chamber with a dehumidifier (25 Pint, Peru) at 30 – 35 °C for 6 days with a drying yield of 10%. Then, dried flakes were ground in an analytical mill (A 11 Basic, IKA, USA), passed through a 500 µm sieve, and retained in a 500 µm sieve (Retsch, Peru). Turmeric flour (TF) was vacuum-packed in polyethylene bags, protected from light, and refrigerated at 5±1 °C until later use.

Chemical reagents

Folin Ciocalteu's phenol reagent (2N), monohydrated gallic acid (≥98.5%, ACS), Trolox (6-hydroxy-2,5,7,8-tetramethylchroman-2-carboxylic acid) ≥96%, potassium iodide solution (>99.0%, ACS), and Acetic acid (≥99.7%, ACS) were obtained from Sigma-Aldrich (Canada). Curcumin standard ≥95% (Bio Basic, Canada). The reagents sodium carbonate (≥99.9%), iron trichloride hexahydrate (ACS), calcium standard (in HNO_3 1,000 mg of Ca in 1 L), acetone (≥99.8%, ACS), methanol (≥99.9%, ACS), chloroform (≥99.8%, ACS) and sodium thiosulfate (ACS) were purchased from Merck (USA). The reagent 2,4,6-Tri(2-pyridyl)-1,3,5-triazine 98% was from Alfa Aesar (Germany), and ethanol (99.5%) was from Scharlau (Spain). Deionized water was supplied by the Barnstead water purification system (Barnstead, Model D11911, Germany). Hydrochloric acid ultrapure reagent (32-35%) (J.T. Baker, Canada), iron standard ICP-27N-5 1,000 µg mL^{-1} (Accustandard, EE. UU.), copper standard ICP-15N-5 1,000 µg mL^{-1} (Accustandard, EE. UU.), zinc standard (1,000 mg L^{-1}, Sigma-Aldrich, Canada), sodium standard ICP-54N-5 1,000 µg mL^{-1} (AccuStandard, EE. UU.), magnesium standard ICP-32N-5 1,000 µg mL^{-1} (AccuStandard, EE. UU.), potassium standard ICP-43N-5 1,000 µg mL^{-1} (AccuStandard, EE. UU.)

Experimental design

To formulate the SFSs, a full factorial design was used with the Minitab statistical program (Table 1), with two factors: Type of fruit with two levels: mango and cocona; and the second factor: turmeric flour content with four levels: 6, 7, 8, and 9% turmeric flour. TF was added to the spicy mango (SMS) and cocona (SCS) sauce as established in Table 1.

The effect of the factors on the following response variables was analyzed: Flavor, TCC, TPC, ABTS, FRAP, DPPH. Optimization was calculated by maximizing flavor score, TCC, and TPC.

Table 1. Experimental design of the formulations of spicy fruit sauces and treatment codes.

Experiments	Treatment code (TF)	Blocks	Fruit	Turmeric flour (%)
1	SMS 6%	1	Mango	6
2	SCS 6%	1	Cocona	6
3	SMS 7%	1	Mango	7
4	SCS 7%	1	Cocona	7
5	SMS 8%	1	Mango	8
6	SCS 8%	1	Cocona	8
7	SMS 9%	1	Mango	9
8	SCS 9%	1	Cocona	9
9	SMS 6%	2	Mango	6
10	SCS 6%	2	Cocona	6
11	SMS 7%	2	Mango	7
12	SCS 7%	2	Cocona	7
13	SMS 8%	2	Mango	8
14	SCS 8%	2	Cocona	8
15	SMS 9%	2	Mango	9
16	SCS 9%	2	Cocona	9

Formulation of the spicy fruit sauce

The studies were conducted in the bioactive compounds laboratories of the Instituto Tecnológico de la Producción, Lima-Peru. The supplies were purchased at the Lima wholesale market. The formulation is shown in Table 2.

Table 2. Formulations in percentage (%) of spicy mango sauce (SMS) and spicy cocona sauce (SCS).

Ingredients	SMS (6%)	SMS (7%)	SMS (8%)	SMS (9%)	SCS (6%)	SCS (7%)	SCS (8%)	SCS (9%)
Yellow chili	20	20	20	20	20	20	20	20
Charapita chili	2.5	2.5	2.5	2.5	2.5	2.5	2.5	2.5
Turmeric	6	7	8	9	6	7	8	9
Mango	41	40	39	38	0	0	0	0
Cocona	0	0	0	0	31	30	29	28
Vegetal spices	2.25	2.25	2.25	2.25	2.25	2.25	2.25	2.25
Pepper	0.1	0.1	0.1	0.1	0.1	0.1	0.1	0.1
Garlic	1	1	1	1	1	1	1	1
Salt	3	3	3	3	3	3	3	3
Oil and vinegar	19	19	19	19	19	19	19	19
Water	5.15	5.15	5.15	5.15	15.15	15.15	15.15	15.15

Sensory evaluation

To control the effect of contrast between samples, a balanced incomplete blocks design (Cochran and Cox 1957) was followed for 28 trained panelists, 14 male and 14 females, between 25 and 60 years old. Workers from the Instituto Tecnológico de la Producción participated; they were selected based on their habit of consuming spicy sauce at least three times a week, and for liking the spicy sensation. The test was developed by a professional from the sensory evaluation laboratory. The 5-point hedonic scale was used to evaluate color, smell, flavor, and texture (consistency). The rating of 5, 4, 3, 2, 1 corresponded to "I like it a lot"; "I like it", "I neither like it nor dislike it", "I dislike it", and "I dislike it a lot", respectively. The rating "3" was considered acceptable, and lower ratings were not acceptable.

Each panelist received two samples according to the balanced incomplete block design (5 g per sample). Pieces of white potato measuring 3x3 cm were used as a sample vehicle. Also, a glass of water was provided, as well as a sensory card that the participants were asked to mark according to their liking. The temperature of the sample at the time of serving was 20±2 °C. The evaluation was carried out in duplicate. The data were processed with R software (Studio version 4.3.1).

Color measurement

The colorimetry equipment (Konica Minolta, CM-5 spectrophotometer, Japan) was used with illuminant D65 and a viewing angle of 0° in reflectance mode, expressing the readings in terms of the CIELab color space (L*, a*, b*). Measurements were made of the values, where L represents luminosity (0 = black, 100 = white), a represents red/green (+ value = redness, - value = greenness), and b represents yellow/blue (+ value = yellowness, - value = blue). The Browning Index (BI) of the sauces was calculated using Equation 1 (S Abd El-Baset and Almoselhy 2023). The BI was used in order to measure how much the SFS increases the brown intensity as TF is added. No references were found with measurements of L*, a*, and b* of spicy fruit sauce; for this reason, the coloration was compared with three commercial samples of chili sauce.

$$BI = \frac{100}{0.17}\left(\frac{a + 1.75\,L}{5.645\,L + a - 0.012\,b} - 0.31\right) \quad (1)$$

Chemical analysis

All the chemical analyses were done in duplicate.

Obtaining extracts

In a 2 mL vial, 1 g of SFS sample was weighed and washed with 1 mL of 96 ° ethanol, then placed in a centrifuge (Centrifuge 5415 C, Germany) at 10,000 rpm for 10 min. The supernatant was placed in a tube, and eight similar washes were performed on the sample in the vial. The entire supernatant was then centrifuged in the refrigerated centrifuge (Centrifuge 5804 R, Germany) at 7,500 rpm for 10 min at 5 °C. Finally, it was rooted in a 10 mL vial and stored frozen until further

analysis. The extract was used for the chemical analysis of total phenolic content, total curcuminoids, antioxidant activity, and antidiabetic activity.

Determination of total phenolic compounds

Total phenolic content (TPC) was determined using the Folin-Ciocalteu procedure described by Barriga-Sánchez et al. (2021) with modifications. 71 µL of extract was combined with 71 µL of Folin-Ciocalteu, 1,430 µL of 6% (w/v) sodium carbonate, and 2,000 µL of deionized water. The mixture was kept in the dark at room temperature for 1 h. The reading was performed at 750 nm using a Genesys 180 model spectrophotometer (Thermo Scientific, USA), and the results were reported as milligram gallic acid equivalents (GAE) per gram of sauce using a curve generated with standard solutions of 50, 100, 150, 200, and 400 mg L^{-1}.

Determination of total Curcuminoids

The methodology was followed as described by Hazra et al. (2015). A standard solution of 500 µg mL^{-1} of curcumin with methanol was prepared in a 10 mL vial, and from it, a calibration curve with the following concentrations: 5, 10, 15 and 20 µg mL^{-1} in ethanol, the absorbances of the points of the calibration curve were measured in the Genesys 180 model spectrophotometer (Thermo Scientific, USA) at 421 nm, and the SFS sample extracts were also directly measured at 421 nm. The results were expressed in mg curcuminoids g^{-1} SFS.

Antioxidant activity

ABTS assay

The 2-2′-azino-bis (3-ethylbenzothiazoline-6-sulfonic acid) (ABTS) radical cation scavenging capacity test of SFS was performed according to Prior et al. (2005). A calibration curve was used with Trolox concentrations of 0.1, 0.5, 1.0, 1.5, and 2.0 mM in ethanol. The calibration curve and the sample extracts were measured in the spectrophotometer. The results were expressed in µmol TE g^{-1} SFS.

DPPH

The antioxidant capacity of SFS was determined using the procedure described by Barriga-Sánchez et al. (2021), using the reagent 2, 2-diphenyl-1-picrylhydrazyl (DPPH). For the calibration curve, Trolox was used as a standard, and a calibration curve was prepared from the sample extracts, from 100 µL to 900 µL. After 30 minutes of reaction in the dark, the absorbance was determined in the spectrophotometer at 518 nm. The results were expressed in µmol TE g^{-1} SFS.

FRAP assay

The antioxidant capacity of the spicy fruit sauce was determined using the FRAP assay as described by Barriga-Sánchez et al. (2022). Samples extracts at the appropriate dilution were added to the FRAP reagent (acetate buffer pH=3.6, TPTZ (2,4,6-tripyridyl-s-triazine) and $FeCl_3 6H_2O$ in a ratio of 25:2.5:2.5). The mixture was incubated at 20 °C for 30 min, and the absorbance was measured with the Spectrophotometer at 595 nm. A calibration curve was prepared using 50, 150, 300, 400, 500, and 600 µM Trolox. The results were expressed in µmol TE g^{-1} SFS.

Antidiabetic activity

α-glucosidase inhibition assay

The quantification of α-glucosidase inhibition was determined using the enzymatic hydrolysis of the substrate p-Nitrophenyl-α-D-glucopyranoside (p-NGP) by the action of the enzyme α-glucosidase (α-GLC) that releases p-nitrophenolate and α-D-glucose units, as described by Artanti et al. (2012) and Srianta et al. (2013) with modifications. Acarbose was used as a positive control (10-1,000 µg mL^{-1}). 50 µL of SFS Sample extract was added to a vial with 100 µL of p-NGP (5 mM) and 330 µL of phosphate buffer (pH=6.8); the same was done for acarbose. 20 µL of α-GLC (0.24 U mL^{-1} in phosphate buffer, pH=6.8) was added, and the vials were incubated at 37 °C for 15 min. The reaction was stopped with 500 µL of Na_2CO_3 (0.2 M), and the absorbance was measured at 405 nm. The results were expressed in IC_{50}, units µg mL^{-1}. The criterion to confirm positive antidiabetic activity consisted of comparing the IC_{50} of the sample and acarbose, and the sample must have a lower IC_{50} compared to acarbose.

Characterization of the optimized SFS (SMS 8% TF)

Proximal composition analysis

The proximal composition was determined as described by Barriga-Sánchez et al. (2022).

The moisture content was estimated by the gravimetric method by drying the sample in an oven (Venticell Ecoline,

Czech Republic). The ash content was determined by incinerating the dried sample overnight in a muffle furnace (Barnstead, Thermolyne, model 48000, USA). Total nitrogen content was determined by the Kjeldahl method using a Kjeldatherm TZ automated block digester (Germany) and a Buchi K-350 distillation unit (Spain). Fat content was determined by the Soxhlet method using a Buchi E-800 Universal Extractor (Switzerland).

Determination of mineral nutrients

Analyses of calcium, iron, copper, zinc, magnesium, sodium, and potassium were performed with an atomic absorption spectrophotometer (Perkin Elmer, Analyst 800, USA) as described by Barriga-Sánchez et al. (2022).

Viscosity determination

The viscosity was determined with a viscometer (Brookfield viscometer, DV2T, USA), and the spindle 64 was used. The apparent viscosity was determined at 3 rpm at 25 °C for the SMS 8TF and three commercial samples.

Determination of pH value

The pH of each spicy sauce was determined by direct reading, using the potentiometer (Thermo Scientific, Orion VersaStar Pro, Indonesia) with a semi-solid sample electrode (Thermo Scientific Orion 8157BNUMD).

Determination of acidity

A TitroLine TL 7000 automatic titrator (Schott GmbH, Germany) was used for the analysis. First, 0.5 g of sauce was weighed, and 50 mL of 96% ethanol, neutralized with phenolphthalein, was added to the sample. The mixture was then homogenized. Titration was carried out using 0.02 N NaOH. A blank sample, consisting of neutralized ethanol titrated with 0.25 N NaOH, was included, and the volume of NaOH consumed during titration was recorded. Equation (2) was used to calculate the percentage of acetic acid.

$$\text{Acetic Acid}(\%) = \frac{V \times N \times F \times 0.060}{W} \times 100 \qquad (2)$$

Where V is the volume of NaOH used in titration (mL), N is the normality of NaOH, F is the NaOH factor, W is the weight of the sauce sample (g), and 0.060 is the Milliequivalents of acetic acid.

Determination of consistency

The consistency of SMS 8 TF was determined using a Bostwick consistometer (Cole-Parmer Consistometer, USA) following the method of Juszczak et al. (2013). The consistometer tank was filled, and the gate was opened. The distance traveled after 30 seconds was recorded, and the results were expressed in centimeters per 30 seconds.

Statistical analysis

With the Minitab v.17 statistical program (Minitab, USA), a full factorial experimental design was obtained and the effect of the factors on the sensory evaluation score, TCC, TPC and antioxidant activity was analyzed; a one-way analysis of variance (ANOVA) and Tukey's multiple comparisons test of means were also performed. Previously, the results of the sensory analysis were analyzed by the RStudio 4.3.1 program, and then a factor analysis was performed. A significance level of $P<0.05$ was used. Results were presented as mean ± standard deviation and calculated using Excel 2016 (Microsoft, USA).

RESULTS AND DISCUSSION

Sensory analysis of the SFS

A sensory acceptable spicy sauce formulation was achieved, successfully masking the unpleasant taste of turmeric.

The attributes color, smell, and texture (consistency), and the spicy sensation, presented ratings higher than "3"; while in the flavor attribute, two of the treatments obtained ratings lower than "3" (Figure 1). The highest flavor scores were obtained by SMS 7% TF and SMS 8% TF (Table 3).

There was a significant effect of the type of fruit on the flavor (P=0.022), color (P=0.044), texture (P=0.029) of the SFS, also of the TF (P=0.017) on the flavor of the SFS (Table 4). There was no significant effect of the addition of TF and the type of fruit on the odor and spicy sensation (Table 4).

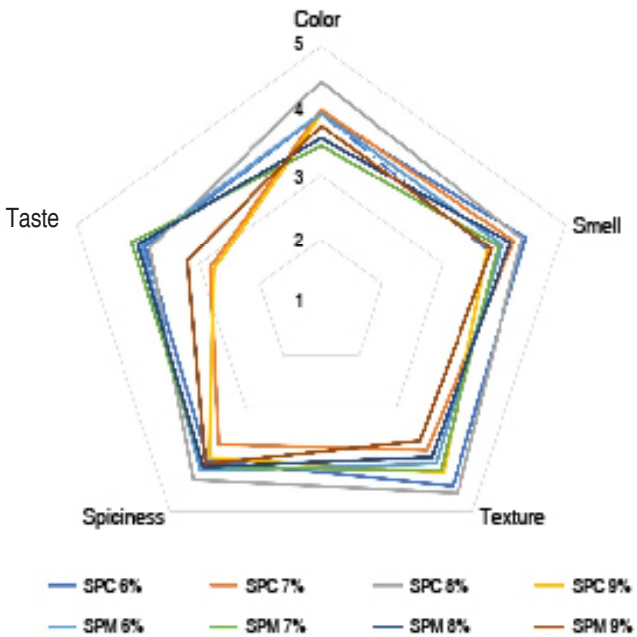

Figure 1. Spicy fruit sauce color, smell, texture, spiciness, and flavor ratings. SCS: spicy cocona sauce, SMS: spicy mango sauce, containing 6%, 7%, 8%, and 9% turmeric flour.

Table 3. Experimental design with results of flavor rating, total curcuminoids (TCC), total phenolic compounds (TPC) of mango (SMS) or cocona (SCS) spicy sauce with 6, 7, 8 and 9% turmeric flour.

Experiments	Treatment (TF)	Flavor	TCC (mg curcumin g^{-1})	TPC (mg GAE g^{-1})
1	SMS 6%	4.11	3.74	2.95
2	SCS 6%	3.86	3.77	3.43
3	SMS 7%	4.48	4.51	3.71
4	SCS 7%	2.98	4.54	4.01
5	SMS 8%	3.61	4.85	4.38
6	SCS 8%	3.98	5.12	4.46
7	SMS 9%	2.98	5.73	4.52
8	SCS 9%	2.86	5.29	4.75
9	SMS 6%	3.77	3.86	2.99
10	SCS 6%	3.89	3.83	3.32
11	SMS 7%	3.77	4.56	3.72
12	SCS 7%	2.64	4.47	3.46
13	SMS 8%	4.39	5.18	4.19
14	SCS 8%	3.64	5.16	4.22
15	SMS 9%	3.39	5.75	4.45
16	SCS 9%	2.64	5.54	4.31

SMS: spicy mango sauce, SCS: spicy cocona sauce.

Table 4. ANOVA of the factorial design of the attributes flavor, color, texture, smell, and spiciness of the Spicy Fruit Sauce.

Attribute		Flavor				Color				Texture			
Source	**DF**	**Adj SS**	**Adj MS**	***F*-Value**	***P*-Value**	**Adj SS**	**Adj MS**	***F*-Value**	***P*-Value**	**Adj SS**	**Adj MS**	***F*-Value**	***P*-Value**
Model	8	4.38	0.55	4.71	0.028	1.71	0.21	1.95	0.196	1.78	0.22	3.55	0.056
Blocks	1	0.03	0.03	0.27	0.616	0.41	0.41	3.78	0.093	0.18	0.18	2.94	0.130
Linear	4	3.39	0.85	7.30	0.012	0.84	0.21	1.92	0.212	0.87	0.22	3.48	0.072
TF(%)	3	2.39	0.80	6.87	0.017	0.18	0.06	0.55	0.665	0.40	0.13	2.13	0.185
Fruit type	1	1.00	1.00	8.62	0.022	0.66	0.66	6.04	0.044	0.47	0.47	7.56	0.029
2-Way Interactions	3	0.95	0.32	2.74	0.123	0.46	0.15	1.39	0.322	0.72	0.24	3.85	0.064
TF(%)*Fruit type	3	0.95	0.32	2.74	0.123	0.46	0.15	1.39	0.322	0.72	0.24	3.85	0.064
Error	7	0.81	0.12			0.77	0.11			0.44	0.06		
Total	15	5.19				2.48				2.21			

Attribute		Smell				Spiciness			
Source	**DF**	**Adj SS**	**Adj MS**	**F-Value**	**P-Value**	**Adj SS**	**Adj MS**	**F-Value**	**P-Value**
Model	8	0.72	0.09	0.70	0.688	0.56	0.07	0.93	0.547
Blocks	1	0.01	0.01	0.04	0.848	0.00	0.00	0.00	1.000
Linear	4	0.62	0.15	1.19	0.393	0.32	0.08	1.06	0.444
TF(%)	3	0.48	0.16	1.23	0.369	0.26	0.09	1.13	0.399
Fruit type	1	0.14	0.14	1.09	0.332	0.06	0.06	0.82	0.394
2-Way Interactions	3	0.10	0.03	0.26	0.851	0.24	0.08	1.06	0.423
TF(%)*Fruit type	3	0.10	0.03	0.26	0.851	0.24	0.08	1.06	0.423
Error	7	0.91	0.13			0.53	0.08		
Total	15	1.63				1.09			

DF: degrees of freedom; AdjSS: Adjusted Sum of Squares); Adj MS: Adjusted Mean Square; F value: Test statistic and *P* value: Is the probability of observing.

No references were found for sensory evaluation studies on turmeric-based spicy fruit sauces. However, Malomo et al. (2022) conducted a sensory evaluation using a 9-point scale to analyze the attributes of canned African catfish in tomato sauce with the addition of 3 and 4% turmeric. The results show that tomato sauce without turmeric (control) obtained better sensory ratings in the attributes of appearance, taste, texture, aroma, and general acceptability, with scores of 7.20, 6.60, 7.20, 7.33, and 7.27, respectively. They conclude that adding turmeric at 4% caused a decrease in sensory acceptance, to scores of 6.93, 5.40, 6.27, 6.33, and 6.00, respectively; this decrease indicated that turmeric negatively affected the sensory perception of the panelists. Similar results were obtained in this study, as the lowest scores corresponded to the spicy fruit sauce with the highest TF content.

Color determination (L*, a* and b*)

The average values of L* of the SCS were in the range of 55.60 to 58.94, and for the mango, from 53.43 to 54.78; and the a* value of the SCS presented lower values than the SMS, indicating that the cocona hot sauce presented greater clarity than the mango hot sauce. The b* value of the SCS 6% TF presented a greater yellow intensity than the rest of the SFSs. No articles on sauces of this type were found in the bibliography consulted. The color coordinates L* and a* presented values very far from those of commercial hot sauces (Table 5), possibly due to the use of turmeric, which is a natural colorant. The commercial sauces used in the comparison with the sauce in this work do not contain fruit or turmeric but represent the varieties of spicy sauces available in supermarkets in Lima, Peru.

The greater the addition of TF, the higher the BI value, indicating the greater intensity of brown color in the SFSs with 9% TF (Table 5).

Table 5. Color parameters (L, a, b*) and Browning Index (BI) of mango and cocona sauces containing 6%, 7%, 8%, and 9% turmeric flour.

Treatment code	L*	a*	b*	BI
SCS 0%	69.38±0.04^{C}	3.22±0.01^{E}	47.92±0.06$^{B, C}$	3.59±0.02^{G}
SCS 6%	58.94±0.13^{E}	16.33±0.20^{B}	57.96±3.03^{A}	19.40±0.20^{D}
SCS 7%	55.73±0.41$^{F, G}$	16.39±0.84^{B}	52.67±2.17$^{A, B, C}$	20.50±1.11$^{C, D}$
SCS 8%	57.11±0.20$^{E, F}$	17.65±0.25^{A}	54.78±2.10$^{A, B}$	21.47±0.22$^{B, C}$
SCS 9%	55.60±0.47$^{F, G}$	17.77±0.30^{A}	51.56±0.99$^{A, B, C}$	22.14±0.18$^{A, B}$
SMS 0%	64.90±0.01^{D}	5.59±0.01^{D}	50.17±0.01$^{A, B, C}$	6.41±0.01^{F}
SMS 6%	53.98±1.71^{G}	17.04±0.02$^{A, B}$	50.94±4.73$^{A, B, C}$	21.89±0.65$^{A, B, C}$
SMS 7%	53.58±0.17^{G}	17.34±0.31$^{A, B}$	51.11±3.83$^{A, B, C}$	22.41±0.34$^{A, B}$
SMS 8%	54.78±0.14$^{F, G}$	17.60±0.15^{A}	51.90±2.29$^{A, B, C}$	22.25±0.14$^{A, B}$
SMS 9%	53.43±1.11^{G}	18.02±0.08^{A}	48.60±1.70$^{B, C}$	23.26±0.35^{A}
Commercial Chili sauce N° 1	77.32±0.01^{A}	1.02±0.02^{F}	48.03±0.04$^{B, C}$	1.19±0.02^{H}
Commercial Chili sauce N° 2	76.23±0.01$^{A, B}$	4.04±0.02^{E}	45.11±0.02^{C}	4.01±0.02^{G}
Commercial Chili sauce N°3	74.05±0.04^{B}	8.93±0.02^{C}	58.09±0.06^{A}	8.80±0.02^{E}

Tukey test. Different letters in the same column indicate a significant difference (P<0.05). Equal letters in the same column indicate no significant difference (P>0.05).

Phenolic compounds, total curcuminoids, and antioxidant capacity (ABTS, FRAP, DPPH)

Total Phenolic Compounds (TPC)

The addition of TF had a significant effect on the phenolic compound content of the sauce (Table 6). As shown in Figure 2, increasing the percentage of flour in the SFS formulation led to a rise in TPC content, reaching values between 2.97 and 4.53 mg GAE g^{-1}, values higher than those reported by Guo et al. (2024), who made a spicy Chinese cabbage sauce (0.86 mg GAE g^{-1}); and by Rahman et al. (2024) when evaluating tomato and pumpkin sauce (0.035 to 0.062 mg GAE g^{-1}). In contrast, El Haggar et al. (2023) found higher TPC values (14.8317 mg GAE g^{-1}) in acai sauce, possibly because the latter contained sweet red peppers and pomegranate sauces as main ingredients. No studies of TPC, TCC, or antidiabetic activity in hot sauces with turmeric were found in the literature.

Table 6. Analysis of variance of factorial regression of total curcuminoids (TCC) and total phenolic compounds (TPC) vs % turmeric flour and type of fruit.

		TCC (mg g^{-1})				TPC (mg GAE g^{-1})			
Source	**DF**	**Adj SS**	**Adj MS**	***F*-Value**	***P*-Value**	**Adj SS**	**Adj MS**	***F*-Value**	***P*-Value**
Model	8	7.1512	0.8939	105.4	0.000	4.7022	0.5878	26.700	0.000
Blocks	1	0.0400	0.0400	4.710	0.067	0.1502	0.1502	6.820	0.035
Linear	4	7.0023	1.7506	206.30	0.000	4.4515	1.1129	50.550	0.000
TF(%)	3	6.9890	2.3297	274.54	0.000	4.3826	1.4609	66.360	0.000
Fruit type	1	0.0132	0.0132	1.560	0.252	0.0689	0.0689	3.1300	0.120
2-Way Interactions	3	0.1089	0.0363	4.280	0.052	0.1006	0.0335	1.520	0.291
TF(%)*Fruit type	3	0.1089	0.0363	4.280	0.052	0.1006	0.0335	1.520	0.291
Error	7	0.0594	0.0085	-	-	0.1541	0.0220	-	-
Total	15	7.2106	-	-	-	4.8563	-	-	-

Total curcuminoid content (TCC)

Turmeric from the Peruvian Amazon is a valuable resource characterized by its high content of bioactive compounds, mainly curcuminoids. There was a significant effect (directly proportional) of the addition of TF (P=0) on the TCC content of the SFS (Table 6), since as the percentage (%) of flour in the SFS increased, the TCC content increased (Figure 2). The TCC content of this study was in the range of 3.8 to 5.74 mg g^{-1} sample.

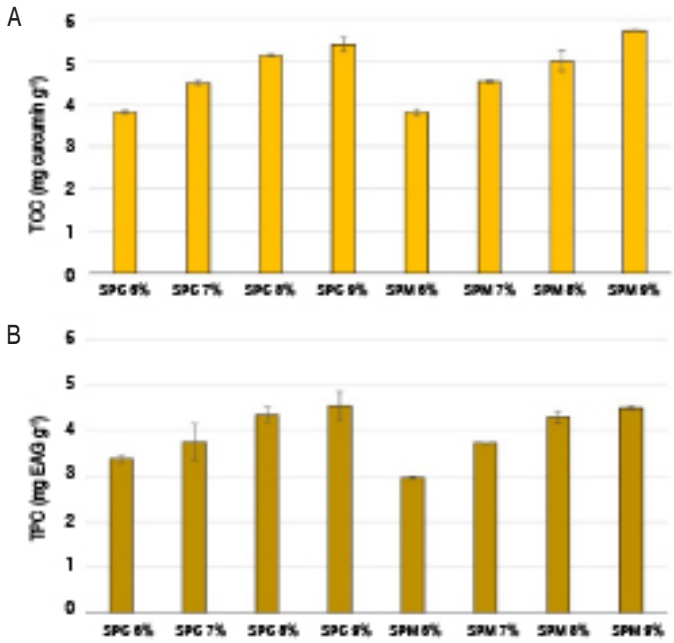

Figure 2. A) Content of total curcuminoids (TCC) and B) Total phenolic compounds (TPC) of spicy fruit sauces of mango (SMS) and cocona (SCS) containing 6%, 7%, 8%, and 9% turmeric flour.

Antioxidant activity

As more TF content is added, the antioxidant activity of FRAP and ABTS increases (Figure 3). In this regard, Barzegar (2012) pointed out that the hydrogen and electron transfer mechanisms explain the antioxidant potential of curcuminoids, which are the mechanisms on which the ABTS and FRAP methods are based, respectively.

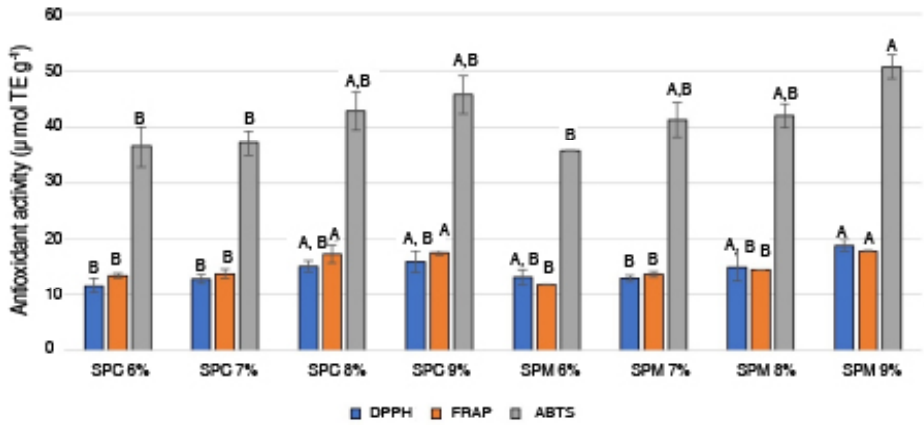

Figure 3. Antioxidant capacity DPPH, FRAP, and ABTS of the SFS, containing 6%, 7%, 8%, and 9% turmeric flour.

The percentage (%) of TF in the SFS formulation had a significant effect on the antioxidant capacity value DPPH (*P*=0.000), FRAP (*P*=0.000), and ABTS (*P*=0.000). As well as the type of fruit (*P*<0.05) on the antioxidant capacity, FRAP, and ABTS (Table 7). No studies reporting the antioxidant capacity of spicy fruit sauces with turmeric or similar formulations were found in the literature review. The following section discusses studies on antioxidant activity in other sauces. Guo et al. (2024) reported the antioxidant capacity (FRAP) of 360 µmol TE L^{-1} of a fermented spicy Chinese cabbage sauce, a value higher than that reported in this study, possibly due to the different technique and inputs used in its process.

Table 7. Analysis of variance of the factorial regression of antioxidant activity vs % turmeric flour and type of fruit.

		DPPH (µmol TE g^{-1})				FRAP (µmol TE g^{-1})				ABTS (µmol TE g^{-1})			
Source	**DF**	**Adj SS**	**Adj MS**	***F*-Value**	***P*-Value**	**Adj SS**	**Adj MS**	***F*-Value**	***P*-Value**	**Adj SS**	**Adj MS**	***F*-Value**	***P*-Value**
Model	8	75.64	9.46	6.60	0.010	68.03	8.50	16.67	0.000	415.71	51.96	35.37	0.000
Blocks	1	5.54	5.54	3.87	0.090	0.20	0.20	0.38	0.560	48.77	48.77	33.20	0.000
Linear	4	64.27	16.07	11.22	0.000	62.00	15.50	30.38	0.000	337.64	84.41	57.46	0.000
TF(%)	3	59.46	19.82	13.83	0.000	57.69	19.23	37.69	0.000	323.63	107.88	73.43	0.000
Fruit type	1	4.81	4.81	3.36	0.110	4.30	4.30	8.43	0.020	14.02	14.02	9.54	0.020
TF(%)*Fruit type	3	5.83	1.94	1.36	0.330	5.84	1.95	3.81	0.070	29.29	9.76	6.65	0.020
Error	7	10.03	1.43	-	-	3.57	0.51	-	-	10.28	1.47	-	-
Total	15	85.67	-	-	-	71.60	-	-	-	425,99	-	-	-

Park and Byun (2014) developed Bulgogi sauce, with soy and apple puree, with the addition of turmeric concentrate at concentrations of 10, 20, 30, and 40%. The Bulgogi sauce increased the DPPH antioxidant capacity value as the turmeric concentration increased. In this study, the addition was in smaller quantities, but an increase in antioxidant capacity was evident in the SFS with 9% TF compared to those with 6% TF. As shown in Figure 3, both TPC and curcuminoid levels increased significantly with the percentage of TF, which are known contributors to antioxidant activity. Therefore, the greater presence of these bioactive compounds in the samples with 9% TF justifies the higher antioxidant activity observed.

The sauces prepared in this study presented antioxidant activity (ABTS) in the range of 35.66 to 50.69 µmol TE g^{-1}, showing greater capacity for eliminating free radicals than that reported in the acai sauce prepared by Da Silva et al. (2021) (1.00 and 1.10 µmol TE g^{-1}), this variation could be due to the fact that turmeric provides greater antioxidant activity.

Spicy Fruit Sauce optimization

The predicted formulation obtained with the full factorial design, maximizing flavor, TCC, and TPC, was SMS 8% TF (Figure 4); the highest desirability was for flavor and TPC, and the desirability when evaluating TCC was lower.

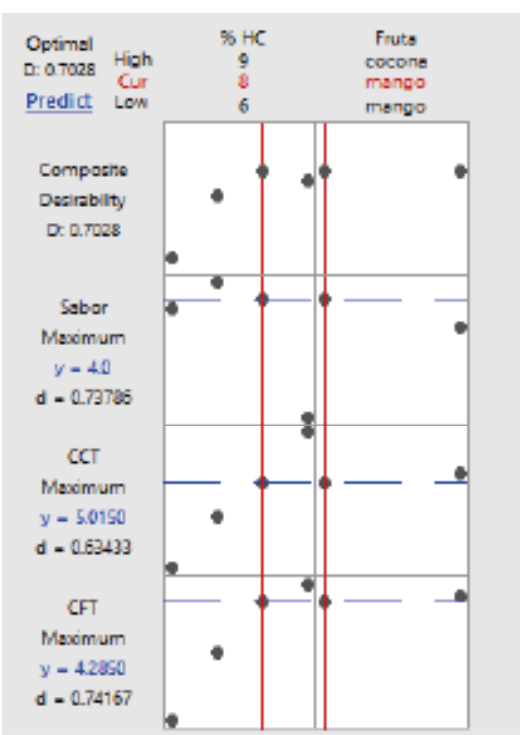

Figure 4. Optimization of spicy fruit sauce formulation.

Antidiabetic activity

The IC_{50} of SMS 8% TF was 69.81±9.42 µg mL^{-1} (IC_{50} of acarbose=415.56±7.20 µg mL^{-1}), indicating antidiabetic activity.) Sabir et al. (2020) found in the ethanolic extract of *C. longa* a greater inhibitory effect on α-GLC (IC_{50}=37.1±0.3 µg mL^{-1}) than in the present work, while Aranda-Ventura et al. (2021) reported a lower inhibition effect on α-glucosidase in ethanolic extract and aqueous extract of *C. longa* (IC_{50} of 81.90 and 171.60 µg mL^{-1}, respectively).

Di Pierro et al. (2015) mention that an overweight person requires consuming *Curcuma longa* at a dose of 800 mg twice a day for 1 month to lose weight and body fat. Likewise, Maithili et al. (2015) conclude that a diabetic patient should consume turmeric in doses of 2 g for 4 weeks to reduce dyslipidemia, LDL, and cholesterol.

Characterization of the optimized SFS (SMS 8% TF)

Proximate composition and mineral nutritional content of the optimal sauce

The proximal composition of the SFS is shown in Table 8, highlighting its mineral nutrient content. The protein and ash content were higher than the cocona hot sauce developed by Terry and Casusol (2018), who reported 1% protein and 3.3% ash. El Haggar et al. (2023) developed a sauce formula as a healthy functional product, with a higher protein content (2.07%) and a lower fat content (0.21%) compared to the present work; with a calcium, magnesium and potassium contribution of 24.53, 5.85 and 68.22 mg 100 g^{-1}, respectively, lower than what was obtained in this study for SMS 8% TF. The opposite was true for copper, iron, and zinc contents (0.85, 1.21, and 1.03 mg per 100 g of the sample, respectively), which were higher than the SMS 8% TF (Table 8).

Table 8. Proximal composition, mineral nutrients, and viscosity of the spicy sauce 8% TF.

Analysis	Component	Values	Commercial Chili sauce N°1	Commercial Chili sauce N°2	Commercial Chili sauce N°3
Proximal composition (g 100 g^{-1})	Moisture	68.11±0.00	-	-	-
	Protein	1.78±0.06	-	-	2.3
	Fat	13.81±0.08	46.6	33.3	26.2
	Saturated fat	1.50±0.01	6.67	5.33	3.2
	Ash	3.67±0.00	-	-	-
Mineral nutrients (mg 100 g^{-1})	Ca	56.87±1.29	-	-	-
	Mg	41.96±2.37	-	-	-
	Na	1185.48±22.57	666.67	733.33	333
	K	295.74±0.96	-	-	-
	Cu	0.24±0.00	-	-	-
	Fe	1.12±0.04	-	-	-
	Zn	0.27±0.01	-	-	-
Viscosity (3 RPM)	-	70500±4946.57^{A}	67550±597.22^{A}	51450±525.99^{B}	42950±191.49^{C}

The values are expressed as the mean ± standard deviation (n = 2).

Commercial sauces 1, 2, and 3 are the most demanded by consumers. The spicy sauce developed in this study exhibited a darker color compared to the commercial ones, while its flavor and consistency were similar to those of commercial sauce N°2.

Commercial sauces 1 and 2 exhibited higher fat and saturated fatty acids content in comparison to the sauce developed in this study.

The product prepared in this work is free of high saturated fat octagon since it presented 1.50±0.01% of saturated fat, which complies with the Peruvian regulations specified by the regulations of the Law for the Promotion of Healthy Eating (Ministerio de Salud del Perú 2017), which establishes that an octagonal symbol is displayed that indicates if the product has a content greater than or equal to 4 g of saturated fat per 100 g of product. However, it does correspond to show an octagon due to its high sodium content.

pH, Acidity, and consistency values

The pH of the sauce was 4.12±0.01, which meets the expected value for the stability of this type of product (Codex standard: pH<4.6). Therefore, the study was conducted using a percentage acidity of 0.53±0.06 acetic acid, at which sensory acceptability was achieved.

The Bostwick consistency in the mango spicy sauce was 2.5 cm per 30 s while the sweet and sour sauces with acai and non-conventional food plants, evaluated by Da Silva et al. (2021), presented 12.7 and 14.5 cm per 30 s of consistency, indicating that SMS is of greater consistency than these sauces, possibly because it has many solids in its formulation.

CONCLUSION

This study contributes to the existing literature of functional foods by providing information related to the antioxidant activity and α-glucosidase inhibition of a product formulated with turmeric flour. Also, it presents a simple technology for the preparation of a fruit-based spicy sauce. The spicy mango sauce with 8% turmeric flour presented the highest sensory score, phenolic compounds, and curcuminoids. This study showed that turmeric flour is a source of bioactive compounds, such as curcuminoids, and has potential antidiabetic properties through α-glucosidase inhibition. Future evaluations of other products using turmeric flour as an ingredient, such as instant soups, and shelf-life studies, and bioavailability of curcuminoids are recommended.

ACKNOWLEDGMENTS

This work was financed by PROCIENCIA (Programa Nacional de Investigación Científica y Estudios avanzados), corresponds to the project FONDECYT 046-2021, executing entity: Instituto Tecnológico de la Producción. We thank German Gonzales for the determination of the antiglycemic activity.

CONFLICT OF INTERESTS

The authors declared no potential conflicts of interest with respect to the research, authorship, and/or publication of this article.

REFERENCES

Aranda-Ventura J, Núñez-Tuesta, L, Villacrés-Vallejo J and González-Aspajo G (2021) Efecto de los alimentos Curcuma longa L, Zingiber officinale Roscoe, Lupinus mutabilis Sweet y Myrciaria dubia (Kunth) McVaugh sobre la inhibición *in vitro* de la alfa-glucosidasa. Revista Peruana de Medicina Integrativa 6(1): 5-12. https://doi.org/10.26722/rpmi.2021.v6n1.48

Artanti N, Firmansyah T and Darmawan A (2012) Bioactivities evaluation of Indonesian mistletoes (*Dendrophthoe pentandra* (L.) Miq.) leaves extracts. Journal of Applied Pharmaceutical Science 2(1): 24-27. https://japsonline.com/abstract.php?article_id=335&sts=2

Awaeloh N, Limsuwan S, Na-Phatthalung P, Kaewmanee T and Chusri S (2025) Novel development and sensory evaluation of extruded snacks from unripe banana (Musa ABB cv. Kluai 'Namwa') and rice flour enriched with antioxidant-rich curcuma longa microcapsules. Foods 14(2): 205. https://doi.org/10.3390/foods14020205

Barriga-Sánchez M, Campos Martinez M, Cáceres H and Rosales-Hartshorn M (2022) Characterization of black borgoña (*Vitis labrusca*) and quebranta (*Vitis vinifera*) grapes pomace, seeds and oil extract. Food Science and Technology 42: e71822. https://doi.org/10.1590/fst.71822

Barriga-Sánchez M, Castro-Rumiche CF, Sanchez-Gonzales G and Rosales-Hartshorn M (2021) Functional and chemical qualities of *Vitis labrusca* grape seed oil extracted by supercritical CO_2. Revista Colombiana de Química 50(3): 3-9. https://doi.org/10.15446/rev.colomb.quim.v50n3.95469

Barzegar A (2012) The role of electron-transfer and H-atom donation on the superb antioxidant activity and free radical reaction of curcumin. Food Chemistry 135(3): 1369-1376. https://doi.org/10.1016/j.foodchem.2012.05.070

Chaudhary M, Midha N, Sukhadiya P, Kumar D and Garg M (2024) Metformin-Induced chronic diarrhea misdiagnosed as irritable bowel syndrome for years. Cureus 16(3): e56828. https://doi.org/10.7759/cureus.56828

CIEN – Centro de Investigación de Economía y Negocios Globales (2023) Panorama del mercado internacional y nacional de cúrcuma. En: CIEN, https://www.cien.adexperu.org.pe/panorama-del-mercado-internacional-y-nacional-de-curcuma/ 25 p.

Cochran WG and GM Cox (1957) Experimental Design. 2a ed. Wiley, New York.

Da Silva M, Lemos T, Rodrigues M, Araujo A, Gomes A, Pereira A, Abreu V, Araújo E and Andrade D (2021) Sweet-and-sour sauce of assai and unconventional food plants with functional properties: An innovation in fruit sauces. International Journal of Gastronomy and Food Science 25: 100372. https://doi.org/10.1016/j.ijgfs.2021.100372

Di Pierro F, Bressan A, Ranaldi D, Rapacioli G, Giacomelli L and Bertuccioli A (2015) Potential role of bioavailable curcumin in weight loss and omental adipose tissue decrease: preliminary data of a randomized, controlled trial in overweight people with metabolic syndrome. Preliminary study. European Review for Medical & Pharmacological Sciences 19(21): 4195–4202. http://www.naturalhealthresearch.org/wp-content/uploads/2017/07/Curcumin-Reduces-Adipose-Tissue-and-Aids-Weight-Loss.pdf

El Haggar E, Mahmoud K, Ramadan M and Zahran H (2023) Tomato-Free wonder sauce: A functional product with health-boosting properties. Journal of Functional Foods 109: 105758 https://doi.org/10.1016/j.jff.2023.105758

Guo J, Jike X, Wu C, Liu L, Wang C, Xu K, Li B, Xu H and Lei H (2024) Phytochemicals, antioxidant capacities and volatile compounds

changes in fermented spicy Chinese cabbage sauces treated by thermal and non-thermal technologies. Food research international 176: 113803 https://doi.org/10.1016/j.foodres.2023.113803

Hazra K, Kumar R, Sarkar B, Chowdary Y, Devgan M and Ramaiah M (2015) UV-visible spectrophotometric estimation of curcumin in nanoformulation. International Journal of Pharmacognosy 2(3): 127-130. http://doi.org/10.13040/IJPSR.0975-8232.IJP.2(3).127-30

Hutachok N, Koonyosying P, Paradee N, Samakradhamrongthai R, Utama-Ang N and Srichairatanakool S (2023) Testing the feasibility and dietary impact of macaroni fortified with green tea and turmeric curcumin extract in diabetic rats. Foods 12(3): 534. https://doi.org/10.3390/foods12030534

Juszczak L, Oczadły Z and Gałkowska D (2013) Effect of modified starches on rheological properties of ketchup. Food and Bioprocess Technology 6: 1251-1260. https://doi.org/10.1007/s11947-012-0813-x

Maithili Karpaga Selvi N, Sridhar M, Swaminathan R and Sripradha R (2015) Efficacy of turmeric as adjuvant therapy in type 2 diabetic patients. Indian Journal of Clinical Biochemistry 30: 180-186. https://doi.org/10.1007/s12291-014-0436-2

Malomo A, Odubanjo O, Olawoye B, Olaniyi O, Lawal M and Fasogbon B (2022) Effect of turmeric on the quality of canned African catfish in tomato sauceduring storage at 25 °C and 45 °C. Food Science and Applied Biotechnology 5(1): 12-21. https://doi.org/10.30721/fsab2022.v5.i1.162

Ministerio de Salud del Perú (2017) Decreto Supremo 017-2017-SA, Reglamento de la Ley de Promoción de la Alimentación Saludable para niños, niñas y adolescentes, N° 30021. En: Gobierno del Perú, https://cdn.www.gob.pe/uploads/document/file/189851/189343_DS_017-2017-SA.PDF20180823-24725-1gajie4.PDF

Modi R and Sahota P (2024) Bio-process optimization for developing a turmeric (*Curcuma longa* Linn.) beverage fermented with functional lactic acid starter cultures. Biocatalysis and Agricultural Biotechnology 61: 103360. https://doi.org/10.1016/j.bcab.2024.103360

Mohanty I, Arya D, Dinda A, Joshi S, Talwar K and Gupta S (2004) Protective effects of *Curcuma longa* on ischemia-reperfusion induced myocardial injuries and their mechanisms. Life sciences 75(14): 1701-1711. https://doi.org/10.1016/j.lfs.2004.02.032

Park S and Byun G (2014) Development of bulgogi sauce added with concentrated *Curcuma longa* L. Culinary Science and Hospitality Research 20(1): 143-158. https://doi.org/10.17495/easdl.2017.10.27.5.512

Perez Gutierrez R (2016) Antidiabetic andantioxidant properties, and α-amylase and α-glucosidase inhibition effects of triterpene saponins from *Piper auritum*. Food Science and Biotechnology 25(1): 229-239. https://doi.org/10.1007/s10068-016-0034-6

Prior R, Wu X and Schaich K (2005) Standardized methods for the determination of antioxidant capacity and phenolics in foods and dietary supplements. Journal of Agricultural and Food Chemistry 53(10): 4290-4302. https://doi.org/10.1021/jf0502698

Rahman M, Hasan S, Sarkar S, Ashik M, Somrat M and Asad A (2024) Effect of formulation on physiochemical, phytochemical, functional, and sensory properties of the bioactive sauce blended with tomato and pumpkin pulp. Applied Food Research 4(1): 100406. https://doi.org/10.1016/j.afres.2024.100406

S Abd El-Baset W and Almoselhy R (2023) Effect of baking temperature on quality and safety of school meal biscuits. Food Science and Applied Biotechnology 6(2): 250-262. https://doi.org/10.30721/fsab2023.v6.i2.258

Sabir S, Zeb A, Mahmood M, Abbas S, Ahmad Z and Iqbal N (2020) Phytochemical analysis and biological activities of ethanolic extract of *Curcuma longa* rhizome. Brazilian Journal of Biology 81(3): 737-740. https://doi.org/10.1590/1519-6984.230628

Seclén S (2015) Diabetes Mellitus en el Perú: hacia dónde vamos. Revista Médica Herediana 26(1): 3-4. http://www.scielo.org.pe/scielo.php?pid=S1018-130X2015000100001&script=sci_arttext&tlng=pt

Srianta I, Kusumawati N, Nugerahani I, Artanti N and Xu G (2013) In vitro α-glucosidase inhibitory activity of Monascus-fermented durian seed extracts. International Food Research Journal 20(2): 533-536. http://repository.ukwms.ac.id/id/eprint/11242

Terry Calderón V and Casusol Perea K (2018) Formulación de una salsa picante a base de pulpa de cocona (*Solanum sessiliflorum*), ají amarillo (*Capsicum baccatum*) y ají Charapita (*Capsicum chinense*). Revista de Investigaciones de la Universidad Le Cordon Bleu 5(1): 5-17. https://doi.org/10.36955/RIULCB.2018v5n1.001

Tshiyoyo K, Bester M, Serem J and Apostolides Z (2022) In-silico reverse docking and *in-vitro* studies identified curcumin, 18α-glycyrrhetinic acid, rosmarinic acid, and quercetin as inhibitors of α-glucosidase and pancreatic α-amylase and lipid accumulation in HepG2 cells, important type 2 diabetes targets. Journal of Molecular Structure 1266: 133492. https://doi.org/10.1016/j.molstruc.2022.133492

Research article

https://revistas.unal.edu.co/index.php/refame

Revista Facultad Nacional de Agronomía

Effect of Trolox and resveratrol supplementation during the refrigeration of boar sperm

Efecto de la suplementación con Trolox y resveratrol durante la refrigeración de semen porcino

https://doi.org/10.15446/rfnam.v78n2.114567

Stephania Madrid Gaviria[1]*, Sergio Morado[1], Pablo Daniel Cetica[1] and Mariana Córdoba[1]

ABSTRACT

This research aimed to evaluate the possibility of improving the boar semen quality already refrigerated in commercial diluent by adding Trolox and/or resveratrol during the refrigeration process. Pools of refrigerated semen from boars of proven fertility were added with a) 200 µM Trolox, b) 50 µM resveratrol, c) 200 µM Trolox + 50 µM resveratrol, or d) no antioxidant supplementation (negative control) and conserved at 17 °C for 7 days. On days 1, 3 and 7 of refrigeration the following sperm parameters were evaluated: Motility, functions of the plasma membrane, pre-capacitated spermatozoa, viability and acrosome integrity, and mitochondrial membrane potential. Additionally, mitochondrial superoxide anion production was evaluated by flow cytometry. *In vitro* fertilization was performed using semen from day 3 of refrigeration. Data were analyzed using ANOVA (P<0.05). Evaluated parameters significantly decreased over refrigeration time (P<0.05), except the percentages of pre-capacitated spermatozoa. Samples supplemented only with Trolox maintained values similar to the control group, except for higher sperm motility on day 3 of preservation (P<0.05), whereas the addition of resveratrol caused a decrease in the studied parameters (P<0.05); the combination of both antioxidants showed intermediate values between each individual antioxidant treatment. No significant variations in mitochondrial superoxide anion production and cleavage rates were detected with each treatment with respect to the control. In conclusion, supplementing boar semen with Trolox and/or resveratrol does not cause a significant improvement in semen quality, once the refrigeration process has started, except for a higher motility with Trolox at day 3 of refrigeration, nor does it alter the mitochondrial production of reactive oxygen species and the fecundity capacity of semen *in vitro*.

Keywords:
Antioxidant
Oxidative stress
Spermatozoa
Sperm preservation
Sperm viability

RESUMEN

El objetivo del presente trabajo fue evaluar la posibilidad de mejorar la calidad de semen porcino ya refrigerado en diluyente comercial por el agregado de Trolox y/o resveratrol durante el proceso de refrigeración. Mezclas de semen refrigerado provenientes de verracos de probada fertilidad fueron adicionadas con a) Trolox 200 µM, b) resveratrol 50 µM, c) Trolox 200 µM + resveratrol 50 µM, o d) sin suplementación antioxidante (control negativo) y conservados a 17 °C por 7 días. En los días 1, 3 y 7 de la refrigeración, se evaluaron los siguientes parámetros espermáticos: motilidad, funcionalidad de la membrana plasmática, espermatozoides precapacitados, viabilidad e integridad acrosomal y potencial de membrana mitocondrial. Además, se evaluó la producción de anión superóxido mitocondrial utilizando citometría de flujo. La fecundación *in vitro* se realizó usando semen del día 3 de refrigeración. Los datos fueron analizados por Análisis de Varianza (P<0,05). Los parámetros evaluados disminuyeron con el tiempo de refrigeración (P<0,05), excepto por los porcentajes de espermatozoides precapacitados. Las muestras suplementadas solo con Trolox mantuvieron valores similares a las del grupo control, excepto por una mayor motilidad espermática en el día 3 de conservación (P<0,05), mientras que la adición de resveratrol causó una disminución de los parámetros estudiados (P<0,05), la combinación de ambos antioxidantes mostró valores intermedios entre cada tratamiento antioxidante individual. No se observaron variaciones en los porcentajes de producción de anión superóxido mitocondrial y de clivaje embrionario en respuesta a la suplementación con cada antioxidante con respecto al control. En conclusión, la suplementación de semen porcino con Trolox y/o resveratrol, una vez que el proceso de refrigeración ha comenzado, no provoca un aumento significativo de la calidad seminal, excepto por una mayor motilidad con Trolox al día 3, ni altera la producción mitocondrial de especies reactivas del oxígeno y la capacidad fecundante del semen *in vitro*.

Palabras clave:
Antioxidante
Estrés oxidativo
Espermatozoides
Conservación espermática
Viabilidad espermática

[1]CONICET – Instituto de Investigaciones en Producción Animal (INPA), Facultad de Ciencias Veterinarias, Instituto de Investigación y Tecnología en Reproducción Animal (INITRA, UBA), Universidad de Buenos Aires, Argentina. smadridgaviria@fvet.uba.ar, smorado@fvet.uba.ar, pcetica@fvet.uba.ar, mcordoba@fvet.uba.ar
*Corresponding author

Received: June 6, 2024; Accepted: October 23, 2024
Rev. Fac. Nac. Agron. Medellín 78(2): 11141-11149. 2025
ISSN 0304-2847 / e-ISSN 2248-7026

CC BY NC SA

The use of assisted reproductive biotechnologies has increased the need to develop reliable techniques for gamete preservation. The porcine species represents a greater challenge for the application of these biotechnologies, as boar sperm is particularly much more sensitive to cold damage due to its lipid composition (Giaretta et al. 2013). Thus, in pigs, frozen semen has a very low survival rate and 99% of artificial inseminations are carried out with refrigerated semen in liquid form between 15 and 17 °C (Yeste 2017). Furthermore, refrigerated boar semen quality can be altered after the refrigeration process due to conservation and transport conditions (Yeste 2017).

It is known that in both frozen and refrigerated semen, the conservation process increases oxidative stress; therefore, among the alternatives to improve the efficiency of these techniques, the supplementation of semen diluents with different types of antioxidants could be introduced. Trolox (6-hydroxy-2,5,7,8-tetramethylchroman-2-carboxylic acid) is a hydrophilic analog of α-tocopherol, the most common and biologically active form of tocopherols (vitamin E) (Giordano et al. 2020). The antioxidant mechanism of vitamin E and its analogues is mainly to inhibit lipid peroxidation of membrane phospholipids or lipoproteins, and to keep iron and other metal elements in a reduced state (Cao et al. 2022). On the other hand, resveratrol (3,5,4´-trihydroxystilbene) is a polyphenol, produced by more than 70 different types of plants in response to stressed conditions (Pasquariello et al. 2020). It has been reported in several cellular models that resveratrol has a reactive oxygen species (ROS) scavenging capacity and, like other phytoestrogen, acts via alpha and beta estrogen receptors activating the transcription of mitochondrial and nuclear target genes, controlling mitochondrial biogenesis and activating antioxidant enzymes (Gambini et al. 2015; Zhu et al. 2019; Pasquariello et al. 2020).

Some studies have reported the beneficial effect of the addition of Trolox or resveratrol to the frozen or refrigerated diluents before boar sperm preservation (Mendez et al. 2013; Varo-Ghiuru et al. 2015; He et al. 2020; Ribas-Maynou et al. 2021; Camporino and Córdoba 2022). However, there are no reports with respect to the addition of these antioxidants, nor their combination once the refrigeration procedure has been completed. Therefore, this research aimed to evaluate the possibility of improving the quality of boar semen already refrigerated in a commercial diluent by adding Trolox and/or resveratrol during the refrigeration process.

MATERIALS AND METHODS

Materials

All chemicals used were of analytical grade and obtained from Sigma-Aldrich (Merk) unless otherwise stated. Fluorochromes were purchased from Sigma-Aldrich (Merk) or Life Technologies (Thermo Fisher).

Research Ethics Statement

No animals were used during this study. Ovaries were donated to our laboratory by a local slaughterhouse and semen was donated by a local farm. The research project was approved by the University of Buenos Aires (20020220300165BA, UBACyT 2023-2016).

Semen sample provision and experimental design

Refrigerated porcine semen samples obtained from fresh samples with a minimum of 70% motile and 80% viable spermatozoa were kindly donated by a local pig genetic company (Agroceres PIC Argentina, https://agrocerespic.com.ar/). These boars belonged to a controlled program of a local artificial insemination centre, and they were kept under uniform feeding and handling conditions during the entire study. Five different pools from boars of proven fertility (three or four F1 Camborough/ line 337, Pietrain x Duroc Jersey males per pool) were refrigerated 1:1 in long-term commercial medium (Androstar Plus, Minitube; at least $31.4x10^6$ spermatozoa mL^{-1}) and transported to the laboratory at controlled temperature conditions (17 °C in an adiabatic container) within the first 24 hours.

Upon arrival at the laboratory, four different sperm aliquots (6 mL) were added with a) 200 µM Trolox (Peña et al. 2003; Varo-Ghiuru et al. 2015), b) 50 µM resveratrol (Longobardi et al. 2017; Zhu et al. 2019), c) 200 µM Trolox + 50 µM resveratrol, or d) no antioxidant supplementation (negative control) and conserved at 17 °C for 7 days. On days 1, 3, and 7 of refrigeration, an aliquot (1 mL) from each treatment was collected, warmed at 37 °C for 10 minutes and then washed by centrifugation at 600x*g* for 5 minutes to remove the refrigeration diluent and to allow later evaluations. -

Sperm motility

Motility was visually determined using an Optic Microscope

(Jenamed 2, Carl Zeiss, Jena, Germany) under 400x magnification with a thermal stage at 37 °C, three times by the same observer (Peña et al. 2003).

Sperm viability and acrosome integrity

The percentage of intact acrosomes in live cells was determined by vital trypan blue stain using differential interference contrast (DIC) microscopy (Jenamed 2, Carl Zeiss, Jena, Germany) at 1000x magnification (Satorre et al. 2018). An aliquot of the sperm suspension was incubated with an equal volume of 0.25% Trypan blue in TALP at 37 °C for 15 minutes. The mixture was then centrifuged at 600×*g* for 10 minutes to remove excess stain and subsequently fixed with 5% formaldehyde in PBS. Live spermatozoa appeared unstained, while dead spermatozoa stained dark blue. Intact acrosomes presented a defined and integral membrane, whereas damaged acrosomes appeared blurred. For each treatment, 200 spermatozoa were analyzed under standardized conditions.

Pre-capacitated spermatozoa

Pre-capacitated spermatozoa percentages were determined through the modifications in fluorescence of chlortetracycline (CTC) patterns using an epifluorescence microscope (Jenamed 2, Carl Zeiss, Jena, Germany) at 400x magnification (Satorre et al. 2018). The CTC solution was freshly prepared daily by dissolving 500 µM CTC in a buffer containing 130 mM NaCl, 5 mM cysteine, and 20 mM Tris, pH=7.8. This solution was protected from light using foil. For the assay, 500 µL of the sperm suspension was mixed with an equal volume of the 500 µM CTC solution, and glutaraldehyde was added to achieve a final concentration of 0.1%. The prepared samples were then placed on a clean slide and sperm capacitation was examined using the epifluorescence microscope (Jenamed 2, Carl Zeiss, Jena, Germany) at 400× magnification. The three sperm patterns were as follows: a) intact non-capacitated sperm, with uniform fluorescence on the head, b) capacitated sperm, with a fluorescence-free band in the postacrosomal region, and c) acrosome-reacted sperm, with a fairly dull fluorescence on the head. The midpiece was fluorescent in all cells.

Sperm plasma membrane functionality

The hypo-osmotic swelling test (HOST) was used to evaluate the functional integrity of the spermatozoa plasma membrane using an Optic Microscope (Jenamed 2, Carl Zeiss, Jena, Germany) under 400x magnification (Satorre et al. 2018). Aliquots (50 µL) of sperm solution were mixed with 500 µL of hypo-osmotic solution (sodium citrate 0.49%, fructose 0.9%, 100 mOsm kg^{-1}) and incubated at 38 °C for 60 min. Spermatozoa with swelling in the tail present a functional plasma membrane. Spermatozoa (n = 200) were counted under differential interference contrast (DIC) microscopy.

Sperm mitochondrial membrane potential

Mitochondrial membrane potential was evaluated using JC-1 (5,5', 6,6'-tetrachloro-1,1', 3,3'-tetraethyl benzimidazolyl carbocyanine iodide) fluorochrome. Aliquots (300 µL) of sperm solution from each treatment were mixed with 15 µL of 2 µM JC-1 (final concentration 0.1 µM) and incubated at 37 °C in the dark for 30 min. Glutaraldehyde (0.1%) was then added to the mixture (Camporino and Córdoba 2022). Spermatozoa were evaluated at 400x magnification using an epifluorescence microscope and 510-570 nm filters (Jenamed 2, Carl Zeiss, Jena, Germany) and classified as low or high membrane potential when showing green or red fluorescence in the middle piece, respectively (Wysokińska 2020). Two hundred spermatozoa were used for the evaluation.

Sperm mitochondrial reactive oxygen species

The amount of mitochondrial superoxide anion produced in sperm cells was evaluated using MitoSOX Red fluorochrome. Aliquots of sperm solution ($1x10^6$ spermatozoa mL^{-1}) from each treatment were incubated with 2 µM MitoSOX Red at 37 °C for 15 min in the dark. Samples were then washed, and MitoSOX Red fluorescence was measured using a flow cytometer (BDFacsCanto II, Becton Dickinson, San Jose, USA). Argon laser excitation at 488 nm was coupled with emission measurements using 580 nm filters. Non-sperm-specific events were gated out and 50,000 cells were examined per independent sample (Zarzycka et al. 2014; He et al. 2017).

***In vitro* fertilizing capacity of Sperm**

Gilt cumulus-oocyte complexes *in vitro* maturation was performed following our laboratory protocol (Morado et al. 2023). Briefly, cumulus-oocyte complexes were obtained by aspiration of antral follicles (3-8 mm) from slaughterhouse ovaries and then matured in medium 199 (GIBCO, Grand Island, NY) supplemented with 50 µg mL^{-1} gentamicin sulfate, 10% (v/v) porcine follicular fluid, 2UI mL^{-1} equine chorionic gonadotropin, 10 ng mL^{-1} epidermal growth

factor, 0.57 mM cysteine, under mineral oil at 39 °C, 5% CO_2 in a humidified atmosphere for 44 h.

To evaluate the *in vitro* fertilizing capacity of refrigerated semen, sperm cells from each treatment at day 3 of refrigeration were washed in TBM (Tris Buffer Medium) by centrifugation and then co-incubated in the same medium at a final concentration of $5x10^5$ spermatozoa mL^{-1} with *in vitro* matured porcine oocytes for 3 h. Fertilized oocytes were washed in NCSU-23 medium (Yamanaka et al. 2009) and the remaining cumulus cells and spermatozoa were removed by gentle pipetting. Presumptive zygotes were incubated in NCSU-23 medium under mineral oil, at 39 °C in a 20% O_2 and 5% CO_2 atmosphere. Cleavage rate was evaluated 48 h post-fertilization. For this experiment, between 25 and 30 COCs were used for each treatment per trial and seven repetitions were performed.

Statistical analysis

Results for spermatic variables were expressed as mean ± standard deviation and were analyzed by two-way ANOVA followed by Tukey test and the comparison of means was carried out at each evaluation time. The normality of the data was evaluated using the modified Shapiro-Wilk test. Cleavage rates were expressed as mean ± standard deviation and were analyzed by one-way ANOVA followed by Tukey test. The normality of the data was evaluated using modified Shapiro-Wilk test. *P* values lower than 0.05 were considered significantly different. The statistical analysis was carried out using Infostat software.

RESULTS AND DISCUSSION

Some studies have attempted to evaluate the effect of Trolox and resveratrol on boar sperm quality, all of them performing the antioxidant supplementation before semen freezing or refrigeration procedures. This study analyzed the possibility of improving the quality of commercial semen by adding these antioxidants once the refrigeration procedure has started. Additionally, the combination of both antioxidants was evaluated considering that they have different antioxidant action mechanisms that could improve their protective capacity.

Five pools of refrigerated boar semen were analyzed in order to evaluate the effect of the addition of Trolox and/or resveratrol during 1, 3, and 7 days of preservation on sperm motility, viability and acrosome integrity, plasma membrane functionality, mitochondrial membrane potential, and pre-capacitated spermatozoa (Figure 1). As expected, except for the percentage of pre-capacitated spermatozoa

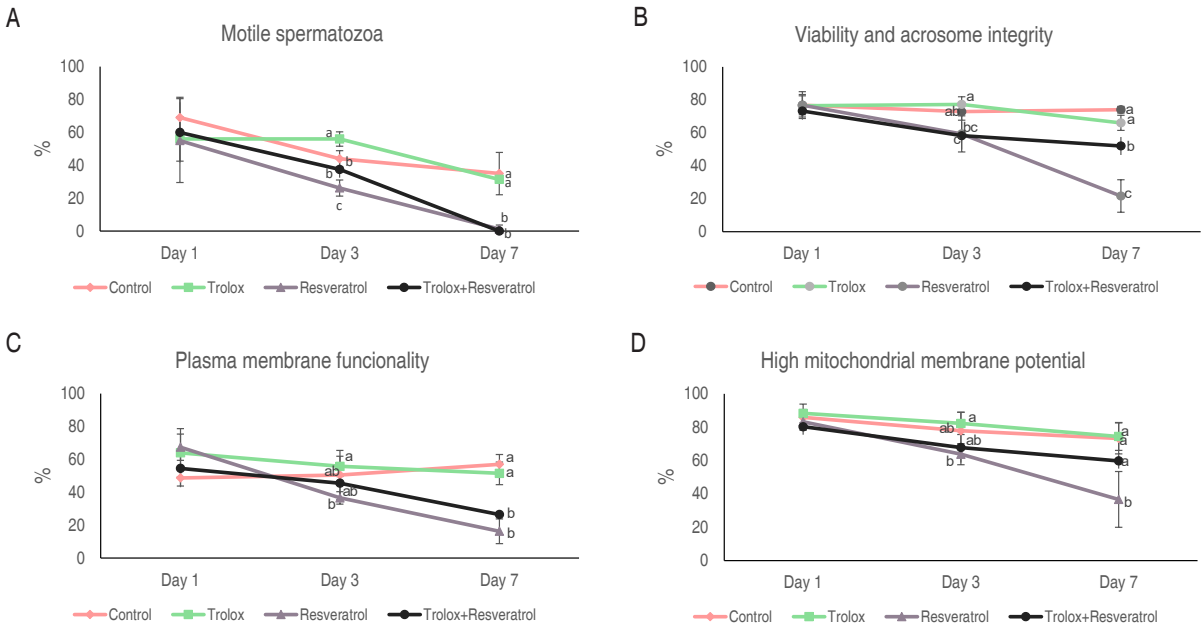

Figure 1. Evaluated sperm parameters. **A.** Percentage of motile spermatozoa. **B.** Percentage of viable spermatozoa with intact acrosome. **C.** Percentage of spermatozoa with functional plasma membrane. **D.** Percentage of spermatozoa with high mitochondrial membrane potential. Data are expressed in percentage ± standard deviation in 5 replicates. [a, b, c] Different letters indicate significant differences between treatments on the same evaluation day ($P<0.05$). All the evaluated parameters significantly decreased over refrigeration time ($P<0.05$).

(day 1=0.2±0.2% to day 7=2.3±0.3%), all the evaluated sperm parameters significantly decreased over the refrigeration time in the four studied groups (control, trolox, resveratrol, and trolox + resveratrol, $P<0.05$).

The addition of Trolox to already refrigerated sperm increased sperm motility at day 3 of preservation ($P<0.05$, Figure 1A), but it maintained similar values with respect to the control group for the other sperm parameters at all evaluated days (Figure 1A-D). The effect of Trolox supplementation on boar sperm is still controversial. It has been reported that the addition of Trolox (200 µM) during the freezing process improves frozen-thawed boar sperm viability, increases motility, mitochondrial activity and acrosome integrity (Peña et al. 2003; Varo-Ghiuru et al. 2015). The addition of Trolox (200 µM) to the refrigeration diluent increases motility and membrane functionality in boar sperm (Camporino and Córdoba 2022). Additionally, supplementation of Trolox (400 µg mL^{-1}) during the processing of pig semen doses to be stored at 15 °C for 72 h reduces malondialdehyde (MDA) production, indicating a reduction in lipid peroxidation (Mendez et al. 2013). On the other hand, it has been reported that the use of trolox (200 µM) in the diluent for boar semen refrigerated for 72 h causes a significant decrease in motility, tail membrane integrity and mitochondrial activity, and a significant increase in DNA fragmentation and lipid peroxidation (Zakošek Pipan et al. 2017). The findings in the present study suggest that the addition of Trolox to the sperm diluent once the refrigeration procedure has started exerts, in general, neither beneficial nor deleterious effect on sperm parameters.

The addition of resveratrol to already refrigerated semen diminished sperm motility ($P<0.05$, days 3 and 7, Figure 1A) and tended to decrease (day 3) or decreased ($P<0.05$, day 7) the other evaluated sperm parameters with respect to the control group (Figure 1A-D). The effect of resveratrol supplementation on boar sperm is also controversial. It was reported that the addition of resveratrol in boar sperm freezing diluent significantly improved post-thawing progressive motility, membrane and acrosome integrity, mitochondrial activity, glutathione level and antioxidant enzyme activity (Zhu et al. 2019). The addition of resveratrol (50 µM) during the refrigeration process improves visual motility, membrane and acrosome integrity, mitochondrial membrane potential, and decreased MDA content (Sun et al. 2020). On the other hand, Martín-Hidalgo et al. (2013) evaluated the addition of resveratrol to the extender of boar semen for its storage at 17 °C, indicating that this supplementation causes a lower response to capacitating stimuli, a decrease in the sperm ATP content and a reduction in mitochondrial membrane potential. Although there are no reports about the addition of resveratrol once the refrigeration process has started, Bucci et al. (2018) performed the antioxidant supplementation during the thawing process of frozen semen and found that the addition of resveratrol (2 mM) to thawing medium causes a negative effect on sperm motility and DNA integrity, while viability, acrosome integrity, mitochondrial function and lipid peroxidation were not influenced. These last studies are in part in line with the results of this study, which indicate that resveratrol addition during the refrigeration process of porcine semen tends to exert or exerts a deleterious effect on the sperm parameters with respect to the control. In this case, as resveratrol was added once the spermatozoa were already refrigerated and their metabolism was decreased, such incorporation in the sperm cells could not be as efficient as expected, increasing its concentration in the extender, which may have shifted their behavior to pro-oxidant activity. A similar idea has been proposed by Vongpralub et al. (2016), who mentioned that these extenders are suitable by themselves for long-term liquid preservation; having in mind that commercial farms retain the seminal plasma in the extended semen, and the plasma contains natural antioxidants, the subsequent addition of antioxidant molecules, may increase their content above the physiological values which may be detrimental to the cells. It was also observed that sperm samples preserved in the presence of resveratrol show the lowest mitochondrial membrane potential. This decrease could be associated with resveratrol ability to regulate mitochondrial permeability transition pore, increase mitochondrial superoxide anion production and to disrupt mitochondrial respiratory chain (Martín-Hidalgo et al. 2013). These events reduce the ATP content of the spermatozoa treated with resveratrol, which could explain the parallel decrease in sperm motility (Martín-Hidalgo et al. 2013); as it was also observed in sperm motility with the addition of resveratrol during refrigeration in the present study.

Interestingly, the percentages of sperm motility, viability and acrosome integrity, plasma membrane functionality and high mitochondrial membrane potential were higher in

samples added with Trolox with respect to those added with resveratrol at days 3 and 7 of preservation (P<0.05, Figure 1A-D). But these sperm parameters showed intermediate values when samples were supplemented with Trolox + resveratrol (Figure 1A-D). These results suggest that Trolox can protect sperm samples from the detrimental effects caused by the presence of resveratrol in the refrigerated diluent.

Sperm mitochondrial ROS production was evaluated with the fluorescent probe MitoSOX Red using flow cytometry. Two distinct subpopulations were observed; a subpopulation of sperm cells that did not bind to the probe (MS(-)), and a subpopulation that reacted to the probe (MS(+)) (representative histograms for days 3 and 7 are shown in Figure 2A). As shown in Figure 2B, mitochondrial ROS production for the MS(+) subpopulation was significantly higher on day 1 in comparison with days 3 and 7 of preservation (P<0.05). It is well known that the cryopreservation process affects sperm functionality, but Awda et al. (2009) demonstrated that intracellular levels of hydrogen peroxide are unchanged after the cryopreservation of boar sperm and that viable frozen-thawed sperm presents significantly less intracellular content of superoxide anion. The reported alterations could be caused by alterations in mitochondrial function and a decrease in oxidative phosphorylation, leading to lower ATP synthesis and ROS generation, causing both the reduction in superoxide anion content and sperm motility (Awda et al. 2009). On the same day of evaluation, no significant differences were observed in the production of mitochondrial superoxide anion between treatments. A possible explanation is presented by Guthrie and Welch (2006), who mentioned that boar sperm naturally presents low basal ROS concentrations, which do not differ between fresh and frozen-thawed sperm. Since physiological ROS production is not high, antioxidant supplementation can have detrimental effects on sperm cells (Bucci et al. 2018). *In vitro* sperm fertilizing capacity was evaluated by co-incubating *in vitro* matured porcine cumulus-oocyte

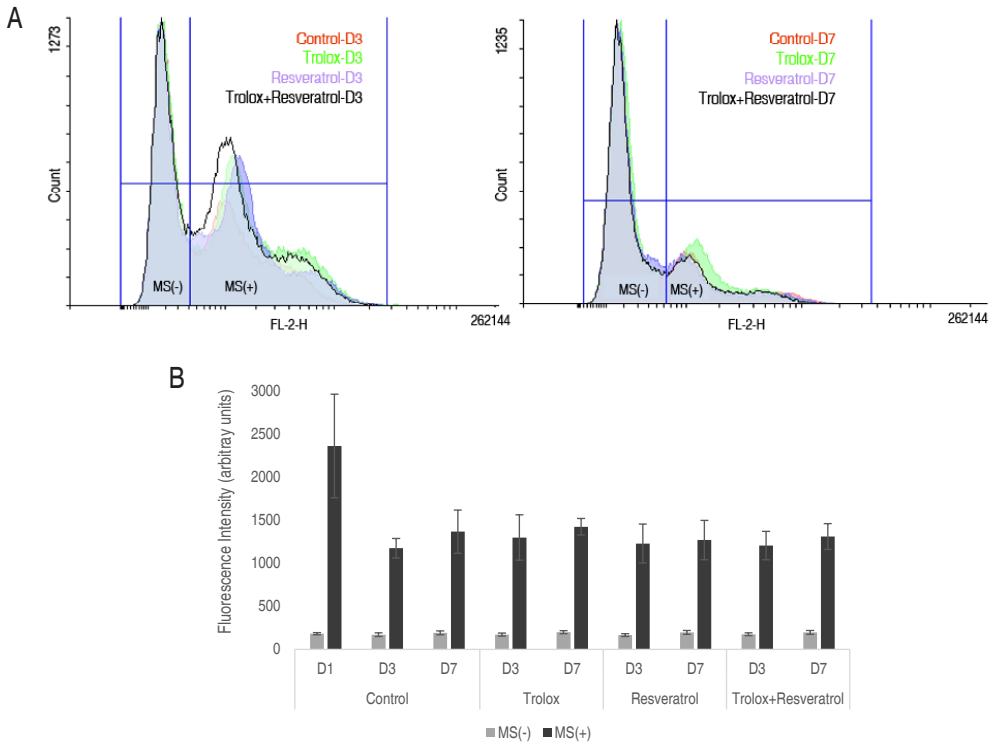

Figure 2. Mitochondrial superoxide anion production. **A**. Representative histograms of mitochondrial superoxide anion production evaluated with MitoSOX Red fluorescent probe using flow cytometry. Two different subpopulations are described; a subpopulation of sperm cells that did not bind to the probe (MS(-)), and a subpopulation that reacted to the probe (MS(+)). **B**. Effect of antioxidant treatment on mitochondrial ROS in refrigerated boar sperm. Results are expressed as arbitrary units of fluorescence intensity ± standard deviation in three replicates for negative (MS(-)) or positive (MS(+)) sperm cells to MitoSOX Red.

complexes with sperm samples treated with antioxidants on day 3 of preservation, because these samples still preserved a good motility. Seven repetitions were performed. As shown in Table 1, no significant differences were observed on cleavage rates between the four groups studied. Surprisingly, despite the differences found for sperm parameters, especially between Trolox and resveratrol, cleavage rates do not differ between treatments. Probably, there are still enough viable spermatozoa to maintain *in vitro* fertilizing capacity in the different sperm samples. These results coincide with several authors (Peña et al. 2003; Pech-Sansores et al. 2011; Maside et al. 2023) who indicated that subjective motility is not a reliable indicator of porcine sperm quality after thawing, and Martín-Hidalgo et al. (2013) who mentioned that conventional boar sperm parameters used to evaluate semen doses are insensitive to assess the fertilization potential of refrigerated semen. Although some studies have evaluated the effect of these antioxidants on classic parameters of boar sperm, to the best of current knowledge, only one has assessed the potential effect of resveratrol on *in vitro* fertilizing capacity. It has been reported that the addition of resveratrol in a frozen medium may increase sperm penetration rate and diminish monospermic rate in comparison with the control (Bucci et al. 2018). This study is the first one that evaluates the effect of Trolox supplementation, alone or combined with resveratrol, on *in vitro* fertilizing capacity of boar refrigerated sperm. Additionally, it would also be interesting to evaluate *in vivo* fertilizing capacity of these sperm samples, considering the effect of female genital tract conditions.

Table 1. Cleavage rate obtained from *in vitro* matured cumulus-oocyte complexes fertilized with refrigerated sperm treated with different antioxidants (Trolox and/or resveratrol).

Sperm treatments	Total number of matured COCs	Total number of cleavage embryos	Mean cleavage rate (%)*
Control	197	102	51.00±4.41
Trolox	201	97	46.41±2.95
Resveratrol	193	100	46.53±9.14
Trolox + Resveratrol	179	92	49.31±8.61

* Percentages are expressed as mean ± standard deviation in seven replicates (n= 25-30 COCs for each treatment per trial; $P<0.05$).

CONCLUSION

Previous studies have evaluated the addition of antioxidants, among them Trolox and resveratrol, to refrigerate diluents before the cooling process to avoid damage related to cold shock. However, there is not enough evidence whether the addition of these antioxidants to the semen extender collaborates to prolong seminal viability once the refrigeration process has been completed, considering that commercial farms sell semen already refrigerated. In this study, it was observed that supplementing refrigerated boar semen with Trolox and resveratrol does not cause a significant improvement in semen quality. When only Trolox is added, viability and acrosome integrity, plasma membrane functionality and mitochondrial membrane potential maintain a similar behavior to the control, except for an increased motility at day 3 of preservation with this antioxidant. Particularly, the addition of resveratrol generates a reduction in the sperm parameters studied over refrigeration time. The presence of Trolox prevents in part, the detrimental effect caused by resveratrol. It is important to highlight that the addition of these antioxidants did not generate changes in mitochondrial superoxide anion production, suggesting that although conservation processes usually increase ROS levels, in refrigerated porcine semen these levels would not exceed the cell physiological control capacity; so, the addition of antioxidant supplements after refrigeration had no beneficial effects. This idea is supported because no significant differences were observed in cleavage rates between treatments, which also was evidenced that commonly evaluated sperm parameters do not necessarily reflect the fertilizing capacity of sperm, at least with respect to *in vitro* embryo production system. Further studies that investigate the endogenous antioxidant sperm capacity could help to develop the proper antioxidant protocol supplementation to improve refrigerated boar sperm performance.

ACKNOWLEDGEMENTS

This study was supported by an UBACyT grant.

CONFLICT OF INTERESTS

The authors have no conflict of interest.

REFERENCES

Awda BJ, Mackenzie-Bell M and Buhr MM (2009) Reactive oxygen species and boar sperm function. Biology of Reproduction 81: 553–561. https://doi.org/10.1095/biolreprod.109.076471

Bucci D, Spinaci M, Yeste M et al (2018) Combined effects of resveratrol and epigallocatechin-3-gallate on post thaw boar sperm and IVF parameters. Theriogenology 117: 16–25. https://doi.org/10.1016/j.theriogenology.2018.05.016

Camporino A and Córdoba M (2022) Effect of Trolox addition as antioxidant in refrigeration medium in porcine spermatozoa. InVet 24: 1–10.

Cao B, Qin J, Pan B et al (2022) Oxidative Stress and Oocyte Cryopreservation: Recent Advances in Mitigation Strategies Involving Antioxidants. Cells 11. https://doi.org/10.3390/cells11223573

Gambini J, Inglés M, Olaso G et al (2015) Properties of resveratrol: *in vitro* and *in vivo* studies about metabolism, bioavailability, and biological effects in animal models and humans. Oxidative Medicine and Cellular Longevity 2015: 1–13. https://doi.org/10.1155/2015/837042

Giaretta E, Spinaci M, Bucci D et al (2013) Effects of resveratrol on vitrified porcine oocytes. Oxidative Medicine and Cellular Longevity 2013: 1–7. https://doi.org/10.1155/2013/920257

Giordano ME, Caricato R and Lionetto MG (2020) Concentration dependence of the antioxidant and prooxidant activity of trolox in hela cells: Involvement in the induction of apoptotic volume decrease. Antioxidants 9: 1–12. https://doi.org/10.3390/antiox9111058

Guthrie HD and Welch GR (2006) Determination of intracellular reactive oxygen species and high mitochondrial membrane potential in Percoll-treated viable boar sperm using fluorescence-activated flow cytometry. Journal of Animal Science 84: 2089–2100. https://doi.org/10.2527/jas.2005-766

He B, Guo H, Gong Y and Zhao R (2017) Lipopolysaccharide-induced mitochondrial dysfunction in boar sperm is mediated by activation of oxidative phosphorylation. Theriogenology 87: 1–8. https://doi.org/10.1016/j.theriogenology.2016.07.030

He W hua, Zhai X hu, Duan X jun and Di H shuang (2020) Effect of resveratrol treatment on apoptosis and apoptotic pathways during boar semen freezing. Journal of Zhejiang University: Science B 21: 485–494. https://doi.org/10.1631/jzus.B1900520

Longobardi V, Zullo G, Salzano A et al (2017) Resveratrol prevents capacitation-like changes and improves *in vitro* fertilizing capability of buffalo frozen-thawed sperm. Theriogenology 88: 1–8. https://doi.org/10.1016/j.theriogenology.2016.09.046

Martín-Hidalgo D, Hurtado de Llera A, Henning H et al (2013) The effect of resveratrol on the quality of extended boar semen during storage at 17ºC. Journal of Agricultural Science 5: 231–242. https://doi.org/10.5539/jas.v5n8p231

Maside C, Recuero S, Salas-Heutos A et al (2023) Animal board invited review: An update on the methods for semen quality evaluation in swine – from farm to the lab. Animal 17(2023): 1-13. https://doi.org/10.1016/j.animal.2023.100720

Mendez MFB, Zangeronimo MG, Rocha LGP et al (2013) Effect of the addition of IGF-I and vitamin e to stored boar semen. Animal 7: 793–798. https://doi.org/10.1017/S1751731112002285

Morado S, Aparicio A, Pinchetti D et al (2023) Variations in metabolic parameters of *in vitro* matured porcine oocytes after vitrification-warming. Open Veterinary Journal 13:1416–1424. https://doi.org/10.5455/OVJ.2023.v13.i11.4

Pasquariello R, Verdile N, Brevini TAL et al (2020) The role of resveratrol in mammalian reproduction. Molecules 25: 1–16. https://doi.org/10.3390/molecules25194554

Pech-Sansores AGC, Centurión-Castro FG, Rodríguez-Buenfil JC et al (2011) Effect of the addition of seminal plasma, vitamin E and incubation time on post-thawed sperm viability in boar semen. Tropical and Subtropical Agroecosystems 14(2011): 965-971.

Peña FJ, Johannisson A, Wallgren M and Rodriguez Martinez H (2003) Antioxidant supplementation *in vitro* improves boar sperm motility and mitochondrial membrane potential after cryopreservation of different fractions of the ejaculate. Animal Reproduction Science 78: 85–98. https://doi.org/10.1016/S0378-4320(03)00049-6

Ribas-Maynou J, Mateo-Otero Y, Delgado-Bermúdez A et al (2021) Role of exogenous antioxidants on the performance and function of pig sperm after preservation in liquid and frozen states: A systematic review. Theriogenology 173: 279–294. https://doi.org/10.1016/j.theriogenology.2021.07.023

Satorre M, Breininger E, Cetica P and Córdoba M (2018) Relation between respiratory activity and sperm parameters in boar spermatozoa cryopreserved with alpha-tocopherol and selected by Sephadex. Reproduction in Domestic Animals 53: 979–985. https://doi.org/10.1111/rda.13197

Sun L, Fan X, Zeng Y et al (2020) Resveratrol protects boar sperm *in vitro* via its antioxidant capacity. Zygote (Cambridge, England) 28: 417–424. https://doi.org/10.1017/S0967199420000271

Varo-Ghiuru F, Miclea I, Hettig A et al (2015) Lutein, Trolox, ascorbic acid and combination of Trolox with ascorbic acid can improve boar semen quality during cryopreservation. Cryo-Letters 36: 1–7

Vongpralub T, Thananurak P, Sittikasamkit C et al (2016) Comparison of effects of different antioxidants supplemented to long-term extender on boar semen quality following storage at 17°C. Thai Journal of Veterinary Medicine 46:119–126. https://doi.org/10.56808/2985-1130.2703

Wysokińska A (2020) Effect of sperm concentration on boar spermatozoa mitochondrial membrane potential and motility in semen stored at 17 °C. Acta Veterinaria Brno 89:333–340. https://doi.org/10.2754/avb202089040333

Yamanaka KI, Sugimura S, Wakai T et al (2009) Difference in sensitivity to culture condition between *in vitro* fertilized and somatic cell nuclear transfer embryos in pigs. Journal of Reproduction and Development 55: 299–304. https://doi.org/10.1262/jrd.20174

Yeste M (2017) State-of-the-art of boar sperm preservation in liquid and frozen state. Animal Reproduction 14: 69–81. https://doi.org/10.21451/1984-3143-AR895

Zakošek Pipan M, Mrkun J, Nemec Svete A and Zrimšek P (2017) Improvement of liquid stored boar semen quality by removing low

molecular weight proteins and supplementation with α-tocopherol. Animal Reproduction Science 186: 52–61. https://doi.org/10.1016/j.anireprosci.2017.09.004

Zarzycka M, Kotwicka M, Jendraszak M et al (2014) Hydroxyflutamide alters the characteristics of live boar spermatozoa. Theriogenology 82: 988–996. https://doi.org/10.1016/j.theriogenology.2014.07.013

Zhu Z, Li R, Fan X et al (2019) Resveratrol Improves Boar Sperm Quality via 5 ′ AMP-Activated Protein Kinase Activation during Cryopreservation. Oxidative Medicine and Cellular Longevity 2019: 1-15. https://doi.org/10.1155/2019/5921503

Research article

https://revistas.unal.edu.co/index.php/refame

Revista Facultad Nacional de Agronomía

Interaction of biological soil crusts with edaphic parameters of carbon and nitrogen in desertified soils

Interacción de las costras biológicas del suelo con los parámetros edáficos de carbono y nitrógeno en suelos desertificados

https://doi.org/10.15446/rfnam.v78n2.111622

Juan Jair Rivera Padilla[1], Julian David Romero Conde[1] and Lizeth Manuela Avellaneda-Torres[2]*

ABSTRACT

This study aimed to assess the influence of biological soil crusts (BSCs) on soil parameters associated with carbon and nitrogen cycling in soils undergoing desertification in Villa de Leyva, Colombia. Soil samples were collected from areas with and without biological soil crusts. Physicochemical variables, including moisture, pH, total nitrogen, and organic carbon, were measured alongside enzymatic activities such as protease, urease, and β-glucosidase. The abundance of microorganisms—including nitrogen-fixing and cellulolytic bacteria, as well as cellulolytic fungi—was also analyzed. Univariate and multivariate statistical analyses were performed. Results indicate that soils with biological crusts harbor a significantly greater abundance of nitrogen-fixing bacteria than those without crusts. Additionally, soils with biological crusts exhibited significant increases in total nitrogen, organic carbon, urease, and β-glucosidase at specific sampling points, suggesting a general trend towards higher values, although average differences were not statistically significant. Biological soil crusts exhibit beneficial properties in soils undergoing desertification, underscoring their potential role in ecosystem restoration and land degradation mitigation.

Keywords:
Cellulolytic microorganisms
Desertification
Enzymatic activities
Nitrogen-fixing bacteria

RESUMEN

Este estudio tuvo como objetivo evaluar la influencia de las costras biológicas del suelo (BSC) en los parámetros edáficos relacionados con el carbono y el nitrógeno en suelos en proceso de desertificación en Villa de Leyva, Colombia. Se recolectaron muestras de suelo en áreas con y sin costras biológicas del suelo. Se midieron variables fisicoquímicas, incluyendo humedad, pH, nitrógeno total y carbono orgánico, junto con actividades enzimáticas como proteasa, ureasa y β-glucosidasa. También se evaluó la abundancia de microorganismos, entre ellos bacterias fijadoras de nitrógeno, bacterias celulolíticas y hongos celulolíticos. Se realizaron análisis estadísticos univariados y multivariados. Los resultados indican que los suelos con costras biológicas del suelo albergan una abundancia significativamente mayor de bacterias fijadoras de nitrógeno en comparación con los suelos sin costra. Además, los suelos con costras biológicas del suelo mostraron incrementos significativos en nitrógeno total, carbono orgánico, ureasa y β-glucosidasa en puntos de muestreo específicos, lo que sugiere una tendencia general hacia valores más altos, aunque las diferencias promedio no fueron estadísticamente significativas. Las costras biológicas del suelo presentan propiedades beneficiosas en suelos en proceso de desertificación, lo que resalta su papel potencial en la restauración de ecosistemas y la mitigación de la degradación del suelo.

Palabras clave:
Microorganismos celulolíticos
Desertificación
Actividades enzimáticas
Bacterias fijadoras de nitrógeno

[1]Facultad de Ingeniería, Universidad Libre, Colombia. juanj-riverap@unilibre.edu.co, juliand-romeroc@unilibre.edu.co
[2]Departamento de Química, Universidad Nacional de Colombia, Colombia. lmavellanedat@unal.edu.co
*Corresponding author

Received: September 13, 2024; Accepted: March 12, 2025
Rev. Fac. Nac. Agron. Medellín 78(2): 11151-11160. 2025.
ISSN 0304-2847 / e-ISSN 2248-7026

CC BY NC SA

Biological soil crusts (BSC) are communities composed of microorganisms, including fungi, microalgae, and cyanobacteria, as well as microorganisms such as lichens and mosses, that inhabit the upper millimeters of the soil surface (Belnap and Lange 2003). BSCs develop in a wide range of ecosystems and under diverse ecological conditions due to the high adaptability of their constituent organisms. These microhabitats include arid and semi-arid regions, with both hot and cold climates, as well as polar zones. BSCs are commonly found in areas where sparse vegetation allows direct solar radiation to reach the soil surface, including regions affected by anthropogenic activities, such as open-pit mines, quarries, and other resource extraction areas (Romero et al. 2021). Their adaptability enables them to persist in extreme environments, and they are often found in landscapes modified by human activities, such as mining and quarrying operations (García et al. 2021).

Soils in arid and degraded regions are characterized by low nitrogen and organic carbon content. In these ecosystems, communities of lichens and cyanobacteria play a crucial role in the cycling of carbon and nitrogen (Castillo-Monroy and Maestre 2011; García 2019). Nitrogen fixation by BSCs is influenced by their composition and the environmental conditions in which they develop (Belnap and Lange 2003). BSCs are essential in arid ecosystems due to their ability to release fixed nitrogen, making it available to vascular plants and other soil microorganisms (Belnap 2002). Additionally, research has demonstrated that soil respiration is closely linked to the extent of BSC coverage and ambient humidity levels (Thomas et al. 2008).

Over time, human activities and climate variations have accelerated global soil desertification (Lozano 2011). This has driven research on BSCs in countries with extensive desert areas, such as Australia, China, the United States, and Israel, which have led to research efforts on these microbial communities (Castillo-Monroy and Maestre 2011). Recent research in China has made significant advances in BSC studies, including key steps in BSC recovery, microorganism selection for cultivation techniques, and the inoculation and monitoring of BSCs to restore highly degraded ecosystems (Zhou et al. 2020). Despite the relevance of BSCs in arid, semi-arid, and anthropogenically degraded ecosystems, studies on BSCs in Latin America remain limited, highlighting a critical research gap in these regions (Castillo-Monroy and Maestre 2011). Research in Latin America has primarily focused on species characterization (Molina et al. 2014), carbon storage and flux in arid soils (Ayala et al. 2018), biological and biochemical properties of crusts under natural vegetation (Toledo 2012), and ecosystem functions and ecological attributes of BSCs (Romero 2019), among others.

In Colombia, a study on the diversity of lichens and bryophytes in arid and degraded regions has been conducted (Pinzón and Linares 2006). However, further research is needed to understand the role of biological soil crusts (BSC) in carbon and nitrogen cycles, especially in areas vulnerable to soil degradation. In this context, the department of Boyacá has garnered special interest, as it contains desert-like areas resulting from unsustainable practices related to the complexity of agricultural activities and resource extraction. According to Pacheco and Giselle (2016), these practices date back to pre-Hispanic times and persisted during the colonization period, with indiscriminate deforestation and vegetation burning to clear land for agriculture and livestock being key contributors to degradation.

A representative case is Villa de Leyva, where degraded soils and the potential presence of BSCs make this region an optimal site for investigating their role in carbon and nitrogen cycles in desert ecosystems. Thus, the primary question guiding this research is: How does the presence of BSCs influence edaphic parameters associated with carbon and nitrogen cycles in desert soils in Villa de Leyva, Colombia? To address this, the following research questions are posed: Which specific areas of the Villa de Leyva desert contain BSCs, and how can they be georeferenced to establish a record of their distribution? What differences exist in physicochemical properties, enzymatic activities, and the abundance of microorganisms in soils with and without BSCs?

MATERIALS AND METHODS

Study area

The study was conducted in the desert of Villa de Leyva, located in the department of Boyacá, Colombia, at coordinates 5°36'48"N and 73°32'40"W, and an elevation of 2,150 meters above sea level (masl). The soils where BSCs were identified and sampled are classified as having miscellaneous erosion, characterized by a loam texture

with natural gravel and a strongly acidic pH (IGAC 2017). These soils are subject to moderate to severe diffuse and concentrated runoff, as well as gully formation due to erosion (Figure 1).

Soil samples with biological crusts were collected by extracting cubic blocks of soil, including the crust, from a depth of 10 cm. For soils lacking biological crusts, samples were obtained from locations 2 to 5 m away from the crusts to ensure similar soil characteristics, using the same extraction method. A total of 18 samples were collected, comprising nine samples from areas with biological crusts and nine from areas without biological crusts. Each sample type was processed in triplicate for subsequent analyses. The samples from areas with biological crusts were designated as "Crust" and those from areas without were termed "Non-Crust." Due to the random distribution of biological soil crusts, samples were taken wherever these crusts were encountered. Each sampling point was georeferenced using GPS, and photographic documentation of each crust was obtained to digitize its location on a map prepared with ArcGIS software (Figure 1). For storage, samples were placed in Ziploc bags and categorized according to the analysis to be performed. Physicochemical samples were stored at room temperature, enzyme assay samples were frozen at -20 °C, and microorganism samples were refrigerated at 4 °C. Prior to analysis, the soil samples were passed through a No. 20 mesh sieve (850 µm) to obtain fine particles for the subsequent processes.

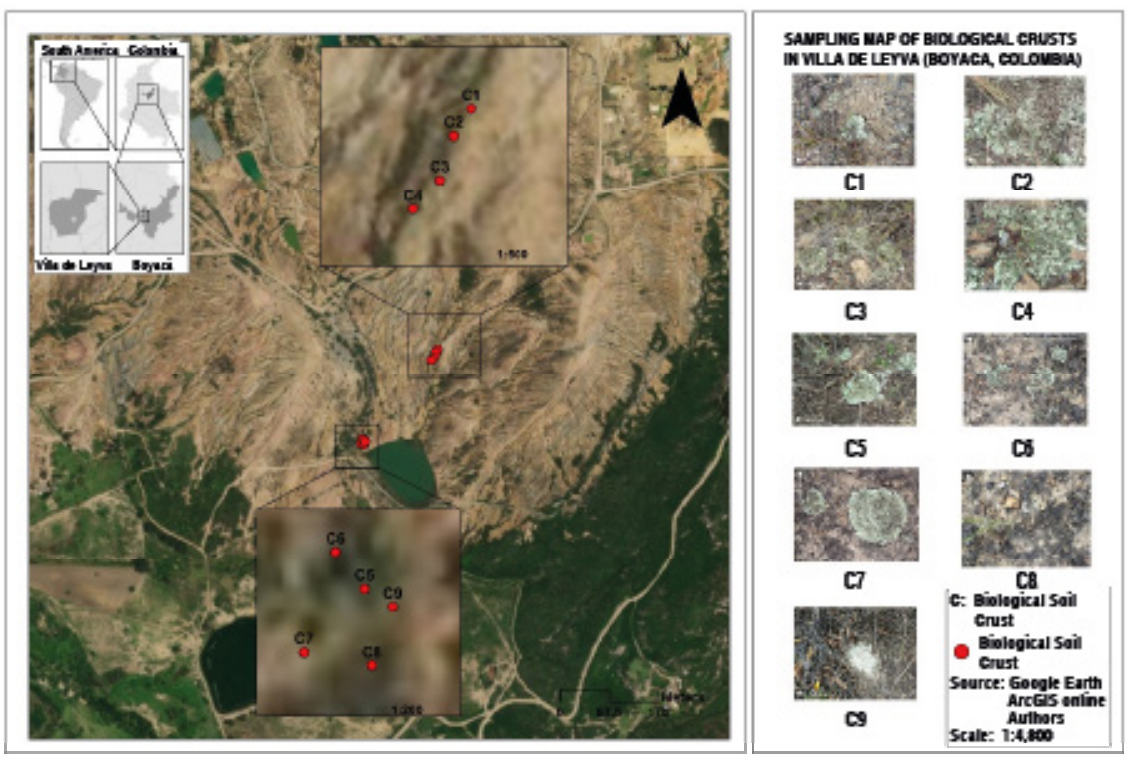

Figure 1. Location of the study area and sampling points for the biological soil crusts (C). The numbering on the map corresponds to each sampled crust and its respective crust-free soil. The photographs correspond to the crusts at each sampling point, numbered accordingly.

Physicochemical analyses

Soil pH was determined using the potentiometric method with a 1:1 (w/v) soil-to-water ratio. Soil moisture content was determined gravimetrically. Total nitrogen was quantified using the Kjeldahl method, while organic carbon was analyzed following the Walkley-Black procedure (IGAC 2006). Each analysis was performed in triplicate.

Enzymatic activities

The enzymatic activities involved in carbon and nitrogen

cycles were determined following the methodology described by Avellaneda et al. (2018). Urease activity was quantified colorimetrically at 690 nm by measuring the amount of ammonia released after incubating the samples with urea as the substrate for 2 h at 37 °C. Protease activity was assessed using casein as the substrate; samples were incubated for 2 h at 50 °C with a pH of 8.1, and the amino acids released during incubation were extracted and reacted with Folin-Ciocalteu reagent in an alkaline solution, with absorbance measured at 700 nm. β-glucosidase activity was measured at 400 nm by quantifying the release of p-nitrophenol after incubating the soil with p-nitrophenyl glucoside solution for 1 h at 37 °C. All analyses were performed in triplicate.

Microorganism abundance

To determine the abundance of microorganisms associated with carbon- and nitrogen-functional groups, colony-forming units per gram of soil (CFU/g) were quantified. For the enumeration and isolation of nitrogen-fixing bacteria, the nitrogen-free selective medium method by Rennie (1981), modified by Avellaneda et al. (2020), was used. Incubation was performed for 48 h at 28 °C. The enumeration and isolation of cellulolytic bacteria and fungi were conducted using Sundara and Paul (1971) medium, modified by Avellaneda et al. (2012), with 1% carboxymethyl cellulose as the sole carbon source. Bacteria were incubated for 48 h at 28°C, while fungi were incubated at 20 °C for 6 days. Each analysis was performed in triplicate.

Statistical analysis

To identify potential significant differences between soil samples from "Crust" and "Non-Crust" categories, and to establish relationships between variables and sampling points, two types of univariate analyses were performed: a general analysis encompassing all sampling points and a specific analysis evaluating each sampling point individually. The assumptions of normality were assessed using the Shapiro-Wilk test (R Core Team 2021), and variance homogeneity was checked with Bartlett's and Fligner-Killeen tests, using the stats package (R Core Team 2021), along with Levene's test from the CAR package (Fox and Weisberg 2019). For variables that did not meet the assumptions of normality and homogeneity of variances, the Mann-Whitney-Wilcoxon (WMW) test from the stats package (R Core Team 2021) was employed. Multivariate data analysis was conducted using Principal Component Analysis (PCA) from the FactoMineR package (Lê et al. 2008). It is essential to interpret these results in the context of the experimental design and the assumptions underlying each statistical test to ensure robust conclusions.

RESULTS AND DISCUSSION

The soil moisture percentage (Figure 2A) indicates that, at five of the nine sampling points under biological soil crusts (Crust), the moisture content was significantly higher compared to the soils without biological soil crusts (Non-Crust). Conversely, at the remaining four points, Non-Crust soils exhibited significantly higher moisture levels. However, when analyzing the data globally (Figure 2E), there is a 2.1% increase in moisture in Non-Crust soils compared to Crust soils, but this difference is not statistically significant. Some types of crusts in sandy soil can reduce rapid water infiltration and help retain soil moisture (Navas et al. 2021). Similarly, Cerdà (1998) notes that soils under BSC tend to maintain more stable moisture levels than Non-Crust soils, likely due to differences in infiltration rates and reduced soil erodibility under BSCs. Additionally, studies suggest that in extreme environments, microorganisms within BSCs can absorb water as an adaptation mechanism to withstand desiccation. In particular, mosses, a key component of many BSCs, are poikilohydric organisms, meaning they can survive extreme dehydration and rehydrate when water becomes available, which may explain the moisture levels observed in BSC-covered soils (Nuñez 2013). However, it is important to acknowledge that the initial water content in crusted soils might influence the observed moisture differences, rather than solely reflecting the effects of BSCs. To minimize this uncertainty, future studies should include sampling across different seasons to assess moisture variations under diverse climatic conditions.

The pH values obtained are generally classified as strongly acidic. Significant differences were observed at four of the nine sampling points (Figure 2B), with three points exhibiting higher pH values in Non-Crust soils. However, when considering all sampling points collectively, no statistically significant differences were detected (Figure 2F). Although the overall acidity is evident, previous studies present differing perspectives. For instance, Kakeh et al. (2018) report no significant differences in pH between soils with and without BSC. In contrast, Wu et al. (2013) suggest that microbial respiration within BSCs may contribute to a reduction in soil pH, which aligns with the

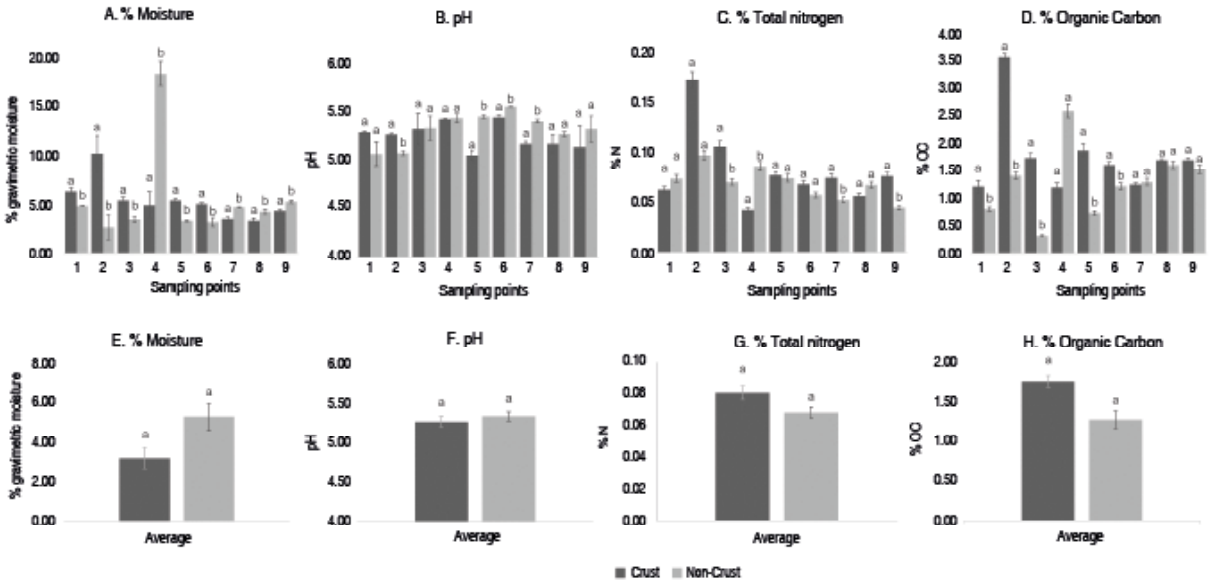

Figure 2. Results of the physicochemical variables by sampling points and average (from 1 to 9). In graphs A, B, C, and D, soils with and without crust are compared individually, while graphs E, F, G, and H show comparisons with the average of soils with and without crust. Significant differences are indicated above the bars with letters a-b when there is a significant difference and a-a when there is not, using a $P \geq 0.05$.

lower pH values observed at three of the four significantly different sampling points.

The total nitrogen content in the soil (Figure 2C) is generally low. Significant differences were observed at four of the nine sampling points, with Crust soils exhibiting higher nitrogen levels at three of these points. However, when analyzing the average data (Figure 2G), Crust soils contain 15.3% more nitrogen than Non-Crust soils, although this difference is not statistically significant. Plata (2019) reports higher total nitrogen percentages in soils with BSC, while Toledo (2012) also notes significantly higher nitrogen levels in BSC soils compared to Non-Crust soils. The observed increase in nitrogen content in some samples may be attributed to microorganisms within the BSC, such as cyanobacteria, which facilitate nitrogen fixation in the soil (García 2019).

The organic carbon content in the soil (Figure 2D) is generally low. Significant differences were found at five of the nine sampling points, with Crust soils exhibiting significantly higher organic carbon content. Additionally, Figure 2H indicates that the organic carbon content in Crust soils is 27.4% higher compared to Non-Crust soils, though this difference is not statistically significant. Studies by Kakeh et al. (2020) and Plata (2019) also, report higher amounts of organic carbon in soils with BSC. Nuñez (2013) studied three different types of BSC and similarly found higher organic carbon levels in soils with BSC. This is supported by Ayala et al. (2018), which affirms that BSCs provide valuable environmental services through carbon sequestration.

Urease enzyme activity (Figure 3A) shows significant differences at four of the nine sampling points, with two points exhibiting higher activity in Crust soils and two in Non-Crust soils. On average (Figure 3D), Crust soils show an 8.5% increase in urease activity compared to Non-Crust soils; however, this difference is not statistically significant. Sun et al. (2020) reported higher enzyme activity in BSC soils compared to Non-Crust soils, though the differences were not significant. In contrast, Xu et al. (2022) found a significant increase in urease activity in BSC soils compared to Non-Crust soils, with a more pronounced effect in hostile environments. Urease activity is highly site-dependent and influenced by factors such as organic carbon content and soil moisture (Rodríguez and Merchancano 2018).

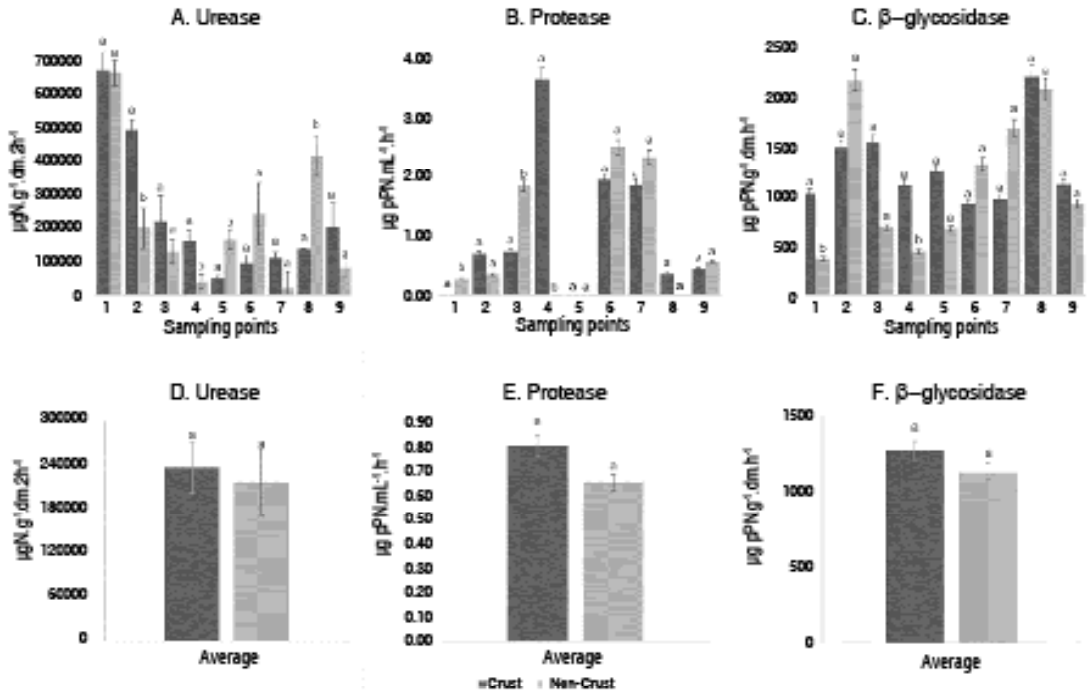

Figure 3. Results of the enzymatic activity variables by sampling points (1 to 9) and average. In graphs A, B, and C, soils with and without crust are compared individually, while graphs D, E, and F show comparisons with the average of soils with and without crust. Significant differences are indicated above the bars with letters a-b when a significant difference is present and a-a when there is no significant difference, using $P \geq 0.05$.

The enzymatic activity of protease (Figure 3B) showed no significant differences at six of the nine sampling points. Among those with significant differences, only one of the three points exhibited higher enzymatic activity in Crust soils. Additionally, Figure 3E shows that protease activity is 18.7% higher in Crust soils compared to Non-Crust soils; however, this difference is not statistically significant. These results indicate that BSCs did not have a significant impact on protease enzymatic activity.

The enzymatic activity of β-glucosidase (Figure 3C) showed significant differences at only two of the nine sampling points, with higher enzymatic activity in Crust soils at both points. On average (Figure 3F), β-glucosidase activity in Crust soils was 11.1% higher compared to that in Non-Crust soils, though this difference was not statistically significant. Miralles et al. (2012) reported significantly higher β-glucosidase activity in soils with BSC. Similarly, Xu et al. (2022) observed a 48.4% increase in β-glucosidase activity in BSC soils, demonstrating a significant difference compared to Non-Crust soils. β-glucosidase activity is strongly associated with organic carbon content (Orellana 2019), which aligns with the results showing higher organic carbon in Crust soils (Figure 2D).

The results obtained for nitrogen-fixing bacteria (Figure 4A) reveal four significant differences out of the nine sampling points, with all significant differences showing higher counts in Crust soils compared to Non-Crust soils. Additionally, on average (Figure 4D), the number of colony-forming units in Crust soils is 41.9% higher than in Non-Crust soils, with this difference being statistically significant. Zhao et al. (2019) found a correlation with the results obtained in this study, demonstrating a higher presence of nitrogen-fixing bacteria in soils with Biological Soil Crust (BSC). The presence of BSC may promote the growth of nitrogen-fixing bacteria due to the presence of aerobic and microaerophilic bacteria that constitute the BSC (Castillo-Monroy and Maestre 2011). Furthermore, Huang et al. (2011) mention that microorganisms within BSCs function as diazotrophic communities. The dominant morphological group in BSCs whether cyanobacteria, mosses, or lichens

can influence their development and ecological functions. However, since no taxonomic identification was performed in this study, these remain as possible explanations rather than definitive conclusions.

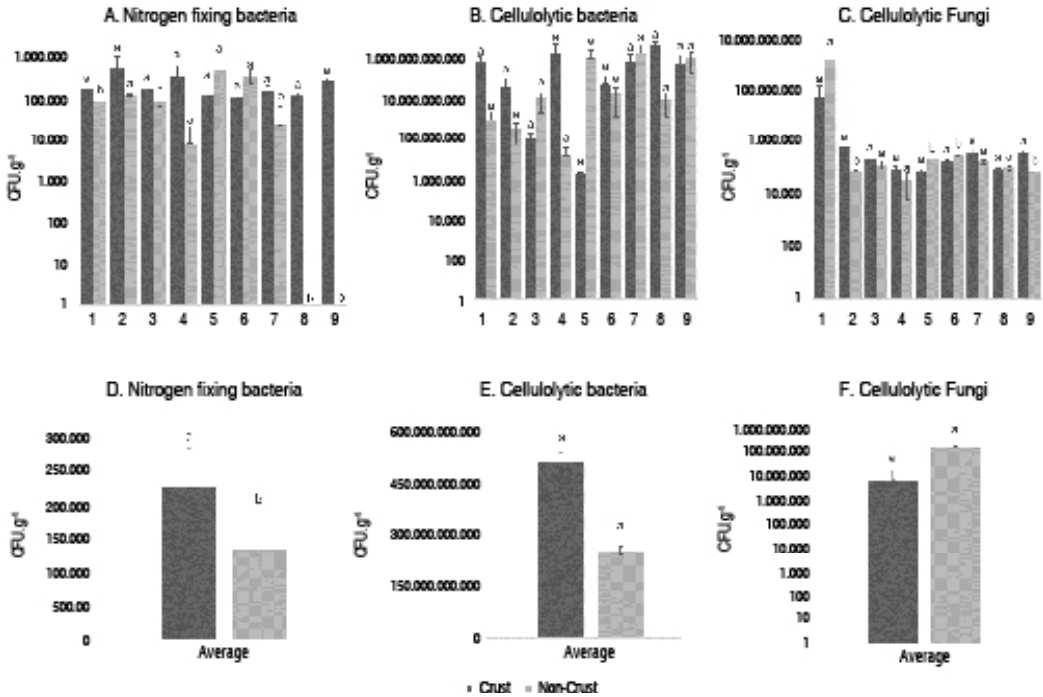

Figure 4. Results of the enumeration of microorganisms associated with carbon and nitrogen cycles by sampling points (from 1 to 9) and the average. In graphs A, B, and C, soils with and without crust are compared individually, while graphs D, E, and F are compared with the average of soils with and without crust. Significant differences are indicated above the bars with letters a-b when there is a significant difference and a-a when there is not, using a $P \geq 0.05$.

The results for cellulolytic bacteria at each sampling point did not show any significant differences (Figure 4B). On average (Figure 4E), cellulolytic bacteria in Crust soils were 50.5% more abundant than in Non-Crust soils, although this difference was not statistically significant. The abundance of cellulolytic fungi showed four significant differences out of the nine sampling points, with two of these differences being higher in Crust soils (Figure 4C) and the remaining two in Non-Crust soils. Conversely, the overall presence of cellulolytic fungi (Figure 4F) was 96% higher in Non-Crust soils than in Crust soils. Biological soil crusts did not significantly affect microorganisms involved in the carbon cycle. One possible explanation is that in extreme environments, microorganisms responsible for decomposing environmental cellulose are significantly reduced (Soares et al. 2012). Another possible explanation could relate to a study examining the contribution of microorganisms in BSCs over time, which shows greater bacterial diversity and abundance compared to fungi at certain times, suggesting that when bacterial populations are higher than fungal populations in BSCs, the crust might be relatively young (Zhao et al. 2019).

The principal component analysis (PCA) included the first three axes, which together explained 65.2% of the variance (Figures 5A and 5B). The PCA indicates a correlation among the variables of moisture, nitrogen percentage, and carbon. However, no clear trend is observed in the behavior of these variables between Crust and Non-Crust points, no single trend is observed. Similarly, Avellaneda et al. (2012) reported an inverse relationship between urease and protease, consistent with the present study (Figures 5A and 5B). The authors suggest that when urease is activated within the same microbial morphotype, protease remains inactive.

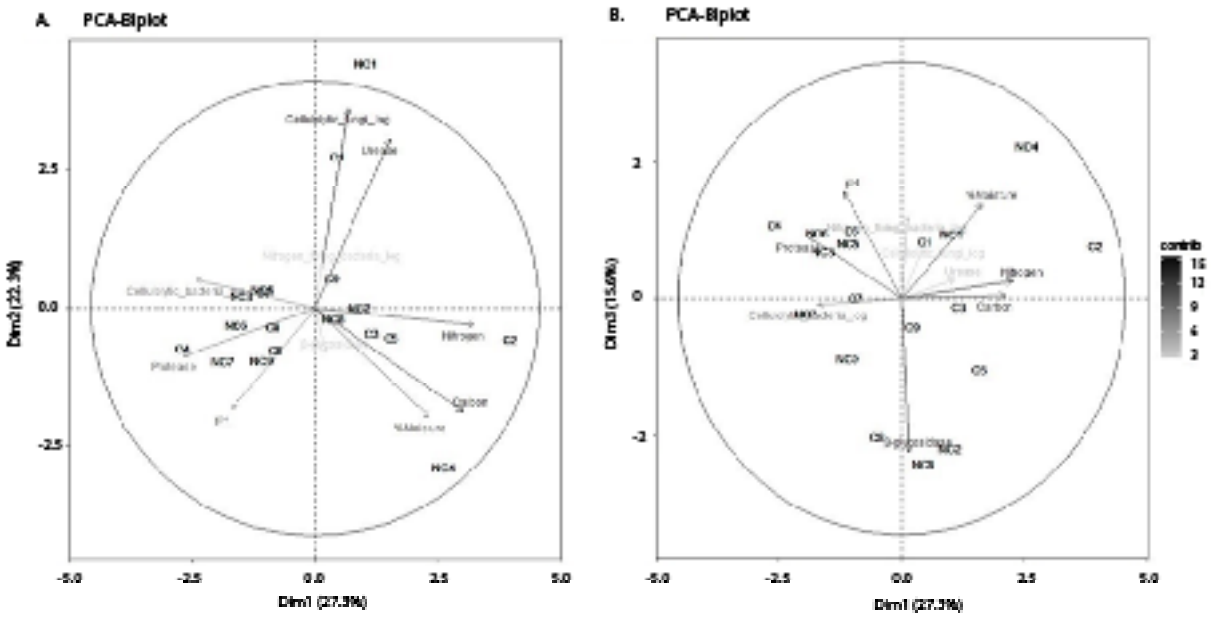

Figure 5. Principal Component Analysis (PCA). The letters C and NC denote soil samples with and without crust, respectively. The numbers preceding C and NC refer to the sampling points. Graph A displays the analysis of Axes 1 and 2, while Graph B shows the analysis of Axes 1 and 3.

When analyzing the overall data for physicochemical variables (Figures 2D to 2H), enzymatic activities (Figures 3D to 3F), and microorganisms (Figures 4D to 4F) in relation to soil quality in Crust and Non-Crust samples it was observed that, although only the nitrogen-fixing bacteria showed a significant individual result (Figure 4A) and an average increase (Figure 4D) in Crust soils, there was a general trend indicating an increase in total nitrogen, organic carbon, urease, and β-glucosidase in Crust soils compared to Non-Crust soils. This suggests that biological soil crusts (BSCs) contribute properties that enhance soil fertility, conservation, and restoration, as discussed in review articles by García (2019) and Castillo-Monroy et al. (2011). These studies highlight that BSC significantly contributes to nitrogen fixation in arid and semi-arid ecosystems, similar to the conditions of the present study, and that BSCs in hot deserts (>25°C) tend to be more efficient than those in cold climates. Recent studies by Gorji et al. (2021) corroborate the findings of this study, reinforcing the importance of BSC in arid ecosystems for soil fertility.

CONCLUSION

The results indicate that soils with biological soil crusts (BSC) exhibit significant ecological benefits. Moisture levels were significantly higher in BSC soils at five out of nine sampling points, suggesting enhanced water retention. In terms of pH, four samples showed significant differences, with three indicating lower values in soils with BSC. Total nitrogen tended to be higher in soils with BSC, as three out of four significant differences pointed to increased nitrogen content, accompanied by a notably greater abundance of nitrogen-fixing bacteria compared to soils without crust. Although organic carbon content displayed an upward trend in five of the nine sampling points, these differences were not statistically significant. Additionally, enzymatic activities—specifically urease and β-glucosidase—were elevated in BSC soils, further suggesting a positive impact on soil quality.

These findings demonstrate that the evaluated BSC possesses beneficial properties for soils in extreme, vegetation-sparse, and erosion-affected environments, underscoring its potential for soil recovery and protection in degraded landscapes. To gain a broader understanding of BSC behavior, it is recommended to extend this research to diverse environmental conditions across Colombia and Latin America. Future studies should also monitor factors such as crust age, conservation status,

and soil depth variations, while expanding the analysis of associated microbial diversity.

CONFLICT OF INTERESTS

The authors declare that they have no known competing financial interests or personal relationships that could have appeared to influence the work reported in this paper.

REFERENCES

Avellaneda LM, León T, Castro EG and Rojas ET (2020) Potato cultivation and livestock effects on microorganism functional groups in soils from the neotropical high andean Páramo. Revista Brasileira de Ciência do Solo 44. https://doi.org/10.36783/18069657RBCS20190122

Avellaneda LM, León TE and Torres E (2018) Impact of potato cultivation and cattle farming on physicochemical parameters and enzymatic activities of Neotropical high Andean Páramo ecosystem soils. Science of The Total Environment 631–632: 1600–1610. https://doi.org/10.1016/J.SCITOTENV.2018.03.137

Avellaneda LM, Muñoz LMM, Cuenca CE and Nieves JS (2012) Actividades Enzimáticas en Consorcios Bacterianos de Suelos Bajo Cultivo de Papa con Manejo Convencional y Bajo Pastizal. Revista Facultad Nacional de Agronomía Medellín 65: 6349–6360. http://www.scielo.org.co/pdf/rfnam/v65n1/v65n1a06.pdf

Ayala F, Maya Y and Troyo E (2018) Carbon storage and flux in arid soils as an environmental service: An example in northwestern Mexico. Terra Latinoamericana 36: 93–104. https://doi.org/10.28940/TERRA.V36I2.334

Belnap J (2002) Nitrogen fixation in biological soil crusts from southeast Utah, USA. Biol Fertil Soils 35: 128–135. https://doi.org/10.1007/S00374-002-0452-X

Belnap J and Lange OL (2003) Biological Soil Crusts: Structure, Function, and Management. Springer Berlin Heidelberg, Berlin, Heidelberg

Castillo-Monroy AP, Bowker MA, Maestre FT et al (2011) Relationships between biological soil crusts, bacterial diversity and abundance, and ecosystem functioning: Insights from a semi-arid Mediterranean environment. Journal of Vegetation Science 22: 165–174. https://doi.org/10.1111/J.1654-1103.2010.01236.X

Castillo-Monroy AP and Maestre FT (2011) La costra biológica del suelo: Avances recientes en el conocimiento de su estructura y función ecológica. Revista Chilena de Historia Natural 84: 1–21. https://doi.org/10.4067/S0716-078X2011000100001

Cerdà A (1998) Influencias de las costras biológicas en el comportamiento hidrológico y erosivo de los suelos en los cordones dunares de Nizzana, Desierto del Negev, Israel. Universidad de Extremadura Servicio de Publicaciones. http://hdl.handle.net/10662/712

Fox J and Weisberg S (2019) An R Companion to Applied Regression, 3°. SAGE Publications, Inc.

García CV (2019) La Costra Biológica del Suelo (CBS) como nuevo ecosistema. Universidad Complutense.

García V, Aranibar J and Villagra P (2021) Propagación de distintos tipos funcionales de la costra biológica del suelo del desierto del Monte, Argentina. Ecología Austral 31: 1–16. http://doi.org/10.25260/EA.21.31.1.0.1158

Gorji M, Bakhosh M, Sohrabi M and Pourbabaei AA (2021) Assessing the Function of Biological Soil Crusts on Soil Fertility (Case Study: Kiamaky Wildlife Refuge, East Azerbaijan, Iran). Eurasian Soil Science 54: 409–416. https://doi.org/10.1134/S1064229321030054

Huang LN, Tang FZ, Song YS et al (2011) Biodiversity, abundance, and activity of nitrogen-fixing bacteria during primary succession on a copper mine tailings. FEMS Microbiol Ecol 78: 439–450. https://doi.org/10.1111/J.1574-6941.2011.01178.X

IGAC (2017) Mapas de Suelos del Territorio Colombiano a escala 1:100.000. Departamento: Boyaca

IGAC (2006) Métodos analíticos del laboratorio de suelos, 6a edn. Instituto Geografico Agustin Codazzi, Bogotá

Kakeh J, Gorji M, Mohammadi MH et al (2020) Biological soil crusts determine soil properties and salt dynamics under arid climatic condition in Qara Qir, Iran. Science of The Total Environment 732: 139168. https://doi.org/10.1016/J.SCITOTENV.2020.139168

Kakeh J, Gorji M, Sohrabi M et al (2018) Effects of biological soil crusts on some physicochemical characteristics of rangeland soils of Alagol, Turkmen Sahra, NE Iran. Soil Tillage Research 181: 152–159. https://doi.org/10.1016/J.STILL.2018.04.007

Lê S, Josse J and Husson F (2008) FactoMineR: An R package for multivariate analysis. Journal of Statistical Software 25: 1–18. https://doi.org/10.18637/JSS.V025.I01

Lozano J (2011) Evaluación del proceso de desertificación en la micro cuenca quebrada La Fundación de la Parroquia Aguedo Felipe Alvarado, municipio Iribarren, Estado Lara. IV Simposio: Humedales, Crisis Climatica y Conservación.

Miralles I, Domingo F, Cantón Y et al (2012) Hydrolase enzyme activities in a successional gradient of biological soil crusts in arid and semi-arid zones. Soil Biology and Biochemistry 53: 124–132. https://doi.org/10.1016/J.SOILBIO.2012.05.016

Molina V, Pando M, Marmolejo J and Alanís E (2014) Diversidad de costras biológicas del suelo en pastizales halófilos del norte de México. Revista Iberoamericana de Ciencias 1: 83–91

Navas AL, Herrera M, Martínez EE and Fernández MC (2021) Influencia de las costras biológicas del suelo en la infiltración y retención de humedad en diferentes texturas de suelo. Multequina 30: 17–30.

Nuñez F (2013) Composición de las costras microbióticas y su influencia en algunas propiedades del suelo en una zona semiárida. Revista de Investigación (Guadalajara) 37: 91–116. https://ve.scielo.org/scielo.php?script=sci_arttext&pid=S1010-29142013000300006&lng=es&tlng=es

Orellana M (2019) Efecto de las labranzas y niveles de fertilización sobre la actividad enzimática en un suelo agrícola. Universidad Central del Ecuador. http://www.dspace.uce.edu.ec/handle/25000/19159

Pacheco M and Giselle K (2016) Prácticas agropecuarias coloniales y degradación del suelo en el Valle de Saquencipá, Provincia de Tunja, siglos xvi y xvii. Universidad Nacional de Colombia. https://repositorio.unal.edu.co/handle/unal/9982

Pinzón M and Linares E (2006) Diversidad De Líquenes y Briofitos En La Region Subxerofitica De La Herrera, Mosquera (Cundinamarca-Colombia). I. Riqueza Y Estructura. Caldasia 28: 243–257. http://www.scielo.org.co/scielo.php?script=sci_arttext&pid=S0366-52322006000200008

Plata J (2019) Influencia de la biocostra del suelo en el balance de Carbono y Nitrógeno en un ecosistema árido - Repositorio Institucional Uanl. Universidad Autónoma de Nuevo León Facultad de Ciencias Forestales. http://eprints.uanl.mx/21387/1/1080313997.pdf

Rennie RJ (1981) A single medium for the isolation of acetylene-reducing (dinitrogen-fixing) bacteria from soils.Canadian Journal of Microbiology 27: 8–14. https://doi.org/10.1139/M81-002

Rodríguez D and Merchancano J (2018) Evaluación de la actividad enzimática del suelo en un sistema de producción ganadero con diferentes usos de suelo en Pasto, Colombia. Universidad de Nariño. https://sired.udenar.edu.co/5458/

Romero A (2019) Funciones ecosistémicas y atributos ecológicos de las costras biológicas en el centro-oeste de la Argentina. Universidad Nacional de Cuyo. http://hdl.handle.net/11336/86060

Romero A, Martinez E and Herrera M (2021) Restauración de costras biológicas del suelo: pasado, presente y futuro. Multequina 30.

Soares FL, Melo IS, Dias ACF and Andreote FD (2012) Cellulolytic bacteria from soils in harsh environments. World Journal of Microbiology and Biotechnology 28: 2195–2203. https://doi.org/10.1007/S11274-012-1025-2

Sun Y, Feng W, Zhang Y et al (2020) Effects of biological soil crusts on soil enzyme activities of *Artemisia ordosica* community in the Mu Us Desert of northwestern China. Journal of Beijing Forestry University 42: 82–90. https://doi.org/10.12171/J.1000-1522.20190082

Sundara WVB and Paul NB (1971) Phosphate-dissolving bacteria in the rhizosphere of some cultivated legumes. Plant Soil 35: 127–132. https://doi.org/10.1007/BF01372637

Thomas AD, Hoon SR and Linton PE (2008) Carbon dioxide fluxes from cyanobacteria crusted soils in the Kalahari. Applied Soil Ecology 39: 254–263. https://doi.org/10.1016/J.APSOIL.2007.12.015

Toledo VF (2012) Evaluación de las propiedades biológicas y bioquímicas de la costra microbiótica de un suelo bajo vegetación natural en la región árida de Quíbor, Venezuela - Dialnet. Revista de Investigación (Guadalajara) 36: 143–162. https://ve.scielo.org/pdf/ri/v36n75/art09.pdf

Wu Y, Rao B, Wu P et al (2013) Development of artificially induced biological soil crusts in fields and their effects on top soil. Plant and Soil 2013 370:1 370: 115–124. https://doi.org/10.1007/S11104-013-1611-6

Xu H, Zhang Y, Shao X and Liu N (2022) Soil nitrogen and climate drive the positive effect of biological soil crusts on soil organic carbon sequestration in drylands: A Meta-analysis. Science of The Total Environment 803: 150030. https://doi.org/10.1016/J.SCITOTENV.2021.150030

Zhao L, Liu Y, Wang Z et al (2019) Bacteria and fungi differentially contribute to carbon and nitrogen cycles during biological soil crust succession in arid ecosystems. Plant and Soil 2019 447: 1 447:379–392. https://doi.org/10.1007/S11104-019-04391-5

Zhou X, Zhao Y, Belnap J et al (2020) Practices of biological soil crust rehabilitation in China: experiences and challenges. Restoration Ecology 28: S45–S55. https://doi.org/10.1111/REC.13148

Research article

https://revistas.unal.edu.co/index.php/refame

Revista Facultad Nacional de Agronomía

Physical and mechanical properties of cross-laminated timber made from *Pinus tecunumanii* wood

Propiedades físicas y mecánica de madera contralaminada fabricada con *Pinus tecunumanii*

https://doi.org/10.15446/rfnam.v78n2.114727

Jhon F. Herrera-Builes[1]*, Juan C. Sierra[1] and Rodolfo Parra[1]

ABSTRACT

Timber from forest plantations is of great relevance to be used as a substitute for timber from natural forests; thus, reducing pressure on them and in such a way indiscriminate felling. Alternative building materials, like cross-laminated timber (CLT), are being sought in the world. In Colombia, the CLT production is not well-studied; thus, this investigation characterized the physical and mechanical behavior of cross-laminated timber (CLT) in three layers made with *Pinus tecunumanii* wood manufactured by Finger Joint and wood plank systems. In each of the CLTs, density, modulus of elasticity and modulus of rupture in static bending were evaluated. Both manufacturing systems produced CLTs with an air-dry medium density and low resistance to static bending. The CLT made with finger joints showed low elasticity, while the CLT made with a solid wood planks system showed medium elasticity. The results of this study, with wood match material *Pinus tecunumanii* showed higher values than those reported for other woods. Future studies should focus on determining changes in the physical and mechanical properties of CLT with quality-rated wood.

Keywords:
Bending static
Density
Finger joint
Wood planks

RESUMEN

Las maderas procedentes de plantaciones forestales son de gran relevancia para ser utilizadas como reemplazos de las procedentes de bosques naturales; con lo cual se disminuye la presión sobre los mismos y de esta forma la tala indiscriminada. En el mundo se están buscando materiales alternativos para la construcción, como es el caso de la madera contralaminada o CLT. En Colombia se encuentran pocos estudios donde se referencien la producción de CLT; por ello, el presente estudio caracterizó el comportamiento físico y mecánico de CLT en 3 capas fabricados con el sistema de Finger Joint y con tablones de madera maciza de *Pinus tecunumanii*. En cada uno de los CLT fueron evaluadas su densidad, módulo de elasticidad y módulo de rotura a la flexión estática, los CLT fabricados por ambos sistemas de fabricación presentaron una mediana densidad seca al aire; además, ambos presentan baja resistencia a la flexión estática; los CLT fabricados con el sistema de Finger Joint presentaron una baja elasticidad y con el sistema con tablones de madera maciza presentaron una mediana elasticidad. Los resultados arrojados en este estudio con material de partido de la madera *Pinus tecunumanii* son mayores a los resultados reportados para otras maderas. Los estudios futuros deben centrarse en determinar los cambios en las propiedades físicas y mecánicas de CLTs con madera con clasificación de calidad.

Palabras clave:
Flexion estática
Densidad
Finger joint
Tablones de madera

[1]Facultad de Ciencias Agrarias, Universidad Nacional de Colombia, Sede Medellín, Colombia. jfherrer@unal.edu.co, jcsierram@unal.edu.co, rhparra@unal.edu.co
*Corresponding author

Received: January 30, 2025; Accepted: April 5, 2025
Rev. Fac. Nac. Agron. Medellín 78(2): 11161-11168. 2025
ISSN 0304-2847 / e-ISSN 2248-7026

CC BY NC SA

The *Pinus tecunumanii* (Schw.) Eguiluz and Perry, is mainly found in Central America and Chiapas, Mexico. It is a remarkable species that frequently can reach 55 meters in height, and the first 30 meters of the trunk are free of lateral branches. It has a very straight stem form (Dvorak and Donahue 1992). Smaller quantities of *P. tecunumanii* are used in plantations, but it is an important plantation species in Colombia and it has acquired importance in Brazil and southern Africa (Dvorak et al. 2000). The mechanical properties of wood make it an efficient option for structural applications in construction (Ramage et al. 2017). Wood constructions are less vulnerable to damage than concrete or brick constructions because they have more flexible material that can better absorb the vibrations of an earthquake (Saxena et al. 2022). The use of wood as a construction material is on the rise in certain countries worldwide, particularly in Europe and Asia. Although wood does not grow as quickly as other materials, it still has other advantages that make it attractive (Heard et al. 2012).

In the early 1990's a new wood product known as Cross-Laminated Timber (CLT) was developed and patented. It is a wood engineering product that consists of an odd number of layers (usually three, five or seven) made of glued sawn timber, where each layer is made up of boards/lamellas placed adjacent to each other, and where the neighboring layers are most often glued at an angle of 90° with each other. As a result, the CLT panels provide high stiffness and strength both in-plane and out of plane (Jele et al. 2018; Fabrizio et al. 2023).

In recent years, the trend for wood materials and building systems has been influenced by the development of CLT. The current trend is to develop new wood products and timber construction systems, which can be optimized for structural use. The use of cross-laminated timber is common in high-demand structural buildings and multi-storey buildings in Europe, Canada, and the USA. In addition, it is a material of low energy consumption and is particularly noted for its exceptional insulation properties, reduced heat transmission and it is an architectural beauty (Ferk 2013; Brandner 2013). The cross laminated timber is competitive and attractive because it is a lighter laminated structure than steel and concrete, allows building elements up to 40 m in length, high chemical resistance to acidic or alkaline environments, a certain tolerance of exposure to fire, greater dimensional stability with respect to solid wood, and optimization of the available resource, among other advantages (Olsson et al. 2025).

Despite important advances in the field of engineering and sustainable building materials, there is no specific information about CLT production in Colombia right now, or on buildings using this material as a structural component. This gap in research and construction practices creates a unique opportunity to explore the potential of this material in the country. CLT, an innovative and increasingly globally applied material, has proven to be an efficient and sustainable alternative to traditional materials such as steel and concrete in architecture and building.

The importance of this study lies in its potential to promote the use of timber from forest plantations as a renewable raw material for the manufacture of non-traditional products in construction, opening new opportunities for the Colombian forestry and construction. This type of research not only contributes to sustainable building practices but can help diversify the use of forest resources and encourage the use of natural materials and their advantages.

Therefore, this work aimed to characterize the physical behavior of density and mechanical static bending of CLT boards made from *Pinus tecunumanii*, to promote its use as an efficient and environmentally friendly alternative in building construction and other structures in Colombia. This study will not only contribute to the development of new non-traditional products, but also strengthen research and technology applied to the country's forestry and construction sectors.

MATERIALS AND METHODS

Materials

Unsawn timber of 22x90x2000 mm (thickness, width, and length, respectively) and wooden lamellas with Finger Joint of 22x60x650 m (thickness, width, and length, respectively) from *Pinus tecunumanii* wood were used. The Company Cipreses de Colombia SA provided the wood, from mature trees (25 years old) collected from plantations located in the municipality of Yolombó (Antioquia, Colombia).

Manufacture of the CLT panels

It was used Polyvinyl alcohol (PVA) adhesive, a water-soluble synthetic polymer used in a variety of applications,

with a density around 1.19 g cm^{-3}, pH in the range of 6.0 to 7.0, making it generally neutral or slightly acidic; resin content usually from 40 to 60% weight. The rate of application was 200 g m^{-2} on one side of the piece of wood. Pressing was carried out at 8.0 MPa for 60 min. In total, 12 three-layer CLT panels were manufactured; six boards with a Finger Joint system (Figure 1) and six with solid wood plank system (Figure 2). Each board sizes up to 240 mm wide x 1,800 mm length and a final thickness of 60 mm (EN 16351). The wood board samples were not organized or oriented in a specific radial, or tangential way. Instead, the tables were joined at random, as can be seen in Figures 1 and 2, where the arrangement is observed without a definite pattern. In addition, in Colombia there is no established standards for the visual structural classification of wood, which prevented such activity.

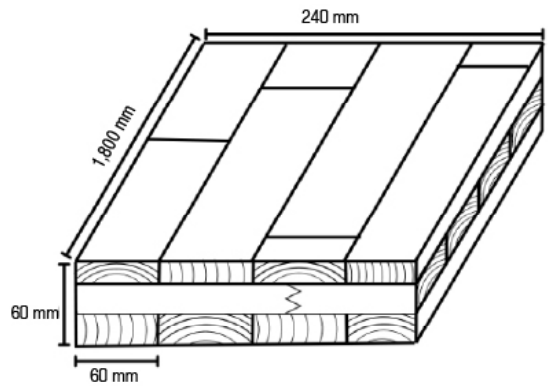

Figure 1. Cross-laminated timber CLT made with Finger Joint.

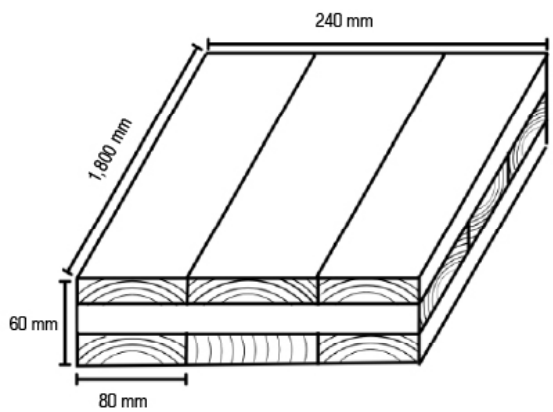

Figure 2. Cross-laminated timber CLT manufactured with solid wood planks.

Evaluation of properties

The properties evaluated in each of the panels were density, modulus of elasticity and modulus of rupture following the method of the UNE-EN 408 standard (UNE 2011). It was performed with a random positional sampling on each CLT panel. Tests were performed using a load frame with a 40,000 kg capacity and a data processor Unitronics (Figure 3).

Figure 3. Loading frame capacity 40,000 kg and data processor Unitronics.

Data analysis

The statistical analysis was performed using a completely randomized design for each test. The information was processed based on the methodology described by Hoshmand (2006).

RESULTS AND DISCUSSION

The results appearing in each box are represented as follows.

$$\bar{y} \quad \pm \quad q$$
$$CVt$$

Where $\bar{y}$ is the Mean; ± q is the 95% Confidence Interval, and CVt is the total coefficient of variation.

CLT Density

The results of the air-dry densities obtained for (CLT) panels made with *Pinus tecunumanii* wood with the Finger Joint and solid wood planks systems are presented in Table 1.

The results of air-dry densities obtained for CLT panels made from *Pinus tecunumanii* wood using two different manufacturing systems, the solid wood planks, and the Finger Joint systems are presented. These results are crucial to assessing the suitability of this species for the manufacture of CLT panels, a material that is increasingly used in construction due to its mechanical and physical properties. As shown in Table 1, the dry density values obtained for CLT panels manufactured with both systems

Table 1. Air-dry density of (CLT) panels made with *Pinus tecunumanii* wood and produced with solid wood planks and Finger Joint systems.

Production system	Density (kg m^{-3})
Solid wood planks	626.05±43.95 to 6.69%
Finger Joint	679.03±56.40 to 7.91%

The same letters in the columns indicate no significant difference, according to Tukey's test ($P \leq 0.05$).

were 626.05 kg m^{-3} for panels produced with the solid wood planks system and 679.03 kg m^{-3} for those manufactured with the Finger Joint system. Both values are in the middle density range, which according to ASTM classification is between 510 and 750 kg m^{-3}, suggesting that *Pinus tecunumanii* CLT panels may be a viable alternative for structural applications. The average densities obtained for the panels with the solid wood planks system and with the Finger Joint system revealed that there was not significant difference (Table 2), indicating that both manufacturing methods result in materials with similar density characteristics. This is relevant as it suggests

that regardless of the manufacturing system used, a material with density characteristics that meets ASTM requirements for the manufacture of medium-density CLTs can be obtained.

Table 2. Analysis of variance for the air-dry density of CLT panels made from *Pinus tecunumanii* wood.

Source	Sum of squares	Df	Mean square	Ratio-F	*P*-value
Between groups	8418.21	1	8418.21	3.63	0.0860
Within groups	23210.5	10	23210.5	-	-
Total (Corrected)	31628.7	11	-	-	-

It is important to note that density is a key parameter in determining the mechanical and physical properties of CLT. The density of a material is directly related to its strength and stiffness, which affects how well cross-laminated timber (CLT) can support structural loads. In this study, the density values obtained for *Pinus tecunumanii* were higher than those reported in other studies conducted with different species of pine, such as *Pinus taeda*, *Pinus elliottii, Pinus radiata, Pinus echinata, Pinus ponderosa*, and *Pinus sylvestris* with density values ranged from 360 to 500 kg m^{-3} for CLT (Godoy et al. 2017; Baño et al. 2018; Glasner et al. 2023; Brandner et al. 2024). This difference could reflect the inherent properties of *Pinus tecunumanii* wood, which has a higher density and therefore could provide a higher quality material for construction.

Mechanical properties

The results of the mechanical characterization for the static bending of CLT panels made of *Pinus tecunumanii* wood, using the Finger Joint and solid wood planks systems, are presented in Table 3. This characterization is essential to evaluate the behavior of CLT panels under bending loads and determine their suitability for structural applications. Both the modulus of rupture (MOR) and the modulus of elasticity (MOE) of panels manufactured with both systems were evaluated. The values obtained for MOR and MOE are indicative of the strength and stiffness of the panels, two key factors for their use in the construction of structural elements.

For panels manufactured with the solid wood planks system, the MOR was significantly higher than that of panels produced with the Finger Joint system, reflecting a greater resistance to static bending in the first system evaluated. This is due to the continuity of wood fiber in solid planks, which contributes to greater structural strength. On the other hand, panels manufactured with the Finger Joint system showed a lower MOE value, which implies a lower stiffness under load.

Table 3. Mechanical resistance to static bending of the CLT panels from *Pinus tecunumanii* wood manufactured with solid wood planks and Finger-Joint methods.

Manufacture method	Modulus of rupture (MOR) MPa	Modulus of elasticity (MOE) MPa
Solid wood planks	41.59±7.08[a] 16.22%	13454.9±2051.89[a] 14.53%
Finger Joint	29.82±11.00[b] 31.15%	9081.86±2914.91[b] 30.58%

Equal letters in the columns indicate no significant difference, according to Tukey's multiple range test ($P \leq 0.05$).

In particular, panels manufactured with the Finger Joint system showed a MOR of 29.82 MPa, which is below the minimum limit recommended by ASTM (39 MPa). This value reflects a very low resistance compared to the requirements for more rigorous structural applications. For the boards manufactured with the Solid wood planks system they showed a higher MOR of 41.59 MPa. In addition, both manufacturing systems presented different values of MOR, with statistically significant differences between them (Table 4), which suggests that

the Solid wood planks system offers a higher strength compared to the Finger Joint system. Comparing these results with those reported for other species of the same genus, such as *Pinus radiata*, *Pinus taeda*, *Pinus echinata* and *Pinus silvesrtis*, the values obtained for *Pinus tecunumanii* were higher than those obtained for CLT manufactured with these species, with a reported MOR between 20-30 MPa (Godoy et al. 2017; Baño et al. 2018; Li et al. 2021; Glasner et al. 2023; Olsson et al. 2025).

Table 4. Analysis of variance for the modulus of rupture to static bending of CLT panels made of *Pinus tecunumanii* wood.

Source	Sum of squares	Df	Mean square	F- ratio	*P*-value
Between groups	415.711	1	415.711	5.35	0.0433
Within groups	777.409	10	777.409	-	-
Total (Corrected)	1193.12	11	-	-	-

Tukey test for modulus of rupture to static bending MPa.

	Cases	Mean	Homogeneous groups
Cross-laminated timber Finger Joint	6	29.8216	X
Cross-laminated timber solid wood planks	6	41.5932	X
Contrast	**Sig.**	**Difference**	**+/- Limits**
Cross-laminated timber Finger Joint - Cross-laminated timber solid wood planks	*	-11,3716	11,3425

* Indicate a significant difference.

The results obtained for the MOE in static bending of CLT panels manufactured with *Pinus tecunumanii* show significant differences between the two manufacturing systems evaluated (Table 5); for the Finger Joint system, the MOE was 9081.86 MPa, with a confidence interval between 6,962 and 9,807 MPa; this value is classified as low according to the standards established by ASTM, which consider a minimum MOE of 10,000 MPa for structural woods in more demanding applications. On the other hand, panels manufactured with the solid wood

Table 5. Analysis of variance for the modulus of elasticity to static bending of CLT panels made of *Pinus tecunumanii* wood.

Source	Sum of squares	Df	Mean square	F- ratio	*P*-value
Between groups	$5{,}73705 \times 10^{7}$	1	5,73705	9.94	0.0103
Within groups	$5{,}76897 \times 10^{7}$	10	5,76897	-	-
Total (Corrected)	$1{,}1506 \times 10^{8}$	11	-	-	-

Tukey test for modulus of elasticity to static bending MPa.

	Cases	Mean	Homogeneous groups
Cross-laminated timber Finger Joint	6	9081.86	X
Cross-laminated timber solid wood planks	6	13,454.9	X
Contrast	**Sig.**	**Difference**	**+/- Limits**
Cross-laminated timber Finger Joint - Cross-laminated timber solid wood planks	*	-14,373.04	3089.81

* Indicate a significant difference.

planks system presented an MOE of 13,454.9 MPa, with a confidence interval between 9,904 and 14,710 MPa; this value is classified as medium strength according to ASTM standards. These statistical differences between the two manufacturing systems were significant, indicating that the solid wood plank system offers greater rigidity compared to the Finger Joint system. This difference could be related to the fiber continuity in panels made of solid wood planks, which provide greater resistance to bending and better load distribution. Compared to CLT boards made from other species, such as *Pinus ellioti*, *Pinus radiata* and *Pinus taeda*, the values obtained for *Pinus tecunumanii* were higher. According to previous studies by Godoy et al. (2017), Baño et al. (2018) and Li et al. (2021), the CLT panels of these species had MOE values in the range of 6,000-8,000 MPa, which are lower than the results obtained in this study for *Pinus tecunumanii*. On the other hand, for *Pinus sylvestris* wood, results were similar, according to Olsson et al. (2025).

CONCLUSION

CLT boards made of *Pinus tecunumanii* wood are promising, as they suggest that this species can offer a suitable material for the manufacture of CLT in construction, using the two processing systems studied. In relation to dry air density, CLT boards manufactured with *Pinus tecunumanii* exhibit characteristics that meet the standards required for structural applications. The similarity between the values obtained for both manufacturing systems indicates that the choice of system does not significantly affect the density of the boards. Manufacturing systems have a direct impact on the mechanical properties of CLT panels. While both systems showed acceptable values for CLT manufacturing, the solid wood planks system presented advantages in terms of static bending strength, which could make it more suitable for applications where a higher load capacity is required. However, the Finger Joint system may be a viable option for optimizing wood use and maintaining a good strength-to-weight ratio. The values obtained for *Pinus tecunumanii* were higher than those reported for other species, such *as Pinus ellioti*, *Pinus radiata* and *Pinus taeda*, suggesting that this species has considerable potential for structural applications, especially if its properties are optimized through improvement techniques. Finally, it is recommended to carry out additional studies on sheare failure rate, surface quality, and compression parallel to fiber to obtain a more complete characterization of CLT boards manufactured with *Pinus tecunumanii*. Studies that improve the understanding of the mechanical behavior of these panels and their building applications.

ACKNOWLEDGMENTS

The authors wish to thank the company of Cipreses de Colombia S.A. for the donation of the wood material used and to the Laboratory of Forest Products “Héctor Anaya López” of the Universidad Nacional de Colombia, Medellín Headquarters and its staff for their support and collaboration.

REFERENCES

Baño V, Godoy D, Domenech L and Moya L (2018) Influencia de las clases resistentes del Pino Uruguayo en el diseño de paneles de madera contralaminada. En: XVI Encontro Brasileiro em Madeiras e em Estruturas de Madeira IBRAMEM. III Congresso Latino-americano de Estruturas de Madeira LaMEM, Escola de Engenharia de São Carlos EESC USP. São Carlos, Brasil.

Brandner R (2013) Production and technology of cross laminated timber (CLT): State-of-the-art-report. Pp. 3-36. In: Focus solid timber solutions - European Conference on cross laminated timber (CLT). University of Bath, Bath.

Brandner R, Ringhofer A and Sieder R (2024) Out-of-plane bending properties of cross laminated timber (CLT). Construction and Building Materials Volume 438 (9): 136991. https://doi.org/10.1016/j.conbuildmat.2024.136991

Dvorak W and Donahue J (1992) Twelve-year review of the CAMCORE Cooperative: 1980–1992. College of Forest Resources, North Carolina State University, Raleigh, NC, USA.

Dvorak W, Hodge G, Gutiérrez E, Osorio L, Malan F and Stanger T (2000) *Pinus tecunumanii*. pp. 188–209. In: Conservation & Testing of Tropical & Subtropical Forest Tree Species by the CAMCORE Cooperative, College of Natural Resources, North Carolina State University, Raleigh, NC, USA.

Fabrizio C, Sciomenta M, Spera L, De Santis Y, Pagliaro S, Di Egidio A and Fragiacomo M (2023) Experimental investigation and beam-theory-based analytical model of cross laminated timber panels buckling behavior. Archives of Civil and Mechanical Engineering 172(3). https://doi.org/10.1007/s43452-023-00713-8

Ferk H (2013) Some building science aspects for building with CLT. pp. 207-250. In: Focus solid timber solutions - European Conference on Cross Laminated Timber (CLT). University of Bath, Bath.

Glasner D, Ringhofer A, Brandner R and Schickhofer G (2023) Rolling shear strength of cross laminated timber (CLT)-Testing, evaluation, and design. Buildings 13: 2831. https://doi.org/10.3390/buildings13112831

Godoy D, Vega A and Baño V (2017) Characterization of cross

laminated timber made from wood of low-mechanical properties of *Pinus taeda* Elliottii. In: Clem + cimad II Congreso Latinoamericano de Estructuras de Maderas II Congreso Ibero – Latinoamericano de la Madera en la Construcción. Universidad Nacional Noroeste NNOBA, Buenos Aires, Argentina.

Heard R, Hendrickson C and McMichael F (2012) Sustainable development and physical infrastructure materials. MRS Bulletin 37(4): 389–394. https://doi.org/10.1557/mrs.2012.7

Hoshmand, R (2006) Design of experiments for agriculture and the natural sciences. Second edition. Chapman and Hall/CRC. https://doi.org/10.1201/9781315276021

Jele M, Varevac D and Raj V (2018) Cross-laminated timber (CLT) – a state-of-the-art report. Građevinar 70: 75-95. https://doi.org/10.14256/JCE.2071.2017

Li X, Ashraf M, Subhani M, Kremer P, Li H and Anwar-Us-Saadat M (2021) Rolling shear properties of cross-laminated timber (CLT) made from australian Radiata pine – An experimental study. Structures 33: 423–432. https://doi.org/10.1016/j.istruc.2021.04.067

Olsson A, Schirén W and Hu M (2025) Dynamic and quasi-static evaluation of stiffness properties of CLT: longitudinal MoE and effective rolling shear modulus. European Journal of Wood and Wood Products 83:16. https://doi.org/10.1007/s00107-024-02185-w

Ramage M, Burridge H, Busse-Wicher M, Fereday G, Reynolds T et al (2017) The wood from the trees: The use of timber in construction. Renewable and Sustainable Energy Reviews (68): 333–359. https://doi.org/10.1016/j.rser.2016.09.107

Saxena A, Buettner W, Kestler L and Kim Y (2022) Opportunities and barriers for wood-based infrastructure in urban Himalayas: A review of selected national policies of Nepal. Trees Forests and People 8 (March): 100244. https://doi.org/10.1016/j.tfp.2022.100244

UNE - Asociación Española de Normalización (2011) UNE-EN 408. Estructuras de madera. Madera aserrada y madera laminada encolada para uso estructural. Determinación de algunas propiedades físicas y mecánicas. Asociación Española de Normalización (UNE), Madrid, España.

Research article

https://revistas.unal.edu.co/index.php/refame

Revista Facultad Nacional de Agronomía

Survival and oviposition of *Tetranychus urticae* Koch (Acari: Tetranychiidae) under exposure to unfractionated botanical extracts

Supervivencia y oviposición de *Tetranychus urticae* Koch (Acari: Tetranychiidae) bajo exposición a extractos botánicos crudos

https://doi.org/10.15446/rfnam.v78n2.111419

Daniel Rodríguez[1]*, Fernando Cantor[1] and Ericsson Coy-Barrera[1]

Keywords:
Botanicals
Ornamental plants
Pest Control
Phytophagous mite

ABSTRACT

Chemically synthesized acaricides are widely used to control *Tetranychus urticae* Koch (Acari: Tetranychidae), a major agricultural pest that causes significant crop damage. However, the excessive use of synthetic acaricides has led to the emergence of resistant mite populations, complicating pest management. This challenge has driven the search for alternative strategies, including cultural and biological control, which have shown promise. Another potential alternative is botanical extracts, which may be effective even at sublethal doses. This study aimed to evaluate the effects of 10 botanical extracts on the mortality and oviposition of *Tetranychus urticae* adults under laboratory conditions. The extracts were tested at a single mean dose (0.06% w/v). The ethanol crude extract of *Nectandra amazonum* exhibited the highest corrected mortality (14.4%) at 96 hours. Significant oviposition alterations were observed throughout the bioassay, with notable effects at 24 and 96 hours (P<0.05). LC-MS analysis of the extracts identified 42 major compounds, including flavonoids, alkaloids, and terpenes, which are likely responsible for the observed effects. These findings indicate that the tested botanical extracts significantly affect *Tetranychus urticae* reproductive capacity, supporting their potential role in integrated pest management strategies.

Palabras clave:
Productos botánicos
Plantas ornamentales
Control de Plagas
Ácaro fitófago

RESUMEN

Aunque los acaricidas sintetizados químicamente han sido una estrategia ampliamente utilizada para controlar el ácaro *Tetranychus urticae* Koch (Acari: Tetranychidae), una plaga económicamente importante debido a su daño significativo causado en cultivos de flores y ornamentales, la utilización indiscriminada de acaricidas sintéticos ha generado poblaciones de ácaros resistentes a tratamientos químicos. Por lo tanto, el control de este fitófago parece ser más desafiante. Este hecho ha llevado a la búsqueda de otras estrategias, como el control cultural y biológico, que han demostrado ser prometedores. Otra alternativa potencial se basa en el uso de extractos botánicos, con efectos incluso a dosis subletales. El propósito de esta investigación fue evaluar el efecto de 10 extractos botánicos sobre la mortalidad y oviposición de *Tetranychus urticae* en condiciones de laboratorio. Los extractos se probaron con una dosis media única (0,06% p/v). La mayor mortalidad corregida (14,4%) fue obtenida con el extracto etanólico crudo de *Nectandra amazonum* a 96 horas. Así mismo, se observaron alteraciones principales en la oviposición a los diferentes tiempos a lo largo de la duración del bioensayo, que implicaron efectos significativamente diferentes después de 24 y 96 horas (P<0,05). El análisis de la composición química de los extractos mediante LC/MS reveló la presencia de 42 compuestos principales que incluyeron flavonoides, alcaloides y terpenos, que podrían ser responsables de los efectos observados en *Tetranychus urticae*. Los resultados indican que los extractos evaluados alteran la capacidad de reproducción de *Tetranychus urticae* como un efecto subletal relevante, que podría aprovecharse para controlar las poblaciones de este fitófago en combinación con otras estrategias de manejo de plagas.

[1]Facultad de Ciencias Básicas y Aplicadas, Universidad Militar Nueva Granada, Bogotá, Colombia. daniel.rodriguez@unimilitar.edu.co, fernando.cantor@unimilitar.edu.co , ericsson.coy@unimilitar.edu.co
*Corresponding author

Received: December 3, 2024; Accepted: March 10, 2025
Rev. Fac. Nac. Agron. Medellín 78(2): 11169-11180. 2025
ISSN 0304-2847 / e-ISSN 2248-7026

CC BY NC SA

Tetranychus urticae Koch (Acari: Tetranychiidae), commonly known as the red spider mite or two-spotted spider mite, is one of the most significant economic pests worldwide (Assouguem et al. 2022b). This phytophagous mite has a broad host range, including flower crops such as roses (Chacón-Hernández et al. 2020b), carnations (Chauhan et al. 2011), and chrysanthemums (Siebert et al. 2020), as well as fruit crops like citrus species (Assouguem et al. 2022a), strawberries, cucurbits, and vegetables such as tomatoes and beans (Assouguem et al. 2022b). Its feeding activity causes aesthetic and physiological damage, significantly reducing the commercial value of crops and their final products.

The red spider mite feeds on foliage, stems, and fruits by piercing plant tissues with its stylophore and sucking the sap, primarily from the undersides of leaves. This feeding behavior produces characteristic stippling on the upper leaf surface. The mite's life cycle consists of four stages: egg, larva, nymph (protonymph and deutonymph), and adult. Females lay eggs on the undersides of leaves, which hatch in approximately 6–7 days at an average temperature of 20 °C. The larvae, initially creamy-colored and lacking dorsal and ventral spots, develop into nymphs after 3 days. Under optimal conditions (21–25 °C and 55% relative humidity in greenhouses), *T. urticae* populations can rapidly increase and complete its life cycle (Daza Vallejos et al. 2010).

Despite the availability of various control strategies, chemically synthesized acaricides remain the most effective and widely used method for managing *T. urticae*. However, their excessive and indiscriminate use has led to the development of resistant mite populations, posing significant challenges for pest control. Synthetic acaricides such as chlorfenapyr, acequinocyl, and fenazaquin achieve nearly 100% efficacy by inhibiting mitochondrial respiration, disrupting growth, and exerting neurotoxic effects (Dekeyser 2005). Other compounds, including abamectins, hexythiazox, and propargite, exhibit high toxicity against the nymph and adult stages of *T. urticae* (Singh et al. 2017). However, prolonged exposure to these acaricides promotes the selection of resistant populations, further complicating pest management (Van Leeuwen et al. 2010).

Given the challenges posed by resistance development and the environmental and health concerns associated with synthetic acaricides, alternative management strategies are increasingly being explored. These approaches consider the biological characteristics of *T. urticae* and incorporate rotation schemes to enhance susceptibility to control measures (Sudo et al. 2018). Among these alternatives, plant-derived extracts offer a promising strategy for developing biopesticides for plant pest management (Khursheed et al. 2022). The advantages of using plant extracts include their rapid degradation, minimal environmental persistence, reduced risk to natural enemies, and safer handling for farmers (Kaur et al. 2023). Particularly, several studies have demonstrated the acaricidal effects of plant extracts against *T. urticae*. A recent review compiled data on 458 botanical extracts from 67 plant families with potential acaricidal properties (Rincón et al. 2019). For instance, Al-Alawi (2014) reported that three plant extracts induced over 50% mortality in *T. urticae* deutonymphs and adults, with *Ruta chalepensis* L. (Rutaceae) being the most effective, causing 65 and 53% mortality in deutonymphs and adults, respectively. Additionally, *Matricaria chamomilla* aqueous extracts and *Pimpinella anisum* hydroethanolic extracts achieved mortality rates of 83% after 120 h and 75% after 24 h in female mites (Tabet et al. 2018). Extracts from wild tomato (*Lycopersicon* sp.) have also demonstrated acaricidal action and repellent properties (Antonious and Snyder 2006).

The anti-mite effects of botanical extracts are attributed to their diverse bioactive specialized metabolites, which are concentrated during extract preparation (Jakubowska et al. 2022). These complex mixtures containing bioactive metabolites can induce single and/or concomitant detrimental effects on mites (Numa et al. 2018), which can ensure a low occurrence of resistance. Moreover, botanical extracts with sublethal effects may play a crucial role in integrated pest management (IPM) programs. Expanding the search for new bioactive botanicals against mites remains a priority in bioprospecting efforts to enhance current knowledge and develop sustainable pest control solutions. Thus, as part of ongoing research on bioacaricides, this study aimed to evaluate the effects of 10 bioactive botanical extracts on the mortality and oviposition of *T. urticae* females under laboratory conditions. The findings may contribute to the development of IPM strategies that incorporate botanical extracts for sustainable and effective *T. urticae* management.

MATERIALS AND METHODS

Plant materials

Plant material for extract preparation was collected from various locations in the Cundinamarca, Casanare, and Meta departments, specifically in Villa Pinzón (5.195608, -73.612221), Aguazul (5.200453, -72.587894), and Puerto López (4.055872, -72.993582), respectively. The Colombian National Herbarium assisted with plant identification, and a voucher specimen for each accession was independently deposited under the corresponding collection number (CN). A total of 10 plant species were collected, and their leaves were selected as test materials based on previous reports of their bioactivity. The selected species and their corresponding CNs were as follows: *Baccharis latifolia* (COL64911), *Genista monspessulana* (COL55658), *Nectandra amazonum* (COL269178), *Galipea trifoliata* (COL71165), *Solanum nigrum* ecotype-1 (collected in Cundinamarca; COL37524), *Solanum nigrum* ecotype-2 (collected in Casanare; COL355705), *Tithonia diversifolia* (COL80466), *Ulex europaeus* (COL60248), *Virola elongata* (COL401848), and *Virola peruviana* (COL369292).

Tetranychus urticae mites

Forty-eight-hour-old adult *T. urticae* females (preovipositing) used in bioassays were obtained from a breeding stock maintained under greenhouse conditions. To avoid overlapping generations and ensure age uniformity, the breeding was conducted in batches, as detailed in Rincón et al. (2024). The stock was fed a mixture of *Fragaria vesca*, *Lupinus bogotensis*, *Alstroemeria pelegrina*, and *Phaseolus vulgaris* in equal proportions to create a heterogeneous feeding environment. Previous studies have indicated that *T. urticae* behavior and susceptibility to chemical agents can vary depending on the host plant (Miresmailli et al. 2006). Mites were maintained under controlled greenhouse conditions (17±2 °C and 70±2% relative humidity) and randomly selected for bioassays to ensure a heterogeneous population.

Crude extracts preparation

Leaves (100 g) from each plant species were used for crude extract preparation. The samples were individually ground under nitrogen (N_2) and dried via lyophilization. Extraction was performed using 96% ethanol by maceration (2:1 ethanol-to-dry leaves ratio, v/w) for 7 days. Daily solvent removal under reduced pressure with a rotary evaporator yielded crude extracts with 10–15% efficiency. The crude extracts were stored at 4 °C without further fractionation until chemical analysis and bioassays.

High-performance liquid chromatography coupled with mass spectrometry (HPLC/MS) analysis

Ethanolic extracts were analyzed using a Shimadzu 8030 liquid chromatography (LC) system (Shimadzu Corp., Nakagyo-ku, Kyoto, Japan) equipped with a photodiode array (PDA) detector, electrospray ionization (ESI), and a mass spectrometry (MS) detector with a triple quadrupole mass analyzer. Separation was performed using a Premier C18 standard column (4.6 × 150 mm, 5 µm) with gradient elution. The mobile phase consisted of 0.005% formic acid and acetonitrile mixtures at a flow rate of 0.7 mL min^{-1}. A 5 µL aliquot of each plant extract solution (2.5 mg mL^{-1} in absolute ethanol) was injected into the LC system. The mass spectrometry method included scanning in both positive and negative ionization modes with an acquisition time of 2–33 min, a mass range of 50–800 m/z, a scan speed of 1,667 μs^{-1}, an event time of 0.5 s, a nebulizer gas flow rate of 1.5 L min^{-1}, an interface temperature of 350 °C, a desolvation line (DL) temperature of 450 °C, a block temperature of 450 °C, and a drying gas flow rate of 9 L s^{-1}. The analysis was monitored at wavelengths between 270 and 330 nm. Metabolite annotation and level 3 putative identification of major and minor metabolites in the test extracts were performed by analyzing their mass spectra, quasimolecular ions, and fragment ions, using the MassBank Project database (www.massbank.jp) for comparison.

Bioassay

Experiments were conducted under laboratory conditions (20±0.2 °C temperature and 55±2% relative humidity). A completely randomized design was used to evaluate the effects of the ethanolic extracts. Absolute (no application), relative (70% ethanol), and positive (Sunfire® commercial acaricide containing 24% chlorfenapyr as the active ingredient) controls were included, along with the 10 botanical crude extracts: *B. latifolia* (Bl), *G. monspessulana* (Gm), *N. amazonum* (Na), *G. trifoliata* (Gt), *S. nigrum* ecotype-1 (Sn1), *S. nigrum* ecotype-2 (Sn2), *T. diversifolia* (Td), *U. europaeus* (Eu), *V. elongata* (Ve), and *V. peruviana* (Vp). Each trial included three replicates per treatment, and each experiment was replicated three times. All test extracts and positive controls were applied at the same concentration (0.06% w/v). Previous research has

successfully demonstrated the direct effects of leaf extracts from various botanical species at this concentration (Numa et al. 2018).

Each experimental unit consisted of a 9-cm Petri dish containing a treated bean leaf disk surrounded by moistened cotton. Bean leaves were immersed in test solutions (0.06% w/v) for 1 min, air-dried for 15 min to remove excess moisture, and placed inside the Petri dish. Twenty *T. urticae* females were then randomly selected from the breeding stock and placed on the abaxial surface of the leaf. Since mites were placed on pre-treated leaves, mortality was expected to result primarily from ingestion or feeding deterrence. To ensure contact toxicity, an additional application of extract solutions (0.06% w/v) was administered over the mites using an airbrush (20 cm height, 96 drops cm^{-2}, 20–30 psi, 1.0 mL). Each experimental unit was sealed with stretch film and placed in a climate-controlled chamber. Mortality and oviposition of *T. urticae* were recorded for up to 96 h, the point at which mortality in the absolute control remained below 10% (Numa et al. 2018).

Data analysis

Daily *T. urticae* mortality data from the three replicates were used to calculate corrected mortality using Abbott's formula (Piepho et al. 2024) for each evaluation day (Equation 1):

$$\text{Corrected mortality}(\%) = \frac{(\text{mortality in treatment}(\%) - \text{mortality in absolute control}(\%)) * 100}{100 - \text{mortality in absolute control}(\%)} \quad (1)$$

The eggs laid by the females placed in each Petri dish were counted under a stereoscope at different evaluation times. Thus, fecundity was calculated as the total number of oviposited eggs per female in each treatment at 24, 48, 72, and 96 h (Equation 2):

$$\text{Total fecundity} = \frac{\text{total number of eggs}}{\text{total number of living females}} \quad (2)$$

Data on corrected mortality and total fecundity at 96 h were analyzed using a generalized linear model (GLM) assuming binomial and Poisson distributions, respectively, using the GLM function in R v4.1.2 (R Core Team 2021).

RESULTS AND DISCUSSION

In this study, mites were intentionally fed on various plants to ensure a generalizable mortality response across different pest populations from a range of host plants. The positive control (Sunfire® at a test concentration of 0.06% w/v) exhibited significantly higher mortality rates (54.6–89.7%) compared to the relative control (0.42–7.6%) from 48 to 96 h (P<0.05) (Table 1). This result aligns with expectations and indicates that the variability in female diet, due to different host plant species, did not significantly alter the response to the evaluated treatments. Unfractionated botanical extracts were prepared using 96% ethanol as the primary extractant due to its availability, ease of recovery, and ability to solubilize and extract a broad range of bioactive specialized metabolites. The bioassay demonstrated that the ethanolic extracts induced mortality and affected oviposition in *T. urticae* females at varying levels at the selected concentration (0.06% w/v). This dose was chosen as a representative value within the concentration range commonly used for biopesticides, such as those derived from *Azadirachta indica* (0.02–0.10% w/v)(Biswas 2013).

The corrected mortality percentages of *T. urticae* females exposed via direct contact with various crude ethanol extracts under laboratory conditions over 24 to 96 h are presented in Table 1. Among the tested extracts, *N. amazonum* exhibited the highest corrected mortality (14.4%) at 96 h, with significant differences from the relative control (P<0.01). *Solanum nigrum*-EC2 showed significantly different mortality rates at 24, 48, and 72 h (P<0.05), whereas *U. europaeus* exhibited its highest mortality at 96 h. Conversely, *S. nigrum*-EC1, *T. diversifolia*, and *V. elongata* displayed low corrected mortality rates, with *S. nigrum*-EC2 reaching a maximum of 8.9% after 96 h. These findings indicate that the test extracts had weak lethal effects (<15%). For *T. diversifolia*, its low impact on *T. urticae* agrees with Pavela et al. (2018), who reported a maximum mortality of 50% at a dose of 150 µg cm^{-3} of a polar extract in acute toxicity assays. The observed low mortality may be attributed to the characteristics and traits of the tested mite population. This observation was

evident from the results obtained for a reference active extract derived from *S. nigrum*-EC2 (collected in Casanare, Colombia) (Numa et al. 2016). This extract was previously tested on a homogeneous *T. urticae* population composed of susceptible individuals, yielding high corrected mortality (85.0±4.3% after 72 h) (Numa et al. 2016). However, when tested on the current heterogeneous population under identical exposure conditions, mortality was markedly lower (5.9±1.6%). To rule out chemical composition differences as a cause of these discrepancies, LC-MS analyses were performed on the botanical extracts, confirming identical chemical profiles. Thus, the differential mortality between assays can be attributed to variations in *T. urticae* populations. In this study, *S. nigrum* ecotype 1 (EC1) was included among the tested botanicals to compare the effects of extracts from the same species growing in different locations. The extract from *S. nigrum*-EC1 (collected in Cundinamarca, Colombia) exhibited lower mortality compared to that of *S. nigrum*-EC2. This difference is likely due to variations in chemical composition, with ecotype 2 containing higher levels of certain metabolites, particularly alkaloidal triterpenes.

Table 1. Corrected mortality percentage of *Tetranychus urticae* adults exposed to crude ethanol extracts under laboratory conditions from 24 to 96 h.

Treatment	Corrected Mortality (%)			
	24 h	48 h	72 h	96 h
Relative Control[a]	0.42±0.08	1.53±1.6	1.7±1.6	7.6±3.3
Positive Control[b]	54.6±6.3**	71.3±5.7**	86.4±4.3**	89.7±3.8**
Baccharis latifolia	2.08±18	3.34±2.3	3.90±2.4	6.21±3.1
Genista monspessulana	2.92±2.1	1.65±1.6	2.91±2.1	7.50±3.3
Nectandra amazonum	0.83±1.2	1.66±1.6	3.46±2.3	14.4±2.3**
Galipea trifoliata	0.83±1.2	2.49±7.84	1.68±1.6	3.05±2.2
Solanum nigrum-EC1[c]	2.08±2.6	2.07±2.9	1.61±3.0	3.92±3.6
Solanum nigrum-EC2[d]	4.40±1.8	5.60±1.84	5.90±1.6	8.90±2.5
Tithonia diversifolia	2.92±2.1	2.92±9.80	1.62±0.8	2.19±1.9
Ulex europaeus	0.83±1.2	2.92±2.1	3.49±2.3	7.97±3.4
Virola elongata	2.08±1.2	1.24±0.4	2.22±0.8	4.39±2.6
Virola peruviana	1.25±1.4	2.93±2.1	3.01±2.2	6.16±3.0

[a]70% ethanol; [b]Commercial acaricide (24% Chlorfenapyr as active ingredient); [c]ecotype 1, collected in Cundinamarca, Colombia; [d]ecotype 2, collected in Casanare, Colombia. Laboratory conditions: 19±0.2 °C and 60±2% relative humidity. Data expressed as mean ± standard error of the mean (SEM). *Significant differences (P<0.05) regarding the relative control, **highly significant differences regarding the relative control (P<0.01).

Despite the low impact on *T. urticae* mortality, the main effect of test botanicals was observed on reproductive alterations. Females from positive control (Sunfire®) increased oviposition at 72 and 96 h of exposure (Table 2). A similar effect was observed for the *N. amazonum*-derived extract, which was the most active botanical in terms of mite mortality. This response can be attributed to physiological stress, leading to hormonal changes that accelerate reproduction. A similar phenomenon has recently been reported in the brown planthooper *Nilaparvata lugens*, where exposure to certain insecticides has been associated with increased juvenile hormone levels, responsible for stimulating egg development and oviposition (Gao et al. 2025).

Significantly lower oviposition rates were recorded for *S. nigrum* (ecotype-2) at 96 h (P<0.05) and *T. diversifolia*, *V elongata*, and *V. peruviana* at 24 h. Additionally, *U. europaeus* induced an oviposition reduction below one egg per day per female at 96 h (Table 2). These extracts exhibited a sublethal effect by reducing *T. urticae* oviposition, consistent with findings for other plant extracts. Pavela et al. (2018) reported that polar extracts from *T. diversifolia*, despite their low direct toxicity, strongly

inhibited oviposition. This effect was attributed to the presence of tagitinin C and A, which act as repellents and antifeedants. In the present study, tagitinin C and A were not detected in the *T. diversifolia* extract; however, a structurally related compound, tagitinin D, was identified. This finding suggests that sesquiterpene lactones such as tagitinins may play a role as bioactive metabolites in the genus *Tithonia*, which has been previously associated with plant defense mechanisms (Chagas-Paula et al. 2012).

Table 2. Effects of crude ethanol extracts on the *Tetranychus urticae* female oviposition under laboratory conditions from 24 to 96 h.

Treatment	Per capita fecundity (eggs/day/female)			
	24 h	48 h	72 h	96 h
Relative Control[a]	1.44±0.20	1.62±0.35	1.36±0.34	1.15±0.15
Positive Control[b]	1.08±0.17	1.83±0.34	1.87±0.50*	2.15±0.74**
Baccharis latifolia	1.18±0.21	1.69±0.34	2.15±0.46**	1.16±0.22
Genista monspessulana	1.42±0.21	1.51±0.19	1.30±0.28	1.83±0.40
Nectandra amazonum	1.40±0.11	1.64±0.24	2.02±0.27	1.35±0.14
Galipea trifoliata	1.01±0.15	1.23±0.21	1.47±0.41	1.29±0.22
Solanum nigrum-EC1[c]	1.15±0.12	1.11±0.24	1.00±0.19	1.34±0.32
Solanum nigrum-EC2[d]	1.30±0.10	1.60±0.30	1.60±0.40	0.60±0.10**
Tithonia diversifolia	0.92±0.14**	1.14±0.24	1.08±0.21	1.13±0.17
Ulex europaeus	1.07±0.18	1.32±0.29	1.32±0.32	0.87±0.23**
Virola elongata	0.84±0.13**	1.15±0.13	1.00±0.15	1.01±0.17
Virola peruviana	0.85±0.12**	1.34±0.20	0.99±0.18*	1.38±0.29

[a]70% ethanol; [b]Commercial acaricide (24% Chlorfenapyr as active ingredient); [c]ecotype 1, collected in Cundinamarca, Colombia; [d]ecotype 2, collected in Casanare, Colombia. Laboratory conditions: 19±0.2 °C and 60±2% relative humidity. Data expressed as mean ± standard error of the mean (SEM) (n=30). *Significant differences (P<0.05) regarding the relative control, **highly significant differences regarding the relative control (P<0.01).

Several studies have investigated the oviposition-deterring effects of plant by-products on *T. urticae*, demonstrating that phenolic- and terpene-rich botanicals significantly impact mite reproduction (Rincón et al. 2019). In this context, flavonoids and phenolics (from *V. elongata*, *V. peruviana*, and *U. europaeus*), alkaloidal triterpenes (from *S. nigrum*-EC2), and sesquiterpenes (from *T. diversifolia*) may be the active phytochemicals responsible for the observed reductions in oviposition. Similar effects have been reported by Chacón-Hernández et al. (2020b), who found that exposure to *Magnolia tamaulipana* powder extract led to a concentration-dependent reduction in *T. urticae* oviposition, with the effect increasing between 5 and 1,000 µg mL^{-1}. Additionally, ethanolic extracts of *Lippia origanoides* and *Gliricidia sepium* at a concentration of 5% v/v inhibited oviposition in *Tetranychus cinnabarinus* by 43.7–57.0% after 72 h of exposure (Sivira et al. 2011). This oviposition-inhibitory effect may have two possible explanations: 1) specialized metabolites produced by plants could directly impair ovarian function (Dimetry et al. 2003), or 2) these compounds may induce incomplete or temporary sterility, leading to reduced oviposition (Hosny et al. 2010). Further research is needed to elucidate the physiological mechanisms underlying these sublethal effects.

Although preference tests were not conducted in this study, previous experiments suggest that botanicals can modify oviposition behavior, as females often avoid locating and ovipositing on treated surfaces (Keskin et al. 2020). This response could be mediated by specific phytoconstituents, such as volatile compounds, present in botanicals (Keskin et al. 2020). In multiple-choice tests, Hata et al. (2020) demonstrated that aromatic plants with low acceptance by *T. urticae* females also induced significantly lower oviposition rates per day.

Similarly, Zhang et al. (2008) reported that an extract derived from *Artemisia annua* leaves significantly reduced *T. cinnabarinus* oviposition. Kumral et al. (2010) further demonstrated the effectiveness of *Datura stramonium* L. seed- and leaf-derived extracts against *T. urticae*, not only as an acaricide but also as a repellent, oviposition deterrent, and hatch rate reducer after 24 h of exposure. These findings highlight the potential efficacy of compounds in the tested extracts for disrupting *T. urticae* reproduction.

LC/MS-based chemical characterization of the unfractionated extracts used in the bioassay detected 42 main compounds (annotated at level three based on their mass spectral data, Table 3), comprising phenolics, flavonoids, alkaloids, and terpene-related metabolites. Some of these compounds shared retention times in certain extracts, while most were detected only in a specific extract, reflecting the taxonomic variability of the tested botanicals (Figure 1, Table 3). Thus, this comparative LC/MS-based analysis provides an overview of the number and semiquantitative levels of metabolites present in a single extract, particularly those derived from leaves, which exhibit highly varied phytoconstituent profiles. These plant-derived metabolites can act as toxic agents or oviposition disruptors for many pests (Numa et al. 2015), causing various single or concomitant effects on mites (Numa et al. 2018). This complexity presents a challenge in identifying the specific compounds responsible for the observed acaricidal activity. However, existing records on the toxicity of certain metabolites can guide further investigation. For instance, by-products from *Eugenia langsdorffii* and *Ocotea* spp. contain high concentrations of sesquiterpenes, primarily found in leaves, which exhibit strong toxic effects on *T. urticae*, attributed to these terpene-related compounds (de Moraes et al. 2017).

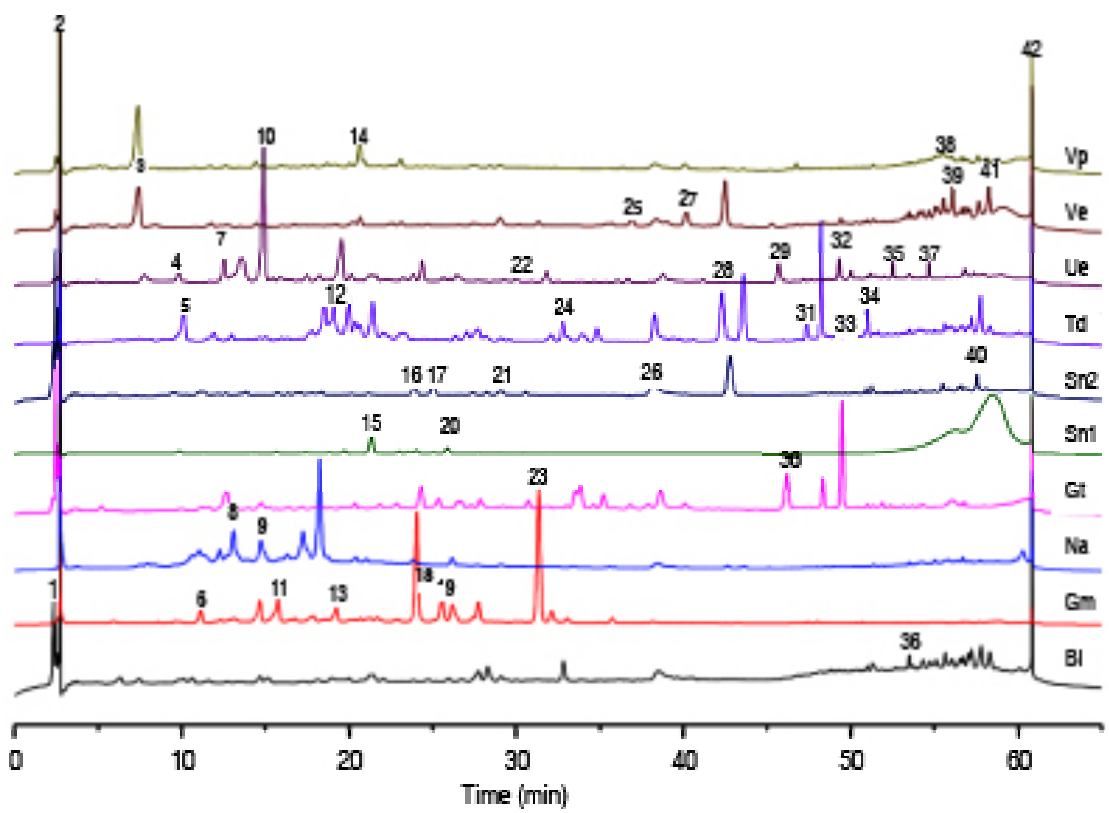

Figure 1. RP-LC-ESI-MS-derived profiles of test extracts: *Baccharis latiflolia* (Bl), *Genista monspessulana* (Gm), *Nectandra amazonun* (Na), *Galipea trifoliata* (Gt), *Solanum nigrum*-EC1 (Sn1), *Solanum nigrum*-EC2 (Sn2), *Tithonia diversifolia* (Td), *Ulex europaeus* (Ue), *Virola elongata* (Ve), *Virola peruviana* (Vp).

Table 3. Chemical composition of test ethanol extracts.

# [a]	R_t (min)	Name	Ct[b]	Molecular Formula	*m/z* [M+H$^+$]	Detection in plant samples[c]									
						1	2	3	4	5	6	7	8	9	10
1	2.46	hispidulin sulfate	f	$C_{16}H_{12}O_9S$	381.03						x				
	2.51	hexahydro-hydroxy-methyl-(methylethyl)-naphthalenecarboxaldehyde	t	$C_{15}H_{22}O_2$	235.52	x									
	2.67	alpinumisoflavone (or isomers)	f	$C_{20}H_{16}O_5$	337.13		x								
	2.73	dimethoxyflavone	f	$C_{17}H_{14}O_4$	282.95										x
2	2.73	monatin	a	$C_{14}H_{16}N_2O_5$	293.11						x				
	2.82	*N*-methylcytisine	a	$C_{12}H_{16}N_2O$	205.55		x								
	2.83	scopolin (or isomers)	p	$C_{16}H_{18}O_9$	353.14							x			
	2.85	glaziovine	a	$C_{18}H_{19}NO_3$	297.24			x							
3	7.43	juruenolide F	p	$C_{25}H_{38}O_5$	391.45									x	
4	9.88	methyltectorigenin apiofuranosylglucopyranoside	f	$C_{28}H_{32}O_{15}$	609. 21								x		
5	10.23	tagitinin D	t	$C_{19}H_{28}O_6$	353.12							x			
6	11.22	dehydrolupanine	a	$C_{15}H_{22}N_2O$	247.45		x								
7	12.53	luteolin rutinoside (or isomers)	f	$C_{27}H_{30}O_{15}$	595.12								x		
8	13.33	reticuline (or isomers)	a	$C_{19}H_{23}NO_4$	329.16			x							
	14.67	unknown	-		446.21		x								
9	14.74	methoxyflindersiamine (or isomer)	a	$C_{14}H_{11}NO_5$	274.51				x						
	14.77	norlirioferine (or isomers)	a	$C_{19}H_{21}NO_4$	327.14			x							
10	14.91	methylgenistein glucoside	f	$C_{22}H_{22}O_{10}$	447.23								x		
11	15.84	*N*-acetylcytisine	a	$C_{13}H_{16}N_2O_2$	431.42		x								
12	18.31	rhombifoline (or isomers)	a	$C_{15}H_{20}N_2O$	245.05								x		
	18.43	corydine (or isomers)	a	$C_{20}H_{23}NO_4$	341.35			x							
13	19.22	cinegalline	a	$C_{23}H_{30}N_2O_6$	429.25		x								
	19.54	genistein glucoside	f	$C_{21}H_{20}O_{10}$	433.21										
	20.18	formononetin rutinoside	f	$C_{28}H_{32}O_{13}$	577.16								x		
14	20.50	yangambin	p	$C_{24}H_{30}O_8$	446.92										x
	20.52	surinamensin or dimethoxylariciresinol	p	$C_{22}H_{28}O_6$	388.11										x
	20.65	unknown	-		265.54									x	
15	21.50	isorhamnetin glucopyranoside	f	$C_{28}H_{32}O_{17}$	641.23					x					
	24.05	ajmaline	a	$C_{20}H_{26}N_2O_2$	327.21						x				
16	24.13	methylgenistein (or isomer)	f	$C_{16}H_{12}O_5$	285.32		x								
	24.33	evoxanthine	a	$C_{16}H_{13}NO_4$	284.35				x						
	24.38	methylgenistein (or isomer)	a	$C_{16}H_{12}O_5$	285.05								x		
17	25.13	calligonine	a	$C_{12}H_{14}N_2$	187.12						x				
18	26.65	daidzein (or isomer)	f	$C_{15}H_{10}O_4$	255.35		x								
19	27.82	luteolin isomer	f	$C_{15}H_{10}O_6$	285.12		x								
20	28.01	solasodoside A	tr	$C_{51}H_{82}O_{21}$	1031.12					x					
	28.90	abutiloside A	a	$C_{49}H_{83}NO_{17}$	958.45					x					

Table 3

# [a]	R_t (min)	Name	Ct[b]	Molecular Formula	*m/z* [M+H$^+$]	Detection in plant samples[c]									
						1	2	3	4	5	6	7	8	9	10
21	29.10	leptomerine	a	$C_{13}H_{15}NO$	201.11						x				
	29.01	grandisin	p	$C_{24}H_{32}O_7$	431.23									x	
	30.05	methylgenistein glucoside	f	$C_{22}H_{22}O_{10}$	445.05								x		
22	30.66	dimethoxyflavone isomer	f	$C_{17}H_{14}O_4$	283.14						x				
	30.73	subaphyllin	p	$C_{14}H_{20}N_2O_3$	264.53				x						
23	31.52	trihydroxyxanthone	p	$C_{15}H_{10}O_5$	271.35		x								
	31.83	resokaempferol	f	$C_{15}H_{10}O_5$	269.21								x		
	32.11	eupafolin	f	$C_{16}H_{12}O_7$	317.18							x			
24	32.96	hispidulin	f	$C_{16}H_{12}O_6$	299.21							x			
	33.00	abutiloside J	a	$C_{48}H_{81}NO_{17}$	943.23					x					
25	36.91	unknown	-		499.31									x	
26	38.28	Hydroxy-methoxy-methyl-formylflavanone isomer	f	$C_{18}H_{16}O_5$	313.11						x				
	38.59	dictamine	a	$C_{12}H_9NO_2$	200.52				x						
27	40.13	unknown	-		223.53									x	
	42.34	nevadensin	f	$C_{18}H_{16}O_7$	345.35							x			
28	42.45	xenognosin B (or isomer)	f	$C_{16}H_{12}O_5$	285.31									x	
	42.84	hydroxy-methoxy-methylflavone	f	$C_{17}H_{14}O_4$	283.12						x				
29	45.71	isowighteone	f	$C_{20}H_{18}O_5$	339.43								x		
30	46.18	tigloyldiderroside	a	$C_{15}H_{15}NO_3$	258.41				x						
31	48.25	homobutein	f	$C_{16}H_{14}O$	287.23							x			
	49.20	abutiloside B	a	$C_{46}H_{77}NO_{17}$	914.21					x					
32	49.31	claussequinone-vestitol	f	$C_{32}H_{28}O_9$	555.22								x		
	49.41	helianyl octanoate	tr	$C_{38}H_{66}O_2$	555.21							x			
	49.47	methoxyflindersiamine (or isomer)	a	$C_{14}H_{11}NO_5$	274.43				x						
33	50.94	hymenoxin	f	$C_{19}H_{18}O_8$	373.14							x			
	50.94	desmethyleucalyptin (or isomer)	f	$C_{18}H_{16}O_5$	313.11						x				
34	51.29	desmethyleucalyptin (or isomer)	f	$C_{18}H_{16}O_5$	313.11						x				
	52.51	onogenin	f	$C_{17}H_{14}O_6$	315.51								x		
35	52.56	limonin	tr	$C_{26}H_{30}O_8$	471.22				x						
	52.57	bisparasin (isomer)	p	$C_{30}H_{28}O_6$	485.25				x						
36	53.64	conycephaloide	t	$C_{20}H_{20}O_5$	339.23	x									
37	54.68	betulin	tr	$C_{30}H_{50}O_2$	443.71								x		
	55.14	unknown	-		255.32										x
38	55.53	artonin U	f	$C_{20}H_{20}O_5$	353.14						x				
	55.58	unknown	-		893.33									x	
39	56.13	xenognosin B (or isomer)	f	$C_{16}H_{12}O_5$	284.06									x	
	56.81	daidzein (or isomer)	f	$C_{15}H_{10}O$	255.41								x		
40	57.63	hydroxysolasodine	a	$C_{27}H_{45}NO_3$	430.33						x				
	57.72	juruenolide E	p	$C_{23}H_{34}O_5$	391.42									x	

Table 3

# [a]	R_t (min)	Name	Ct[b]	Molecular Formula	*m/z* [M+H$^+$]	Detection in plant samples[c]									
						1	2	3	4	5	6	7	8	9	10
41	58.24	formononetin	f	$C_{16}H_{12}O_4$	269.25									x	
	60.84	verrucosin	P	$C_{20}H_{24}O_5$	344.09										x
	60.86	solasodine	a	$C_{27}H_{43}NO$	398.34						x				
42	60.87	ichangensin	tr	$C_{25}H_{32}O_7$	445.28				x						
	60.91	dihydro-(hydroxyphenyl)-pyranocatechinone	f	$C_{24}H_{20}O_8$	436.16			x							
	60.93	methyl-[tetrahydromethylbutadienyl) methylene-oxofuranyl]-butenal (or isomers)	t	$C_{15}H_{18}O_3$	247.44							x			
	60.94	geranyllinalololide (or isomers)	t	$C_{20}H_{30}O_3$	319.55	x									

[a]Numbering according to detection order showed in Figure 1; [b]Ct = Compound type: flavonoid (f), phenolics (p), alkaloid (a), terpenoid (t), triterpene (tr); [c]Compound distribution among test plant-derived extracts: **1**= *Baccharis latiflolia* (Bl), **2**= *Genista monspessulana* (Gm), **3**= *Nectandra amazonun* (Na), **4**= *Galipea trifoliata* (Gt), **5**= *Solanum nigrum* 1 *(*Sn1), **6**= *Solanum nigrum* 2 *(*Sn2), **7**= *Tithonia diversifolia* (Td), ***8***= *Ulex europaeus* (Ue), **9**= *Virola elongata* (Ve). **10**= *Virola Peruviana* (Vp).

The findings of this study serve as a foundation for developing alternative control strategies targeting *T. urticae* reproduction using test plant extracts, particularly *U. europaeus*, an invasive species in South America. In this context, quinolizidine alkaloids (e.g., rhombifoline) and prenylated isoflavones (e.g., isowighteone) were identified in the *U. europaeus* extract and may contribute to oviposition inhibition (Isman 2020). Indeed, prenylated isoflavones, precursors of rotenoids, have demonstrated acaricidal activity and completely inhibited the oviposition of the female tick *Rhipicephalus appendiculatus* (Van Puyvelde et al. 1987), while matrine-type quinolizidine alkaloids have been shown to affect *T. urticae* oviposition (Marčić and Među 2014). Additionally, nitrogenated triterpenes (e.g., abutiloside J), lignans (e.g., grandisin), and sesquiterpene lactones (e.g., tagitinin D) were detected in extracts with the highest oviposition inhibitory effects, such as those from *S. nigrum*, *V. elongata*, and *T. diversifolia*. These findings warrant further bio-guided fractionation studies to isolate and evaluate the active compounds responsible for anti-mite effects, defining the active principles and their specific roles in *T. urticae* oviposition alteration.

T. urticae susceptibility to acaricidal agents has been primarily assessed through acute contact toxicity assays. However, resistance development is well-documented and is often linked to genetic traits enabling adaptation to acaricide pressure via transposable elements in its genome (Rincón et al. 2019). Resistance mechanisms include reduced target site sensitivity, metabolic detoxification, and decreased penetration, all classified as physiological resistance, while behavioral adaptations remain poorly studied (Adesanya et al. 2019). Developing behavioral manipulation techniques is a promising approach to mitigating resistance and optimizing synthetic insecticide use (de França et al. 2013). From this perspective, botanical extracts from *S. nigrum*, *T. diversifolia*, *V. elongata*, and *U. europaeus* show potential for use as oviposition inhibitors or disruptors. Information on the extraction yield and crop productivity of these plants is essential for assessing the feasibility of incorporating oviposition inhibitors into integrated pest management (IPM) programs for controlling *T. urticae*. Additionally, further studies should evaluate the dose-dependent effectiveness of the most promising extracts under laboratory conditions to validate their potential in *T. urticae* management through targeted field trials. Once high effectiveness is confirmed, standardization processes must be established, including plant selection, cultivation management, and formulation development for field application. A common challenge with botanical products is the inconsistency in efficacy and lack of reproducibility, often due to variations in agronomic practices and extract stability (Ivase et al. 2021). Therefore, caution is advised in generalizing these findings, as physiological and behavioral aspects may influence the magnitude of the observed effects (Thompson and Reddy 2016).

CONCLUSION

This study evaluated the capacity of 10 leaf-derived unfractionated ethanol extracts to alter *T. urticae* survival and oviposition behavior, identifying promising candidates

for disrupting its reproduction. Among the tested extracts, *S. nigrum* EC2 and *U. europaeus* significantly inhibited oviposition after 96 h, while *N. amazonum*, *S. nigrum* EC1, and *T. diversifolia* were most effective in inducing mite mortality. These findings suggest that specific phytochemicals, such as alkaloidal triterpenes, phenolics, and sesquiterpenes, may play crucial roles in these biological activities. The results highlight the importance of understanding phytochemical-pest interactions and emphasize the need for further research to isolate and characterize the active compounds responsible for these effects. Additionally, the observed reduction in *T. urticae* oviposition may be attributed to the sublethal effects of the extracts, potentially leading to decreased population growth and reduced dependence on synthetic pesticides. This research underscores the potential of botanical extracts as sustainable IPM tools, offering an environmentally friendly alternative to conventional chemical controls and contributing to the reduction of pesticide use in commercial agriculture.

ACKNOWLEDGMENTS

The authors thank the Universidad Militar Nueva Granada (UMNG) for the financial support. This study was funded by Vicerrectoría de Investigaciones at UMNG through the research project INV-CIAS-2054, validity 2016.

CONFLICT OF INTERESTS

The authors have no conflict of interest**.**

ETHICS IN RESEARCH AND LEGAL REGULATIONS

The authors declare they have not violated or omitted ethical or legal norms when conducting this study.

REFERENCES

Adesanya AW, Beauchamp MJ, Lavine MD et al (2019) Physiological resistance alters behavioral response of *Tetranychus urticae* to acaricides. Scientific Reports 9:19308. https://doi.org/10.1038/s41598-019-55708-4

Al-Alawi MS (2014) Acaricidal Activity of Medicinal Plants Against the developmental stages of the two spotted spider mite, *Tetranychus urticae* (Acari: Tetranychidae). International Journal of Agricultural Research 9: 38–46. https://doi.org/10.3923/ijar.2014.38.46

Antonious GF and Snyder JC (2006) Natural products: Repellency and toxicity of wild tomato leaf extracts to the two-spotted spider mite, *Tetranychus urticae* Koch. Journal of Environmental Science and Health, Part B 41: 43–55. https://doi.org/10.1080/03601230500234893

Assouguem A, Farah A, Ullah R et al (2022a) Evaluation of the varietal impact of two citrus species on fluctuations of *Tetranychus urticae* (Acari: Tetranychidae) and beneficial Phytoseiid mites. Sustainability 14: 3088. https://doi.org/10.3390/su14053088

Assouguem A, Kara M, Mechchate H et al (2022b) Current situation of *Tetranychus urticae* (Acari: Tetranychidae) in Northern Africa: The Sustainable Control Methods and Priorities for Future Research. Sustainability 14: 2395. https://doi.org/10.3390/su14042395

Biswas G (2013) Comparative effectiveness of neem extracts and synthetic organic insecticide against mustard aphid. Bangladesh Journal of Agricultural Research 38: 181–187. https://doi.org/10.3329/bjar.v38i2.15881

Chacón-Hernández JC, Cerna-Chávez E, Aguirre-Uribe LA et al (2020b) Resistance of four rose varieties to *Tetranychus urticae* (Acari: Tetranychidae) under greenhouse conditions. Florida Entomologist 103: 404–407. https://doi.org/10.1653/024.103.0315

Chagas-Paula DA, Oliveira RB, Rocha BA and Da Costa FB (2012) Ethnobotany, chemistry, and biological activities of the genus *Tithonia* (Asteraceae). Chemistry & Biodiversity 9: 210–235. https://doi.org/10.1002/cbdv.201100019

Chauhan U, Gupta PR and Sharma A (2011) Management of the two spotted spidermite on carnation with the use of biopesticides and the predator *Neoseiulus longispinosus* (Evans) (Acari: Tetranychidae, Phytoseiidae)*. Zoosymposia 6: 135–138. https://doi.org/10.11646/zoosymposia.6.1.23

Daza Vallejos MA, Bustos Rodriguez HA, Cantor Rincon F et al (2010) Criterios para la producción de *Phytoseiulus persimilis* (Parasitiformes: Phytoseiidae) bajo condiciones de invernadero. Acta Biológica Colombiana 15: 37–46. https://revistas.unal.edu.co/index.php/actabiol/article/view/9225

de França SM, Breda MO, Badji B and de Oliveira JV (2013) The use of behavioral manipulation techniques on synthetic insecticides optimization. In: Trdan S (ed) Insecticides. IntechOpen, Rijeka, p Ch. 6.

de Moraes MM, da Camara CAG and da Silva MMC (2017) Comparative toxicity of essential oil and blends of selected terpenes of *Ocotea* species from Pernambuco, Brazil, against *Tetranychus urticae* Koch. Anais da Academia Brasileira de Ciências 89: 1417–1429. https://doi.org/10.1590/0001-3765201720170139

Dekeyser MA (2005) Acaricide mode of action. Pest Management Science 61: 103–110. https://doi.org/10.1002/ps.994

Dimetry NZ, Amer SAA and El-Gengaihi S (2003) Toxicological evaluation and biological potency of petroleum ether extract of two plants and their isolates towards the two spotted spider mite *Tetranychus urticae* Koch. Acarologia 43: 67–73

Gao Y, Su S-C, Xing J-Y et al (2025) Pesticide-induced resurgence in brown planthopper is mediated by action on a suite of genes that promote juvenile hormone biosynthesis and female fecundity. https://doi.org/10.7554/elife.91774.2

Hata FT, Béga VL, Ventura MU et al (2020) Plant acceptance for oviposition of *Tetranychus urticae* on strawberry leaves is influenced by aromatic plants in laboratory and greenhouse intercropping experiments. Agronomy 10: 193. https://doi.org/10.3390/agronomy10020193

Hosny AH, Keratum AY and Hasan NE (2010) Comparative efficiency of pesticides and some predators to control spider mites: II- Biological and behavioral characteristics of predators *Stethorus gilvifrons*, *Amblyseius gossipi* and *Phytoseiulus macropili* and their host two spotted spider mite, *Tetranychus urticae* under some chemicals treatments. Journal of Plant Protection and Pathology 1: 1065–1085.

https://doi.org/10.21608/jppp.2010.86971

Isman MB (2020) Botanical insecticides in the twenty-first century—fulfilling their promise? Annual Review of Entomology 65: 233–249. https://doi.org/10.1146/annurev-ento-011019-025010

Ivase TJ-P, Nyakuma BB, Otitolaiye VO et al (2021) Standardization, quality control, and bio- enhancement of botanical insecticides: A review. DRC Sustainable Future: Journal of Environment, Agriculture, and Energy 2: 104–111. https://doi.org/10.37281/DRCSF/2.2.2

Jakubowska M, Dobosz R, Zawada D and Kowalska J (2022) A Review of crop protection methods against the two-spotted spider mite—*Tetranychus urticae* Koch (Acari: Tetranychidae)—with special reference to alternative methods. Agriculture 12: 898. https://doi.org/10.3390/agriculture12070898

Kaur A, Chhabra R, Sharma R et al (2023) Botanical extracts: A step towards eco-friendly pest management strategy. Agric Res J 60:167–176.

Keskin G, Kumral NA and Kaçar O (2020) A laboratory study of the acaricidal, repellent and oviposition deterrent effects of three botanical oils on *Tetranychus urticae* (Koch, 1836) (Acari: Tetranychidae). Turkish Journal of Entomology 44: 305–318. https://doi.org/10.16970/entoted.702157

Khursheed A, Rather MA, Jain V et al (2022) Plant based natural products as potential ecofriendly and safer biopesticides: A comprehensive overview of their advantages over conventional pesticides, limitations and regulatory aspects. Microbial Pathogenesis 173: 105854. https://doi.org/10.1016/j.micpath.2022.105854

Kumral NA, Çobanoğlu S and Yalcin C (2010) Acaricidal, repellent and oviposition deterrent activities of *Datura stramonium* L. against adult *Tetranychus urticae* (Koch). Journal of Pest Science 83: 173–180. https://doi.org/10.1007/s10340-009-0284-7

Marčić D and Međo I (2014) Acaricidal activity and sublethal effects of an oxymatrine-based biopesticide on two-spotted spider mite (Acari: Tetranychidae). Experimental and Applied Acarology 64: 375–391. https://doi.org/10.1007/s10493-014-9831-x

Miresmailli S, Bradbury R and Isman MB (2006) Comparative toxicity of *Rosmarinus officinalis* L. essential oil and blends of its major constituents against *Tetranychus urticae* Koch (Acari: Tetranychidae) on two different host plants. Pest Management Science 62: 366–371. https://doi.org/10.1002/ps.1157

Numa S, Rodríguez-Coy, Rodríguez D and Coy-Barrera E (2016) Effect of acaricidal activity of *Solanum nigrum* on *Tetranychus urticae* Koch under laboratory conditions. African Journal of Biotechnology 15: 363–369. https://doi.org/10.5897/AJB2015.15054

Numa S, Rodríguez-Coy, Rodríguez D and Coy-Barrera E (2015) Susceptibility of *Tetranychus urticae* Koch to an ethanol extract of *Cnidoscolus aconitifolius* leaves under laboratory conditions. SpringerPlus 4: 338. https://doi.org/10.1186/s40064-015-1127-z

Numa S, Rodríguez-Coy, Rodríguez D and Coy-Barrera E (2018) Examination of the acaricidal effect of a set of colombian native plants-derived extracts against *Tetranychus urticae* Koch under laboratory conditions. Journal of Biopesticides 11: 30–37. https://jbiopestic.com/archivesbrief.php?id=99

Pavela R, Dall'Acqua S, Sut S et al (2018) Oviposition inhibitory activity of the Mexican sunflower *Tithonia diversifolia* (Asteraceae) polar extracts against the two-spotted spider mite *Tetranychus urticae* (Tetranychidae). Physiological and Molecular Plant Pathology 101: 85–92. https://doi.org/10.1016/j.pmpp.2016.11.002

Piepho H-P, Malik WA, Bischoff R et al (2024) Efficacy assessment in crop protection: a tutorial on the use of Abbott's formula. Journal of Plant Diseases and Protection 131: 2139–2160. https://doi.org/10.1007/s41348-024-00968-0

Rincón RA, Rodríguez D and Coy-Barrera E (2019) Botanicals against *Tetranychus urticae* Koch under laboratory conditions: a survey of alternatives for controlling pest mites. Plants 8:272. https://doi.org/10.3390/plants8080272

Rincón RA, Rodríguez D and Coy-Barrera E (2024) Susceptibility of *Tetranychus urticae* to the alkaloidal extract of *zanthoxylum schreberi* Bark: phenotypic and biochemical insights for biotechnological exploitation. BioTech 13:5. https://doi.org/10.3390/biotech13010005

Siebert JC, Wurlitzer WB, Lambert GH et al (2020) Population fluctuation of *Tetranychus urticae* (Acari: Tetranychidae) in Different chrysanthemum varieties in greenhouses. Oecologia Australis 24:957–963. https://doi.org/10.4257/oeco.2020.2404.19

Singh S, Rana RS, Sharma KC et al (2017) Chemical control of two spotted spider mite *Tetranychus urticae* (Acari: Tetranychidae) on rose under polyhouse conditions. Journal of Entomology and Zoology Studies 5: 104–107. https://www.entomoljournal.com/archives/?year=2017&vol=5&issue=6&ArticleId=2579

Sivira A, Sanabria M, Valera N and Vásquez C (2011) Toxicity of ethanolic extracts from *Lippia origanoides* and *Gliricidia sepium* to *Tetranychus cinnabarinus* (Boisduval) (Acari: Tetranychidae). Neotropical Entomology 40: 375–379.

Sudo M, Takahashi D, Andow DA et al (2018) Optimal management strategy of insecticide resistance under various insect life histories: Heterogeneous timing of selection and interpatch dispersal. Evolutionary Applications 11: 271–283. https://doi.org/10.1111/eva.12550

Tabet VG, Vieira MR, Martins GLM and Sousa CGNM de (2018) Plant extracts with potential to control of two-spotted spider mite. Arquivos do Instituto Biológico 85: e0762015. https://doi.org/10.1590/1808-1657000762015

Thompson BM and Reddy GVP (2016) Effect of temperature on two bio-insecticides for the control of confused flour beetle (Coleoptera: Tenebrionidae). The Florida Entomologist 99:67–71

Van Leeuwen T, Vontas J, Tsagkarakou A et al (2010) Acaricide resistance mechanisms in the two-spotted spider mite *Tetranychus urticae* and other important Acari: A review. Insect Biochemistry and Molecular Biology 40: 563–572. https://doi.org/10.1016/j.ibmb.2010.05.008

Van Puyvelde L, De Kimpe N, Mudaheranwa JP et al (1987) Isolation and structural elucidation of potentially insecticidal and acaricidal isoflavone-type compounds from *Neorautanenia mitis*. Journal of Natural Products 50: 349–356. https://doi.org/10.1021/np50051a002

Zhang Y, Ding W, Zhao Z et al (2008) Studies on acaricidal bioactivities of *Artemisia annua* L. extracts against *Tetranychus cinnabarinus* Bois. (Acari: Tetranychidae). Agricultural Sciences in China 7: 577–584. https://doi.org/10.1016/S1671-2927(08)60055-3

Research article

https://revistas.unal.edu.co/index.php/refame

Revista Facultad Nacional de Agronomía

Camellia cattienensis: phytochemical and biological properties from the leaf extract

Camellia cattienensis: propiedades fitoquímicas y biológicas del extracto de hojas

https://doi.org/10.15446/rfnam.v78n2.115865

Hanh Thi Dieu Nguyen[1], Ngoc An Nguyen[1], Thi Nha Xuyen Nguyen[1], Trong Thao Nguyen[1], Le Pham Tan Quoc[1], Hong Thien Van[1], Thanh Tho Le[2], Van Hop Nguyen[3,4], Quoc Hung Nguyen[5] and Tan Viet Pham[1*]

ABSTRACT

Camellia consists of many plants of high economic importance that are used in different fields, especially in the food industry. *Camellia cattienensis* is a rare species and is native to Vietnam. Studies on the phytochemical and biological properties of this species have been unknown so far. In this study, the chemical components of the acetone extract from *C. cattienensis* leaves and its fractions, including n-hexane, chloroform, and ethyl acetate, were investigated using gas chromatography-mass spectrometry assay. Accordingly, 2-pentanone, 4-hydroxy-4-methyl- was the most abundant compound in the acetone extract and the ethyl acetate fraction, while phenol, 2,4-bis(1,1-dimethylethyl)-, phosphite (3:1) and hexanedioic acid, bis(2-ethylhexyl) ester are the richest components in the chloroform and n-hexane fractions, respectively. Furthermore, the acetone extract was active against four tested bacteria, including *Klebsiella pneumoniae*, *Staphylococcus aureus*, and *Staphylococcus saprophyticus* BAA750. The acetone extract of the *C. cattienensis* leaves also possessed DPPH, and ABTS free radical scavenging with the IC_{50} values of 91.63±1.88 and 13.32±0.49 µL, respectively. The outcomes of this study hold promise for potential applications of *C. cattienensis* leaves in food product development, especially in the future beverage industry.

Keywords:
Antibacterial
Antioxidant
Cat Tien camellia
GC/MS

RESUMEN

La *Camelia* se compone de muchas plantas de alto valor económico y se utilizan en diferentes campos, especialmente en la industria alimentaria. *Camellia cattienensis* es una especie rara y originaria de Vietnam. Hasta el momento se desconocen los estudios sobre las propiedades fitoquímicas y biológicas de esta especie. En este estudio, se investigaron los componentes químicos del extracto de acetona de las hojas de *C. cattienensis* y sus fracciones, como n-hexano, acetato de etilo y cloroformo, mediante un ensayo de cromatografía de gases/espectrometría de masas. En consecuencia, 2-pentanona, 4-hidroxi-4-metil-fue el compuesto más abundante en el extracto de acetona y la fracción de acetato de etilo, mientras que fenol, 2,4-bis(1,1-dimetiletil)-, fosfito (3:1) y el ácido hexanodioico, el éster bis(2-etilhexílico) son los componentes más ricos en las fracciones de cloroformo y n-hexano, respectivamente. Además, se descubrió que el extracto de acetona era eficaz contra cuatro bacterias analizadas, incluidas *Klebsiella pneumoniae, Staphylococcus aureus,* y *Staphylococcus saprophyticus*. El extracto de acetona de las hojas de *C. cattienensis* también poseía eliminación de radicales libres DPPH y ABTS con valores de IC_{50} de 91,63±1,88 y 13,32±0,49 µL, respectivamente. Los resultados de este estudio son prometedores para aplicaciones potenciales de las hojas de *C. cattienensis* en el desarrollo de productos alimenticios, especialmente en la industria de bebidas en el futuro.

Palabras clave:
Antibacterianas
Antioxidantes
Cat tien camellia
GC/MS

[1]Institute of Biotechnology and Food Technology, Industrial University of Ho Chi Minh City, Vietnam. nguyenthidieuhanh@iuh.edu.vn, nguyenngocan.cnsh@iuh.edu.vn, nhaxuyen121019@gmail.com, kentrong357@gmail.com, lephamtanquoc@iuh.edu.vn, vanhongthien@iuh.edu.vn , phamtanviet@iuh.edu.vn
[2]Center of Analytical Services and Experimentation HCMC, Vietnam. tholt@case.vn
[3]Faculty of Natural Resources and Environment, Vietnam National University of Forestry-Dongnai Campus, Vietnam. hopvfu@gmail.com
[4]College of Forestry, Fujian Agriculture & Forestry University, Fujian Province, China.
[5]Bureau Veritas AQ Vietnam Company Limited, No. 36-38 Nguyen Van Troi Street, Phu Nhuan District, Ho Chi Minh City, Vietnam. ngqhung2005@gmail.com
*Corresponding author

Received: February 3, 2025; Accepted: March 23, 2025
Rev. Fac. Nac. Agron. Medellín 78(2): 11181-11190. 2025
ISSN 0304-2847 / e-ISSN 2248-7026

CC BY NC SA

Camellia is a large genus in the family of Theaceae, comprising over 280 species distributed in many countries around the world, and about 95 species have been found in Vietnam (Quach et al. 2021). Many members of the Camellia genus are plants of high economic value due to their byproducts, including oil seeds, tea, ornamental plants, and iconic flowering shrubs (Yang et al. 2016). Additionally, various solvent extracts obtained from Camellia plants have been reported to possess numerous pharmaceutical properties, including antibacterial, antifungal, antitumor, and antioxidant activities (Yang et al. 2016). Notably, *Camellia sinensis*, commonly known as the tea plant, is cultivated in tropical and subtropical regions. Additionally, leaf extracts from this species are recognized as the second most consumed beverage in the world (Chitsazan 2015). Moreover, they contain numerous beneficial compounds, such as catechins (Gaur and Bao 2021), steroids, alkaloids, polyphenols, and terpenoids (Anand et al. 2015). Furthermore, the oil extracted from certain *Camellia* species, particularly *C. oleifera* and *C. japonica*, is known as 'Asian olive oil' due to its high content of major chemical compounds, such as oleic acid and neutral lipids (Kim et al. 2014).

Camellia cattienensis Orel was first reported as a new species for the flora of Vietnam by Orel and Wilson (2011). This species, whose type specimen was collected from Cat Tien National Park, Dong Nai Province, Vietnam. To date, it is a rare plant and is found only in the type collection (Orel and Wilson 2011). The phytochemical and biological effects of this species have been unknown so far. This study, thus, provided the chemical constituents, antioxidants, and antibacterial activities of *C. cattienensis* for the first time.

MATERIALS AND METHODS

Materials

The leaf specimens of *Camellia cattienensis* were collected from Bau Sau station, Cat Tien National Park, (Dong Nai Province, Vietnam) by Van Hop Nguyen, where its type specimen was collected. The voucher specimen was CT22092022, and it was deposited in the herbarium of the Faculty of Natural Resources and Environment, Vietnam National University of Forestry-Dong Nai Campus, Vietnam.

Bacterial strains

Ten bacterial strains were used to identify the antibacterial activity of the studied species, including six Gram-negative strains (*Escherichia coli* ATCC 25922, *Salmonella typhimurium* ATCC 13311, *Klebsiella pneumoniae* ATCC 13883, *Klebsiella pneumoniae* ATCC 700603, *Shigella flexneri* ATCC 9199, *Enterobacter hormaechei* ATCC 700323) and four Gram-positive strains (*Staphylococcus saprophyticus* BAA750, *Staphylococcus aureus* ATCC 29213, *Staphylococcus aureus* ATCC 25923, *Bacillus cereus* ATCC 13883).

Extraction procedures

The leaves of *C. cattienensis* were freshly harvested, well-washed, air-dried at 50 °C, and evenly ground into fine powder. 500 mL of acetone solution (99%, Thermo Fisher Scientific, USA) was used to immerse 100 g of powder for 72 h; after that, the supernatant was collected and filtered. The remaining solid matter underwent two more rounds of acetone extraction, and the end product was recovered by combining all the filtered fractions. The solvent was then eliminated in vacuum condition at 45 °C.

Three grams of acetone extract were dissolved in 30 mL of distilled water in an extraction flask. Then, 30 mL n-hexane was added, shaken, and left standing for layer formation. The hexane layer on the top was collected, and this procedure was performed again two more times to pick up 90 mL of the n-hexane extract. This extract was also eliminated under vacuum conditions at 45 °C to obtain the hexane fraction. The same process done above was used to obtain ethyl acetate and chloroform (Le et al. 2021).

Gas chromatography-mass spectrometry assays

The chemical constituents of the acetone extract and its fractions (n-hexane, ethyl acetate, and chloroform) from *C. cattienensis* leaves were determined using the TRACE 1310 Gas Chromatograph in conjunction with the ISQ 7000 mass spectrometer (Thermo Fisher Scientific, USA). The DB-5MS column (Agilent, USA) was used as a stationary phase with GC/MS, and run parameters were configured as previously described by Nguyen et al. (2023). Acquired mass spectral data were used to compare with the NIST 2017 library to determine the exact chemical compositions.

Determination of antibacterial activity

The disk diffusion method was employed to assess the antibacterial efficacy of the acetone extract from the

studied species, following the Clinical and Laboratory Standards Institute guidelines (CLSI 2016). Acetone extracts at concentrations of 100, 150, and 200 mg mL^{-1} in 15% dimethyl sulfoxide were used for the test. As a positive control, a 10-µg gentamicin disk (Nam Khoa BioTek, Vietnam) was used, while 15% DMSO served as the negative control. The experiment was conducted in triplicate, and Fisher's least significant difference (LSD) and one-way analysis of variance (ANOVA) were employed for statistical analysis.

DPPH radical scavenging assay

DPPH radical scavenging activity of the acetone extract from the studied species was determined by DPPH assay (Nguyen et al. 2023) with slight modifications. Methanol 99.8% was used to dissolve the extract into different concentrations. The mixture, composed of 0.3 mL of extract and 3.7 mL of DPPH 0.1 mM was incubated at room temperature for 30 min in the dark. Absorbance measurement was done using a UV-Vis spectrophotometer (Genesys 20, USA) at 517 nm. DPPH radical scavenging activity was calculated as follows the Equation 1:

$$DPPH(\%) = \frac{A_0 - A_i}{A_0} \times 100 \qquad (1)$$

Where A_o and A_i are the absorbance of the DPPH solution and the sample-DPPH mixture, respectively. The DPPH radical scavenging effect was determined by IC_{50} value in comparison with the control ascorbic acid.

ABTS radical scavenging assay

Antioxidant activity was determined by ABTS radical scavenging assay described by Re et al. (1999) with slight modifications. Initially, solution A comprised 7 mM ABTS and 2.45 mM $K_2S_2O_8$, was prepared and incubated at 37 °C for 18 h in the dark. Subsequently, a mixture of 3 mL of solution A, 0.1 mL of the studied extract, and 1.9 mL of acetone was made, followed by 15 min incubation in the dark. To assess the ABTS radical scavenging activity, the absorbance of the solution was measured at 734 nm using a UV-VIS spectrophotometer (UVS 2800, Labome, USA) equipped with UVWin6 Software. Ascorbic acid served as the reference standard, and the standard curve for ascorbic acid (0 to 15 ppm) was constructed. The sample concentration was determined from the standard curve equation and expressed as µg mL^{-1} ascorbic acid.

RESULTS AND DISCUSSION

Chemical components of the acetone extract and chloroform, ethyl acetate, and hexane fractions from *Camellia cattienensis*

The chemical components of the acetone extract and chloroform, ethyl acetate, and hexane fractions of *C. cattienensis* are shown in Table 1 and Figure 1. A total of 54 compounds were found in the four extracts studied. The acetone extract was found to be rich in 2-pentanone, 4-hydroxy-4-methyl (22.85%); 3,7,11,15-tetramethyl-2-hexadecen-1-ol (17.14%); neophytadiene (16.97%); stigmasterol (12.78%); α-amyrin (5.29%); and n-hexadecanoic acid (4.75%). The chloroform fraction possessed phenol, 2,4-bis(1,1-dimethylethyl)-, phosphite (3:1) (74.91%); n-hexadecanoic acid (8.30%); and 7,9-di-tert-butyl-1-oxaspiro (4,5) deca-6,9-diene-2,8-dione (5.08%) as the major compounds. The ethyl acetate fraction was mainly composed of 2-pentanone, 4-hydroxy-4-methyl (54.68%); phenol, 2,4-bis(1,1-dimethylethyl)-, phosphite (3:1) (9.17%); n-hexadecanoic acid (8.25%); and 5-hydroxymethylfurfural (8.08%) whereas hexanedioic acid, bis(2-ethylhexyl) ester (30.89%); neophytadiene (25.21%); 3,7,11,15-tetramethyl-2-hexadecen-1-ol (11.58%); n-hexadecanoic acid (10.26%); and 9,12,15-octadecatrienoic acid, (Z,Z,Z)- (8.44%) were the major compounds in the n-hexane fraction.

Previous studies have also demonstrated the chemical compositions of various *Camellia* species collected from Vietnam. For example, the essential oil of the *C. longii* flower was found to be rich in α-eudesmol (16.1%), (E)-nerolidol (13.0%), and β-eudesmol (8.9%) (Tran et al. 2023). Hoang et al. (2014) determined 35 volatile compounds that could be the main factor responsible for the black tea's aroma quality (*Camellia sinensis*), of which α-ionone, ethyl caprylate, 3-hydroxy-β-damascone, β-ionone, 2(4H)-benzofuranone were the main factors contributing for this (Hoang et al. 2014). The seed oil of the *Camellia ninhii* was characterized by the predominance of oleic acid (45.43%), palmitic acid (27.83%), and *trans*-cinnamic acid (4.83%) (Tran et al. 2022).

Table 1. Chemical components of the acetone extract and its fractions.

STT	RT	Compounds	Relative percentage (%)			
			CAT	CATC	CATE	CATH
1	2.20	Acetic acid, butyl ester	-	-	1.55	-
2	2.41	3-Furaldehyde	-	-	0.74	-
3	2.43	3-Penten-2-one, 4-methyl-	1.77	-	-	-
4	2.48	2-Pentanone, 4-hydroxy-4-methyl-	22.85	-	54.68	0.24
5	2.82	Benzene, 1,3-dimethyl	-	-	0.15	-
6	3.04	2-Propenoic acid, butyl ester	-	-	1.65	-
7	3.09	1,3,5,7-Cyclooctatetraene	-	-	0.23	-
8	3.81	2-Heptanol, acetate	0.47	-	-	-
9	5.81	Ethanol, 2,2'-oxybis-, diacetates	0.10	-	-	-
10	6.33	Dodecane	-	-	1.35	-
11	6.43	2,6-Dimethyldecane	-	-	0.22	-
12	7.44	Linalool	0.38	-	-	-
13	7.96	Octanoic acid	-	-	0.42	-
14	8.03	2,6-Dimethyl-6-nitro-2-hepten-4-one	0.35	-	-	-
15	8.14	Benzoic acid	0.18	-	-	-
16	8.27	Azulene	-	-	0.69	-
17	8.51	Undecane, 2,6-dimethyl	-	-	0.22	-
18	8.61	Dodecane, 4-methyl	-	-	0.17	-
19	8.74	5-Hydroxymethylfurfural	0.20	-	8.08	-
20	9.02	Tetradecane, 5-methyl-	-	-	0.50	-
21	9.14	Dodecane, 2,6,11-trimethyl-	-	-	1.38	-
22	10.08	Undecane, 4,7-dimethyl-	-	0.56	-	-
23	10.84	1-Iodo-2-methylundecane	-	-	1.45	-
24	10.97	Pentanoic acid, 5-hydroxy-, 2,4-di-t-butylphenyl esters	-	0.30	-	-
25	11.53	Phenol, 2,4,6-tri-tert-butyl-	-	0.62	-	-
26	12.19	Tetradecane, 2,6,10-trimethyl-	-	0.93	1.40	-
27	12.66	Benzyl Benzoate	-	0.79	-	-
28	12.96	Neophytadiene	16.97	2.13	-	25.21
29	13.36	7,9-Di-tert-butyl-1-oxaspiro (4,5) deca-6,9-diene-2,8-dione	-	5.08	1.43	-
30	13.37	3,7,11,15-Tetramethyl-2-hexadecen-1-ol	17.14	-	-	11.58
31	13.57	n-hexadecenoic acid	4.75	8.30	8.25	10.26
32	14.45	9,12,15-Octadecatrienoic acid, 2,3-dihydroxypropyl ester, (Z,Z,Z)-	-	-	2.01	-
33	14.46	9,12,15-Octadecatrienoic acid, (Z,Z,Z)-	-	-	-	8.44
34	14.55	Octadecanoic acid	0.56	2.53	2.25	1.97
35	14.63	Phytol	1.34	-	-	1.01
36	14.72	9,12-Octadecadienoic acid (Z,Z)-	0.28	-	-	-
37	15.36	Octadecane, 3-ethyl-5-(2-ethylbutyl)-	-	0.85	-	-
38	15.50	17-Pentatriacontene	0.35	-	-	-

Table 1

STT	RT	Compounds	Relative percentage (%)			
			CAT	CATC	CATE	CATH
40	15.66	Oleic Acid	0.29	-	-	-
41	16.18	Benzenepropanoic acid, 3,5-bis(1,1-dimethylethyl)-4-hydroxy-, 2-ethylhexyl ester	-	2.08	-	-
42	16.41	Bis(2-ethylhexyl) phthalate	-	-	-	1.61
43	16.59	Octadecane, 3-ethyl-5-(2-ethylbutyl)-	0.51	-	-	-
44	16.70	Hexadecenoic acid, 1-(hydroxymethyl)-1,2-ethanediyl ester	0.72	-	-	-
45	16.80	Oleic acid, 3-(octadecyloxy)propyl ester	0.73	-	0.18	-
46	16.83	Octadecanal, 2-bromo	0.65	-	-	-
47	17.26	Octadecane, 3-ethyl-5-(2-ethylbutyl)-	0.58	-	-	-
48	18.15	1,2-Cyclohexanedicarboxylic acid, dinonyl ester	-	-	-	2.35
49	18.54	Squalene	2.42	-	-	2.84
50	24.05	dl-α-Tocopherol	2.26	-	-	-
51	27.26	Stigmasterol	12.78	-	-	3.42
52	27.63	Phenol, 2,4-bis(1,1-dimethylethyl)-, phosphite (3:1)	-	74.91	9.17	-
53	28.03	α-Amyrin	5.29	-	-	-
54	28.30	β-Sitosterol	4.30	-	-	-
		Total	98.22	99.08	98.17	98.82

Note: CAT: acetone extract, CATC: chloroform, CATE: ethyl acetate, and CATH: hexane.

Furthermore, a recent study reported that the leaf and flower of *C. tonkinensis* consisted of Zn (10.20 and 13.40 mg kg^{-1}) and saponin (58.30 and 87.10 mg g^{-1}) whereas various amino acids were also present in two organs of this plant, including aspartate, glutamate, serine, histamine, glycine, arginine, threonine, alanine, cysteine, tyrosine, valine, phenylalanine, methionine, leucine, isoleucine, proline, and lysine with the contents ranging from 3.512 to 42.087 g kg^{-1} (Dang et al. 2022).

Studies have identified the chemical compounds in various *Camellia* species extracts using different solvents and analyzed them with gas chromatography-mass spectrometry. For instance, the methanol extract isolated from *Camellia sinensis* leaves collected from Bangladesh mainly contained caffeine (27.44%), hexadecanoic acid, methyl ester (14.02%), 9,12,15-octadecatrienoic acid methyl ester (Z, Z, Z) (3.95%) (Hasan et al. 2024). Similarly, the chloroform: methanol extract of the *C. sinensis* leaves grown in Ambala Cantt., India was found to be rich in caffeine (48.21%), *trans*-13-octadecenoic acid (18.30%), *cis*-11-eicosenoic acid (15.15%) (Gupta and Kumar 2017). In addition, the methanol extract of *C. sinensis* leaves from Dehradun, India, was mainly composed of *n*-heptadecanol-1 (68.63%); 2-pentanone, 4-hydroxy-4-methyl- (3.82%); and 7-hexadecanoic acid, methyl ester, (Z) (2.32%) (Pradhan and Dubey 2021). The phytochemistry of the methanol extract of *C. sinensis* leaves collected from six regions of India was also investigated. Accordingly, the sample extracts from Moonar (Kerala) and Kodaikanal (Tamil Nadu) were characterized by the predominance of caffeine (46.25-57.17%); 1,2,3-benzenetriol (18.40-16.28%); and 1,3,4,5-tetrahydroxycyclohexanecarbonyl (13.96-9.64%). Meanwhile, the extracts grown in Ootacamund (Tamil Nadu) and Bengaluru (Karnataka) contained caffeine 1,3,7-trimethyl-3,7-dihydro-1H-purine-2,6-dione (56.48-57.52%);1,2,3-benzenetriol (28.36-21.55%) as the major compounds. Finally, 1,3,7-trimethyl-3,7-dihydro-1H-purine-2,6-dione (42.75-59.79%) as the most abundant compound in the extracts from Assam (Assam) and Kolkata (West Bengal) (Senthilkumar et al. 2015). Apart from that, the major constituents of the ethanol extract of the *C. sinensis* leaves from Uganda were caffeine (82.69%); naphthacene-5,12-dione, 6,11

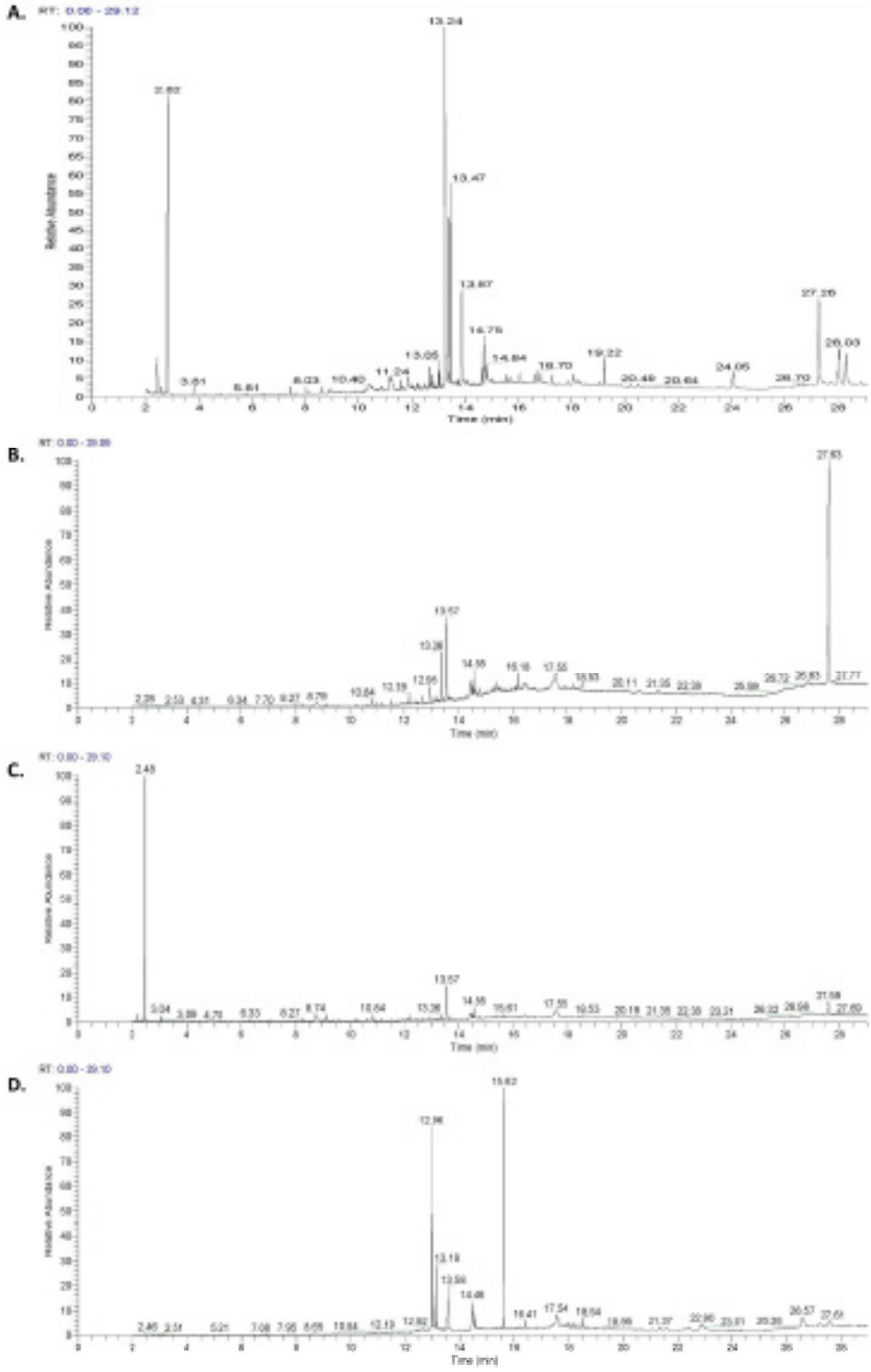

Figure 1. The GC chromatogram of **A.** acetone extract from *Camellia cattienensis* and **B**. chloroform, **C.** ethyl acetate, and **D**. hexane fractions from *Camellia cattienensis.*

-dihydroxy-2,3,8,9-tetramethyl- (3.73%); and estra-1,3,5(10)-trien-17-ol, 2,3,4-trimethoxy-, (17.β.)- (3.73%) (Hope et al. 2022).

The benzene-ethanol extracts of *Camellia oleifera* leaves collected from Hunan, China, were found rich in butyraldehyde, semicarbazone (11.58%); hexatriacontane (8.04%); and 1,6-anhydro-β-D-glucopyranose (7.54%) (Liu et al. 2009). The chemical constituents of different extracts of *C. oleifera* fruit grown in Hunan, China, were also reported. For instance, the methanol extract contained a mixture of γ-sitosterol (43.32%); 5-hydroxymethylfurfural (22.07%); and *cis*-vaccenic acid (12.71%). The ethanol extract was mainly composed of 5-hydroxymethylfurfural (58.78%) and furfural (4.74%), while *cis*-vaccenic acid (45.20%); *n*-hexadecanoic acid (10.98%); and 9-octadecenamide, (Z)- (5.82%) were the main compounds in the ethyl acetate extract (Xie et al. 2018). Moreover, the acetone extract of *Camellia assamica* leaves collected from Dehradun, India was characterized by the predominance of 2′,6′dihydroxyacetophenone, bis(trimethylsilyl) ether (17.58%); *N*(trifluoracetyl) *O*,*O*',*O*"tris(trimethylsilyl) epinephrine (15.83%); and tetracosamethyl cyclododecasiloxane (10.62%) (Pradhan and Dubey 2021).

Antibacterial activity of acetone extract from *Camellia cattienensis*

The antibacterial property of *C. cattienensis* acetone extract was presented in Table 2. Accordingly, the studied extract was found to be effective against four out of eight bacterial strains, including *K. pneumoniae* ATCC 700603, *S. aureus* ATCC 29213, *S. aureus* ATCC 25923, and *S. saprophyticus* BAA750. Overall, at a concentration of 200 mg mL^{-1}, the studied extract exhibits a stronger antibacterial effect against four bacterial strains in comparison with the remaining concentrations (Table 2).

Table 2. Antibacterial property of acetone extracts from *Camellia cattienensis*.

Bacterial strains	**Zone of inhibition (mm)**				
	100 (mg mL^{-1})	**150 (mg mL^{-1})**	**200 (mg mL^{-1})**	**Gentamycin**	**Negative control**
B. cereus ATCC 13883	-	-	-	14.17±0.29	-
E. coli ATCC 25922	-	-	-	13.33±0.58	-
E. hormaechei ATCC 700323	-	-	-	8.83±0.76	-
K. pneumoniae ATCC 700603	4.00±0.87^{a}	4.83±0.29^{a}	5.33±1.15^{a}	12.83±0.76^{b}	-
K. pneumoniae ATCC 13883	-	-	-	13.50±0.87	-
S. aureus ATCC 29213	2.50±0.50^{a}	4.00±0.50^{b}	4.33±0.58^{b}	13.67±1.53^{c}	-
S. aureus ATCC 25923	2.67±1.15^{a}	4.33±0.58^{a}	6.67±0.76^{b}	13.00±1.00^{c}	-
S. flexneri ATCC 9199	-	-	-	12.00±0.87	-
S. saprophyticus BAA750	2.33±0.58^{a}	2.50±0.50^{a}	3.67±0.29^{b}	13.33±0.58^{c}	-
S. typhimurium ATCC 13311	-	-	-	14.50±0.87	-

Different superscript lower-case letters in the same row denote significant difference (P<0.05). (-) Not active.

Studies provided the antimicrobial activities of different solvent extracts from *Camellia* species. For example, the chloroform: methanol extract of the *Camellia sinensis* leaves grown in Ambala Cantt., India had an inhibitory effect on *Staphylococcus aureus, Escherichia coli*, *Pseudomonas aeruginosa*, and *Candida albicans* (Gupta and Kumar 2017). The methanol extract of the *C. sinensis* and *C. assamica* leaves from Dehradun, India and its various fractions such as water, ethanol, methanol, chloroform, and petroleum ether were reported to possess antimicrobial effects against *Escherichia coli, Salmonella typhi, Klebsiella pneumoniae, Listeria monocytogenes, Staphylococcus aureus, Pseudomonas aeruginosa*, and *Candida albicans* (Pradhan and Dubey 2021). In another report, the antibacterial effects of the hot water extract isolated from the green, herbal, and black teas (*C. sinensis*) were also investigated. Accordingly, the first extract was found to be effective against three bacterial strains, including *Micrococcus luteus*, *Bacillus cereus*, and *Staphylococcus aureus*, while the latter

extracts exhibited an inhibitory effect on *Micrococcus luteus* and *Bacillus cereus* (Chan et al. 2011).

The ethanol extract of *C. sinensis* leaves from Uganda was demonstrated to be effective against different pathogenic bacteria, especially *Salmonella* and *Escherichia coli* (Hope et al. 2022). Also, the leaf ethanol extract of this plant collected from Chennai, India, displayed activity against *Streptococcus mutans* and *Lactobacillus acidophilus* (Anita et al. 2015). The ethanol extract of *C. sinensis* leaves grown in Iran was effective against 30 *Escherichia coli* strains isolated from the urine cultures of patients in three hospitals in Zabol, southeastern Iran (Sepehri et al. 2014). Additionally, the organic acids and phenolic components from the seeds of *Camellia oleifera* cake, collected in Jiangxi, China, exhibited antimicrobial activity against six fungal and bacterial strains, including *Aspergillus oryzae*, *Rhizopus stolonifer*, *Mucor racemosus*, *Bacillus subtilis*, *Staphylococcus aureus*, and *Escherichia coli* (Zhang et al. 2020). Furthermore, another study demonstrated the antibacterial effects of the methanol extract fractioned into basic, neutral, and acid fractions obtained from *Camellia japonica* grown in Yeosoo, Korea. Accordingly, the methanol extract, neutral, and acid fractions displayed activity against some bacterial strains, including *Escherichia coli*, *Salmonella typhimurium*, *Listeria monocytogenes*, and *Staphylococcus aureus* (Kim et al. 2001).

Antioxidant activity of acetone extract from *Camellia cattienensis*

The antioxidant effects of the tested extract from *C. cattienensis* were shown in Figure 2. Accordingly, the extract had the DPPH, ABTS free radical scavenging with the IC_{50} values of 91.63±1.88 and 13.32±0.49 µg mL^{-1}, respectively.

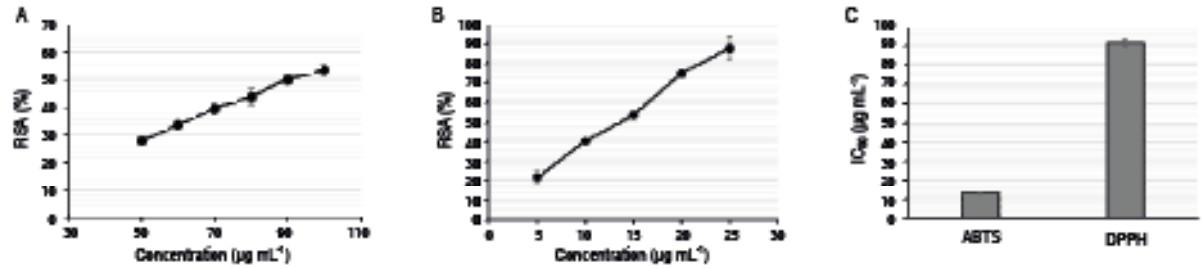

Figure 2. The free radical scavenging activity of the acetone extract from *Camellia catienensis* was measured using **A.** the DPPH assay, **B**. the ABTS assay, and **C**. the corresponding IC_{50} values.

Compared to other *Camellia* species, the results show moderate antioxidant potential. For example, the methanol extract of *C. sinensis* leaves from Bangladesh showed a stronger DPPH scavenging effect with an IC_{50} value of 69.51 µg mL^{-1}, indicating better antioxidant activity compared to *C. cattienensis* (Hasan et al. 2024). Conversely, the acetone extract of *C. oleifera* seed oil from Taiwan exhibited a much lower antioxidant effect, with only 4.46% inhibition at 200 µg mL^{-1}, significantly weaker than *C. cattienensis* (Lee and Yen 2006). Similarly, the ethyl acetate extract of *C. oleifera* seed oil showed only 5.92% inhibition, while the methanol extract performed better, with 66.50% inhibition at the same concentration (Lee and Yen 2006). In another study, the organic acids and phenolic components of *C. oleifera* seed cake from Jiangxi, China, demonstrated weaker antioxidant activity than *C. cattienensis*, with IC_{50} values of 184 mg L^{-1} and 103 mg L^{-1}, respectively (Zhang et al. 2020). Furthermore, the ethanol extract of *C. japonica* flowers from Korea demonstrated a DPPH inhibition of up to 60% at 50 µg mL^{-1} (Piao et al. 2011), while the ethanol extract of *C. japonica* leaves from Jeonnam, Korea, showed a stronger antioxidant effect with an IC_{50} value of 38.53 µg mL^{-1} (Yoon et al. 2017).

Overall, the acetone extract of *C. cattienensis* leaves displayed a moderate antioxidant effect, stronger than that of *C. oleifera* extracts but weaker compared to the more potent antioxidant effects of *C. sinensis* and *C. japonica* ethanol and methanol extracts. These differences likely reflect the variations in solvent choice, plant parts used, and regional factors influencing the phytochemical composition.

CONCLUSION

Camellia cattienensis is a rare species that, to date, has

only been documented from the type collection at Nam Cat Tien National Park, Dong Nai Province, Vietnam. In the present study, a limited number of samples of this species were utilized for experimental purposes to prioritize its conservation. Furthermore, phytochemical, antioxidant, and antibacterial properties are recognized as prominent features in *Camellia* species. Therefore, the present study provides these characteristics for the first time from the acetone extract of *C. cattienensis*. As a result, the various acetone sub-extracts were found to contain several bioactive compounds, with 2-pentanone, 4-hydroxy-4-methyl-phenol, 2,4-bis(1,1-dimethylethyl)-, phosphite (3:1); and hexanedioic acid, bis(2-ethylhexyl) identified as the most abundant compounds. The acetone extracts of *C. cattienensis* exhibited moderate effects against bacterial strains, including *Klebsiella pneumoniae*, *Staphylococcus aureus*, and *Staphylococcus saprophyticus*. Notably, this extract demonstrated potent antioxidant activity, as evaluated using the DPPH and ABTS assays, with IC_{50} values of 91.63±1.88 and 13.32±0.49 µg mL^{-1}, respectively. The results of analyses, such as the antioxidant and antibacterial activities of the n-hexane, chloroform, and ethyl acetate fractions, will be reported in a subsequent study. Given the versatile applications of various *Camellia* species in the food industry, the findings of this study contribute to a deeper understanding of the potential food uses of *C. cattienensis*, particularly in the beverage industry.

CONFLICT OF INTERESTS

The author declares no conflict of interest.

REFERENCES

Anand J, Upadhyaya B, Rawat P and Rai N (2015) Biochemical characterization and pharmacognostic evaluation of purified catechins in green tea (*Camellia sinensis*) cultivars of India. 3 Biotech 5(3): 285–294. https://doi.org/10.1007/s13205-014-0230-0

Anita P, Balan In, Ethiraj S et al (2015) In vitro antibacterial activity of *Camellia sinensis* extract against cariogenic microorganisms. Journal of Basic and Clinical Pharmacy 6(1): 35-39. https://www.jbclinpharm.org/articles/in-vitro-antibacterial-activity-of-camellia-sinensis-extract-against-cariogenic-microorganisms.pdf

Chan EW, Tie P, Soh E and Law Y (2011) Antioxidant and antibacterial properties of green, black, and herbal teas of *Camellia sinensis*. Pharmacognosy Research 3(4): 266–272. https://doi.org/10.4103/0974-8490.89748

Chitsazan A (2015) Anti-cancer properties of green Tea probed via quantum mechanics calculations. Oriental Journal of Chemistry 31(1): 393–408. https://doi.org/10.13005/ojc/310147

CLSI - Clinical & Laboratory Standards Institute (2016) Methods for antimicrobial dilution and disk susceptibility testing of infrequently isolated or fastidious bacteria. 3rd ed. CLSI guideline M45. Wayne PA. Clinical and Laboratory Standard Institute.

Dang VH, Nguyen TC, Le VQ et al (2022) Content of some chemical components from Ba Vi yellow *Camellia* plant (*Camellia tonkinensis* (Pit.) Cohen-Stuart). Vietnam Journal of Agriculture and Rural Development 434: 72-76.

Gaur R and Bao GH (2021) Chemistry and pharmacology of natural catechins from camellia sinensis as anti-MRSA agents. Current Topics in Medicinal Chemistry 21(17): 1519-1537. https://doi.org/10.2174/1568026621666210524100632

Gupta D and Kumar M (2017) Evaluation of in vitro antimicrobial potential and GC–MS analysis of *Camellia sinensis* and *Terminalia arjuna*. Biotechnology Reports 13: 19–25. https://doi.org/10.1016/j.btre.2016.11.002

Hasan R, Haque MM, Hoque A et al (2024) Antioxidant activity study and GC-MS profiling of *Camellia sinensis* Linn. Heliyon 10(1): e23514. https://doi.org/10.1016/j.heliyon.2023.e23514

Hoang QT, Tham BHP, Vu HS et al (2014) Sensory aroma and related volatile flavor compound profiles of different black tea grades (*Camellia sinensis*) produced in Northern Vietnam. In: Valentin D, Chollet S, Le S et al (2014) Summer Program in Sensory Evaluation 2014, Vietnam. VNU-HCM Publishing House, 113-119.

Hope O, Bright IE and Alagbonsi AI (2022) GC-MS biocomponents characterization and antibacterial potency of ethanolic crude extracts of *Camellia sinensis*. SAGE Open Medicine 10: 1-13. https://doi.org/10.1177/20503121221116859

Kim JK, Park HG, Kim CR et al (2014) Quality evaluation on use of *Camellia* oil as an alternative method in dried seaweed preparation. Preventive Nutrition and Food Science 19(3): 234–241. https://doi.org/10.3746/pnf.2014.19.3.234

Kim KY, Davidson PM and Chung H J (2001) Antibacterial activity in extracts of *Camellia japonica* L. petals and its application to a model food system. Journal of Food Protection 64(8): 1255–1260. https://doi.org/10.4315/0362-028X-64.8.1255

Le HT, Luu TN, Nguyen HMT et al (2021) Antibacterial, antioxidant and cytotoxic activities of different fractions of acetone extract from flowers of *Dipterocarpus intricatus* Dyer (Dipterocarpaceae). Plant Science Today 8(2): 273–277. https://doi.org/10.14719/pst.2021.8.2.1086

Lee CP and Yen GC (2006) Antioxidant activity and bioactive compounds of tea seed (*Camellia oleifera* Abel.) oil. Journal of Agricultural and Food Chemistry 54(3): 779–784. https://doi.org/10.1021/jf052325a

Liu QM, Peng WX, Wu YX et al (2009) Analysis of biomedical components of *Camellia oleifera* Leaf and kernel hull by GC/MS. 2009 3rd International Conference on Bioinformatics and Biomedical Engineering IEEE 1-4.

Nguyen ND, Trinh NN, Nguyen QH et al (2023) Chemical profiles and biological activities of acetone extracts of nine Annonaceae plants. Journal of Applied Botany & Food Quality 96: 148-156. https://doi.org/10.5073/JABFQ.2023.096.019

Orel G and Wilson PG (2011) *Camellia cattienensis*: a new species of *Camellia* (sect. Archaecamellia: Theaceae) from Vietnam. Kew Bulletin 66(4): 565–569. https://www.jstor.org/stable/23216738

Piao MJ, Yoo ES, Koh YS et al (2011) Antioxidant effects of the ethanol extract from flower of *Camellia japonica* via scavenging

of reactive oxygen species and induction of antioxidant enzymes. International Journal of Molecular Sciences 12(4): 2618–2630. https://doi.org/10.3390/ijms12042618

Pradhan S and Dubey RC (2021) GC–MS analysis and molecular docking of bioactive compounds of *Camellia sinensis* and *Camellia assamica*. Archives of Microbiology 203(5): 2501–2510. https://doi.org/10.1007/s00203-021-02209-6

Quach V H, Luong VD, Doudkin RV et al (2021) Diversity of the genus *Camellia* L. (Theaceae) in Lam Dong Province. Academia Journal of Biology 43: 129-138. https://www.researchgate.net/publication/357451755

Re R, Pellegrini N, Proteggent, A et al (1999) Antioxidant activity applying an improved ABTS radical cation decolorization assay. Free radical biology and medicine 26: 1231-1237. https://doi.org/10.1016/s0891-5849(98)00315-3

Senthilkumar SR, Sivakumar T, Arulmozhi KT and Mythili N (2015) Gas chromatography-mass spectroscopy evaluation of bioactive phytochemicals of commercial green teas (*Camellia sinensis*) of India. Asian Journal of Pharmaceutical and Clinical Research 8: 278-282

Sepehri Z, Hassanshahian M, Shahi Z et al (2014) Antibacterial effect of ethanol extract of *Camellia sinensis* L. against *Escherichia coli*. Asian Pacific Journal Microbiology Research 2: 6-8.

Tran TTQ, Trinh TD, Nguyen TTU and Le VS (2022) Fatty acid composition and antioxidant activity of *Camellia ninhii* seed oil collected in Lam Dong province. Dalat University Journal of Science 12(3): 27–33. https://doi.org/10.37569/DalatUniversity.12.3.993(2022)

Tran TH, Nguyen TC, Dung VC et al (2023) Characterization and evaluation of the in vitro antioxidant, α-glucosidase inhibitory activities of *Camellia longii* Orel and Luu. (Theaceae) llower essential oil and extracts from Vietnam. Natural Product Communications 18(11). https://doi.org/10.1177/1934578X231208348

Xie Y, Ge S, Jiang S et al (2018) Study on biomolecules in extractives of *Camellia oleifera* fruit shell by GC–MS. Saudi Journal of Biological Sciences 25(2): 234–236. https://doi.org/10.1016/j.sjbs.2017.08.006

Yang C, Liu X, Chen Z et al (2016) Comparison of oil content and fatty acid profile of ten new *Camellia oleifera* cultivars. Journal of Lipids 2016, 3982486. https://doi.org/10.1155/2016/3982486

Yoon IS, Park DH, Kim JE et al (2017) Identification of the biologically active constituents of *Camellia japonica* leaf and anti-hyperuricemic effect in vitro and in vivo. International Journal of Molecular Medicine 39(6): 1613–1620. https://doi.org/10.3892/ijmm.2017.2973

Zhang D, Nie S, Xie M and Hu J (2020) Antioxidant and antibacterial capabilities of phenolic compounds and organic acids from *Camellia oleifera* cake. Food Science and Biotechnology 29(1): 17–25. https://doi.org/10.1007/s10068-019-00637-1

ÍNDICE DE AUTORES

Almaguer-Vargas Gustavo. Gibberellic acid and warm incubation temperatures as germination stimulants in yellow kiwifruit seeds (*Actinidia chinensis* var. *chinensis*). Vol. 78(2): 11069-11076. 2025.

Araya-Bastías Carolina. Application of tomato peels (*Solanum lycopersicum* L.) in baking: effects on nutritional and sensory quality. Vol. 78(2): 11117-11125. 2025.

Avellaneda-Torres Lizeth Manuela. Interaction of biological soil crusts with edaphic parameters of carbon and nitrogen in desertified soils. Vol. 78(2): 11151-11160. 2025.

Ávila Rocío. Application of tomato peels (*Solanum lycopersicum* L.) in baking: effects on nutritional and sensory quality. Vol. 78(2): 11117-11125. 2025.

Barriga-Sánchez Maritza. Effect of turmeric flour on sensory rating and antioxidant capacity in spicy fruit sauce. Vol. 78(2): 11127-11140. 2025.

Cantor Fernando. Survival and oviposition of *Tetranychus urticae* Koch (Acari: Tetranychiidae) under exposure to unfractionated botanical extracts. Vol. 78(2): 11169-11180. 2025.

Castañeda-Garzón Sandra Liliana. Growth models of *Hevea brasiliensis* genotypes in clonal fields of the Colombian Orinoquia. Vol. 78(2): 11057-11067. 2025.

Castañeda-Vildozola Álvaro. Gibberellic acid and warm incubation temperatures as germination stimulants in yellow kiwifruit seeds (*Actinidia chinensis* var. *chinensis*). Vol. 78(2): 11069-11076. 2025.

Cetica Pablo Daniel. Effect of Trolox and resveratrol supplementation during the refrigeration of boar sperm. Vol. 78(2): 11141-11149. 2025.

Chiffelle Ítalo. Application of tomato peels (*Solanum lycopersicum* L.) in baking: effects on nutritional and sensory quality. Vol. 78(2): 11117-11125. 2025.

Ciro Velásquez Héctor José. Protein concentrates from Colombian cheese acid whey as a source of antioxidant hydrolysates obtained by proteolysis. Vol. 78(2): 11077-11088. 2025.

Córdoba Mariana. Effect of Trolox and resveratrol supplementation during the refrigeration of boar sperm. Vol. 78(2): 11141-11149. 2025.

Correa-Londoño Guillermo. Characterization of rejected green banana flour: morphological, structural, and techno-functional properties. Vol. 78(2): 11089-11102. 2025.

Coy-Barrera Ericsson. Survival and oviposition of *Tetranychus urticae* Koch (Acari: Tetranychiidae) under exposure to unfractionated botanical extracts. Vol. 78(2): 11169-11180. 2025.

Cristobal Alania Patricia. Effect of turmeric flour on sensory rating and antioxidant capacity in spicy fruit sauce. Vol. 78(2): 11127-11140.

Cruz-Castillo Juan Guillermo. Gibberellic acid and warm incubation temperatures as germination stimulants in yellow kiwifruit seeds (*Actinidia chinensis* var. *chinensis*). Vol. 78(2): 11069-11076. 2025.

Durango Restrepo Diego Luis. Protein concentrates from Colombian cheese acid whey as a source of antioxidant hydrolysates obtained by proteolysis. Vol. 78(2): 11077-11088. 2025.

Escobar Adriana. Application of tomato peels (*Solanum lycopersicum* L.) in baking: effects on nutritional and sensory quality. Vol. 78(2): 11117-11125. 2025.

Flores Marcos. Application of tomato peels (*Solanum lycopersicum* L.) in baking: effects on nutritional and sensory quality. Vol. 78(2): 11117-11125. 2025.

Gil González Jesús Humberto. Protein concentrates from Colombian cheese acid whey as a source of antioxidant hydrolysates obtained by proteolysis. Vol. 78(2): 11077-11088. 2025.

Gil-González Jesús. Characterization of rejected green banana flour: morphological, structural, and techno-functional properties. Vol. 78(2): 11089-11102. 2025.

Guerra-Ramírez Diana. Gibberellic acid and warm incubation temperatures as germination stimulants in yellow kiwifruit seeds (*Actinidia chinensis* var. *chinensis*). Vol. 78(2): 11069-11076. 2025.

Hernández Angarita David Ricardo. Growth models of *Hevea brasiliensis* genotypes in clonal fields of the Colombian Orinoquia. Vol. 78(2): 11057-11067. 2025.

Herrera-Builes Jhon F. Physical and mechanical properties of cross-laminated timber made from *Pinus tecunumanii* wood. Vol. 78(2): 11161-11167. 2025.

Le Thanh Tho. *Camellia cattienensis*: phytochemical and biological properties from the leaf extract. Vol. 78(2): 11181-11190. 2025.

Manjarres-Pinzón Katherine. Characterization of rejected green banana flour: morphological, structural, and techno-functional properties. Vol. 78(2): 11089-11102. 2025.

Marguet Emilio R. Silage production from agro-industrial by-products fermented with lactic acid bacteria isolated from the marine environment. Vol. 78(2): 11103-11116. 2025.

Mora Garcés Argenis Antonio. Growth models of *Hevea brasiliensis* genotypes in clonal fields of the Colombian Orinoquia. Vol. 78(2): 11057-11067. 2025.

Morado Sergio. Effect of Trolox and resveratrol supplementation during the refrigeration of boar sperm. Vol. 78(2): 11141-11149. 2025.

Nguyen Hanh Thi Dieu. *Camellia cattienensis*: phytochemical and biological properties from the leaf extract. Vol. 78(2): 11181-11190. 2025.

Nguyen Ngoc An. *Camellia cattienensis*: phytochemical and biological properties from the leaf extract. Vol. 78(2): 11181-11190. 2025.

Nguyen Quoc Hung. Camellia cattienensis: phytochemical and biological properties from the leaf extract. Vol. 78(2): 11181-11190. 2025.

Nguyen Thi Nha Xuyen. *Camellia cattienensis*: phytochemical and biological properties from the leaf extract. Vol. 78(2): 11181-11190. 2025.

Nguyen Trong Thao. *Camellia cattienensis*: phytochemical and biological properties from the leaf extract. Vol. 78(2): 11181-11190. 2025.

Nguyen Van Hop. *Camellia cattienensis*: phytochemical and biological properties from the leaf extract. Vol. 78(2): 11181-11190. 2025.

Parra Rodolfo. Physical and mechanical properties of cross-laminated timber made from *Pinus tecunumanii* wood. Vol. 78(2): 11161-11167. 2025.

Pham Tan Viet. *Camellia cattienensis*: phytochemical and biological properties from the leaf extract. Vol. 78(2): 11181-11190. 2025.

Quitral Vilma. Application of tomato peels (*Solanum lycopersicum* L.) in baking: effects on nutritional and sensory quality. Vol. 78(2): 11117-11125. 2025.

Quoc Le Pham Tan. *Camellia cattienensis*: phytochemical and biological properties from the leaf extract. Vol. 78(2): 11181-11190. 2025.

Reina-García Jhusua David. Gibberellic acid and warm incubation temperatures as germination stimulants in yellow kiwifruit seeds (*Actinidia chinensis* var. *chinensis*). Vol. 78(2): 11069-11076. 2025.

Rivera Padilla Juan Jair. Interaction of biological soil crusts with edaphic parameters of carbon and nitrogen in desertified soils. Vol. 78(2): 11151-11160. 2025.

Rodríguez Daniel. Survival and oviposition of *Tetranychus urticae* Koch (Acari: Tetranychiidae) under exposure to unfractionated botanical extracts. Vol. 78(2): 11169-11180. 2025.

Rodríguez-Sandoval Eduardo. Characterization of rejected green banana flour: morphological, structural, and techno-functional properties. Vol. 78(2): 11089-11102. 2025.

Romero Conde Julian David. Interaction of biological soil crusts with edaphic parameters of carbon and nitrogen in desertified soils. Vol. 78(2): 11151-11160. 2025.

Sánchez-Mesa Nelly. Characterization of rejected green banana flour: morphological, structural, and techno-functional properties. Vol. 78(2): 11089-11102. 2025.

Sepúlveda Valencia José Uriel. Protein concentrates from Colombian cheese acid whey as a source of antioxidant hydrolysates obtained by proteolysis. Vol. 78(2): 11077-11088. 2025.

Sierra Juan C. Physical and mechanical properties of cross-laminated timber made from *Pinus tecunumanii* wood. Vol. 78(2): 11161-11167. 2025.

Sosa Franco M. Silage production from agro-industrial by-products fermented with lactic acid bacteria isolated from the marine environment. Vol. 78(2): 11103-11116. 2025.

Tarazona Yanes Maribel. Growth models of *Hevea brasiliensis* genotypes in clonal fields of the Colombian Orinoquia. Vol. 78(2): 11057-11067. 2025.

Vallejo Marisol. Silage production from agro-industrial by-products fermented with lactic acid bacteria isolated from the marine environment. Vol. 78(2): 11103-11116. 2025.

Van Hong Thien. *Camellia cattienensis*: phytochemical and biological properties from the leaf extract. Vol. 78(2): 11181-11190. 2025.

Zapata Bustamante Sandra. Protein concentrates from Colombian cheese acid whey as a source of antioxidant hydrolysates obtained by proteolysis. Vol. 78(2): 11077-11088. 2025.